

MOMENT RESISTING STEEL-CONCRETE COMPOSITE FRAMES UNDER THE COLUMN LOSS SCENARIO: DESIGN OF AN EXPERIMENTAL STUDY

Riccardo Zandonini ¹

Nadia Baldassino ¹

Fabio Freddi ²

¹ Department of Civil, Environmental and Mechanical Engineering, University of Trento, Trento, Italy

² Department of Civil, Environmental & Geomatic Engineering, University College of London, London, WC1E 6BT, U.K.,
formerly Department of Civil, Environmental and Mechanical Engineering, University of Trento, Trento, Italy



UNIVERSITÀ DEGLI STUDI
DI TRENTO

ISBN (online) 978-88-8443-816-4

DOI 10.15168/11572_219133

Publisher: Università degli Studi di Trento, via Calepina, 14 – 38122 Trento (Italy)

Title: Moment resisting steel-concrete composite frames under the column loss scenario:
design of an experimental study

Authors: Riccardo Zandonini, Nadia Baldassino, Fabio Freddi

Date of publication: November 2018

All rights reserved

Riccardo Zandonini, Nadia Baldassino, Fabio Freddi

Table of Contents

1	INTRODUCTION	1
2	DESIGN OF THE CASE STUDY STRUCTURES	2
2.1	Geometry	2
2.2	Finite Element Model	11
2.3	Materials	11
2.4	Actions	12
2.5	Load Combinations	15
2.6	Imperfection for global analysis of frames	26
2.7	Creep and Shrinkage of the concrete	26
2.8	Symmetric Structure	27
2.9	Asymmetric Structure	37
2.10	Calculation of the shear connectors - ULS	47
2.11	Design of composite joints	49
3	DESIGN OF THE EXPERIMENTAL TESTS	62
3.1	Numerical analysis of the experimental test	65
3.2	Design of the test setup	76
4	PRODUCTION OF THE SPECIMENS	87
4.1	Steel components	87
4.2	Restraints	89
4.3	Rebars	91
5	CONCLUDING REMARKS	96
6	LITERATURE	98
	ANNEX A: FULL-SCALE TESTS - STEEL COMPONENTS	A-1
	ANNEX B: RESTRAINTS	B-1
	ANNEX C: SLAB'S REINFORCEMENT	C-1

1 INTRODUCTION

Robustness is a very topical research issue, and several research work have been carried out in recent years. The University of Trento was involved in the project 'Robust impact design of steel and composite building structures' (acronym ROBUSTIMPACT). The project was financially supported in the framework of the European RFCS program (Research Fund for Coal and Steel). This document concerns the experimental activities carried out at the Laboratory of Material and Structural Testing (LMST) of the University of Trento.

The project focuses on the behaviour of composite steel and concrete framed buildings subject to accidental actions. Within the project, several experimental analyses were performed by the partners ranging from the local to the global response.

As to the global behaviour, at LMST two 3D full-scale tests on steel-concrete composite sub-frames simulating the total loss of an impacted column were performed. The purpose of the study is to improve the state of knowledge on the contribution offered by the joints and by the 3D slab system in terms of activation of an alternative mechanisms of resistance. The research assumes two reference case studies of steel and concrete five-story buildings differing for in-plane column layout. Two sub-frames were 'extracted' from these structures and tested in the laboratory.

The plan of the experimental tests required preliminary studies devoted to:

- selection and definition of a reference buildings assumed as case studies,
- design of the reference buildings according to the Eurocodes;
- identification of representative substructures (slab-beam system, columns and joints) from the reference structures to be experimentally investigated;
- design of the testing set-up

This report concern the design of the case studies, of the specimens and of the testing set-up.

In particular, Section 2 illustrates the design, based on the relevant Eurocodes, of the reference structures for both the geometric configurations. Section 3 reports the design of the sub-structures including also the numerical analysis and the design of the testing setup. Finally, Section 4 provides the details of the components of the two specimens as needed for their fabrication, and of the testing set-up. All the related drawings are reported in Annexes A-C.

2 DESIGN OF THE CASE STUDY STRUCTURES

2.1 Geometry

A five-story composite steel and concrete structure has been selected as case study structure. The total dimensions of the building are 34.2 *m* in *X* direction, 11.4 *m* in *Y* direction and the total height is of 18 *m* and it consists of six bays in the *X* direction and two bays in the *Y* direction. Two different geometric configurations of the frames are investigated. The first configuration is symmetric with respect to *X* and *Y* direction (Figure 2-1) while the second configuration is symmetric only with respect to the *Y* direction (Figure 2-6). The two case study structures will be called hereinafter as “*Symmetric*” and “*Asymmetric*” configurations respectively.

Both the building configurations are made by using the same steel sections type for beams (*IPE 240*) and columns (*HEB 220*) and the same thickness of the slab (150 *mm*). This choice is made in order to reduce the number of variables and hence, in order to simplify the comparison of the results between the two structures. Also the joint connections of the two geometric configurations are made in the same way and the only difference is in the rebars dimension and layout of the slab.

The steel braces designed to resist the horizontal forces in *X* direction are positioned in the frames *A* and *C* (Figure 2-1 and Figure 2-6), while, those needed to resist the horizontal forces in *Y* direction are positioned in the frames *4* and *7* (Figure 2-1 and Figure 2-6). Even if it is not the optimal solution to obtain a good seismic behavior, this choice is made in order to identify a portion of structure that is free from steel braces which can be hence simply reproduced in laboratory. Moreover, this make the sub-structure more representative of a general case.

In the *Symmetric* structure the two bays in *Y* direction have the same dimension of 5.7 *m*. Figure 2-1, Figure 2-2 and Figure 2-3 reports the typical floor framing plan and the frame elevation respectively in *X* and *Y* direction. The characteristics of the floor framing plan are the same at all the stories. In the *Asymmetric* structure the two bays in *Y* direction have different dimensions of 7.125 *m* and 4.275 *m*. Figure 2-6, Figure 2-7 and Figure 2-8 reports the typical floor framing plan and the frame elevation respectively in *X* and *Y* direction. The characteristics of the floor framing plan are the same at all the stories.

The cover of the rebars is equal to 20 *mm*. Wires of $\phi 10/150 \times 150$ *mm* are uniformly distributed in the top and bottom side of the slab. Moreover, several additional reinforcements are required in several zones. Figure 2-4 and Figure 2-5 illustrate the distribution of the reinforcements in the slab respectively in the upper side and in the lower side of the *Symmetric* structure. While, Figure 2-9 and Figure 2-10 illustrate the distribution of the reinforcements in the slab respectively in the upper side and in the lower side of the *Asymmetric* structure.

MOMENT RESISTING STEEL-CONCRETE COMPOSITE FRAMES UNDER THE COLUMN LOSS SCENARIO:
DESIGN OF THE REFERENCE FRAMES AND OF THE FULL-SCALE SUB-FRAME SPECIMENS

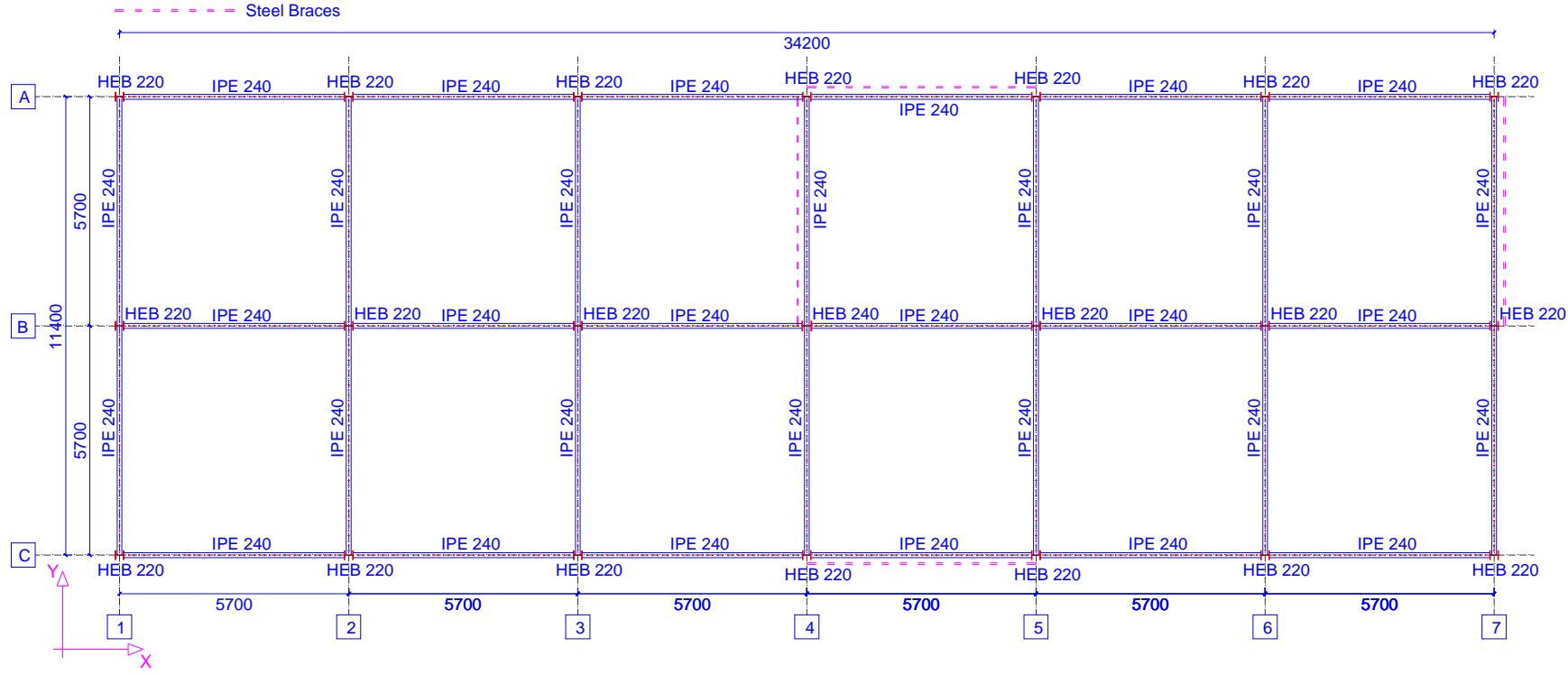


Figure 2-1. Floor Framing Plan – Symmetric Configuration (length unit mm)

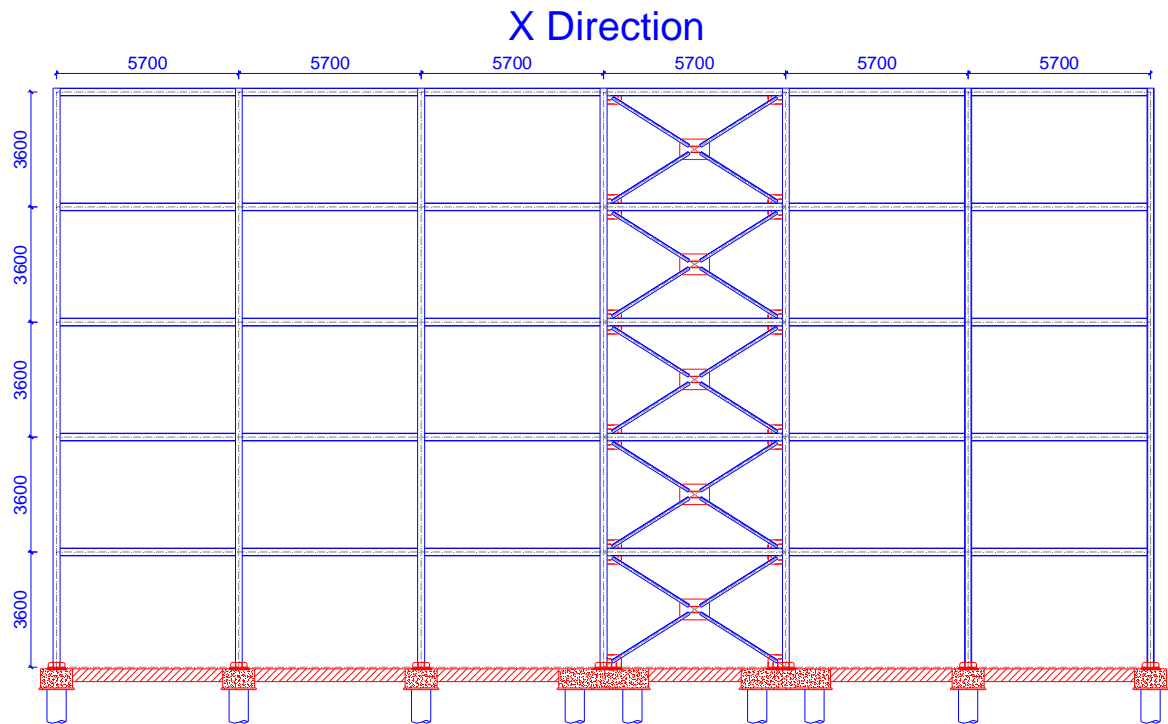


Figure 2-2. Frame Elevation – X direction – Symmetric Configuration (length unit mm)

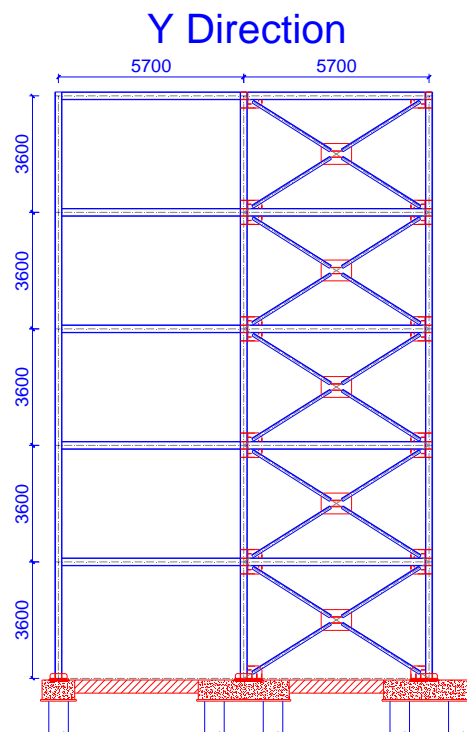


Figure 2-3. Frame Elevation – Y direction – Symmetric Configuration (length unit mm)

**MOMENT RESISTING STEEL-CONCRETE COMPOSITE FRAMES UNDER THE COLUMN LOSS SCENARIO:
DESIGN OF THE REFERENCE FRAMES AND OF THE FULL-SCALE SUB-FRAME SPECIMENS**

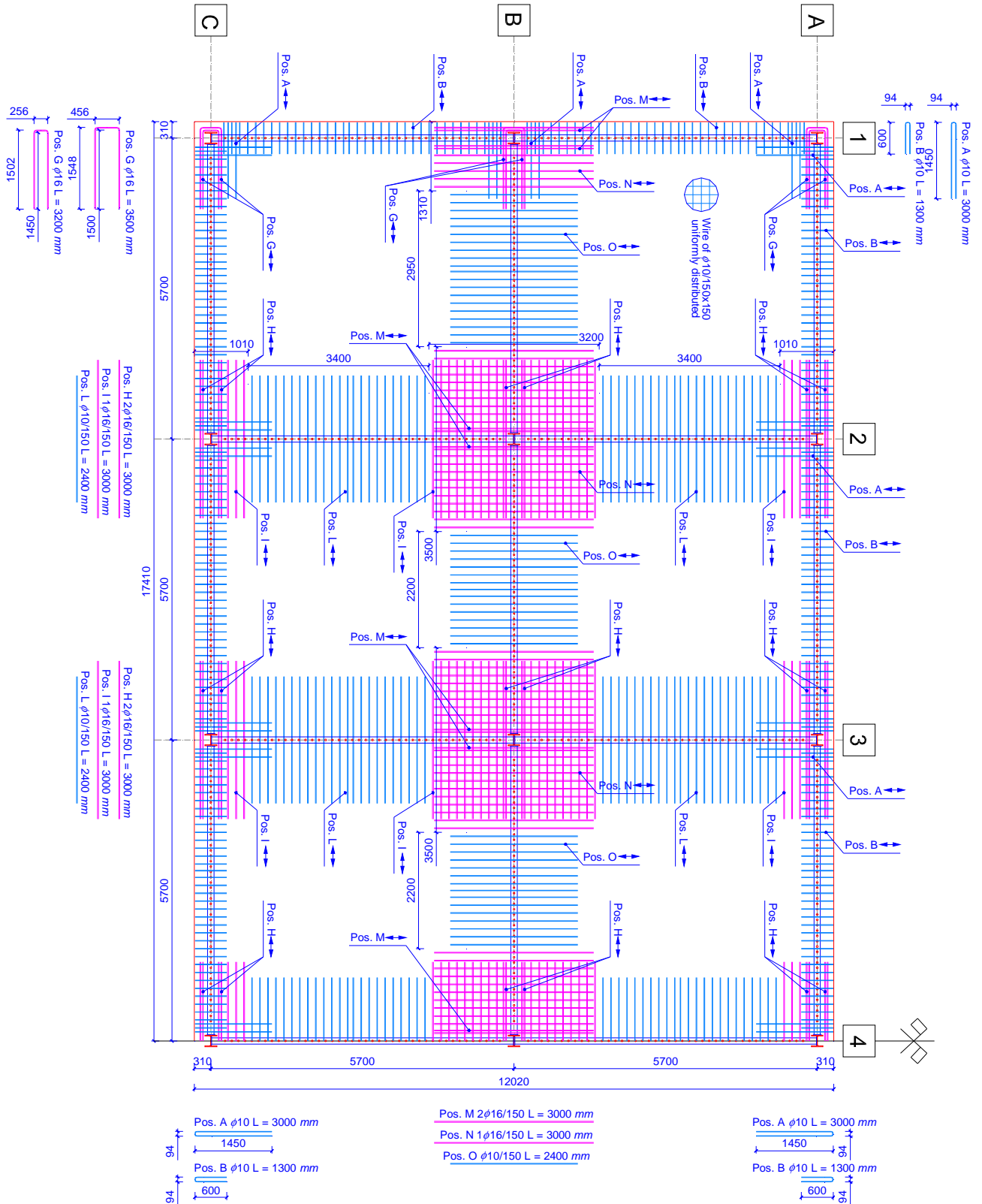


Figure 2-4. Slab Rebars - Upper Side – Symmetric Configuration (length unit mm)

**MOMENT RESISTING STEEL-CONCRETE COMPOSITE FRAMES UNDER THE COLUMN LOSS SCENARIO:
DESIGN OF THE REFERENCE FRAMES AND OF THE FULL-SCALE SUB-FRAME SPECIMENS**

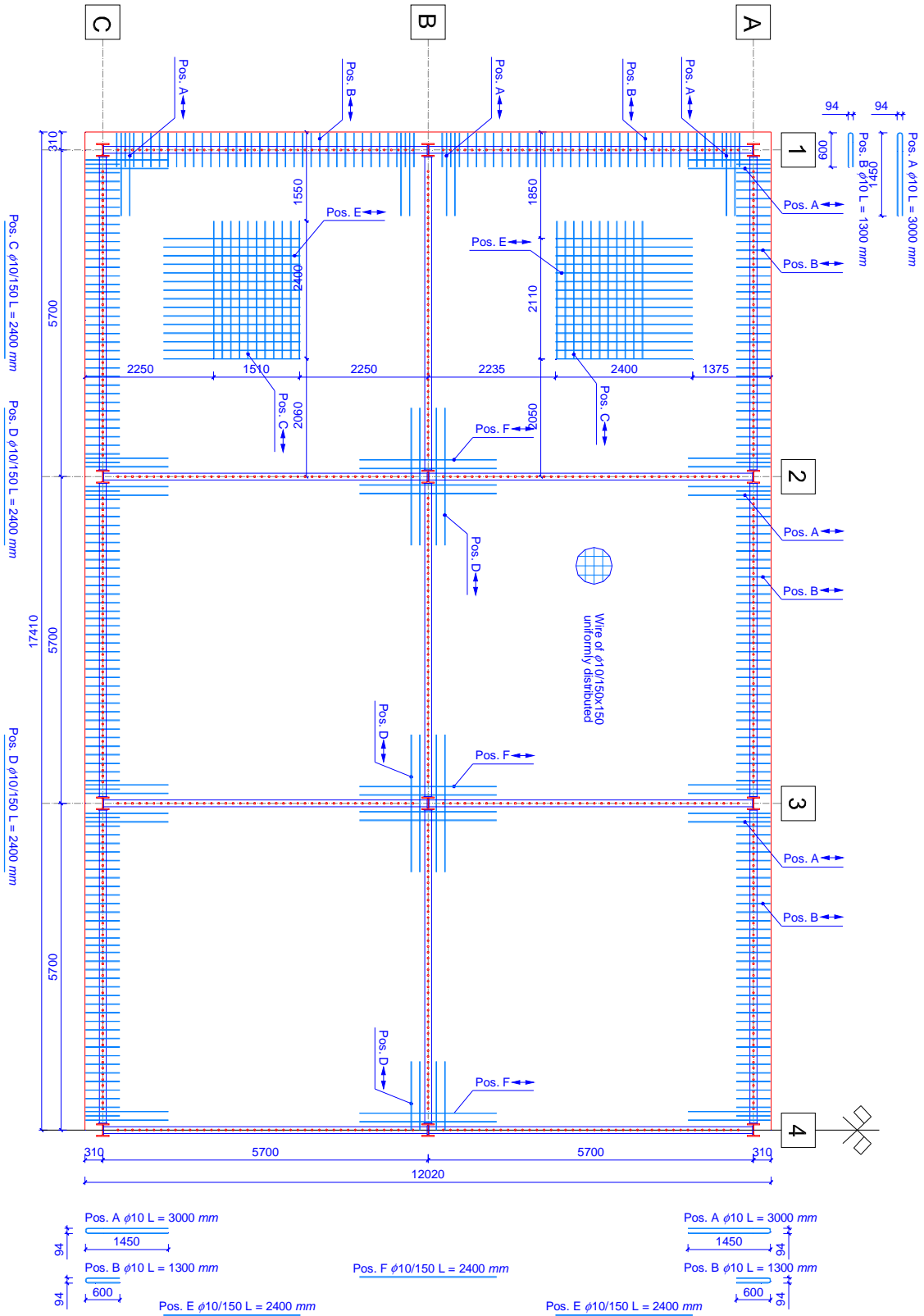


Figure 2-5. Slab Rebars - Lower Side – Symmetric Configuration (length unit mm)

MOMENT RESISTING STEEL-CONCRETE COMPOSITE FRAMES UNDER THE COLUMN LOSS SCENARIO:
DESIGN OF THE REFERENCE FRAMES AND OF THE FULL-SCALE SUB-FRAME SPECIMENS

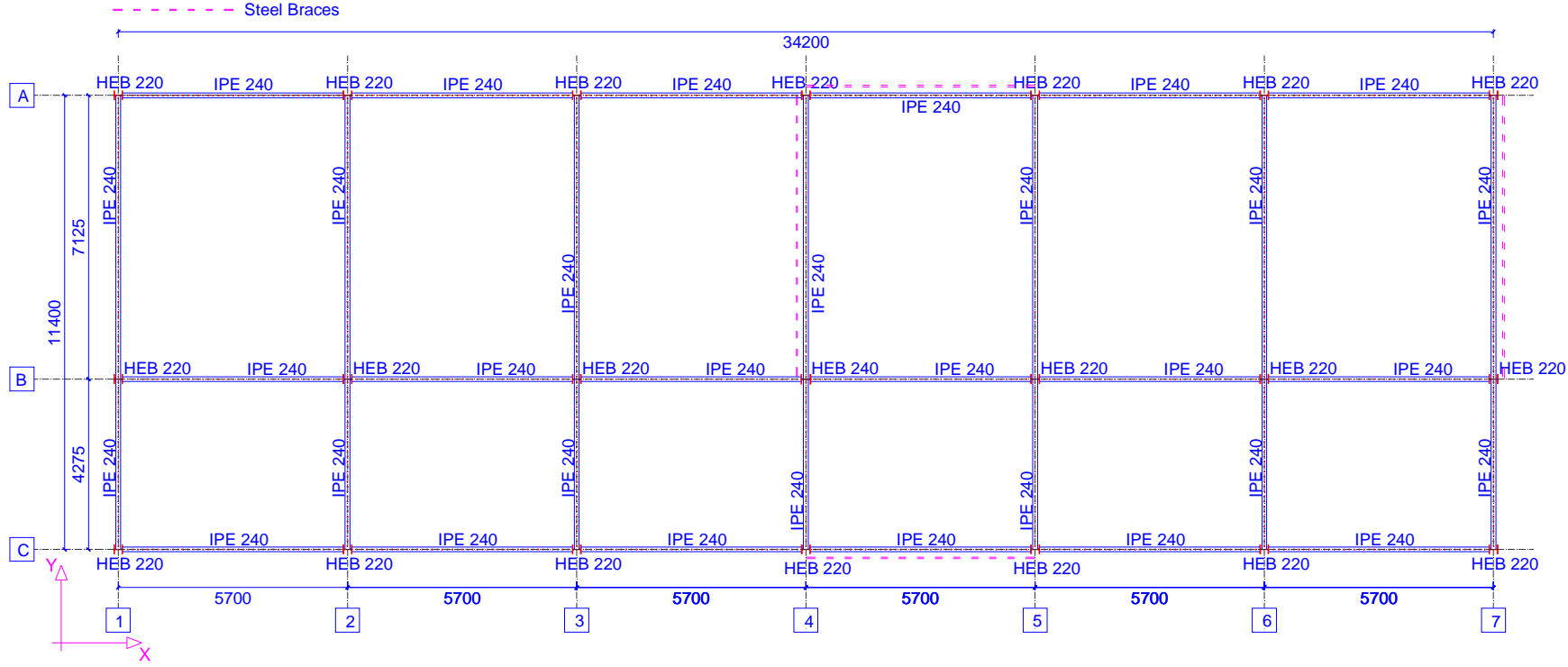


Figure 2-6. Floor Framing Plan – Asymmetric Configuration (length unit mm)

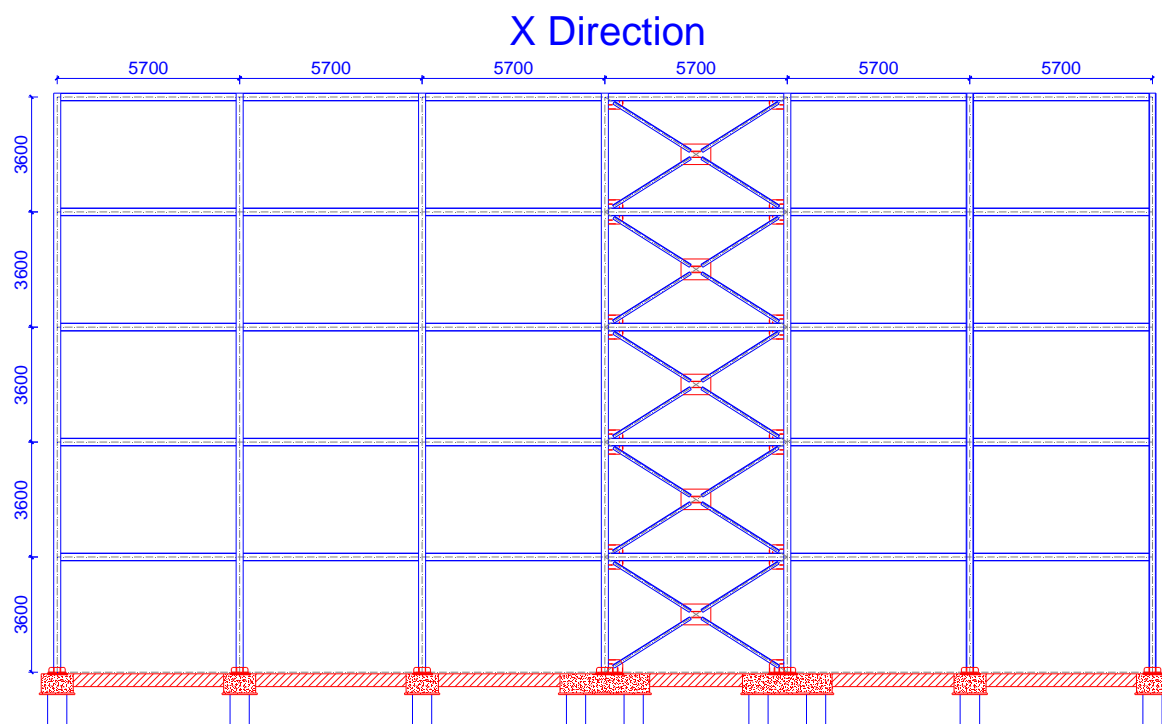


Figure 2-7. Frame Elevation – X direction – Asymmetric Configuration (length unit mm)

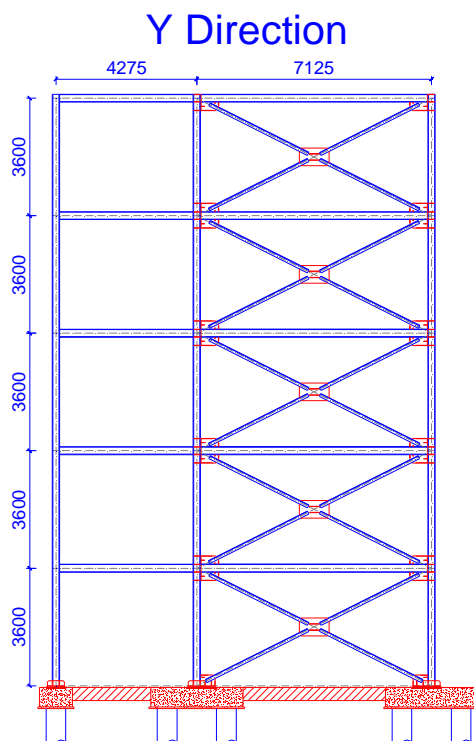


Figure 2-8. Frame Elevation – Y direction – Asymmetric Configuration (length unit mm)

**MOMENT RESISTING STEEL-CONCRETE COMPOSITE FRAMES UNDER THE COLUMN LOSS SCENARIO:
DESIGN OF THE REFERENCE FRAMES AND OF THE FULL-SCALE SUB-FRAME SPECIMENS**

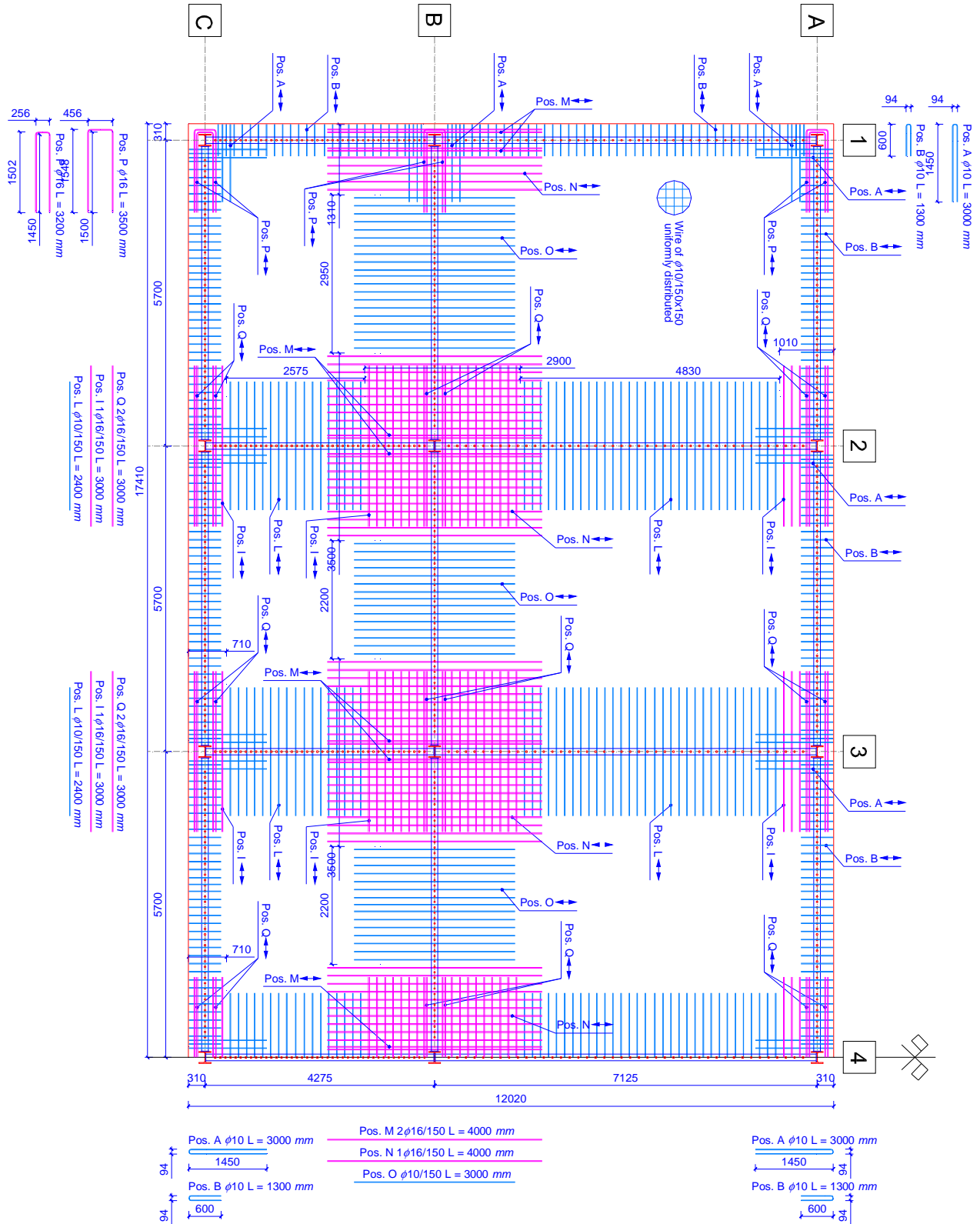


Figure 2-9. Slab Rebars - Upper Side – Asymmetric Configuration (length unit mm)

**MOMENT RESISTING STEEL-CONCRETE COMPOSITE FRAMES UNDER THE COLUMN LOSS SCENARIO:
DESIGN OF THE REFERENCE FRAMES AND OF THE FULL-SCALE SUB-FRAME SPECIMENS**

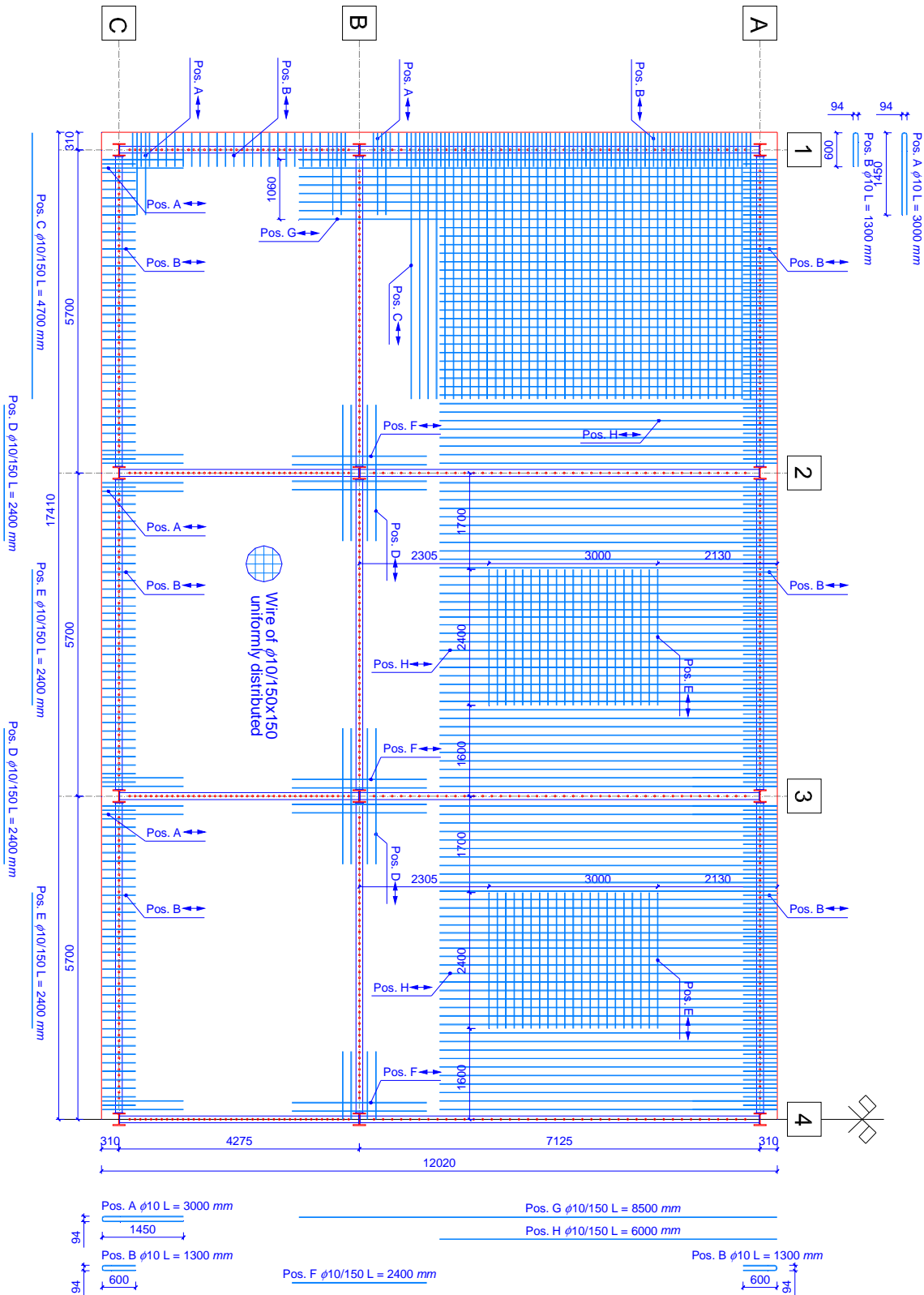


Figure 2-10. Slab Rebars - Lower Side – Asymmetric Configuration (length unit mm)

2.2 Finite Element Model

In order to design the case study structures, the Finite Element Model of the 3-D frame has been developed by using the SAP 2000 program [1]. The frame is fixed at the base in both the directions and employs steel braces modeled as elastic elements to resist to the horizontal forces. The model employs the elastic 2-D elements “*Frame*” to model the behavior of beams and columns and elastic “*Shell*” elements to model the behavior of the slab. The slab is rigidly connected to the beams in order to simulate the behavior of the complete interaction given by the shear connection. The connection between beams and columns is modeled by a pinned connection in the *Y* direction where the beams are connected to the web of the column, differently, in the *X* direction the beam-column connections are characterized by an adequate stiffness calculated by following the instructions of EN 1993-1-8 [2].

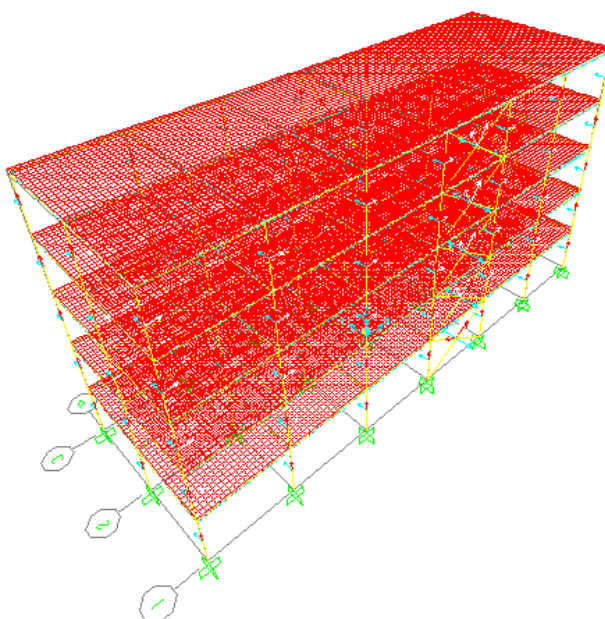


Figure 2-11. 3-D Finite Element Model – Symmetric Configuration

2.3 Materials

The materials used for the design of the structures are listed below. There is no difference between the materials used in the *Symmetric* and in the *Asymmetric* structure.

Concrete – C30/37 (EN 1992-1-1 §2.4.2.4 and EN 1992-1-1 Table 2.1N [3])

$$f_{ck} = 30 \text{ MPa};$$

$$R_{ck} = 37 \text{ MPa};$$

$$f_{cm} = 38 \text{ MPa};$$

$$f_{ctm} = 2.896 \text{ MPa};$$

$$E_{cm} = 32.836 \text{ GPa};$$

$$\gamma_c = 1.5 \text{ for persistent and transient design situations};$$

$$\gamma_c = 1.2 \text{ for accidental design situations};$$

Rebars – B450C	(EN 1992-1-1 §2.4.2.4 and EN 1992-1-1 Table 2.1N [3]) $f_{yk} = 450 \text{ MPa};$ $f_{tk} = 540 \text{ MPa};$ $E_s = 210 \text{ GPa};$ $\gamma_s = 1.15$ for persistent and transient design situations; $\gamma_s = 1.00$ for accidental design situations;
Steel – S355	(EN 1993-1-1 Table 3.1 and EN 1993-1-1 §6.1 [4]) $f_y = 355 \text{ MPa};$ $f_u = 510 \text{ MPa};$ $E_s = 210 \text{ GPa};$ $\gamma_{M0} = 1.00$ for resistance of cross-sections; $\gamma_{M1} = 1.00$ for resistance of members to instability; $\gamma_{M2} = 1.25$ for resistance of cross-section in tension to fracture;
Bolts – Class 10.9	(EN 1993-1-8 Table 3.1 [2] and EN 1992-1-1 Table 2.1N [3]) $f_{yb} = 900 \text{ MPa};$ $f_{ub} = 1000 \text{ MPa};$ $\gamma_{M2} = 1.25$ for resistance of bolts;

2.4 Actions

The actions considered for the design of the structures are reported in the following sections. There is no difference between the actions of the *Symmetric* and of the *Asymmetric* structure.

2.4.1 Self-Weight

- Slab $G_{k,slab} = 3.75 \text{ kN/m}^2$
- Beam IPE 240 $G_{k,beam} = 0.301 \text{ kN/m}$
- Column HEB 220 $G_{k,col} = 0.701 \text{ kN/m}$
- Finishes $G_{k,2} = 2.00 \text{ kN/m}^2$

2.4.2 Variable Action

- Imposed load, Category B $Q_k = 3.00 \text{ kN/m}^2$
- Movable partition $G_{k,mp} = 1.20 \text{ kN/m}^2$

2.4.3 Wind Load

The wind load is evaluated by following the EN 1991-1-4 §4.3.3 [5].

- Wind on the long side (Y direction)

$$q_p(z_e) = q_p(z_i) = 0.823 \frac{kN}{m^2}$$

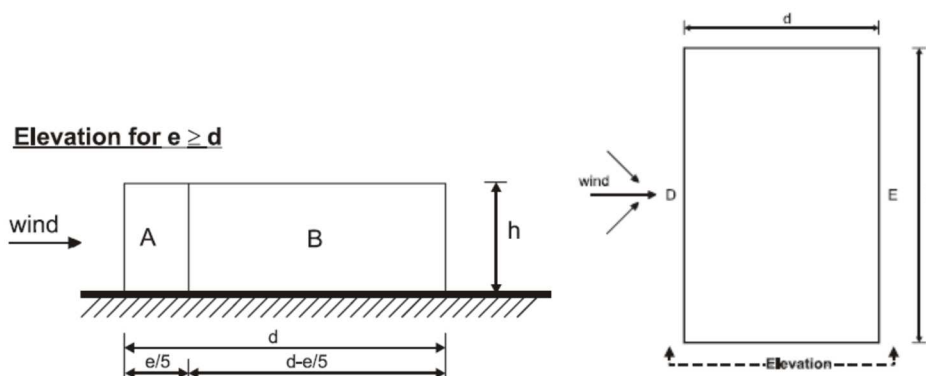


Figure 2-12. Key for vertical walls

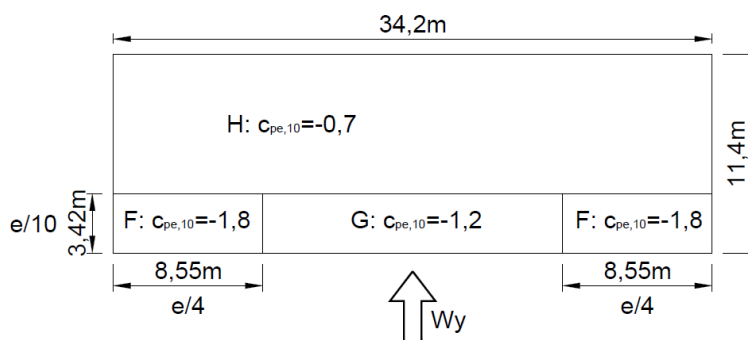


Figure 2-13. Key for flat roof with wind in Y direction

Table 2-1. Wind pressures for normal design situations on the long side (Y direction)

Wind pressure [kN/m^2]							
zone	Vertical walls				Roof		
	A	B	D	E	F	G	H
c_{pe}	-1.2	-0.8	0.8	-0.529	-1.8	-1.2	-0.7
$c_{pi} = +0,2$	-0.974	-0.704	0.375	-0.521	-1.379	-0.974	-0.637
$c_{pi} = -0,3$	-0.562	-0.293	0.787	-0.110	-0.967	-0.562	-0.225

Table 2-2. Wind pressures for accidental design situations on the long side (Y direction)

Wind pressure [kN/m^2]							
zone	Vertical walls				Roof		
	A	B	D	E	F	G	H
c_{pe}	-1.2	-0.8	0.8	-0.529	-1.8	-1.2	-0.7
$c_{pi} = +0,72$	-1.402	-1.132	-0.053	-0.949	-1.807	-1.402	-1.065
$c_{pi} = -1,08$	0.080	0.349	1.429	0.532	-0.325	0.080	0.417

- Wind on the short side (X direction)

$$q_p(z_e) = q_p(z_i) = 0.701 \frac{kN}{m^2} \quad \text{for} \quad 0 m < z < 11.4 m$$

$$q_p(z_e) = q_p(z_i) = 0.823 \frac{kN}{m^2} \quad \text{for} \quad 11.4 m < z < 18 m$$

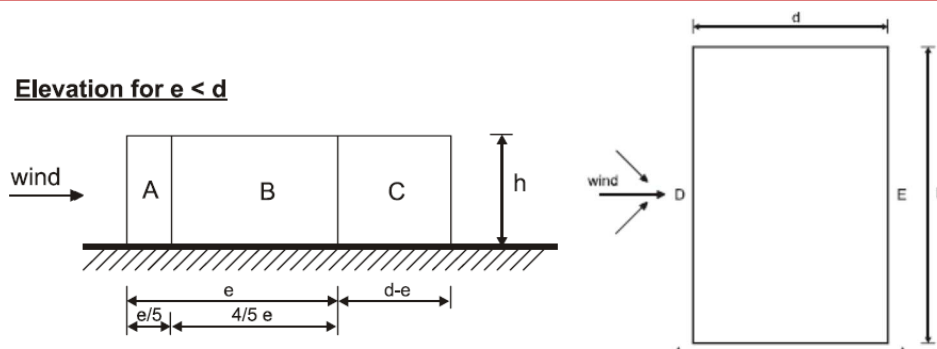


Figure 2-14. Key for vertical walls

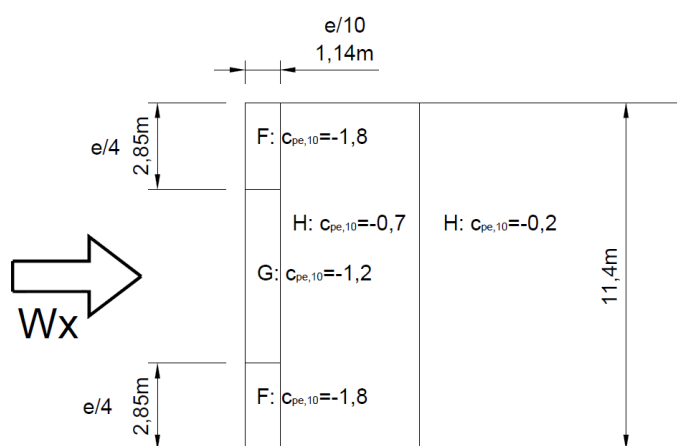


Figure 2-15. Key for flat roof with wind in X direction

Table 2-3. Wind pressures for normal design situations on the short side (X direction)

Wind pressure [kN/m^2]										
zone		Vertical walls					Roof			
c_{pe}		A	B	C	D	E	F	G	H	I
$c_{pi} = +0,2$	$0 \leq z \leq 11,4 m$	-0,872	-0,628	-0,445	0,309	-0,368	-1,238	-0,872	-0,567	-0,262
	$11,4 < z \leq 18 m$	-1,024	-0,738	-0,523	0,363	-0,432	-1,454	-1,024	-0,666	-0,308
$c_{pi} = -0,3$	$0 \leq z \leq 11,4 m$	-0,522	-0,278	-0,095	0,660	-0,018	-0,888	-0,522	-0,217	0,088
	$11,4 < z \leq 18 m$	-0,612	-0,326	-0,111	0,775	-0,021	-1,042	-0,612	-0,254	0,104

Table 2-4. Wind pressures for accidental design situations on the short side (X direction)

Wind pressure [kN/m^2]										
zone		Vertical walls					Roof			
c_{pe}		A	B	C	D	E	F	G	H	I
$c_{pi} = +0,72$	$0 \leq z \leq 11,4 m$	-1,237	-0,993	-0,810	-0,055	-0,733	-1,603	-1,237	-0,932	-0,627
	$11,4 < z \leq 18 m$	-1,452	-1,166	-0,951	0,065	-0,860	-1,882	-1,452	-1,094	-0,736
$c_{pi} = -1,08$	$0 \leq z \leq 11,4 m$	0,025	0,269	0,452	1,207	0,529	-0,341	0,025	0,330	0,635
	$11,4 < z \leq 18 m$	0,030	0,316	0,531	1,417	0,621	-0,400	0,030	0,388	0,746

2.4.4 Snow Load

The snow loads on the roof are obtained by following the instruction of EN 1991-1-3 §5 [6].

- Persistent/Transient design situations $s = 1.2kN/m^2$
- Accidental design situations $s = 2.4kN/m^2$

2.5 Load Combinations

The load combinations are defined in accordance with the EN 1990 [7]. In all the combinations, the *self-weight* is uniformly distributed overall the structure. Differently, the *variable* actions are distributed by following different load distributions in order to maximize the stresses in all the structural elements. Figure 2-16 shows all the load combination schemes considered for the typical floor framing plan for the variable loads for both the *Symmetric* and *Asymmetric* structures.

The symbols used in Figure 2-16 are:

- q_1 Variable loads distribution to maximize the forces on the slab;
- q_2 Variable loads distribution to maximize the forces on the slab;
- q_{1v} Variable loads distribution to maximize the forces on the beams in *X* direction;
- q_{2v} Variable loads distribution to maximize the forces on the beams in *X* direction;
- q_{1o} Variable loads distribution to maximize the forces on the beams in *Y* direction;
- q_{2o} Variable loads distribution to maximize the forces on the beams in *Y* direction;
- $q_1 + q_2$ Variable loads distribution to maximize the forces on the supports;

All the considered variable loads are listed in the follow:

- q Imposed load;
- q_s Snow load;
- q_{mp} Mobile partitions load;
- $W_{x_cpi+0.2}$ Wind in *X* direction with coefficient $c_{pi} = + 0.2$;
- $W_{x_cpi-0.3}$ Wind in *X* direction with coefficient $c_{pi} = - 0.3$;
- $W_{y_cpi+0.2}$ Wind in *Y* direction with coefficient $c_{pi} = + 0.2$;
- $W_{y_cpi-0.3}$ Wind in *Y* direction with coefficient $c_{pi} = - 0.3$.

Maximization of loads

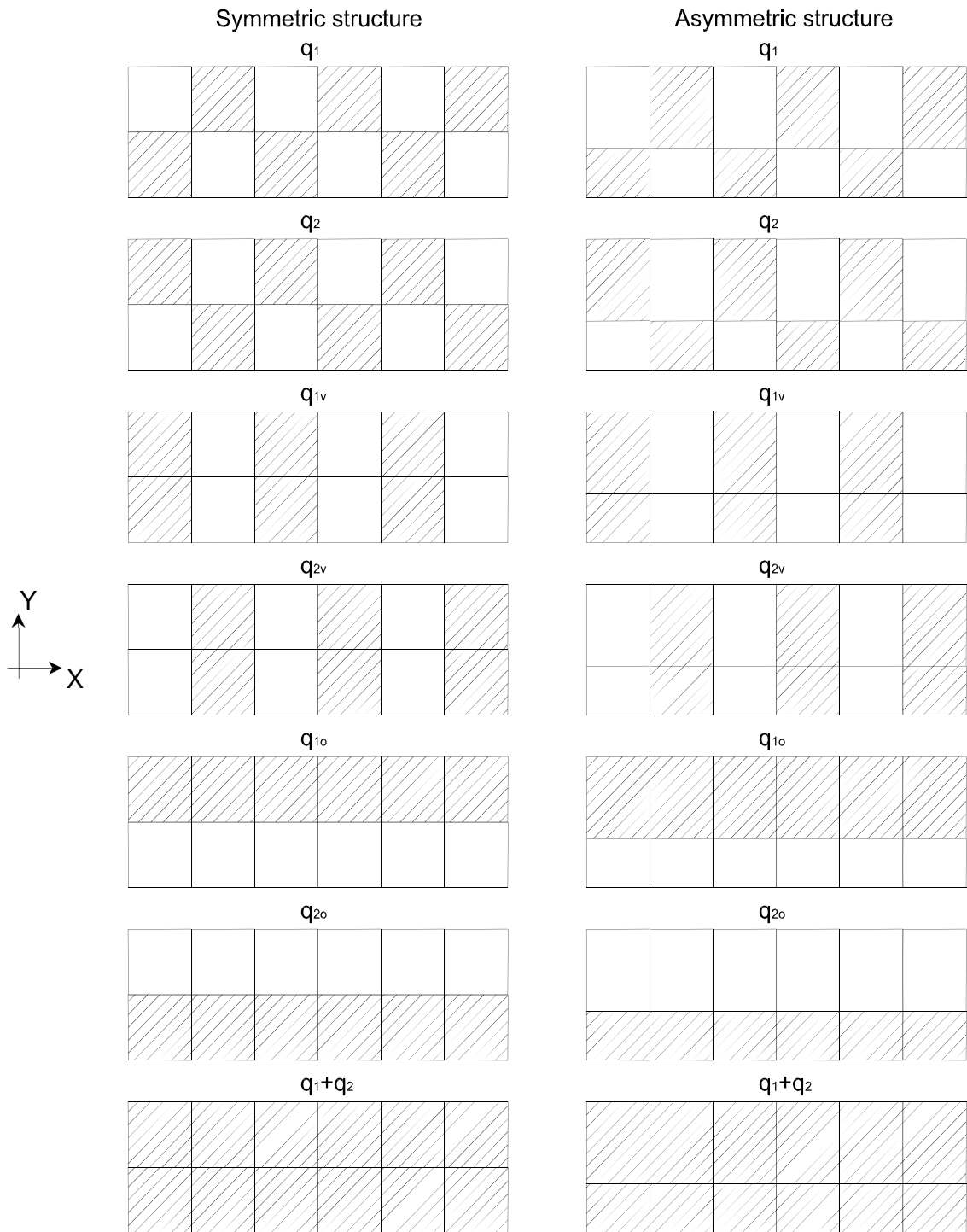


Figure 2-16. Load Combination Schemes on the Typical Floor Framing Plan

The load combination schemes on the *Symmetric* structure for the variable loads in the transversal (Y direction) and longitudinal (X direction) frames are reported in the follow (Figure 2-17 to Figure 2-20).

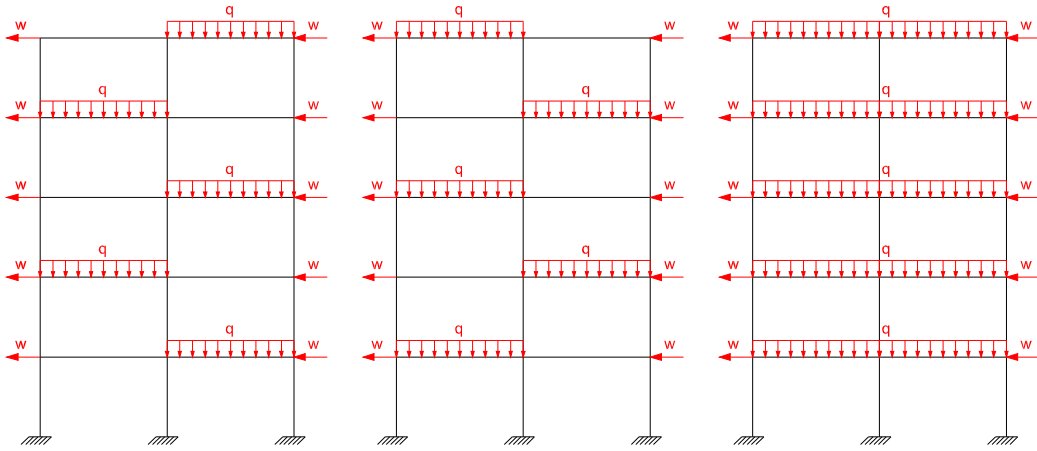


Figure 2-17. Load Combination Schemes on the Frame in Y direction

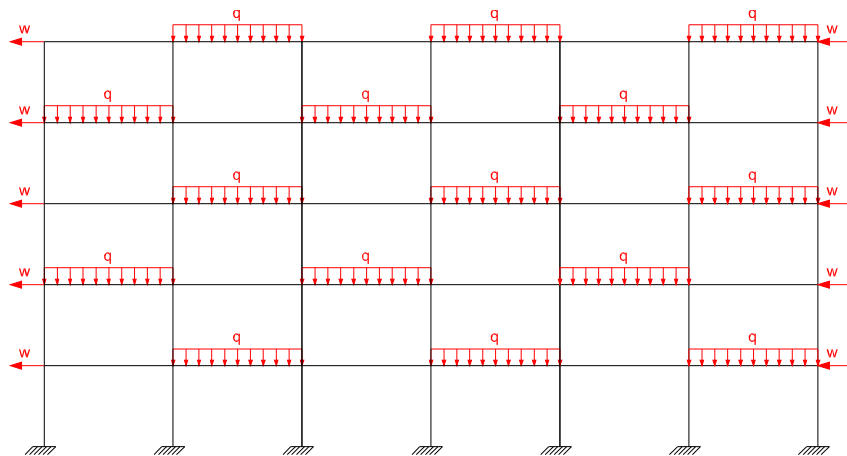


Figure 2-18. Load Combination Schemes on the Frame in X direction

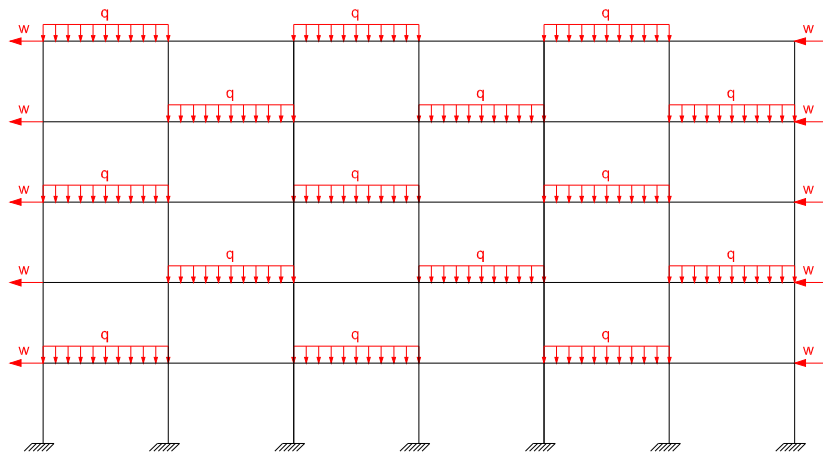


Figure 2-19. Load Combination Schemes on the Frame in X direction

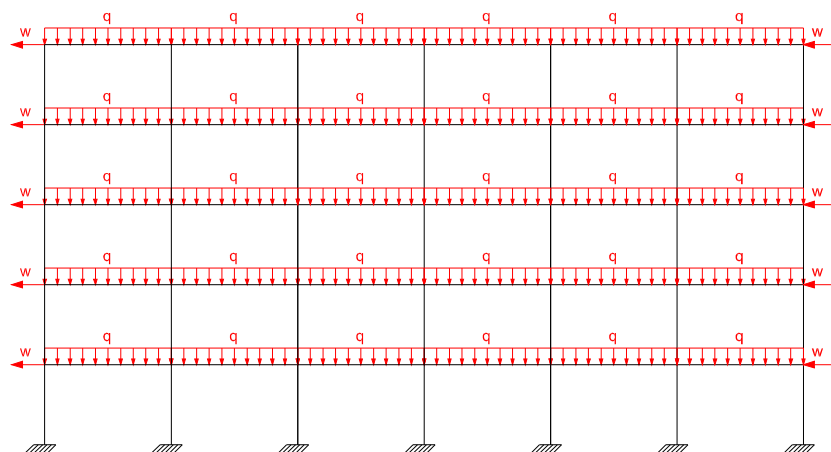


Figure 2-20. Load Combination Schemes on the Frame in X direction

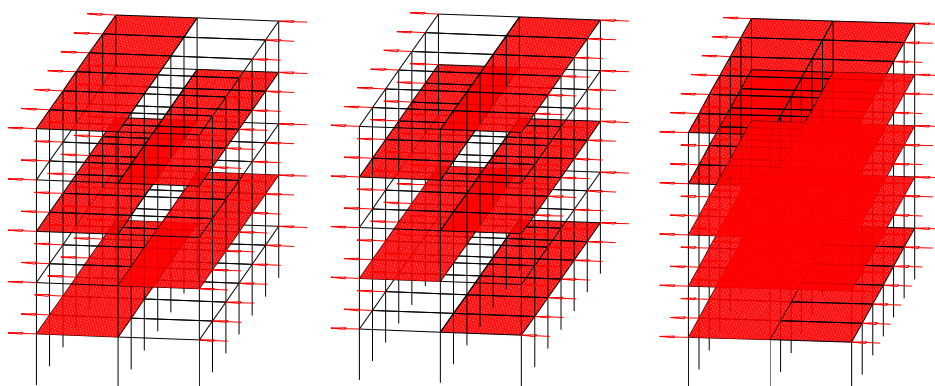


Figure 2-21. 3-D Load Combination Schemes on the Frame in Y direction

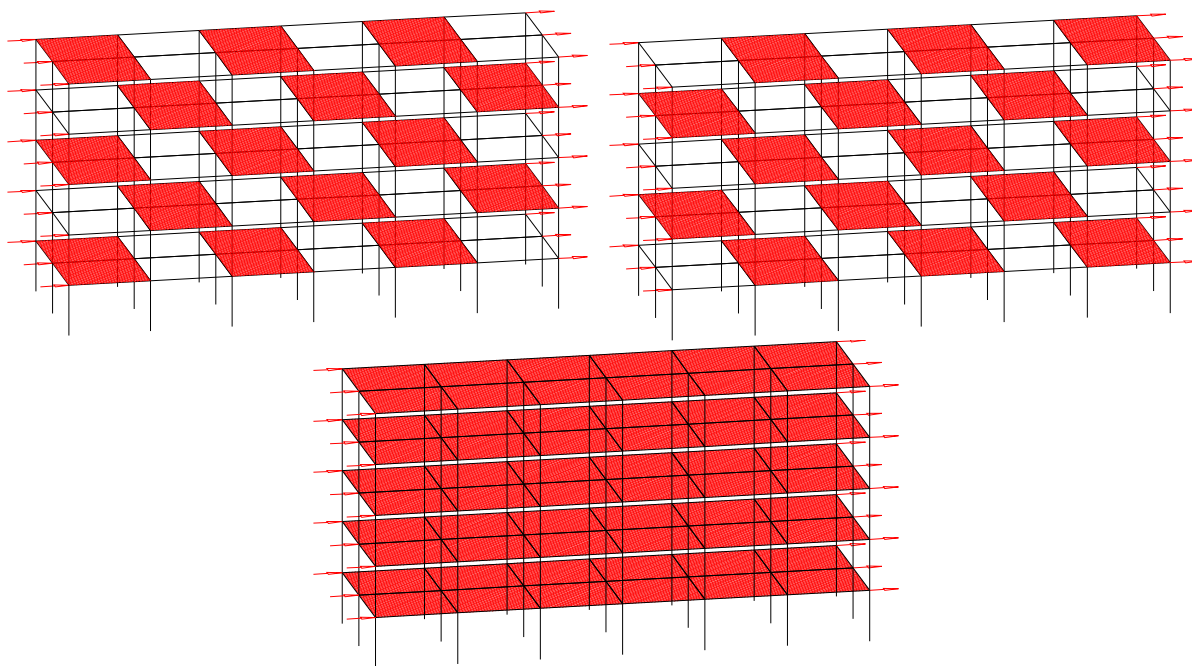


Figure 2-22. 3-D Load Combination Schemes on the Frame in X direction

The load combination schemes on the *Symmetric* frames for the variable loads in the transversal (Y direction) and longitudinal (X direction) frames are reported in the follow (Figure 2-23 to Figure 2-26).

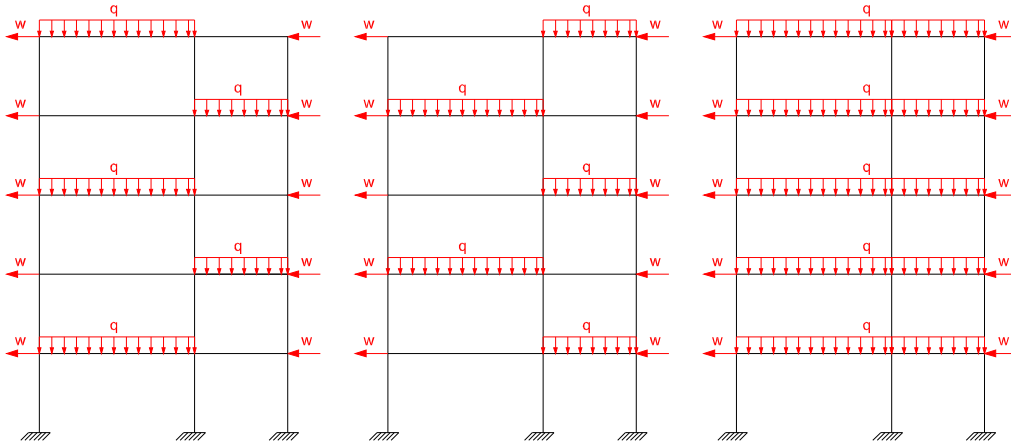


Figure 2-23. Load Combination Schemes on the Frame in Y direction

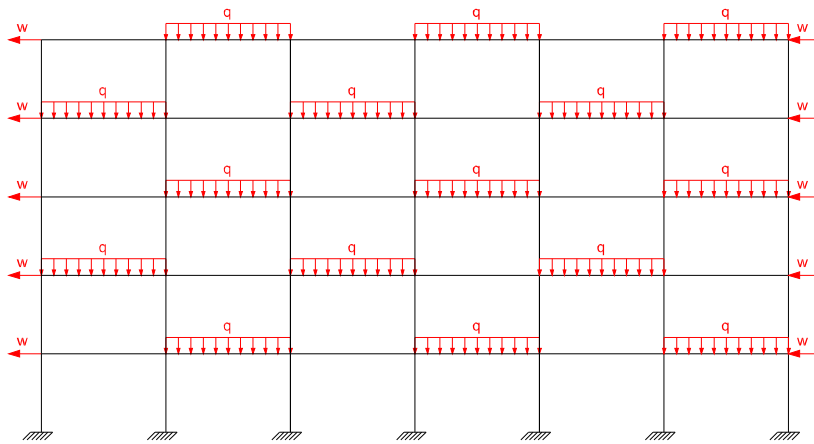


Figure 2-24. Load Combination Schemes on the Frame in X direction

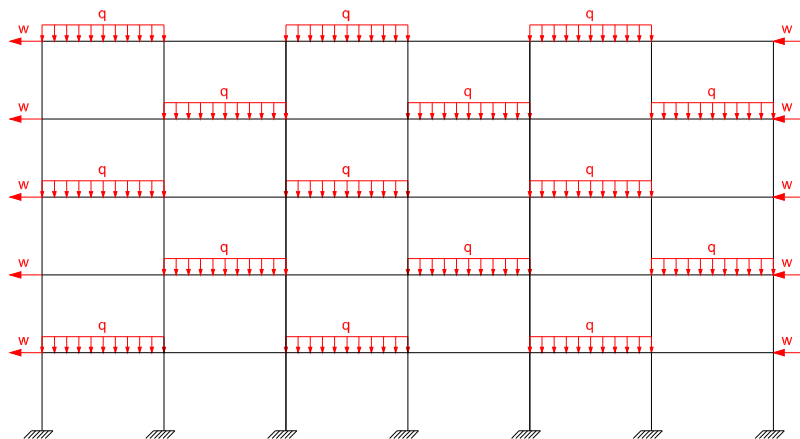


Figure 2-25. Load Combination Schemes on the Frame in X direction

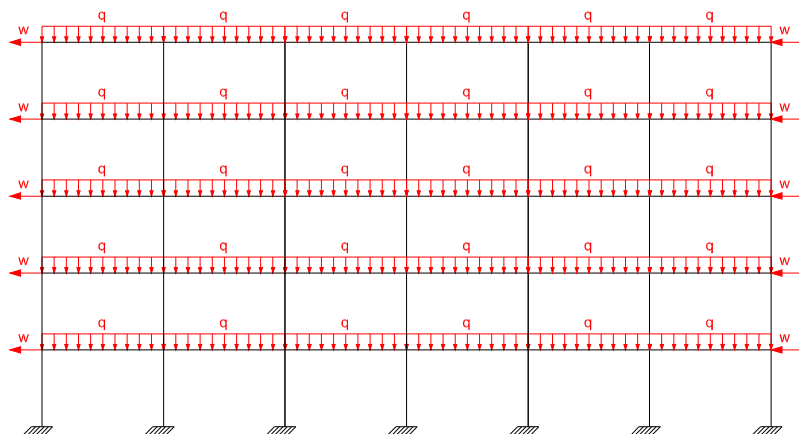


Figure 2-26. Load Combination Schemes on the Frame in X direction

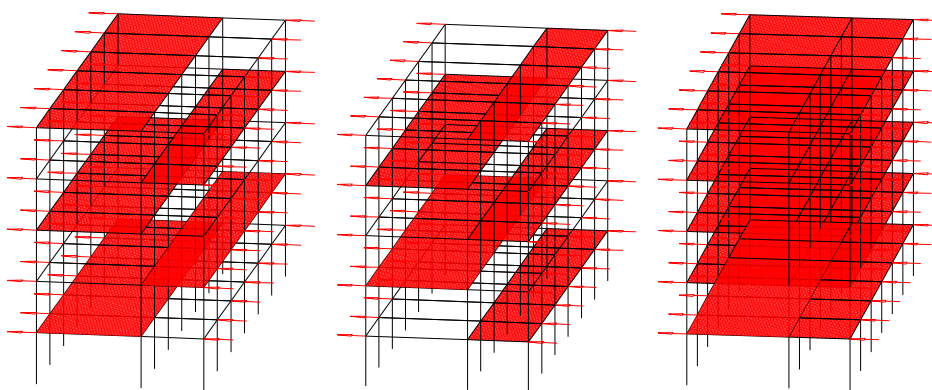


Figure 2-27. 3-D Load Combination Schemes on the Frame in Y direction

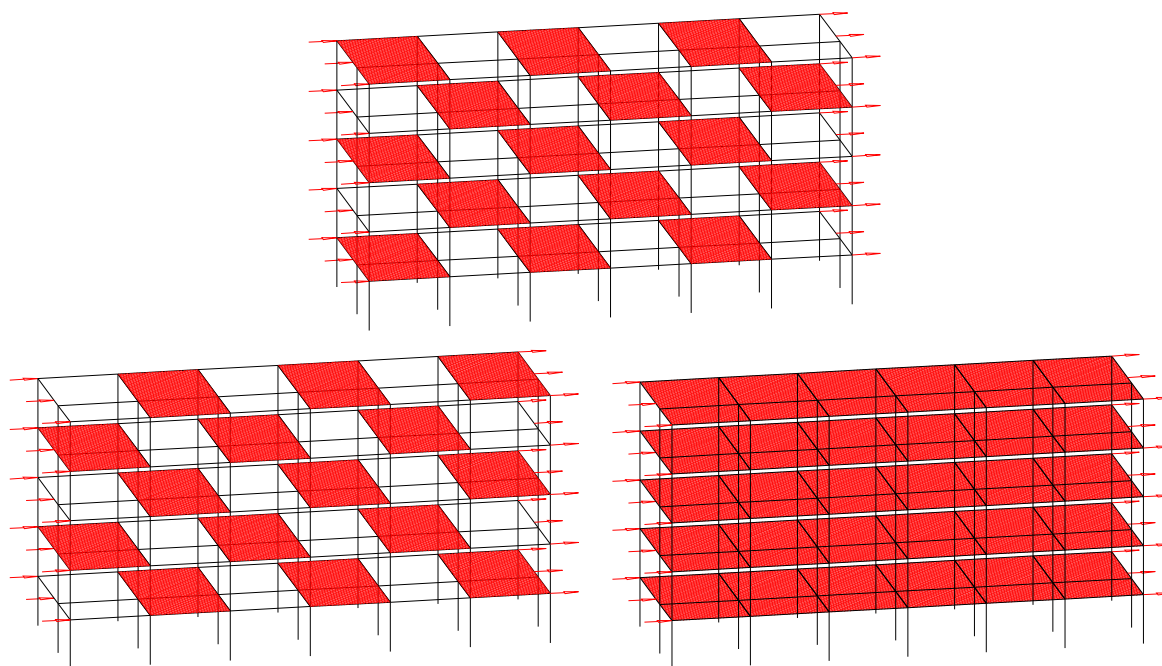


Figure 2-28. 3-D Load Combination Schemes on the Frame in X direction

2.5.1 Ultimate Limit State - ULS

The symbols defined in Figure 2-16 (q_1 , q_2 , q_{1o} , q_{2o} , q_{1v} and q_{2v}) are used in the following tables to report the Load Combinations considered in the study.

The load combinations used for the *Ultimate Limit State* (ULS) are:

$$\sum_{j \geq 1} \gamma_{G,j} G_{k,j} + \gamma_p P + \gamma_{Q,1} Q_{k,1} + \sum_{i > 1} \gamma_{Q,i} \psi_{0,i} Q_{k,i} \quad (2.1)$$

Table 2-5. Load Combinations for Ultimate Limit State

$\gamma_{G,1}$	G_1	$+ \gamma_{G,2} G_2 + \gamma_{Q,1} Q_1$	$+ \gamma_{Q,2} \psi_{0,2} Q_2$	$+ \gamma_{Q,3} \psi_{0,3} Q_3$	$+ \gamma_{Q,4} \psi_{0,4} Q_4$	
1,35	DEAD	+ 1,35 g_2 + 1,5	q_1	+ 1,5 0,7	$w_{y_cpi+0,2}$	q_{1s}
1,35	DEAD	+ 1,35 g_2 + 1,5	q_1	+ 1,5 0,7	$w_{y_cpi-0,3}$	q_{1s}
1,35	DEAD	+ 1,35 g_2 + 1,5	q_2	+ 1,5 0,7	$w_{y_cpi+0,2}$	q_{2s}
1,35	DEAD	+ 1,35 g_2 + 1,5	q_2	+ 1,5 0,7	$w_{y_cpi-0,3}$	q_{2s}
1,35	DEAD	+ 1,35 g_2 + 1,5	q_1+q_2	+ 1,5 0,7	$w_{y_cpi+0,2}$	$q_{1s}+q_{2s}$
1,35	DEAD	+ 1,35 g_2 + 1,5	q_1+q_2	+ 1,5 0,7	$w_{y_cpi-0,3}$	$q_{1s}+q_{2s}$
1,35	DEAD	+ 1,35 g_2 + 1,5	q_1	+ 1,5 0,7	$w_{x_cpi+0,2}$	q_{1s}
1,35	DEAD	+ 1,35 g_2 + 1,5	q_1	+ 1,5 0,7	$w_{x_cpi-0,3}$	q_{1s}
1,35	DEAD	+ 1,35 g_2 + 1,5	q_2	+ 1,5 0,7	$w_{x_cpi+0,2}$	q_{2s}
1,35	DEAD	+ 1,35 g_2 + 1,5	q_2	+ 1,5 0,7	$w_{x_cpi-0,3}$	q_{2s}
1,35	DEAD	+ 1,35 g_2 + 1,5	q_1+q_2	+ 1,5 0,7	$w_{x_cpi+0,2}$	$q_{1s}+q_{2s}$
1,35	DEAD	+ 1,35 g_2 + 1,5	q_1+q_2	+ 1,5 0,7	$w_{x_cpi-0,3}$	$q_{1s}+q_{2s}$
1,35	DEAD	+ 1,35 g_2 + 1,5	q_{1o}	+ 1,5 0,7	$w_{y_cpi+0,2}$	q_{1so}
1,35	DEAD	+ 1,35 g_2 + 1,5	q_{1o}	+ 1,5 0,7	$w_{y_cpi-0,3}$	q_{1so}
1,35	DEAD	+ 1,35 g_2 + 1,5	q_{2o}	+ 1,5 0,7	$w_{y_cpi+0,2}$	q_{2so}
1,35	DEAD	+ 1,35 g_2 + 1,5	q_{2o}	+ 1,5 0,7	$w_{y_cpi-0,3}$	q_{2so}
1,35	DEAD	+ 1,35 g_2 + 1,5	q_{1o}	+ 1,5 0,7	$w_{x_cpi+0,2}$	q_{1so}
1,35	DEAD	+ 1,35 g_2 + 1,5	q_{1o}	+ 1,5 0,7	$w_{x_cpi-0,3}$	q_{1so}
1,35	DEAD	+ 1,35 g_2 + 1,5	q_{2o}	+ 1,5 0,7	$w_{x_cpi+0,2}$	q_{2so}
1,35	DEAD	+ 1,35 g_2 + 1,5	q_{2o}	+ 1,5 0,7	$w_{x_cpi-0,3}$	q_{2so}
1,35	DEAD	+ 1,35 g_2 + 1,5	q_{1v}	+ 1,5 0,7	$w_{y_cpi+0,2}$	q_{1sv}
1,35	DEAD	+ 1,35 g_2 + 1,5	q_{1v}	+ 1,5 0,7	$w_{y_cpi-0,3}$	q_{1sv}
1,35	DEAD	+ 1,35 g_2 + 1,5	q_{2v}	+ 1,5 0,7	$w_{y_cpi+0,2}$	q_{2sv}
1,35	DEAD	+ 1,35 g_2 + 1,5	q_{2v}	+ 1,5 0,7	$w_{y_cpi-0,3}$	q_{2sv}
1,35	DEAD	+ 1,35 g_2 + 1,5	q_{1v}	+ 1,5 0,7	$w_{x_cpi+0,2}$	q_{1sv}
1,35	DEAD	+ 1,35 g_2 + 1,5	q_{1v}	+ 1,5 0,7	$w_{x_cpi-0,3}$	q_{1sv}
1,35	DEAD	+ 1,35 g_2 + 1,5	q_{2v}	+ 1,5 0,7	$w_{x_cpi+0,2}$	q_{2sv}
1,35	DEAD	+ 1,35 g_2 + 1,5	q_{2v}	+ 1,5 0,7	$w_{x_cpi-0,3}$	q_{2sv}
1,35	DEAD	+ 1,35 g_2 + 1,5	$w_{y_cpi+0,2}$	+ 1,5 0,7	q_1	q_{1s}
1,35	DEAD	+ 1,35 g_2 + 1,5	$w_{y_cpi-0,3}$	+ 1,5 0,7	q_1	q_{1s}
1,35	DEAD	+ 1,35 g_2 + 1,5	$w_{y_cpi+0,2}$	+ 1,5 0,7	q_2	q_{2s}

**MOMENT RESISTING STEEL-CONCRETE COMPOSITE FRAMES UNDER THE COLUMN LOSS SCENARIO:
DESIGN OF THE REFERENCE FRAMES AND OF THE FULL-SCALE SUB-FRAME SPECIMENS**

1,35 DEAD + 1,35 g ₂ + 1,5 w _{y_cpi-0,3} + 1,5 0,7	q ₂	+ 1,5 0,7	q _{2s}	+ 1,5 0,7	Q _{2mp}
1,35 DEAD + 1,35 g ₂ + 1,5 w _{y_cpi+0,2} + 1,5 0,7	q ₁ +q ₂	+ 1,5 0,7	q _{1s} +q _{2s}	+ 1,5 0,7	Q _{1mp} +Q _{2mp}
1,35 DEAD + 1,35 g ₂ + 1,5 w _{y_cpi-0,3} + 1,5 0,7	q ₁ +q ₂	+ 1,5 0,7	q _{1s} +q _{2s}	+ 1,5 0,7	Q _{1mp} +Q _{2mp}
1,35 DEAD + 1,35 g ₂ + 1,5 w _{x_cpi+0,2} + 1,5 0,7	q ₁	+ 1,5 0,7	q _{1s}	+ 1,5 0,7	Q _{1mp}
1,35 DEAD + 1,35 g ₂ + 1,5 w _{x_cpi-0,3} + 1,5 0,7	q ₁	+ 1,5 0,7	q _{1s}	+ 1,5 0,7	Q _{1mp}
1,35 DEAD + 1,35 g ₂ + 1,5 w _{x_cpi+0,2} + 1,5 0,7	q ₂	+ 1,5 0,7	q _{2s}	+ 1,5 0,7	Q _{2mp}
1,35 DEAD + 1,35 g ₂ + 1,5 w _{x_cpi-0,3} + 1,5 0,7	q ₂	+ 1,5 0,7	q _{2s}	+ 1,5 0,7	Q _{2mp}
1,35 DEAD + 1,35 g ₂ + 1,5 w _{x_cpi+0,2} + 1,5 0,7	q ₁ +q ₂	+ 1,5 0,7	q _{1s} +q _{2s}	+ 1,5 0,7	Q _{1mp} +Q _{2mp}
1,35 DEAD + 1,35 g ₂ + 1,5 w _{x_cpi-0,3} + 1,5 0,7	q ₁ +q ₂	+ 1,5 0,7	q _{1s} +q _{2s}	+ 1,5 0,7	Q _{1mp} +Q _{2mp}
1,35 DEAD + 1,35 g ₂ + 1,5 w _{y_cpi+0,2} + 1,5 0,7	q _{1o}	+ 1,5 0,7	q _{1so}	+ 1,5 0,7	Q _{1mpo}
1,35 DEAD + 1,35 g ₂ + 1,5 w _{y_cpi-0,3} + 1,5 0,7	q _{1o}	+ 1,5 0,7	q _{1so}	+ 1,5 0,7	Q _{1mpo}
1,35 DEAD + 1,35 g ₂ + 1,5 w _{y_cpi+0,2} + 1,5 0,7	q _{2o}	+ 1,5 0,7	q _{2so}	+ 1,5 0,7	Q _{2mpo}
1,35 DEAD + 1,35 g ₂ + 1,5 w _{y_cpi-0,3} + 1,5 0,7	q _{2o}	+ 1,5 0,7	q _{2so}	+ 1,5 0,7	Q _{2mpo}
1,35 DEAD + 1,35 g ₂ + 1,5 w _{x_cpi+0,2} + 1,5 0,7	q _{1o}	+ 1,5 0,7	q _{1so}	+ 1,5 0,7	Q _{1mpo}
1,35 DEAD + 1,35 g ₂ + 1,5 w _{x_cpi-0,3} + 1,5 0,7	q _{1o}	+ 1,5 0,7	q _{1so}	+ 1,5 0,7	Q _{1mpo}
1,35 DEAD + 1,35 g ₂ + 1,5 w _{x_cpi+0,2} + 1,5 0,7	q _{2o}	+ 1,5 0,7	q _{2so}	+ 1,5 0,7	Q _{2mpo}
1,35 DEAD + 1,35 g ₂ + 1,5 w _{x_cpi-0,3} + 1,5 0,7	q _{2o}	+ 1,5 0,7	q _{2so}	+ 1,5 0,7	Q _{2mpo}
1,35 DEAD + 1,35 g ₂ + 1,5 w _{y_cpi+0,2} + 1,5 0,7	q _{1v}	+ 1,5 0,7	q _{1sv}	+ 1,5 0,7	Q _{1mpv}
1,35 DEAD + 1,35 g ₂ + 1,5 w _{y_cpi-0,3} + 1,5 0,7	q _{1v}	+ 1,5 0,7	q _{1sv}	+ 1,5 0,7	Q _{1mpv}
1,35 DEAD + 1,35 g ₂ + 1,5 w _{y_cpi+0,2} + 1,5 0,7	q _{2v}	+ 1,5 0,7	q _{2sv}	+ 1,5 0,7	Q _{2mpv}
1,35 DEAD + 1,35 g ₂ + 1,5 w _{y_cpi-0,3} + 1,5 0,7	q _{2v}	+ 1,5 0,7	q _{2sv}	+ 1,5 0,7	Q _{2mpv}
1,35 DEAD + 1,35 g ₂ + 1,5 w _{x_cpi+0,2} + 1,5 0,7	q _{1v}	+ 1,5 0,7	q _{1sv}	+ 1,5 0,7	Q _{1mpv}
1,35 DEAD + 1,35 g ₂ + 1,5 w _{x_cpi-0,3} + 1,5 0,7	q _{1v}	+ 1,5 0,7	q _{1sv}	+ 1,5 0,7	Q _{1mpv}
1,35 DEAD + 1,35 g ₂ + 1,5 w _{x_cpi+0,2} + 1,5 0,7	q _{2v}	+ 1,5 0,7	q _{2sv}	+ 1,5 0,7	Q _{2mpv}
1,35 DEAD + 1,35 g ₂ + 1,5 w _{x_cpi-0,3} + 1,5 0,7	q _{2v}	+ 1,5 0,7	q _{2sv}	+ 1,5 0,7	Q _{2mpv}
1,35 DEAD + 1,35 g ₂ + 1,5 q _{1s} + 1,5 0,7	q ₁	+ 1,5 0,7	w _{y_cpi+0,2}	+ 1,5 0,7	Q _{1mp}
1,35 DEAD + 1,35 g ₂ + 1,5 q _{1s} + 1,5 0,7	q ₁	+ 1,5 0,7	w _{y_cpi-0,3}	+ 1,5 0,7	Q _{1mp}
1,35 DEAD + 1,35 g ₂ + 1,5 q _{2s} + 1,5 0,7	q ₂	+ 1,5 0,7	w _{y_cpi+0,2}	+ 1,5 0,7	Q _{2mp}
1,35 DEAD + 1,35 g ₂ + 1,5 q _{2s} + 1,5 0,7	q ₂	+ 1,5 0,7	w _{y_cpi-0,3}	+ 1,5 0,7	Q _{2mp}
1,35 DEAD + 1,35 g ₂ + 1,5 q _{1s} +q _{2s} + 1,5 0,7	q ₁ +q ₂	+ 1,5 0,7	w _{y_cpi+0,2}	+ 1,5 0,7	Q _{1mp} + Q _{2mp}
1,35 DEAD + 1,35 g ₂ + 1,5 q _{1s} +q _{2s} + 1,5 0,7	q ₁ +q ₂	+ 1,5 0,7	w _{y_cpi-0,3}	+ 1,5 0,7	Q _{1mp} + Q _{2mp}
1,35 DEAD + 1,35 g ₂ + 1,5 q _{1s} + 1,5 0,7	q ₁	+ 1,5 0,7	w _{x_cpi+0,2}	+ 1,5 0,7	Q _{1mp}
1,35 DEAD + 1,35 g ₂ + 1,5 q _{1s} + 1,5 0,7	q ₁	+ 1,5 0,7	w _{x_cpi-0,3}	+ 1,5 0,7	Q _{1mp}
1,35 DEAD + 1,35 g ₂ + 1,5 q _{2s} + 1,5 0,7	q ₂	+ 1,5 0,7	w _{x_cpi+0,2}	+ 1,5 0,7	Q _{2mp}
1,35 DEAD + 1,35 g ₂ + 1,5 q _{2s} + 1,5 0,7	q ₂	+ 1,5 0,7	w _{x_cpi-0,3}	+ 1,5 0,7	Q _{2mp}
1,35 DEAD + 1,35 g ₂ + 1,5 q _{1s} +q _{2s} + 1,5 0,7	q ₁ +q ₂	+ 1,5 0,7	w _{x_cpi+0,2}	+ 1,5 0,7	Q _{1mp} + Q _{2mp}
1,35 DEAD + 1,35 g ₂ + 1,5 q _{1s} +q _{2s} + 1,5 0,7	q ₁ +q ₂	+ 1,5 0,7	w _{x_cpi-0,3}	+ 1,5 0,7	Q _{1mp} + Q _{2mp}
1,35 DEAD + 1,35 g ₂ + 1,5 q _{1so} + 1,5 0,7	q _{1o}	+ 1,5 0,7	w _{y_cpi+0,2}	+ 1,5 0,7	Q _{1mpo}
1,35 DEAD + 1,35 g ₂ + 1,5 q _{1so} + 1,5 0,7	q _{1o}	+ 1,5 0,7	w _{y_cpi-0,3}	+ 1,5 0,7	Q _{1mpo}
1,35 DEAD + 1,35 g ₂ + 1,5 q _{2so} + 1,5 0,7	q _{2o}	+ 1,5 0,7	w _{y_cpi+0,2}	+ 1,5 0,7	Q _{2mpo}
1,35 DEAD + 1,35 g ₂ + 1,5 q _{2so} + 1,5 0,7	q _{2o}	+ 1,5 0,7	w _{y_cpi-0,3}	+ 1,5 0,7	Q _{2mpo}
1,35 DEAD + 1,35 g ₂ + 1,5 q _{1so} + 1,5 0,7	q _{1o}	+ 1,5 0,7	w _{x_cpi+0,2}	+ 1,5 0,7	Q _{1mpo}
1,35 DEAD + 1,35 g ₂ + 1,5 q _{1so} + 1,5 0,7	q _{1o}	+ 1,5 0,7	w _{x_cpi-0,3}	+ 1,5 0,7	Q _{1mpo}
1,35 DEAD + 1,35 g ₂ + 1,5 q _{2so} + 1,5 0,7	q _{2o}	+ 1,5 0,7	w _{x_cpi+0,2}	+ 1,5 0,7	Q _{2mpo}

**MOMENT RESISTING STEEL-CONCRETE COMPOSITE FRAMES UNDER THE COLUMN LOSS SCENARIO:
DESIGN OF THE REFERENCE FRAMES AND OF THE FULL-SCALE SUB-FRAME SPECIMENS**

1,35 DEAD + 1,35 g ₂ + 1,5	q _{2so}	+ 1,5 0,7	q _{2o}	+ 1,5 0,7	w _{x_cpi-0,3}	+ 1,5 0,7	q _{2mpo}
1,35 DEAD + 1,35 g ₂ + 1,5	q _{1sv}	+ 1,5 0,7	q _{1v}	+ 1,5 0,7	w _{y_cpi+0,2}	+ 1,5 0,7	q _{1mpv}
1,35 DEAD + 1,35 g ₂ + 1,5	q _{1sv}	+ 1,5 0,7	q _{1v}	+ 1,5 0,7	w _{y_cpi-0,3}	+ 1,5 0,7	q _{1mpv}
1,35 DEAD + 1,35 g ₂ + 1,5	q _{2sv}	+ 1,5 0,7	q _{2v}	+ 1,5 0,7	w _{y_cpi+0,2}	+ 1,5 0,7	q _{2mpv}
1,35 DEAD + 1,35 g ₂ + 1,5	q _{2sv}	+ 1,5 0,7	q _{2v}	+ 1,5 0,7	w _{y_cpi-0,3}	+ 1,5 0,7	q _{2mpv}
1,35 DEAD + 1,35 g ₂ + 1,5	q _{1sv}	+ 1,5 0,7	q _{1v}	+ 1,5 0,7	w _{x_cpi+0,2}	+ 1,5 0,7	q _{1mpv}
1,35 DEAD + 1,35 g ₂ + 1,5	q _{1sv}	+ 1,5 0,7	q _{1v}	+ 1,5 0,7	w _{x_cpi-0,3}	+ 1,5 0,7	q _{1mpv}
1,35 DEAD + 1,35 g ₂ + 1,5	q _{2sv}	+ 1,5 0,7	q _{2v}	+ 1,5 0,7	w _{x_cpi+0,2}	+ 1,5 0,7	q _{2mpv}
1,35 DEAD + 1,35 g ₂ + 1,5	q _{2sv}	+ 1,5 0,7	q _{2v}	+ 1,5 0,7	w _{x_cpi-0,3}	+ 1,5 0,7	q _{2mpv}
1 DEAD + 1 g ₂ + 1,5	w _{y_cpi+0,2}	+ 1,5 0,7	q ₁	+ 1,5 0,7	q _{1s}	+ 1,5 0,7	q _{1mp}
1 DEAD + 1 g ₂ + 1,5	w _{y_cpi-0,3}	+ 1,5 0,7	q ₁	+ 1,5 0,7	q _{1s}	+ 1,5 0,7	q _{1mp}
1 DEAD + 1 g ₂ + 1,5	w _{y_cpi+0,2}	+ 1,5 0,7	q ₂	+ 1,5 0,7	q _{2s}	+ 1,5 0,7	q _{2mp}
1 DEAD + 1 g ₂ + 1,5	w _{y_cpi-0,3}	+ 1,5 0,7	q ₂	+ 1,5 0,7	q _{2s}	+ 1,5 0,7	q _{2mp}
1 DEAD + 1 g ₂ + 1,5	w _{y_cpi+0,2}	+ 1,5 0,7	q ₁ +q ₂	+ 1,5 0,7	q _{1s} +q _{2s}	+ 1,5 0,7	q _{1mp} +q _{2mp}
1 DEAD + 1 g ₂ + 1,5	w _{y_cpi-0,3}	+ 1,5 0,7	q ₁ +q ₂	+ 1,5 0,7	q _{1s} +q _{2s}	+ 1,5 0,7	q _{1mp} +q _{2mp}
1 DEAD + 1 g ₂ + 1,5	w _{x_cpi+0,2}	+ 1,5 0,7	q ₁	+ 1,5 0,7	q _{1s}	+ 1,5 0,7	q _{1mp}
1 DEAD + 1 g ₂ + 1,5	w _{x_cpi-0,3}	+ 1,5 0,7	q ₁	+ 1,5 0,7	q _{1s}	+ 1,5 0,7	q _{1mp}
1 DEAD + 1 g ₂ + 1,5	w _{x_cpi+0,2}	+ 1,5 0,7	q ₂	+ 1,5 0,7	q _{2s}	+ 1,5 0,7	q _{2mp}
1 DEAD + 1 g ₂ + 1,5	w _{x_cpi-0,3}	+ 1,5 0,7	q ₂	+ 1,5 0,7	q _{2s}	+ 1,5 0,7	q _{2mp}
1 DEAD + 1 g ₂ + 1,5	w _{x_cpi+0,2}	+ 1,5 0,7	q ₁ +q ₂	+ 1,5 0,7	q _{1s} +q _{2s}	+ 1,5 0,7	q _{1mp} +q _{2mp}
1 DEAD + 1 g ₂ + 1,5	w _{x_cpi-0,3}	+ 1,5 0,7	q ₁ +q ₂	+ 1,5 0,7	q _{1s} +q _{2s}	+ 1,5 0,7	q _{1mp} +q _{2mp}
1 DEAD + 1 g ₂ + 1,5	w _{y_cpi+0,2}	+ 1,5 0,7	q _{1o}	+ 1,5 0,7	q _{1so}	+ 1,5 0,7	q _{1mpo}
1 DEAD + 1 g ₂ + 1,5	w _{y_cpi-0,3}	+ 1,5 0,7	q _{1o}	+ 1,5 0,7	q _{1so}	+ 1,5 0,7	q _{1mpo}
1 DEAD + 1 g ₂ + 1,5	w _{y_cpi+0,2}	+ 1,5 0,7	q _{2o}	+ 1,5 0,7	q _{2so}	+ 1,5 0,7	q _{2mpo}
1 DEAD + 1 g ₂ + 1,5	w _{y_cpi-0,3}	+ 1,5 0,7	q _{2o}	+ 1,5 0,7	q _{2so}	+ 1,5 0,7	q _{2mpo}
1 DEAD + 1 g ₂ + 1,5	w _{x_cpi+0,2}	+ 1,5 0,7	q _{1o}	+ 1,5 0,7	q _{1so}	+ 1,5 0,7	q _{1mpo}
1 DEAD + 1 g ₂ + 1,5	w _{x_cpi-0,3}	+ 1,5 0,7	q _{1o}	+ 1,5 0,7	q _{1so}	+ 1,5 0,7	q _{1mpo}
1 DEAD + 1 g ₂ + 1,5	w _{x_cpi+0,2}	+ 1,5 0,7	q _{2o}	+ 1,5 0,7	q _{2so}	+ 1,5 0,7	q _{2mpo}
1 DEAD + 1 g ₂ + 1,5	w _{x_cpi-0,3}	+ 1,5 0,7	q _{2o}	+ 1,5 0,7	q _{2so}	+ 1,5 0,7	q _{2mpo}
1 DEAD + 1 g ₂ + 1,5	w _{y_cpi+0,2}	+ 1,5 0,7	q _{1v}	+ 1,5 0,7	q _{1sv}	+ 1,5 0,7	q _{1mpv}
1 DEAD + 1 g ₂ + 1,5	w _{y_cpi-0,3}	+ 1,5 0,7	q _{1v}	+ 1,5 0,7	q _{1sv}	+ 1,5 0,7	q _{1mpv}
1 DEAD + 1 g ₂ + 1,5	w _{y_cpi+0,2}	+ 1,5 0,7	q _{2v}	+ 1,5 0,7	q _{2sv}	+ 1,5 0,7	q _{2mpv}
1 DEAD + 1 g ₂ + 1,5	w _{y_cpi-0,3}	+ 1,5 0,7	q _{2v}	+ 1,5 0,7	q _{2sv}	+ 1,5 0,7	q _{2mpv}
1 DEAD + 1 g ₂ + 1,5	w _{x_cpi+0,2}	+ 1,5 0,7	q _{1v}	+ 1,5 0,7	q _{1sv}	+ 1,5 0,7	q _{1mpv}
1 DEAD + 1 g ₂ + 1,5	w _{x_cpi-0,3}	+ 1,5 0,7	q _{1v}	+ 1,5 0,7	q _{1sv}	+ 1,5 0,7	q _{1mpv}
1 DEAD + 1 g ₂ + 1,5	w _{x_cpi+0,2}	+ 1,5 0,7	q _{2v}	+ 1,5 0,7	q _{2sv}	+ 1,5 0,7	q _{2mpv}
1 DEAD + 1 g ₂ + 1,5	w _{x_cpi-0,3}	+ 1,5 0,7	q _{2v}	+ 1,5 0,7	q _{2sv}	+ 1,5 0,7	q _{2mpv}

2.5.2 Serviceability Limit State - ULS

The symbols defined in Figure 2-16 (q₁, q₂, q_{1o}, q_{2o}, q_{1v} and q_{2v}) are used in the following tables to report the load combinations considered in the study. The load combinations used for the *Serviceability Limit State* (SLS) are reported in the follow.

SLS: *Characteristic load combination*

$$\sum_{j \geq 1} G_{k,j} + P + Q_{k,1} + \sum_{i > 1} \psi_{0,i} Q_{k,i} \quad (2.2)$$

Table 2-6. Load Combinations for Serviceability Limit State - Characteristic

G ₁	+ G ₂	+ Q ₁	+ ψ _{0,2}	Q ₂	+ ψ _{0,3}	Q ₃	+ ψ _{0,4}	Q ₄
DEAD	+ g ₂	+ q ₁ +q ₂	+ 0,7	W _{y_cpi+0,2}	+ 0,7	q _{1s} +q _{2s}	+ 0,7	q _{1mp} +q _{2mp}
DEAD	+ g ₂	+ q ₁ +q ₂	+ 0,7	W _{y_cpi-0,3}	+ 0,7	q _{1s} +q _{2s}	+ 0,7	q _{1mp} +q _{2mp}
DEAD	+ g ₂	+ q ₁ +q ₂	+ 0,7	W _{x_cpi+0,2}	+ 0,7	q _{1s} +q _{2s}	+ 0,7	q _{1mp} +q _{2mp}
DEAD	+ g ₂	+ q ₁ +q ₂	+ 0,7	W _{x_cpi-0,3}	+ 0,7	q _{1s} +q _{2s}	+ 0,7	q _{1mp} +q _{2mp}
DEAD	+ g ₂	W _{y_cpi+0,2}	+ 0,7	q ₁ +q ₂	+ 0,7	q _{1s} +q _{2s}	+ 0,7	q _{1mp} +q _{2mp}
DEAD	+ g ₂	W _{y_cpi-0,3}	+ 0,7	q ₁ +q ₂	+ 0,7	q _{1s} +q _{2s}	+ 0,7	q _{1mp} +q _{2mp}
DEAD	+ g ₂	W _{x_cpi+0,2}	+ 0,7	q ₁ +q ₂	+ 0,7	q _{1s} +q _{2s}	+ 0,7	q _{1mp} +q _{2mp}
DEAD	+ g ₂	W _{x_cpi-0,3}	+ 0,7	q ₁ +q ₂	+ 0,7	q _{1s} +q _{2s}	+ 0,7	q _{1mp} +q _{2mp}
DEAD	+ g ₂	q _{1s} +q _{2s}	+ 0,7	q ₁ +q ₂	+ 0,7	W _{y_cpi+0,2}	+ 0,7	q _{1mp} +q _{2mp}
DEAD	+ g ₂	q _{1s} +q _{2s}	+ 0,7	q ₁ +q ₂	+ 0,7	W _{y_cpi-0,3}	+ 0,7	q _{1mp} +q _{2mp}
DEAD	+ g ₂	q _{1s} +q _{2s}	+ 0,7	q ₁ +q ₂	+ 0,7	W _{x_cpi+0,2}	+ 0,7	q _{1mp} +q _{2mp}
DEAD	+ g ₂	q _{1s} +q _{2s}	+ 0,7	q ₁ +q ₂	+ 0,7	W _{x_cpi-0,3}	+ 0,7	q _{1mp} +q _{2mp}

SLS: Frequent Load Combination

$$\sum_{j \geq 1} G_{k,j} + P + \psi_{1,1} Q_{k,1} + \sum_{i > 1} \psi_{2,i} Q_{k,i} \quad (2.3)$$

Table 2-7. Load Combinations for Serviceability Limit State - Frequent

G ₁	+ G ₂	+ ψ _{1,1}	Q ₁	+ ψ _{2,2}	Q ₂	+ ψ _{2,3}	Q ₃	+ ψ _{2,4}	Q ₄
DEAD	+ g ₂	+ 0,5	q ₁ +q ₂	+ 0,3	W _{y_cpi+0,2}	+ 0,3	q _{1s} +q _{2s}	+ 0,3	q _{1mp} +q _{2mp}
DEAD	+ g ₂	+ 0,5	q ₁ +q ₂	+ 0,3	W _{y_cpi-0,3}	+ 0,3	q _{1s} +q _{2s}	+ 0,3	q _{1mp} +q _{2mp}
DEAD	+ g ₂	+ 0,5	q ₁ +q ₂	+ 0,3	W _{x_cpi+0,2}	+ 0,3	q _{1s} +q _{2s}	+ 0,3	q _{1mp} +q _{2mp}
DEAD	+ g ₂	+ 0,5	q ₁ +q ₂	+ 0,3	W _{x_cpi-0,3}	+ 0,3	q _{1s} +q _{2s}	+ 0,3	q _{1mp} +q _{2mp}
DEAD	+ g ₂	+ 0,5	W _{y_cpi+0,2}	+ 0,3	q ₁ +q ₂	+ 0,3	q _{1s} +q _{2s}	+ 0,3	q _{1mp} +q _{2mp}
DEAD	+ g ₂	+ 0,5	W _{y_cpi-0,3}	+ 0,3	q ₁ +q ₂	+ 0,3	q _{1s} +q _{2s}	+ 0,3	q _{1mp} +q _{2mp}
DEAD	+ g ₂	+ 0,5	W _{x_cpi+0,2}	+ 0,3	q ₁ +q ₂	+ 0,3	q _{1s} +q _{2s}	+ 0,3	q _{1mp} +q _{2mp}
DEAD	+ g ₂	+ 0,5	W _{x_cpi-0,3}	+ 0,3	q ₁ +q ₂	+ 0,3	q _{1s} +q _{2s}	+ 0,3	q _{1mp} +q _{2mp}
DEAD	+ g ₂	+ 0,5	q _{1s} +q _{2s}	+ 0,3	q ₁ +q ₂	+ 0,3	W _{y_cpi+0,2}	+ 0,3	q _{1mp} +q _{2mp}
DEAD	+ g ₂	+ 0,5	q _{1s} +q _{2s}	+ 0,3	q ₁ +q ₂	+ 0,3	W _{y_cpi-0,3}	+ 0,3	q _{1mp} +q _{2mp}
DEAD	+ g ₂	+ 0,5	q _{1s} +q _{2s}	+ 0,3	q ₁ +q ₂	+ 0,3	W _{x_cpi+0,2}	+ 0,3	q _{1mp} +q _{2mp}
DEAD	+ g ₂	+ 0,5	q _{1s} +q _{2s}	+ 0,3	q ₁ +q ₂	+ 0,3	W _{x_cpi-0,3}	+ 0,3	q _{1mp} +q _{2mp}

SLS: *Quasi Permanent Load Combination*

$$\sum_{j \geq 1} G_{k,j} + P + \sum_{i > 1} \psi_{2,i} Q_{k,i} \quad (2.4)$$

Table 2-8. Load Combinations for Serviceability Limit State – Quasi-Permanent

G₁	+	G₂	+	ψ_{1,1}	Q₁	+	ψ_{2,2}	Q₂	+	ψ_{2,3}	Q₃
DEAD	+	g ₂	+	0,3	q ₁ +q ₂	+	0,3	w _{y_cpi+0,2}	+	0,3	q _{1s} +q _{2s}
DEAD	+	g ₂	+	0,3	q ₁ +q ₂	+	0,3	w _{y_cpi-0,3}	+	0,3	q _{1s} +q _{2s}
DEAD	+	g ₂	+	0,3	q ₁ +q ₂	+	0,3	w _{x_cpi+0,2}	+	0,3	q _{1s} +q _{2s}
DEAD	+	g ₂	+	0,3	q ₁ +q ₂	+	0,3	w _{x_cpi-0,3}	+	0,3	q _{1s} +q _{2s}

2.6 Imperfection for global analysis of frames

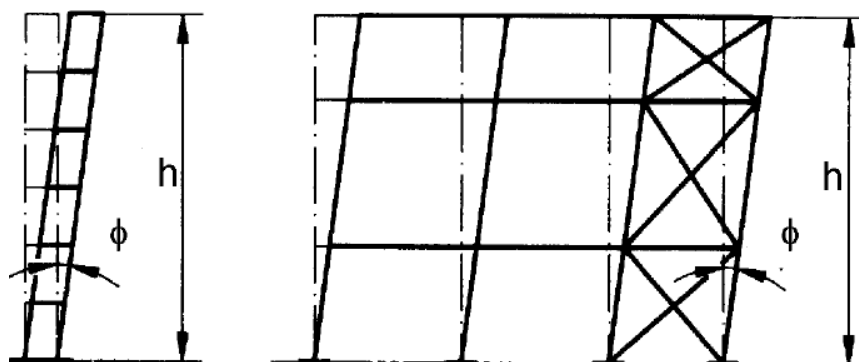


Figure 2-29. Equivalent sway imperfections

The effect of the global initial sway imperfections has been accounted by including these in the geometry of the finite element model. The effect of the bow imperfections has been considered in the study as suggested in the EN 1993-1-1 §6.3 [4]. The global initial sway imperfection may be evaluated by the following formula (EN 1993-1-1 §5.3.2 [4]) :

$$\phi = \phi_0 \cdot \alpha_h \cdot \alpha_m \quad (2.5)$$

The global initial sway imperfections for both the directions are reported in the follow:

- Global initial sway imperfection - X direction

$$\phi_0 = 1/200 \quad \alpha_h = 0.667 \quad \alpha_m = 0.756 \quad \phi_x = 0.00252$$

- Global initial sway imperfection - Y direction

$$\phi_0 = 1/200 \quad \alpha_h = 0.667 \quad \alpha_m = 0.816 \quad \phi_y = 0.00272$$

2.7 Creep and Shrinkage of the concrete

The calculation of the creep coefficient based on EN 1992-1-1 Annex B and EN 1992-1-1 §5.4.2.2 [3]. The relative humidity of the ambient is RH = 75 % and the age of the concrete considered is $t = \infty$. The creep coefficient is calculated as follow.

$$\varphi(t, t_0) = \varphi_0 \cdot \beta_c(t, t_0) \quad (2.6)$$

For the creep, the age of loading t_0 is assumed to be 28 days while for shrinkage, the age of loading t_0 is assumed to be 1 day.

$$\varphi(t, 28) = \varphi_0 \cdot \beta_c(t, 28) = 1.893 \quad \varphi(t, 1) = \varphi_0 \cdot \beta_c(t, 1) = 3.523$$

The modular ratios are calculated for short and for long term loading by following the EN 1994-1-1 §5.4.2.2 [8]. For short-term loading:

$$n_0 = E_s / E_{cm} = 6.395$$

For long-term loading the creep multiplier (ψ_L) depends on the type of loading. It can be taken as 1.1 for permanent load and 0.55 for primary and secondary effect of shrinkage. The modular ratios and effective modulus of elasticity of the concrete for long-term loading are calculated as follow:

- Permanent Load

$$n_L = n_0(1 + \psi_L \phi(t, t_0)) = 19.706 \quad E_{c,eff} = E_s / n_L = 10656.5 \text{ MPa}$$

- Primary and secondary effects of shrinkage

$$n_L = n_0(1 + \psi_L \phi(t, t_0)) = 18.782 \quad E_{c,eff} = E_s / n_L = 11180.7 \text{ MPa}$$

2.8 Symmetric Structure

The following sections report the calculation of the components of the Symmetric structure.

2.8.1 Slab - Maximum Bending Moments - ULS

The bending moments for the design of the slab in both the directions have been obtained by using the finite element model previously described. Figure 2-30 up to Figure 2-33 show the maximum and minimum bending moments in X and Y direction for the Envelope of all the ULS combinations.

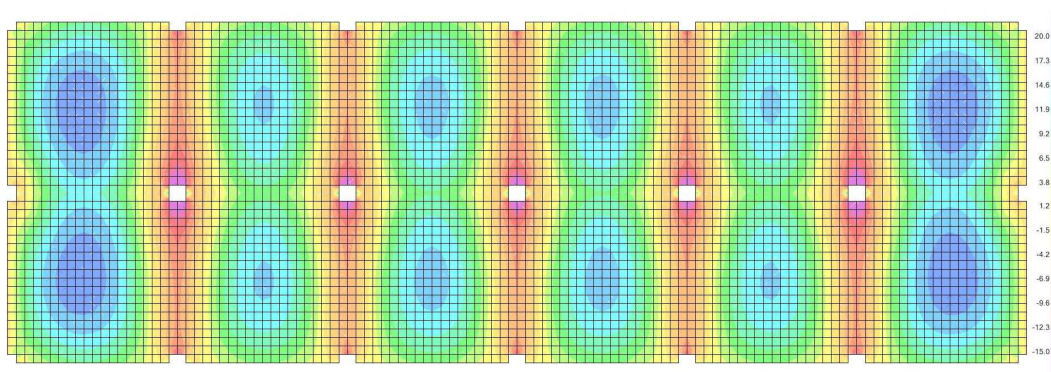


Figure 2-30. Maximum Bending Moments in X direction (ULS Envelope)

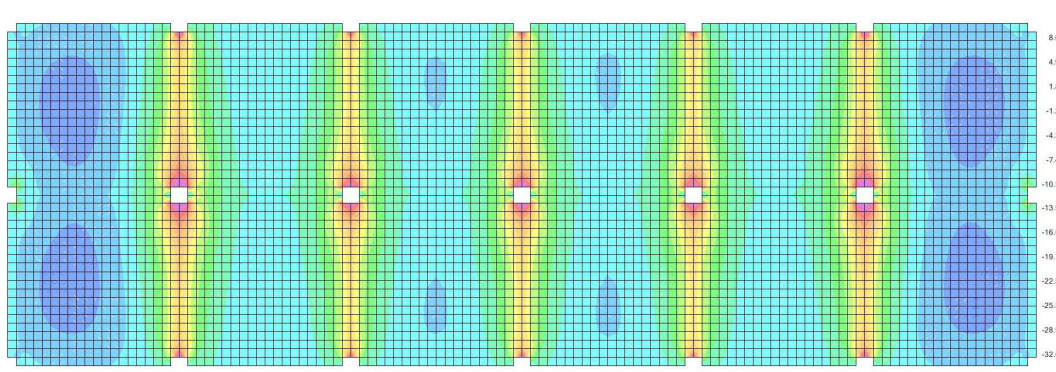


Figure 2-31. Minimum Bending Moments in X direction (ULS Envelope)

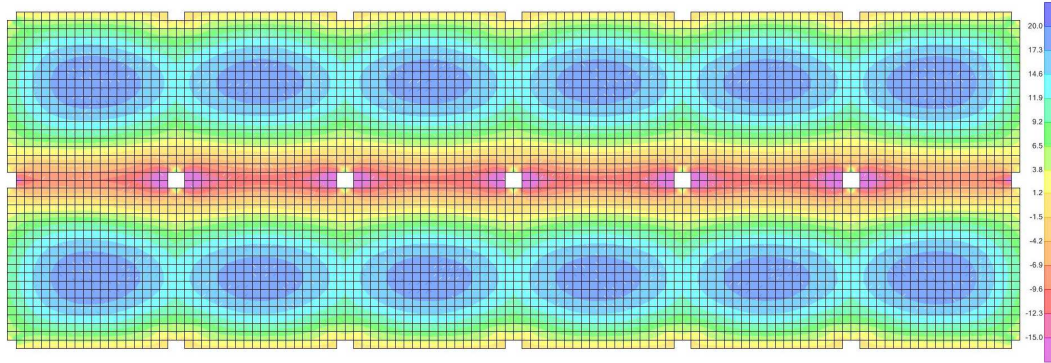


Figure 2-32. Maximum Bending Moments in Y direction (ULS Envelope)

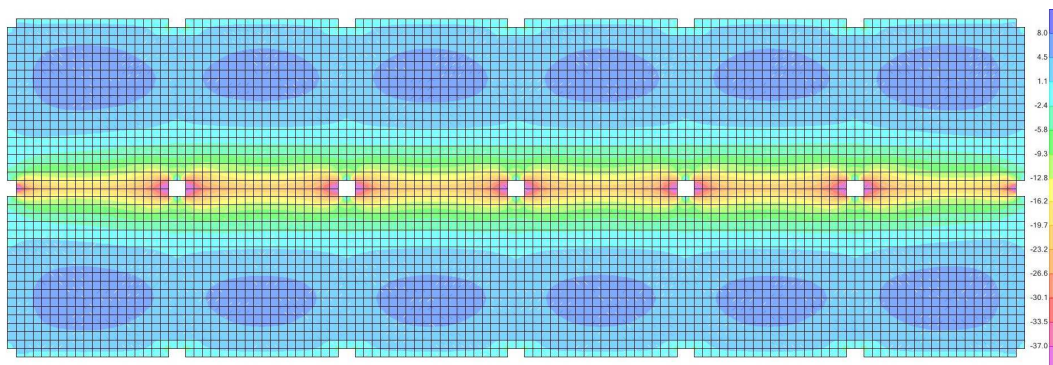


Figure 2-33. Minimum Bending Moments in Y direction (ULS Envelope)

2.8.2 Slab - Maximum traction force in the layers of rebars - ULS

The amount of rebars is based on the maximum traction force in each layer of rebars for the Envelope of all the ULS combinations as reported in Figure 2-34 up to Figure 2-37. The minimum and maximum steel percentages and the maximum spacing of rebars are defined in the EN 1992-1-1 §9.2.1 and EN 1992-1-1 §9.3 [3]. They are respectively:

$$A_{y,\min} = 150.8 \text{ mm}^2/\text{m} \quad \text{minimum steel percentage}$$

$$A_{y,\max} = 6000 \text{ mm}^2/\text{m} \quad \text{maximum steel percentage}$$

$$s_{\max,slab} = 400 \text{ mm} \quad \text{maximum spacing of rebars}$$

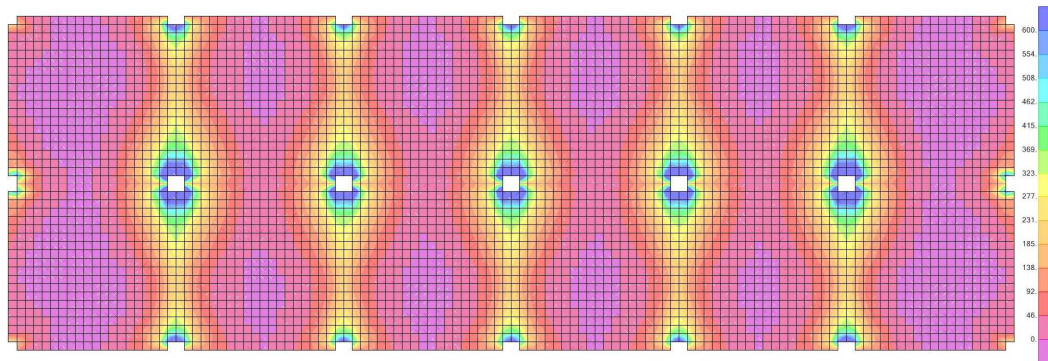


Figure 2-34. Maximum Traction Force in the upper rebars in X direction (ULS Envelope)

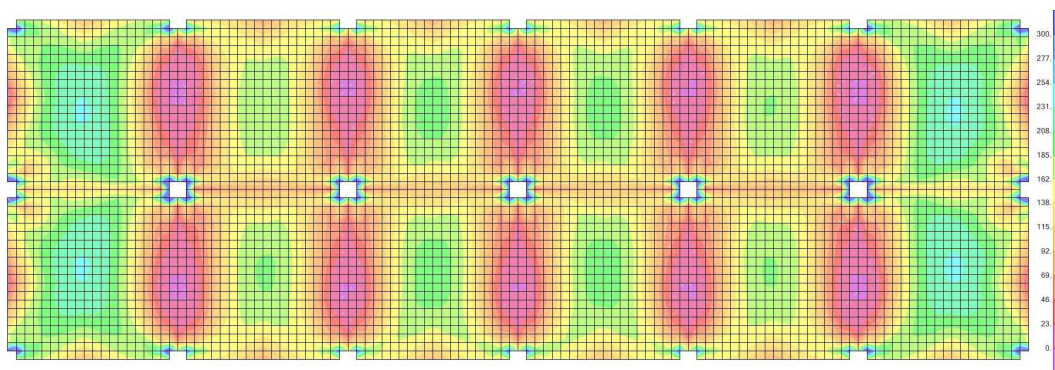


Figure 2-35. Maximum Traction Force in the lower rebars in X direction (ULS Envelope)

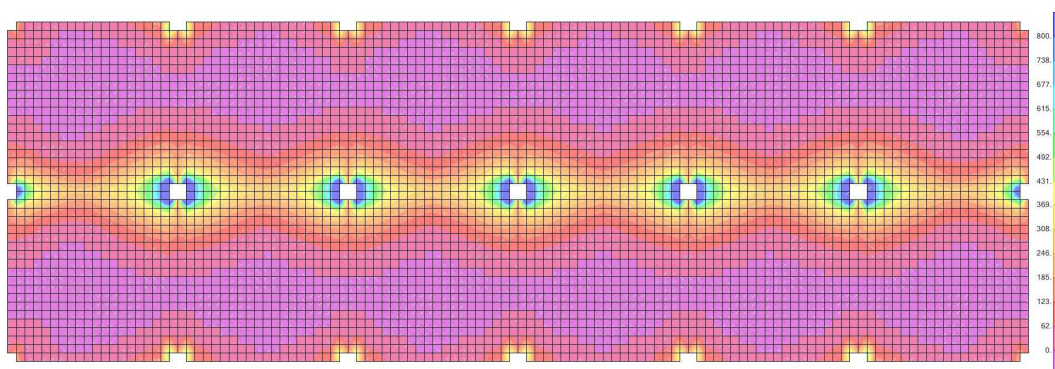


Figure 2-36. Maximum Traction Force in the upper rebars in Y direction (ULS Envelope)

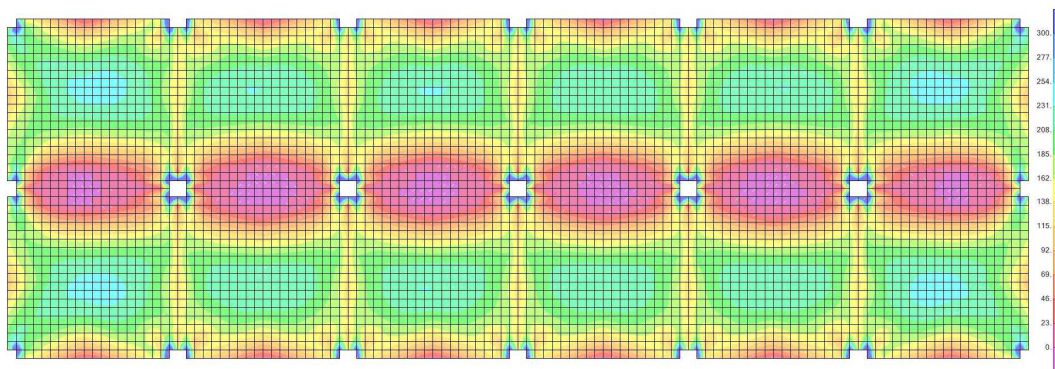


Figure 2-37. Maximum Traction Force in the lower rebars in Y direction (ULS Envelope)

**MOMENT RESISTING STEEL-CONCRETE COMPOSITE FRAMES UNDER THE COLUMN LOSS SCENARIO:
DESIGN OF THE REFERENCE FRAMES AND OF THE FULL-SCALE SUB-FRAME SPECIMENS**

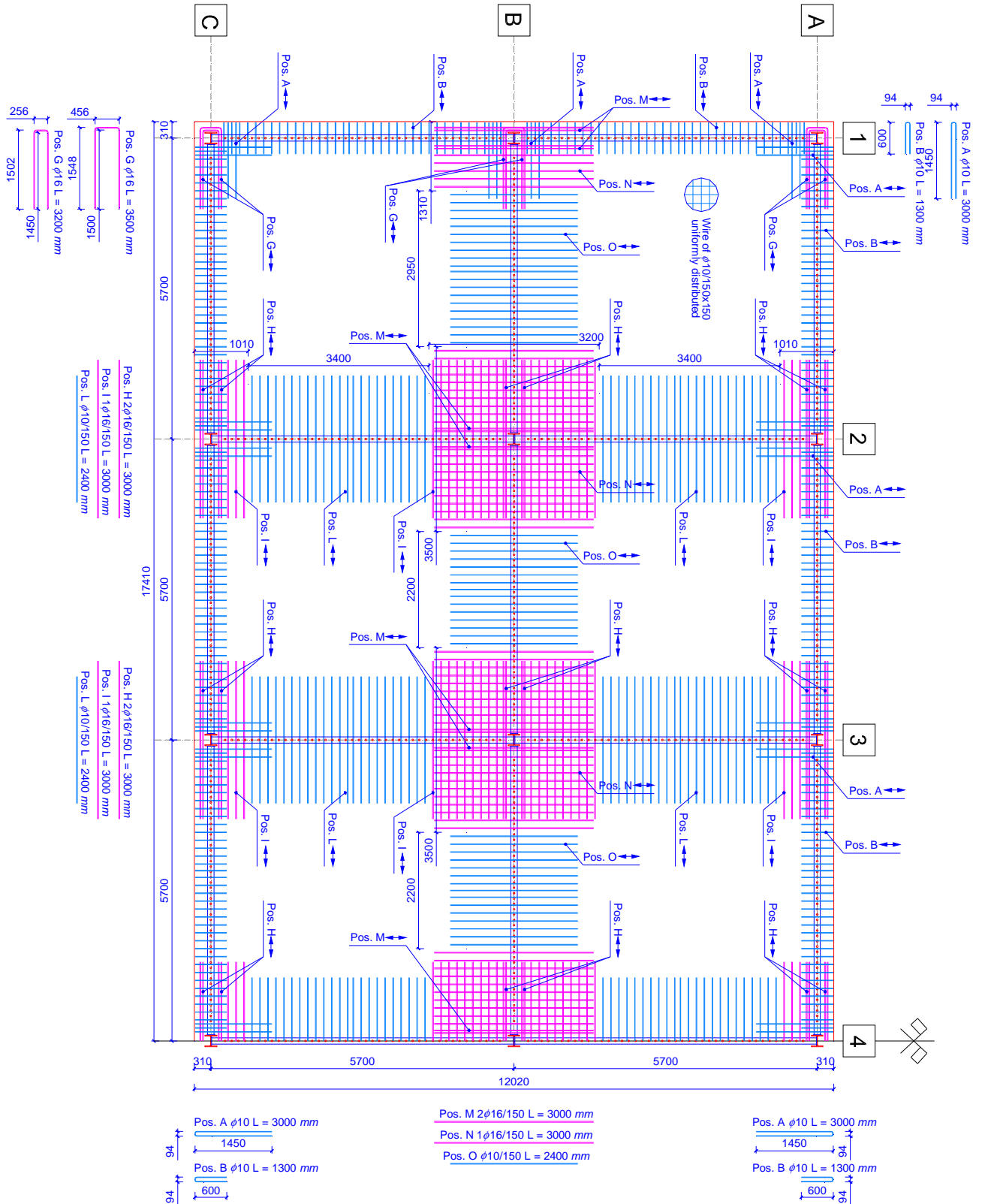


Figure 2-38. Slab Rebars - Upper Side – Symmetric Configuration (length unit mm)

**MOMENT RESISTING STEEL-CONCRETE COMPOSITE FRAMES UNDER THE COLUMN LOSS SCENARIO:
DESIGN OF THE REFERENCE FRAMES AND OF THE FULL-SCALE SUB-FRAME SPECIMENS**

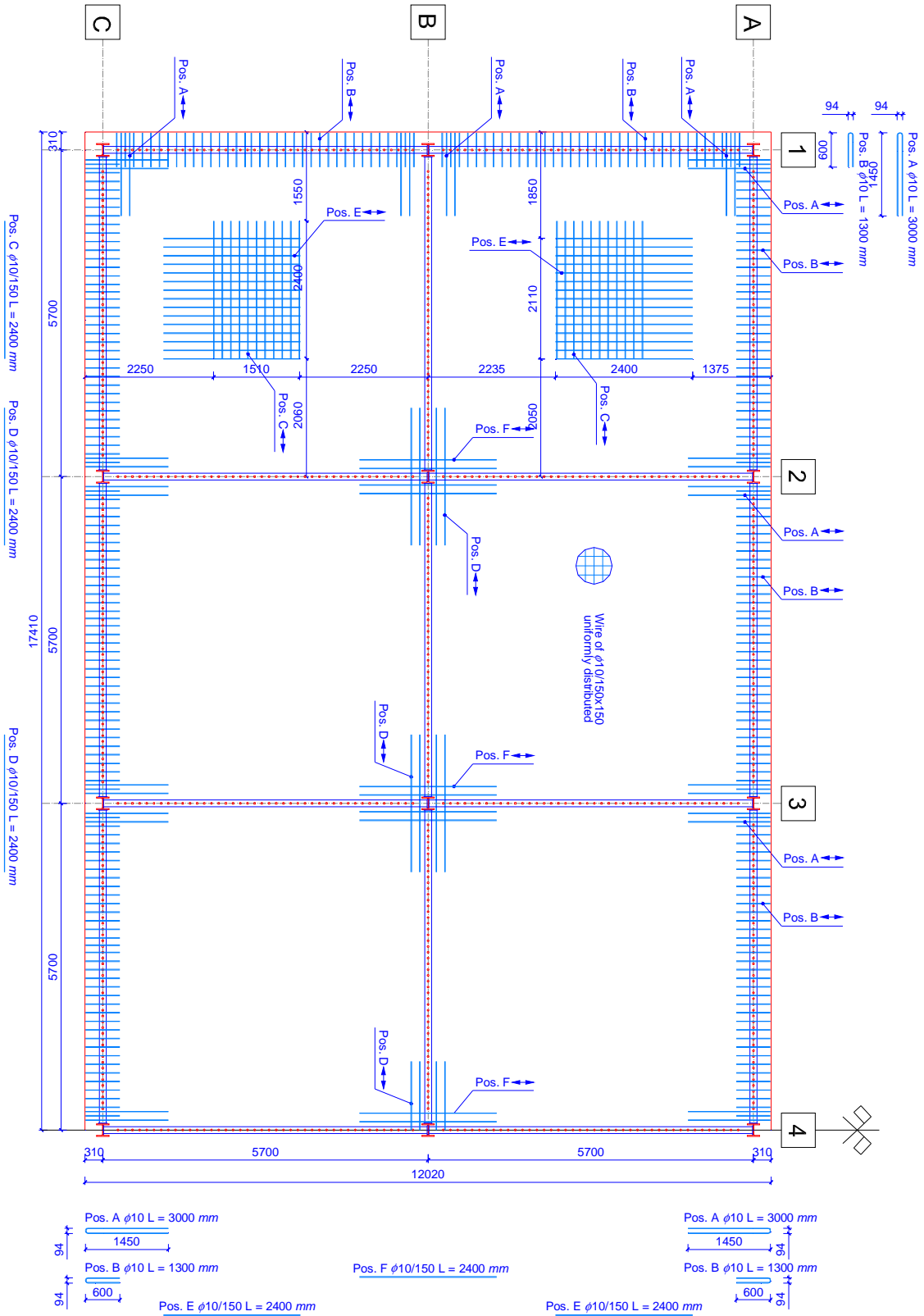


Figure 2-39. Slab Rebars - Lower Side – Symmetric Configuration (length unit mm)

2.8.3 Slab Shear - ULS

The slab is verified against shear forces by following the EN 1992-1-1 §6.2 [3]. The design forces at the ULS are:

$$V_{Ed,max} = 22 \text{ kN/m} \quad N_{Ed,max} = -40 \text{ kN/m (traction)}$$

The design value for the shear resistance $V_{Rd,c}$ in members not requiring design shear reinforcement is calculated as specified in the EN 1992-1-1 §6.2.2 [3]:

$$V_{Rd,c} = \max \left\{ C_{Rd,c} k (100 \rho_l f_{ck})^{1/3} + k_1 \sigma_{cp}; (v_{min} + k_1 \sigma_{cp}) b_w d \right\} = 78.97 \text{ kN/m} > V_{Ed}$$

2.8.4 Slab Deflection - SLS

The maximum slab deflection has been evaluated by considering the **Quasi Permanent** load combination as required in EN 1992-1-1 §7.4 [3]. The design value of the bending moment in a portion of the slab of unitary width is:

$$M_{Ed,max} = 8.58 \text{ kNm}$$

Considering a portion of the slab of unitary width and neglecting the presence of rebars the bending moment at cracking is:

$$f_{cm,fl} = \max \left[(1.6 - h/1000) f_{cm}; f_{cm} \right] = 4.20 \text{ MPa} \quad M_{cr} = f_{cm,fl} \cdot \frac{b \cdot h^2}{6} = 15.75 \text{ kNm} > M_{Ed}$$

The slab is not cracked since $M_{cr} > M_{Ed}$. The evaluation of the maximum deflection is conducted considering the moment of inertia of the uncracked section. The finite element model with the effective modulus of elasticity of the concrete in the case of long-term permanent load have been employed for the deflection evaluation as required in the EN 1992-1-1 §7.4.3(4) [3]. The maximum displacement is equal to $\delta = 11.09 \text{ mm}$. The maximum dimension of the slab is equal to $L = 5.700 \text{ m}$ and hence, the ratio L/δ is equal to 513.98.

2.8.5 Slab Stresses - SLS

The stresses on the concrete and on the rebars of the slab are checked with reference to the **Characteristic** and the **Quasi-Permanent** load combinations as required in EN 1992-1-1 §7.2 [3]. The stresses are directly obtained as results of the model of the analysis.

- Characteristic Load Combination

$$\sigma_{c,max} = 8.35 \text{ MPa} < 0.6 f_{ck} = 18 \text{ MPa}$$

$$\sigma_{s,max} = 268 \text{ MPa} < 0.8 f_{yk} = 360 \text{ MPa}$$

- Quasi-Permanent Load Combination

$$\sigma_{c,max} = 5.81 \text{ MPa} < 0.45 f_{ck} = 13.5 \text{ MPa}$$

2.8.6 Beams - Effective width of flange for shear lag

The beams section type is IPE 240. It is a section class 1 in bending and section class 2 in compression. The dimensions of the effective width of flange for shear lag is calculated by following the indications of EN 1994-1-1 §5.4.1.2 [8].

L_e in the different parts of the beams is defined by following the indications reported in Figure 5.1 of EN 1994-1-1 [8]. Figure 2-40 and Figure 2-41 reports the effective width of flanges for shear lag of beams respectively in X e Y directions.

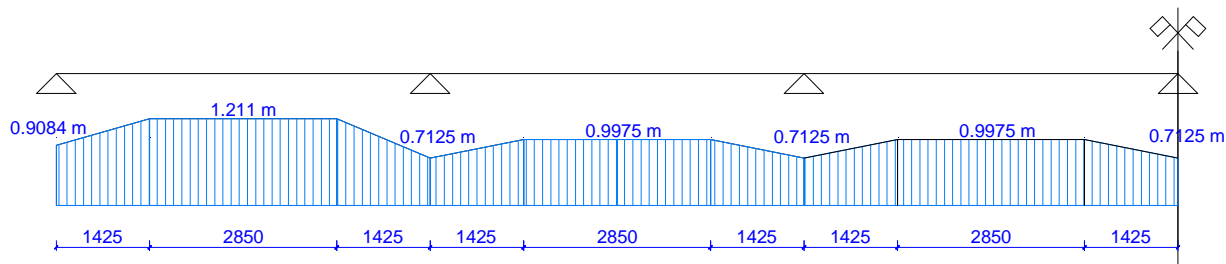


Figure 2-40. Effective width of flanges for shear lag of beams in X direction

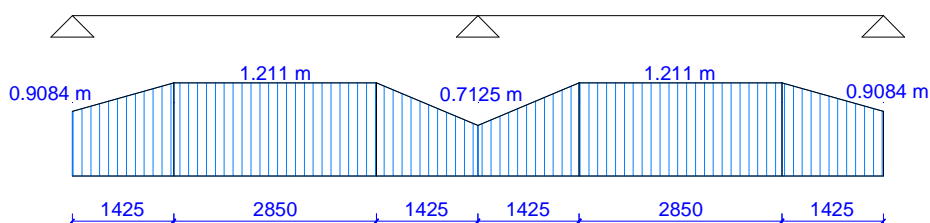
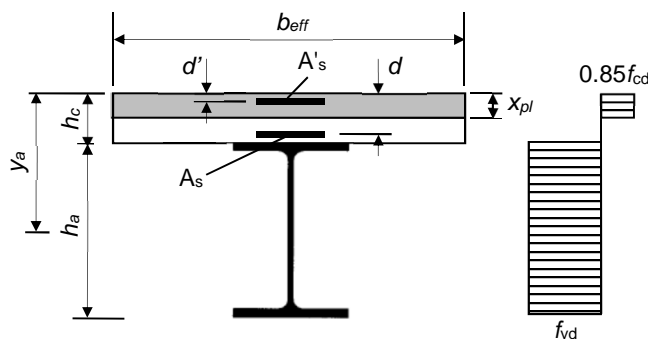


Figure 2-41. Effective width of flanges for shear lag of beams in Y direction

2.8.7 Beams - Maximum positive bending moment at mid span - ULS

The maximum positive bending moment of the beam at mid-span is equal to $M_{Ed} = 130.49 \text{ kNm}$.



The beams section type is IPE 240 and the effective width of flange in this position is equal to $b_{eff} = 1.2110 \text{ m}$. The calculation of the resisting moment for the ULS condition is reported in the follow.

$$F_{c,max} = 0.85 \cdot h_c \cdot b_{eff} \cdot \frac{f_{ck}}{\gamma_c} = 3088.05 \text{ kN} \quad \text{Plastic resistance of the concrete section}$$

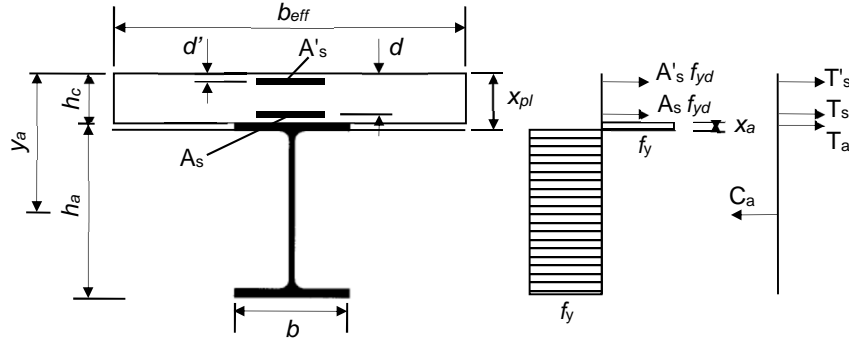
$$F_{a,max} = A \cdot \frac{f_y}{\gamma_{M0}} = 1388.05 \text{ kN} \quad \text{Plastic resistance of the steel section}$$

$$x_{pl} = \frac{F_{a,max}}{0.85 \cdot \frac{f_{ck}}{\gamma_c} \cdot b_{eff}} = 67.42 \text{ mm} \quad \text{Neutral axis position}$$

$$M_{pl} = F_{s, \max} \left(\frac{h_a}{2} + h_c - \frac{x_{pl}}{2} \right) = 327.98 \text{ kNm} > M_{Ed}$$

2.8.8 Beams - Maximum negative bending moment at the support- ULS

The maximum negative bending moment of the beam at the support is equal to $M_{Ed} = 109.18 \text{ kNm}$.



The beams section type is IPE 240 and the effective width of flange in this position is equal to $b_{eff} = 712.5 \text{ mm}$. The amount of rebars contained in the effective width of flange are $A_s' = 1363.45 \text{ mm}^2$ ($2\phi 10 + 6\phi 16$, $d' = 34 \text{ mm}$) and $A_s = 471.24 \text{ mm}^2$ ($6\phi 10$, $d = 116 \text{ mm}$) respectively for the upper and lower layers.

$$T'_s = A_s' \frac{f_{yd}}{\gamma_s} = 533.52 \text{ kN} \quad \text{Tensile force in the rebars;}$$

$$T_s = A_s \frac{f_{yd}}{\gamma_s} = 184.40 \text{ kN} \quad \text{Tensile force in the rebars;}$$

$$T_a = \frac{1}{2} \left(A \frac{f_y}{\gamma_{M0}} - T'_s - T_s \right) = 335.42 \text{ kN} \quad \text{Tensile force in steel section;}$$

$$x_{pl} = h_c + \frac{T_a}{b \frac{f_y}{\gamma_{M0}}} = 157.87 \text{ mm} \quad \text{Neutral axis position}$$

$$C_a = A \frac{f_y}{\gamma_{M0}} - T_a = 1053.34 \text{ kN} \quad \text{Compressive force in the steel section;}$$

$$M_{pl} = C_a(x_{Ca} - x_{pl}) + T_a(x_{pl} - x_{Ta}) + T_s(x_{pl} - x_s) + T'_s(x_{pl} - x'_s) = 189.09 \text{ kN} > M_{Ed}$$

2.8.9 Beams - Maximum shear force at the support- ULS

As suggested in EN 1993-1-1 §6.2.6, only the beams section IPE 240 is considered for the shear resistance. The maximum shear force on the beam is equal to $V_{Ed} = 145.68 \text{ kN}$.

$$V_{Rd} = \frac{A_v \frac{f_{yk}}{\sqrt{3}}}{\gamma_{M0}} = 392.45 \text{ kN} > V_{Ed}$$

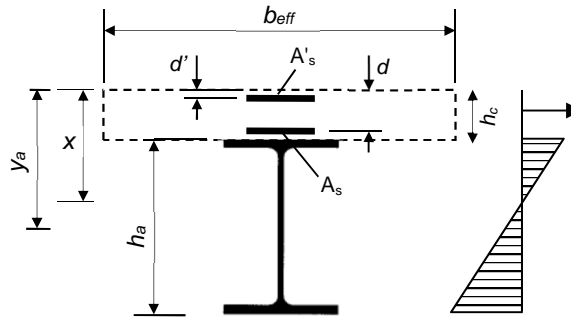
2.8.10 Beams - Calculation of the crack widths - ULS

The crack width is calculated by following the EN 1992-1-1 §7.3.4 [3] as follow.

$$w_k = s_{r,\max}(\varepsilon_{sm} - \varepsilon_{cm}) \quad (2.7)$$

The structure is subjected to the exposure class XC3 where the maximum crack width is equal to $w_{\max} = 0.3 \text{ mm}$ while considering the **Quasi-Permanent** load combination. (EN 1992-1-1 Table 7.1N [3]). The beams section type is IPE 240 and the effective width of flange in this position is equal to $b_{\text{eff}} = 712.5 \text{ mm}$

The amount of rebars contained in the effective width of flange are $A'_s = 1363.45 \text{ mm}^2$ ($2\emptyset 10 + 6\emptyset 16, d' = 34 \text{ mm}$) and $A_s = 471.24 \text{ mm}^2$ ($6\emptyset 10, d = 116 \text{ mm}$) respectively for the upper and lower layers. The negative bending moment of the beam at the support is equal to $M_{\text{Ed}} = 54.87 \text{ kNm}$.



$$A = A_u + A_s + A'_s = 5746.69 \text{ mm}^2 \quad \text{Total area of resisting elements in tension;}$$

$$x = \frac{1}{A}(A_u y_a + A_s d + A'_s d') = 201.38 \text{ mm} \quad \text{Position of the neutral axis;}$$

$$J = J_u + A_u (y_a - x)^2 + A_s (x - d)^2 + A'_s (x - d')^2 = 6100.45 \text{ cm}^4 \quad \text{Moment of inertia}$$

$$\sigma_{s,t} = \frac{M}{J}(x - d') = 150.55 \text{ MPa} \quad \text{Tensile stress in the upper layer of rebars;}$$

$$\varepsilon_{sm} - \varepsilon_{cm} = \frac{\sigma_{s,t}}{E_s} = 0.000717$$

$$s_{r,\max} = 115.6$$

$$w_k = s_{r,\max}(\varepsilon_{sm} - \varepsilon_{cm}) = 0.0829 \text{ mm} < w_{\max}$$

2.8.11 Columns - Maximum axial force- ULS

The column section type is HEB 220. It is class 1 both in bending and in compression. The maximum axial force on the column is checked by the EN 1993-1-1 §6.2.4 [4]. The maximum axial force on the columns is equal to $N_{\text{Ed}} = 2596.91 \text{ kN}$

$$N_{\text{Rd}} = \frac{A f_y}{\gamma_{M0}} = 3231 \text{ kN} > N_{\text{Ed}}$$

2.8.12 Columns - Maximum shear force- ULS

The column section type is HEB 220. It is class 1 both in bending and in compression. The maximum shear force on the column is checked by the EN 1993-1-1 §6.2.6 [4]. The maximum shear force on the column is equal to $V_{\text{Ed}} = 22.72 \text{ kN}$.

$$A_v = A - 2bt_f + (t_w + 2r)t_f = 2792.00 \text{ mm}^2$$

$$V_{Rd} = \frac{A_v \frac{f_{yk}}{\sqrt{3}}}{\sqrt{3}} = 572.25 \text{ kN} > V_{Ed}$$

2.8.13 Columns - Member in bending and axial compression - ULS

The column section type is HEB 220. It is class 1 both in bending and in compression. In order to verify the members which are subjected to combined bending and axial compression, the formulations reported in EN 1993-1-1 §6.3.3 [4] have to be satisfied.

The forces acting in the more stressed column are:

$$N_{Ed} = 2596.91 \text{ kN}$$

$$M_{y,Ed,A} = -14.72 \text{ kNm} \quad M_{z,Ed,A} = -7.50 \text{ kNm}$$

$$M_{y,Ed,B} = 4.42 \text{ kNm} \quad M_{z,Ed,B} = 4.43 \text{ kNm}$$

The reduction factors for buckling for lateral torsional buckling χ_y , χ_z and χ_{LT} have been calculated by following the instruction of EN 1993-1-1 §6.2.1.2, EN 1993-1-1 §6.3.2.2 and EN 1993-1-1 §6.3.2.3 [4].

$$\chi_y = \frac{1}{\phi_y + \sqrt{\phi_y^2 - \bar{\lambda}_y^2}} = 0.989 \quad \chi_z = \frac{1}{\phi_z + \sqrt{\phi_z^2 - \bar{\lambda}_z^2}} = 0.917 \quad \chi_{LT} = \frac{1}{\phi_{LT} + \sqrt{\phi_{LT}^2 - \beta \bar{\lambda}_{LT}^2}} = 0.963$$

The parameters N_{Rk} , $M_{y,Rk}$ and $M_{z,Rk}$ are calculated as define in EN 1993-1-1 Table 6.7 [4].

$$N_{Rk} = f_y A = 355 \text{ MPa} \cdot 9104 \text{ mm}^2 = 3231.92 \text{ kN}$$

$$M_{y,Rk} = f_y W_{pl,y} = 355 \text{ MPa} \cdot 827 \cdot 10^3 \text{ mm}^3 = 293.59 \text{ kNm}$$

$$M_{z,Rk} = f_y W_{pl,z} = 355 \text{ MPa} \cdot 393 \cdot 10^3 \text{ mm}^3 = 139.83 \text{ kNm}$$

The interaction coefficients have been calculated by using the approach reported in EN 1993-1-1 Annex B [4].

$$k_{yy} = \min \left(C_{my} \left(1 + (\bar{\lambda}_y - 0.2) \frac{N_{Ed}}{\chi_y N_{Rk} / \gamma_{M1}} \right); C_{my} \left(1 + 0.8 \frac{N_{Ed}}{\chi_y N_{Rk} / \gamma_{M1}} \right) \right) = 0.499$$

$$k_{zz} = \min \left(C_{mz} \left(1 + (2\bar{\lambda}_z - 0.6) \frac{N_{Ed}}{\chi_z N_{Rk} / \gamma_{M1}} \right); C_{mz} \left(1 + 1.4 \frac{N_{Ed}}{\chi_z N_{Rk} / \gamma_{M1}} \right) \right) = 0.485$$

$$k_{yz} = 0.6k_{zz} = 0.291$$

$$k_{zy} = 0.6k_{yy} = 0.300$$

$$\frac{N_{Ed}}{\chi_y N_{Rk} / \gamma_{M1}} + k_{yy} \frac{M_{y,Ed} + \Delta M_{y,Ed}}{\chi_{LT} \frac{M_{y,Rk}}{\gamma_{M1}}} + k_{yz} \frac{M_{z,Ed} + \Delta M_{z,Ed}}{\gamma_{M1}} = 0.854 \leq 1$$

$$\frac{N_{Ed}}{\chi_z N_{Rk} / \gamma_{M1}} + k_{zy} \frac{M_{y,Ed} + \Delta M_{y,Ed}}{\chi_{LT} \frac{M_{y,Rk}}{\gamma_{M1}}} + k_{zz} \frac{M_{z,Ed} + \Delta M_{z,Ed}}{\gamma_{M1}} = 0.935 \leq 1$$

2.8.14 Steel Diagonal Bracing - ULS

The forces on the steel braces have been obtained by employing the finite element model previously described without the compressed braces assuming that they do not have compressive resistance as consequence of the buckling.

The bracing section type is the equal length angle L120×120×10 in X direction and the double equal length angle L120×120×10 in Y direction. The resistance of the net section is evaluated by following the instructions of EN 1993-1-8 §3.10.3 [2]. The use of bolts M20 is considered.

The maximum axial force acting in the braces for the X direction is equal to $N_{Ed} = 208.04$ kN.

$$A_{Net} = A - d_0 t = 2098 \text{ mm}^2 \quad N_{u,Rd} = \frac{\beta_3 A_{Net} f_u}{\gamma_{M2}} = 599.2 \text{ kN} > N_{Ed}$$

The maximum axial force acting in the braces for the Y direction is equal to $N_{Ed} = 635.38$ kN.

$$A_{Net} = A - d_0 t = 2098 \text{ mm}^2 \quad N_{u,Rd} = 2 \frac{\beta_3 A_{Net} f_u}{\gamma_{M2}} = 1198.4 \text{ kN} > N_{Ed}$$

2.9 Asymmetric Structure

The following sections report the calculation of the components of the Asymmetric structure.

2.9.1 Slab - Maximum Bending Moments - ULS

The bending moments for the design of the slab in both the directions have been obtained by using the finite element model previously described. Figure 2-42 up to Figure 2-45 show the maximum and minimum bending moments in X and Y direction for the Envelope of all the ULS combinations.

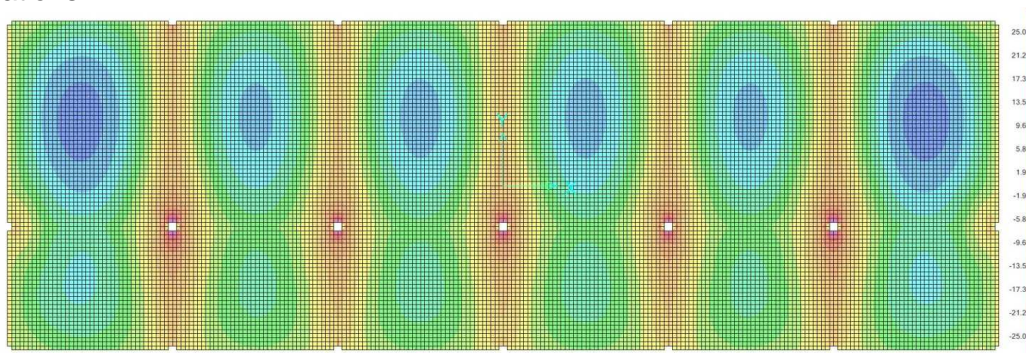


Figure 2-42. Maximum Bending Moments in X direction (ULS Envelope)

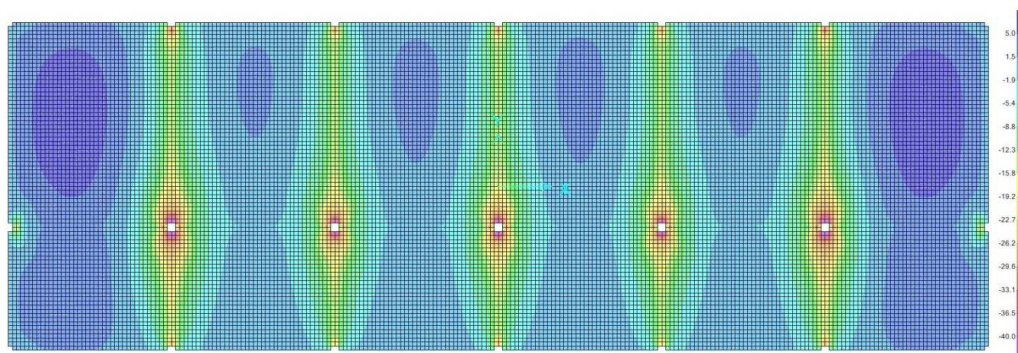


Figure 2-43. Minimum Bending Moments in X direction (ULS Envelope)

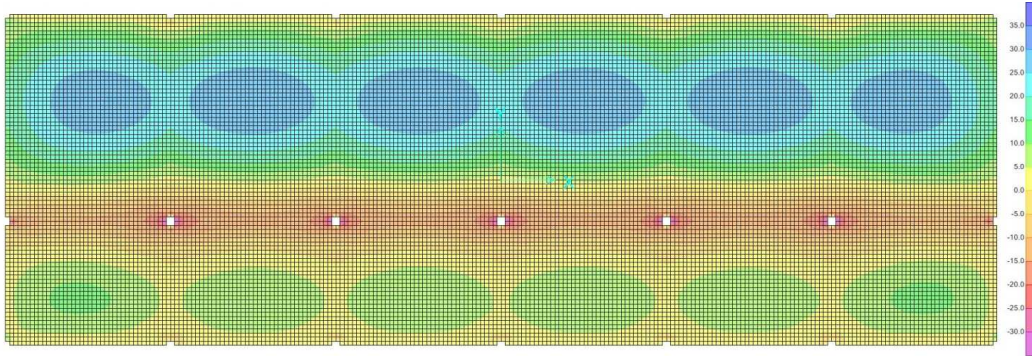


Figure 2-44. Maximum Bending Moments in Y direction (ULS Envelope)

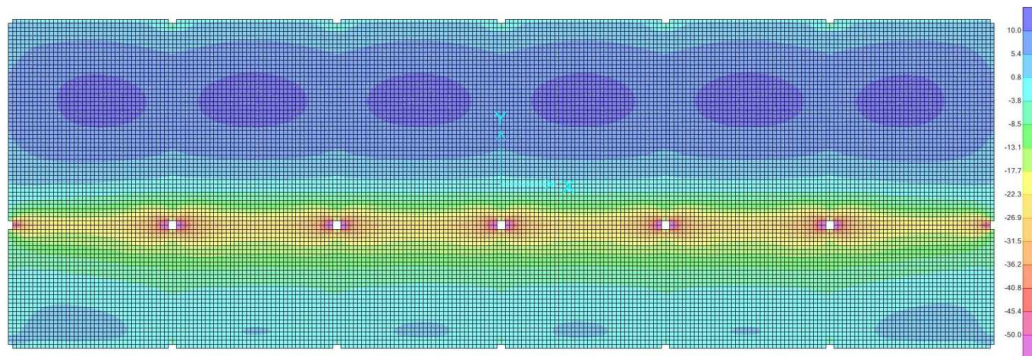


Figure 2-45. Minimum Bending Moments in Y direction (ULS Envelope)

2.9.2 Slab - Maximum traction force in the layers of rebars - ULS

The amount of rebars is based on the maximum traction force in each layer of rebars for the Envelope of all the ULS combinations as reported in Figure 2-46 up to Figure 2-49.

The minimum and maximum steel percentages and the maximum spacing of rebars are defined in the EN 1992-1-1 §9.2.1 and EN 1992-1-1 §9.3 [3]. They are respectively:

$$A_{s,\min} = 150.8 \text{ mm}^2/\text{m} \quad \text{minimum steel percentage}$$

$$A_{s,\max} = 6000 \text{ mm}^2/\text{m} \quad \text{maximum steel percentage}$$

$$s_{\max,slab} = 400 \text{ mm} \quad \text{maximum spacing of rebars}$$

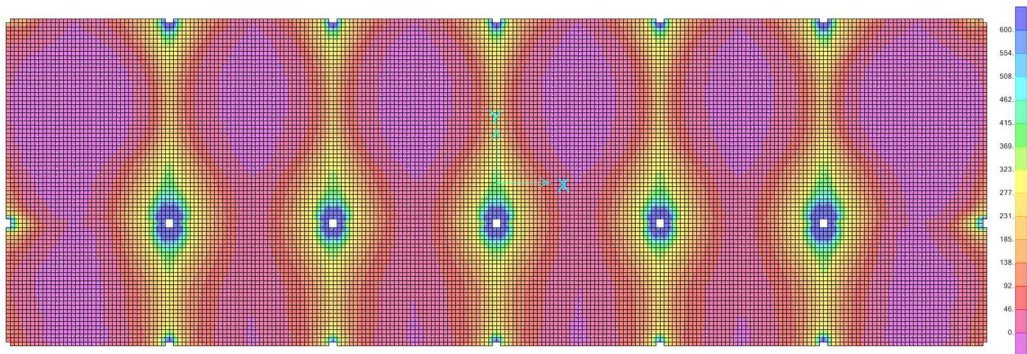


Figure 2-46. Maximum Traction Force in the upper rebars in X direction (ULS Envelope)

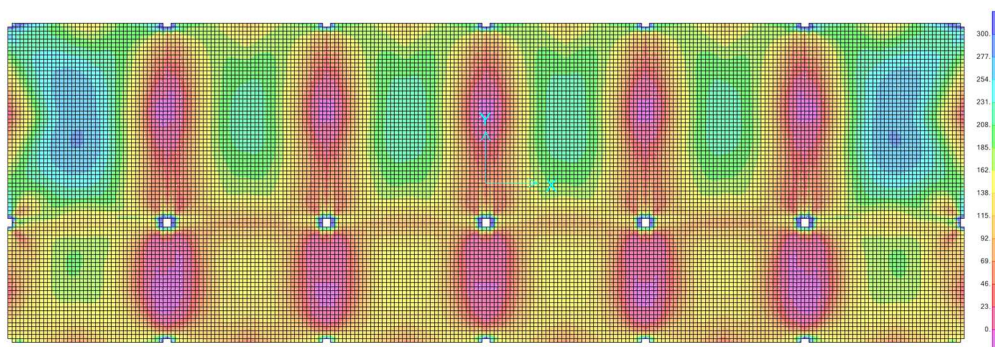


Figure 2-47. Maximum Traction Force in the lower rebars in X direction (ULS Envelope)

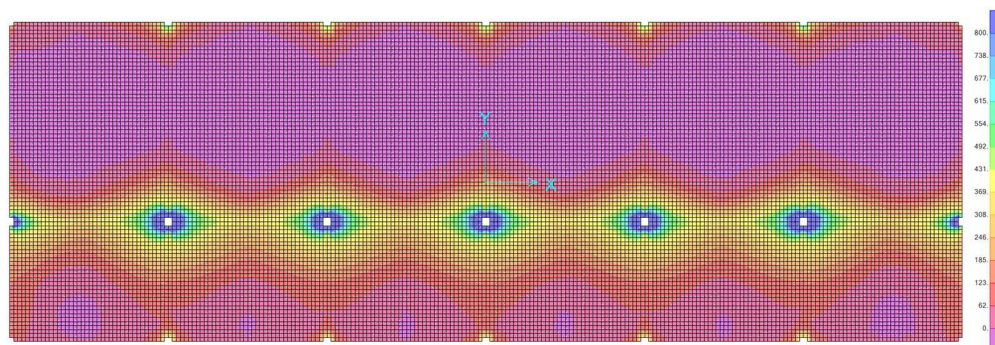


Figure 2-48. Maximum Traction Force in the upper rebars in Y direction (ULS Envelope)

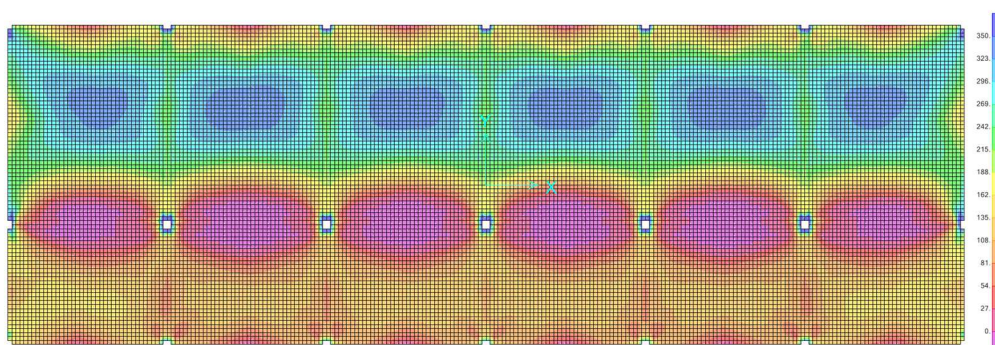


Figure 2-49. Maximum Traction Force in the lower rebars in Y direction (ULS Envelope)

**MOMENT RESISTING STEEL-CONCRETE COMPOSITE FRAMES UNDER THE COLUMN LOSS SCENARIO:
DESIGN OF THE REFERENCE FRAMES AND OF THE FULL-SCALE SUB-FRAME SPECIMENS**

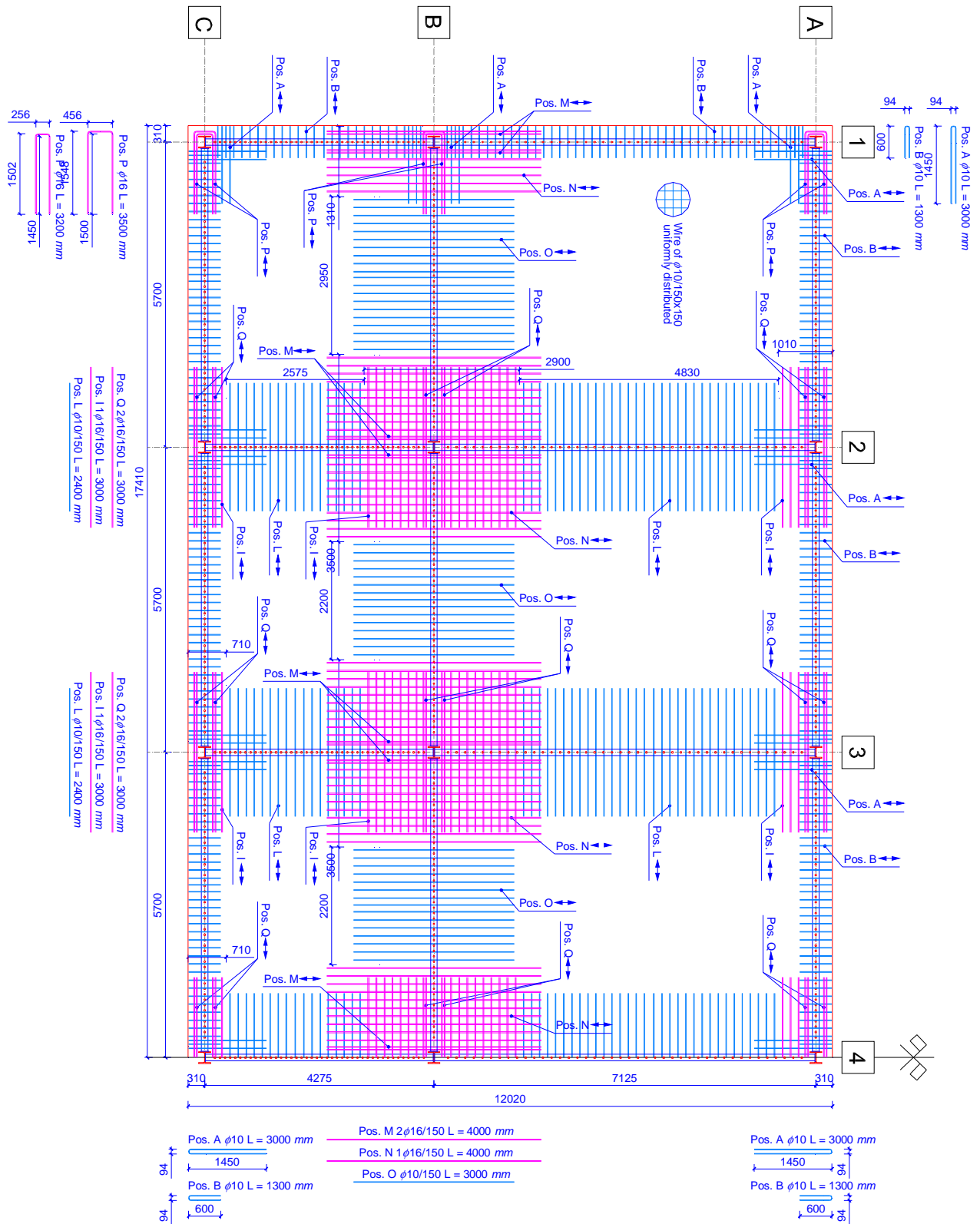


Figure 2-50. Slab Rebars - Upper Side – Asymmetric Configuration (length unit mm)

**MOMENT RESISTING STEEL-CONCRETE COMPOSITE FRAMES UNDER THE COLUMN LOSS SCENARIO:
DESIGN OF THE REFERENCE FRAMES AND OF THE FULL-SCALE SUB-FRAME SPECIMENS**

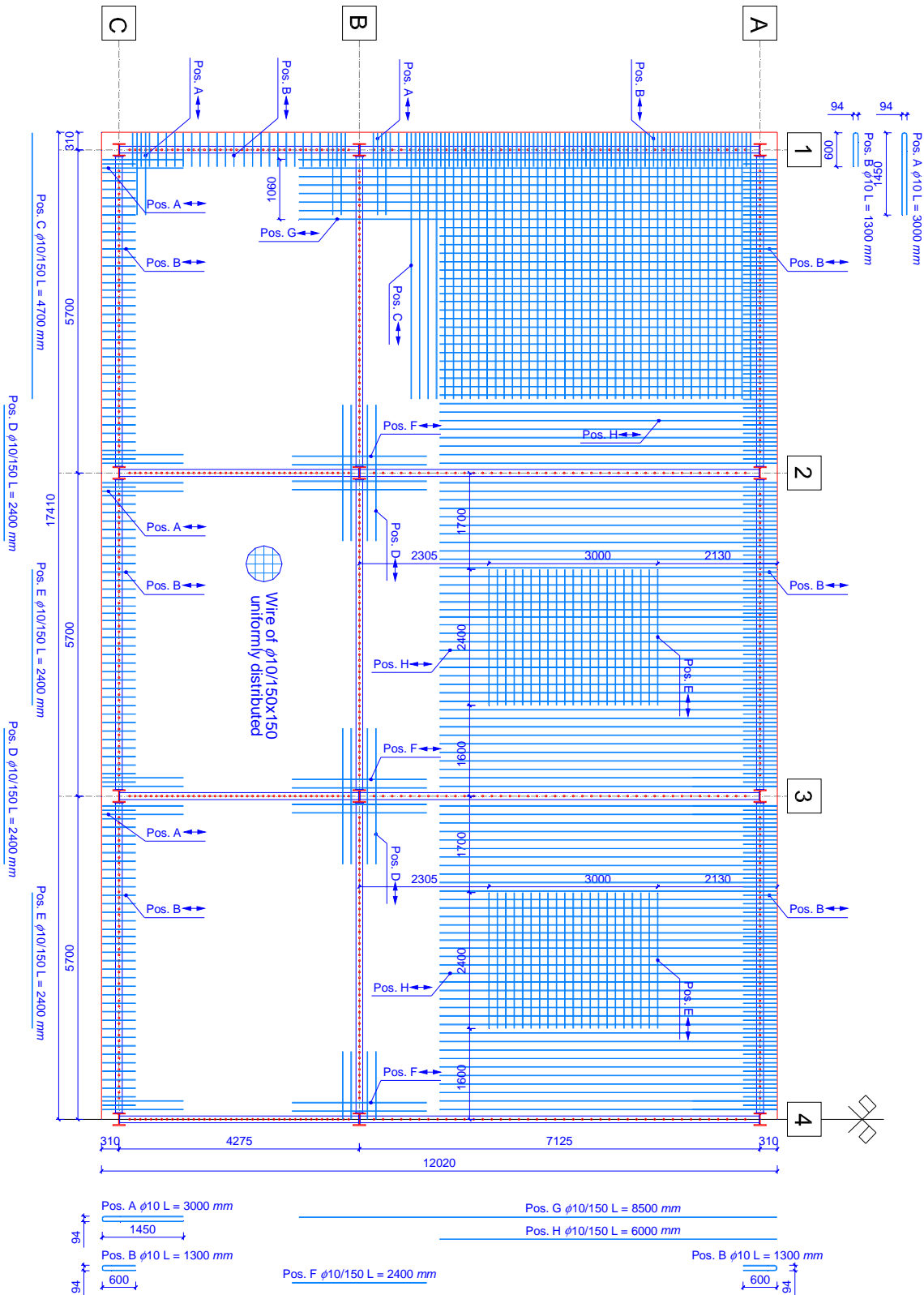


Figure 2-51. Slab Rebars - Lower Side – Asymmetric Configuration (length unit mm)

2.9.3 Slab Shear - ULS

The slab is verified against shear forces by following the EN 1992-1-1 §6.2 [3]. The design forces at the ULS are:

$$V_{Ed,max} = 30 \text{ kN/m} \quad N_{Ed,max} = -40 \text{ kN/m (traction)}$$

The design value for the shear resistance $V_{Rd,c}$ in members not requiring design shear reinforcement is calculated as specified in the EN 1992-1-1 §6.2.2 [3]:

$$V_{Rd,c} = \max \left\{ \left[C_{Rd,c} k (100 \rho_l f_{ck})^{1/3} + k_1 \sigma_{cp} \right] b_w d; (v_{min} + k_1 \sigma_{cp}) b_w d \right\} = 76.65 \text{ kN/m} > V_{Ed}$$

2.9.4 Slab Deflection - SLS

The maximum slab deflection has been evaluated by considering the **Quasi Permanent** load combination as required in EN 1992-1-1 §7.4 [3]. The design value of the bending moment in a portion of the slab of unitary width is:

$$M_{Ed,max} = 12.33 \text{ kNm}$$

Considering a portion of the slab of unitary width and neglecting the presence of rebars the bending moment at cracking is:

$$f_{cm,fl} = \max \left[(1.6 - h/1000) f_{cm}; f_{cm} \right] = 4.20 \text{ MPa} \quad M_{cr} = f_{cm,fl} \cdot \frac{b \cdot h^2}{6} = 15.75 \text{ kNm} > M_{Ed}$$

The slab is not cracked since $M_{cr} > M_{Ed}$. The evaluation of the maximum deflection is conducted considering the moment of inertia of the uncracked section. The finite element model with the effective modulus of elasticity of the concrete in the case of long-term permanent load have been employed for the deflection evaluation as required in the EN 1992-1-1 §7.4.3(4) [3]. The maximum displacement is equal to $\delta = 20.476 \text{ mm}$. The maximum dimension of the slab is equal to $L = 7.125 \text{ m}$ and hence, the ratio L/δ is equal to 347.97.

2.9.5 Slab Stresses - SLS

The stresses on the concrete and on the rebars of the slab are checked with reference to the **Characteristic** and the **Quasi-Permanent** load combinations as required in EN 1992-1-1 §7.2 [3]. The stresses are directly obtained as results of the model of the analysis.

- Characteristic Load Combination

$$\sigma_{c,max} = 12.28 \text{ MPa} < 0.6 f_{ck} = 18 \text{ MPa}$$

$$\sigma_{s,max} = 348 \text{ MPa} < 0.8 f_{yk} = 360 \text{ MPa}$$

- Quasi-Permanent Load Combination

$$\sigma_{c,max} = 8.55 \text{ MPa} < 0.45 f_{ck} = 13.5 \text{ MPa}$$

2.9.6 Beams - Effective width of flange for shear lag

The beams section type is IPE 240 and it is a section class 1 in bending and section class 2 in compression. The dimensions of the effective width of flange for shear lag is calculated by following the indications of EN 1994-1-1 §5.4.1.2 [8]. L_e in the different parts of the beams is defined by following the indications reported in Figure 5.1 of EN 1994-1-1 [8]. Figure 2-52 and

Figure 2-53 reports the effective width of flanges for shear lag of beams respectively in X e Y directions.

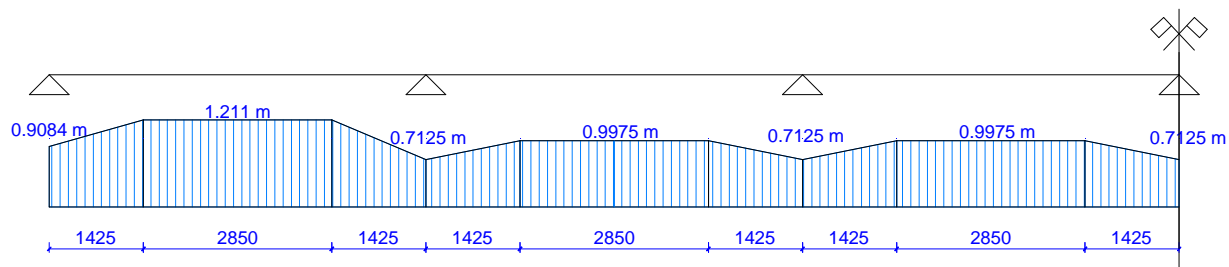


Figure 2-52. Effective width of flanges for shear lag of beams in X direction

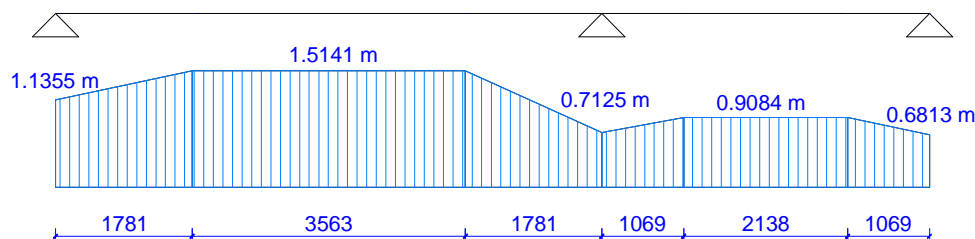
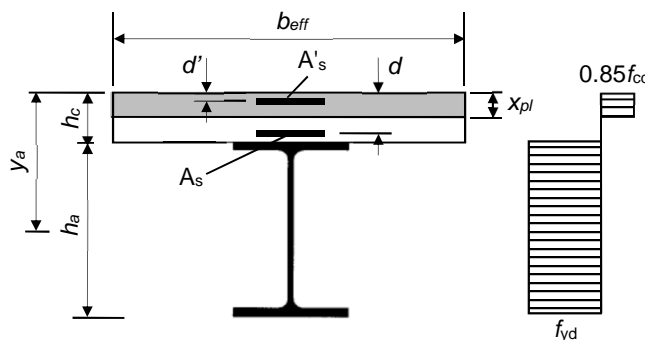


Figure 2-53. Effective width of flanges for shear lag of beams in Y direction

2.9.7 Beams - Maximum positive moment at mid span - Long Span - ULS

The maximum positive bending moment of the beam at mid-span is equal to $M_{Ed} = 216.93 \text{ kNm}$. The beams section type is IPE 240 and the effective width of flange in this position is equal to $b_{eff} = 1.514 \text{ m}$. The calculation of the resisting moment for the ULS condition is reported in the follow.



$$F_{c,max} = 0.85 \cdot h_c \cdot b_{eff} \cdot \frac{f_{ck}}{\gamma_c} = 3860.70 \text{ kN}$$

Plastic resistance of the concrete section

$$F_{a,max} = A \cdot \frac{f_y}{\gamma_{M0}} = 1388.05 \text{ kN}$$

Plastic resistance of the steel section

$$x_{pl} = \frac{F_{a,max}}{0.85 \cdot \frac{f_{ck}}{\gamma_c} \cdot b_{eff}} = 53.93 \text{ mm}$$

Neutral axis position

$$M_{pl} = F_{s,max} \left(\frac{h_a}{2} + h_c - \frac{x_{pl}}{2} \right) = 337.34 \text{ kNm} > M_{Ed}$$

2.9.8 Beams - Maximum positive moment at mid span - Short Span - ULS

The maximum positive bending moment of the beam at mid-span is equal to $M_{Ed} = 49.30 \text{ kNm}$. The beams section type is IPE 240 and the effective width of flange in this position is equal to $b_{eff} = 0.9084 \text{ m}$. The calculation of the resisting moment for the ULS condition is reported in the follow.

$$F_{c,max} = 0.85 \cdot h_c \cdot b_{eff} \cdot \frac{f_{ck}}{\gamma_c} = 2316.42 \text{ kN} \quad \text{Plastic resistance of the concrete section}$$

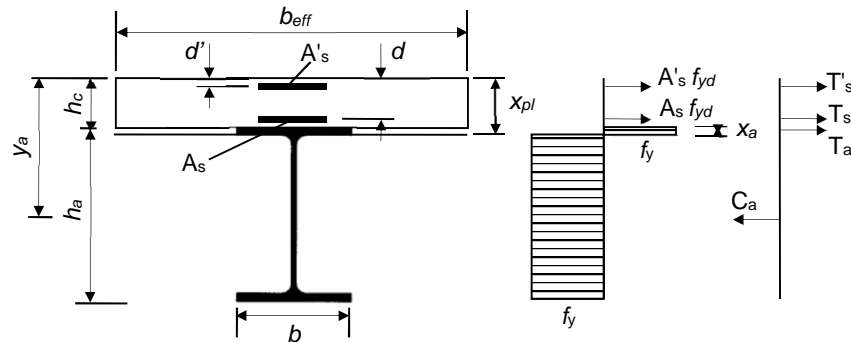
$$F_{a,max} = A \cdot \frac{f_y}{\gamma_{M0}} = 1388.05 \text{ kN} \quad \text{Plastic resistance of the steel section}$$

$$x_{pl} = \frac{F_{a,max}}{0.85 \cdot \frac{f_{ck}}{\gamma_c} \cdot b_{eff}} = 89.88 \text{ mm} \quad \text{Neutral axis position}$$

$$M_{pl} = F_{s,max} \left(\frac{h_a}{2} + h_c - \frac{x_{pl}}{2} \right) = 312.39 \text{ kNm} > M_{Ed}$$

2.9.9 Beams - Maximum negative bending moment at the support- ULS

The maximum negative bending moment of the beam at the support is equal to $M_{Ed} = 149.88 \text{ kNm}$.



The beams section type is IPE 240 and the effective width of flange in this position is equal to $b_{eff} = 712.5 \text{ mm}$. The amount of rebars contained in the effective width of flange are $A'_s = 1363.45 \text{ mm}^2$ ($2\phi 10 + 6\phi 16$, $d' = 34 \text{ mm}$) and $A_s = 471.24 \text{ mm}^2$ ($6\phi 10$, $d = 116 \text{ mm}$) respectively for the upper and lower layers.

$$T'_s = A'_s \cdot \frac{f_{yd}}{\gamma_s} = 533.52 \text{ kN} \quad \text{Tensile force in the rebars;}$$

$$T_s = A_s \cdot \frac{f_{yd}}{\gamma_s} = 184.40 \text{ kN} \quad \text{Tensile force in the rebars;}$$

$$T_a = \frac{1}{2} \left(A \cdot \frac{f_y}{\gamma_{M0}} - T'_s - T_s \right) = 335.42 \text{ kN} \quad \text{Tensile force in steel section;}$$

$$x_{pl} = h_c + \frac{T_a}{b \cdot \frac{f_y}{\gamma_{M0}}} = 157.87 \text{ mm} \quad \text{Neutral axis position}$$

$$C_a = A \frac{f_y}{\gamma_{M0}} - T_a = 1053.34 \text{ kN}$$

Compressive force in the steel section;

$$M_{pl} = C_a(x_{Ca} - x_{pl}) + T_a(x_{pl} - x_{Ta}) + T_s(x_{pl} - x_s) + T'_s(x_{pl} - x'_s) = 189.09 \text{ kN} > M_{Ed}$$

2.9.10 Beams - Maximum shear force at the support- ULS

As suggested in EN 1993-1-1 §6.2.6 [4], only the beams section IPE 240 is considered for the shear resistance. The maximum shear force on the beam is equal to $V_{Ed} = 173.56 \text{ kN}$.

$$V_{Rd} = \frac{A_v \frac{f_{yk}}{\sqrt{3}}}{\gamma_{M0}} = 392.45 \text{ kN} > V_{Ed}$$

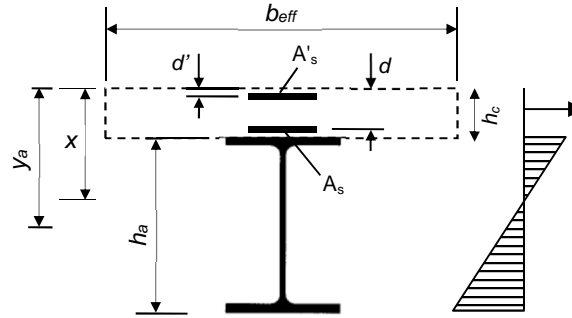
2.9.11 Beams - Calculation of the crack widths - ULS

The crack width is calculated by following the EN 1992-1-1 §7.3.4 [3] as follow.

$$w_k = s_{r,\max}(\varepsilon_{sm} - \varepsilon_{cm}) \quad (2.8)$$

The structure is subjected to the exposure class XC3 where the maximum crack width is equal to $w_{\max} = 0.3 \text{ mm}$ while considering the **Quasi-Permanent** load combination. (EN 1992-1-1 Table 7.1N [3]).

The beams section type is IPE 240 and the effective width of flange in this position is equal to $b_{\text{eff}} = 712.5 \text{ mm}$. The amount of rebars contained in the effective width of flange are $A'_s = 1363.45 \text{ mm}^2$ ($2\emptyset 10 + 6\emptyset 16, d' = 34 \text{ mm}$) and $A_s = 471.24 \text{ mm}^2$ ($6\emptyset 10, d = 116 \text{ mm}$) respectively for the upper and lower layers. The negative bending moment of the beam at the support is equal to $M_{Ed} = 77.56 \text{ kNm}$.



$$A = A_a + A_s + A'_s = 5746.69 \text{ mm}^2$$

Total area of resisting elements in tension;

$$x = \frac{1}{A} (A_a y_a + A_s d + A'_s d') = 201.38 \text{ mm}$$

Position of the neutral axis;

$$J = J_a + A_a (y_a - x)^2 + A_s (x - d)^2 + A'_s (x - d')^2 = 6100.45 \text{ cm}^4$$

Moment of inertia

$$\sigma_{s,t} = \frac{M}{J} (x - d') = 212.80 \text{ MPa}$$

Tensile stress in the upper layer of rebars;

$$\varepsilon_{sm} - \varepsilon_{cm} = \frac{\sigma_{s,t}}{E_s} = 0.001013$$

$$s_{r,\max} = 115.6$$

$$w_k = s_{r,\max} (\varepsilon_{sm} - \varepsilon_{cm}) = 0.1171 \text{ mm} < w_{\max}$$

2.9.12 Columns - Maximum axial force- ULS

The column section type is HEB 220. It is class 1 both in bending and in compression. The maximum axial force on the column is checked by the EN 1993-1-1 §6.2.4 [4]. The maximum axial force on the columns is equal to $N_{Ed} = 2689.47 \text{ kN}$

$$N_{Rd} = \frac{A f_y}{\gamma_{M0}} = 3231 \text{ kN} > N_{Ed}$$

2.9.13 Columns - Maximum shear force- ULS

The column section type is HEB 220. It is class 1 both in bending and in compression. The maximum shear force on the column is checked by the EN 1993-1-1 §6.2.6 [4]. The maximum shear force on the column is equal to $V_{Ed} = 22.75 \text{ kN}$.

$$A_v = A - 2bt_f + (t_w + 2r)t_f = 2792.00 \text{ mm}^2$$

$$V_{Rd} = \frac{A_v f_{yk}}{\sqrt{3} \gamma_{M0}} = 572.25 \text{ kN} > V_{Ed}$$

2.9.14 Columns - Member in bending and axial compression - ULS

The column section type is HEB 220. It is class 1 both in bending and in compression. In order to verify the members which are subjected to combined bending and axial compression, the formulations reported in EN 1993-1-1 §6.3.3 [4] have to be satisfied.

The forces acting in the more stressed column are:

$$N_{Ed} = 2689.47 \text{ kN}$$

$$M_{y,Ed,A} = -17.48 \text{ kNm}$$

$$M_{z,Ed,A} = -7.67 \text{ kNm}$$

$$M_{y,Ed,B} = 2.15 \text{ kNm}$$

$$M_{z,Ed,B} = 3.91 \text{ kNm}$$

The reduction factors for buckling for lateral torsional buckling χ_y , χ_z and χ_{LT} have been calculated by following the instruction of EN 1993-1-1 §6.2.1.2, EN 1993-1-1 §6.3.2.2 and EN 1993-1-1 §6.3.2.3 [4].

$$\chi_y = \frac{1}{\phi_y + \sqrt{\phi_y^2 - \bar{\lambda}_y^2}} = 0.989$$

$$\chi_z = \frac{1}{\phi_z + \sqrt{\phi_z^2 - \bar{\lambda}_z^2}} = 0.917$$

$$\chi_{LT} = \frac{1}{\phi_{LT} + \sqrt{\phi_{LT}^2 - \beta \bar{\lambda}_{LT}^2}} = 0.963$$

The parameters N_{Rk} , $M_{y,Rk}$ and $M_{z,Rk}$ are calculated as define in EN 1993-1-1 Table 6.7 [4].

$$N_{Rk} = f_y A = 355 \text{ MPa} \cdot 9104 \text{ mm}^2 = 3231.92 \text{ kN}$$

$$M_{y,Rk} = f_y W_{pl,y} = 355 \text{ MPa} \cdot 827 \cdot 10^3 \text{ mm}^3 = 293.59 \text{ kNm}$$

$$M_{z,Rk} = f_y W_{pl,z} = 355 \text{ MPa} \cdot 393 \cdot 10^3 \text{ mm}^3 = 139.83 \text{ kNm}$$

The interaction coefficients have been calculated by using the approach reported in EN 1993-1-1 Annex B [4].

$$k_{yy} = \min \left(C_{my} \left(1 + (\bar{\lambda}_y - 0.2) \frac{N_{Ed}}{\chi_y N_{Rk} / \gamma_{M1}} \right); C_{my} \left(1 + 0.8 \frac{N_{Ed}}{\chi_y N_{Rk} / \gamma_{M1}} \right) \right) = 0.574$$

$$k_{zz} = \min \left(C_{mz} \left(1 + (2\bar{\lambda}_z - 0.6) \frac{N_{Ed}}{\chi_z N_{Rk} / \gamma_{M1}} \right); C_{mz} \left(1 + 1.4 \frac{N_{Ed}}{\chi_z N_{Rk} / \gamma_{M1}} \right) \right) = 0.488$$

$$k_{yz} = 0.6k_{zz} = 0.293$$

$$k_{zy} = 0.6k_{yy} = 0.344$$

$$\frac{N_{Ed}}{\chi_y N_{Rk}} + k_{yy} \frac{M_{y,Ed} + \Delta M_{y,Ed}}{\chi_{LT} \frac{M_{y,Rk}}{\gamma_{M1}}} + k_{yz} \frac{M_{z,Ed} + \Delta M_{z,Ed}}{\gamma_{M1}} = 0.894 \leq 1$$

$$\frac{N_{Ed}}{\chi_z N_{Rk}} + k_{zy} \frac{M_{y,Ed} + \Delta M_{y,Ed}}{\chi_{LT} \frac{M_{y,Rk}}{\gamma_{M1}}} + k_{zz} \frac{M_{z,Ed} + \Delta M_{z,Ed}}{\gamma_{M1}} = 0.977 \leq 1$$

2.9.15 Steel Diagonal Bracing - ULS

The forces on the steel braces have been obtained by employing the finite element model previously described without the compressed braces assuming that they do not have compressive resistance as consequence of the buckling.

The bracing section type is the equal length angle L120×120×10 in X direction and the double equal length angle L120×120×10 in Y direction. The resistance of the net section is evaluated by following the instructions of EN 1993-1-8 §3.10.3 [2]. The use of bolts M20 is considered.

The maximum axial force acting in the braces for the X direction is equal to $N_{Ed} = 238.78$ kN.

$$A_{Net} = A - d_0 t = 2098 \text{ mm}^2 \quad N_{u,Rd} = \frac{\beta_3 A_{Net} f_u}{\gamma_{M2}} = 599.2 \text{ kN} > N_{Ed}$$

The maximum axial force acting in the braces for the Y direction is equal to $N_{Ed} = 670.68$ kN.

$$A_{Net} = A - d_0 t = 2098 \text{ mm}^2 \quad N_{u,Rd} = 2 \frac{\beta_3 A_{Net} f_u}{\gamma_{M2}} = 1198.4 \text{ kN} > N_{Ed}$$

2.10 Calculation of the shear connectors - ULS

The beams section type is IPE 240 and it is a section class 1 in bending and section class 2 in compression. The design resistance of a headed stud automatically welded is calculated as reported in EN 1994-1-1 §6.6.3.1 [8]. The number of studs is designed for the full shear connection. The properties of the studs employed are reported in the follow:

$d = 19 \text{ mm}$ Diameter of the shank of the stud;

$h_{sc} = 100 \text{ mm}$ Overall nominal height of the stud;

$f_u = 450 \text{ MPa}$ Ultimate tensile strength of the material of the stud;

$$P_{s,Rd} = \frac{0.8 \cdot f_u \cdot \frac{\pi \cdot d^2}{4}}{\gamma_V} = 81.66 \text{ kN}$$

$$P_{c,Rd} = \frac{0.29 \cdot \alpha \cdot d^2 \sqrt{f_{ck} E_{cm}}}{\gamma_V} = 83.13 \text{ kN}$$

$$P_{Rd} = \min(P_{c,Rd}, P_{s,Rd}) = 81.66 \text{ kN}$$

Design resistance of a headed stud

2.10.1 Beams in X direction

As conservative assumption the internal beam is considered for the design of the studs.

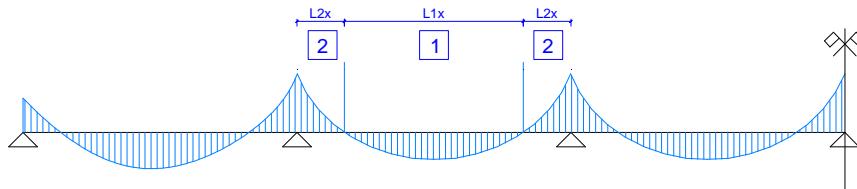


Figure 2-54. Zones for the calculation of the shear connection – X direction

Zone 1

$$V_L = \min(F_{c,\max}, F_{a,\max}) = 1388.76 \text{ kN} \quad n_{stud} = 2 \frac{V_L}{P_{Rd}} = 2 \frac{1388.76 \text{ kN}}{81.66 \text{ kN}} = 34$$

Zone 2

$$V_L = \min(F_{s,\max}, F_{a,\max}) = 717.92 \text{ kN} \quad n_{stud} = \frac{V_L}{P_{Rd}} = \frac{717.92 \text{ kN}}{81.66 \text{ kN}} = 8.8$$

The total number of studs on a beam is equal to $n_{Tot} = 34 + 2 \cdot 9 = 52$. The connectors are spaced uniformly over the length of the beam as reported in EN 1994-1-1 §6.6.1.3 (3) [8].

2.10.2 Beams in Y direction

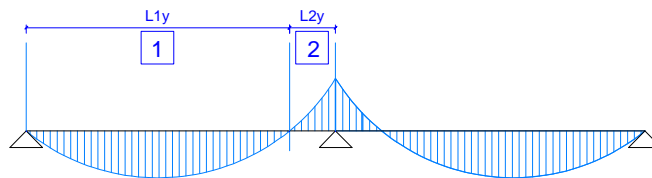


Figure 2-55. Zones for calculation of shear connection – Symmetric structure – Y direction

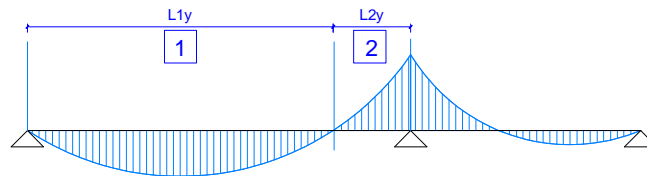


Figure 2-56. Zones for calculation of shear connection – Asymmetric structure – Y direction

Zone 1

$$V_L = \min(F_{c,\max}, F_{a,\max}) = 1388.76 \text{ kN} \quad n_{stud} = 2 \frac{V_L}{P_{Rd}} = 2 \frac{1388.76 \text{ kN}}{81.66 \text{ kN}} = 34$$

Zone 2

$$V_L = \min(F_{s,\max}, F_{a,\max}) = 717.92 \text{ kN} \qquad n_{stud} = \frac{V_L}{P_{Rd}} = 8.8$$

The total number of studs on a beam is equal to $n_{Tot} = 34 + 9 = 43$. The connectors are spaced uniformly over the length of the beam as reported in EN 1994-1-1 §6.6.1.3 (3) [8].

2.11 Design of composite joints

These composite joints employed for this structure are beam-to-column flush end-plate connections. The evaluation of moment resistance and stiffness is based on EN 1993-1-1 [4], EN 1993-1-8 [2] and EN 1994-1-1 [8]. Six different joint configurations have been identified in the model as illustrated in Figure 2-59.

The elements employed in the joints are:

- Column HE 220B;
- Beam IPE 240;
- Solid slab with $h_c = 150 \text{ mm}$;
- Bolts M20 Class 10.9;

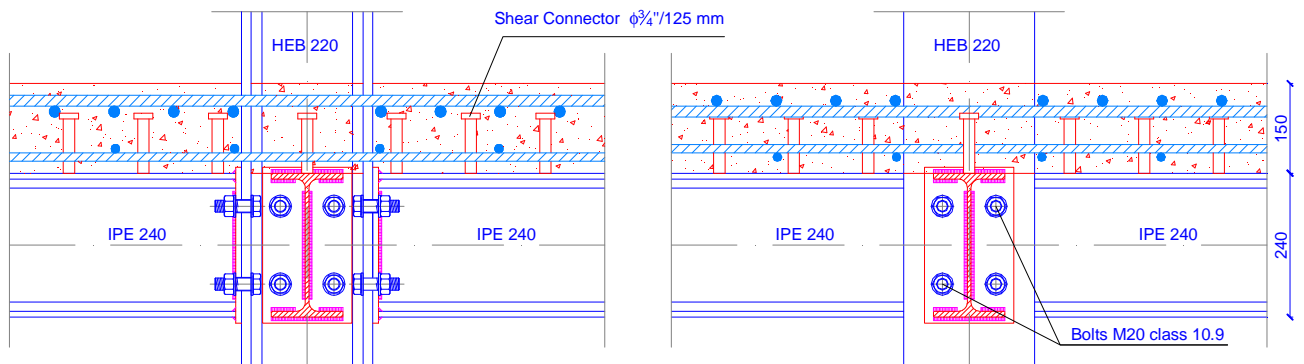


Figure 2-57. Details of the Interior Joint

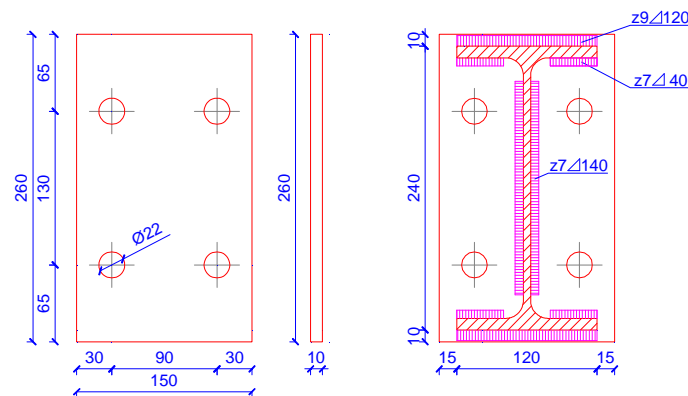


Figure 2-58. Details of the End Plate

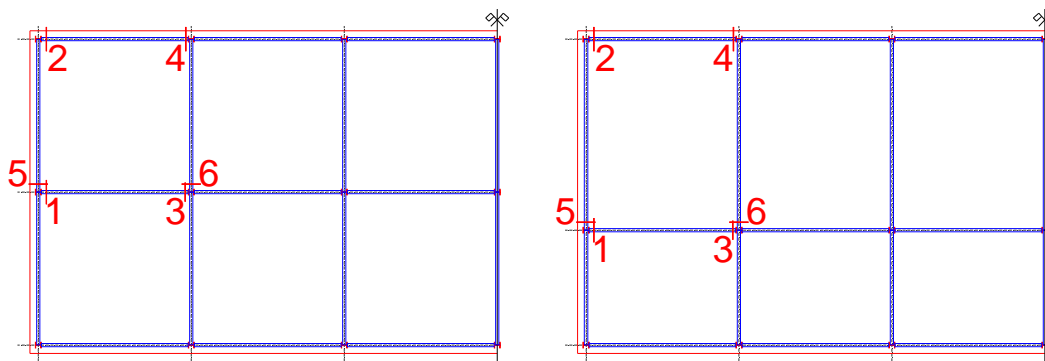


Figure 2-59. Different Joint types for the Symmetric and Asymmetric structure

Joints 1 and 2 are single side joints with the beam that is connected on the flange of the column, which differs for the amount of rebars within the effective width.

Joints 3 and 4 are double side joints with the beam that is connected on the flange of the column, which differs for the amount of rebars within the effective width.

Joints 5 and 6 are double side joints with the beam that is connected on the web of the column, which differs for the amount of rebars within the effective width.

2.11.1 Joint type 1, X direction (single sided joint, $\beta=1$)

The components involved in the calculation of the resistance and stiffness of the joint illustrated in

Figure 2-60 are reported in the follow:

- usrt - Upper slab reinforcement in tension
 - lsrt - Lower slab reinforcement in tension
 - cws - Column web panel in shear
 - cwc - Column web in transverse compression
 - cwt - Column web in transverse tension
 - cfb - Column flange in bending
 - epb - End-plate in bending
 - bfwc - Beam flange and web in compression
 - bwt - Beam web in tension
 - bt - Bolt in tension
- EN 1993-1-8 §6.2.6.1 and §6.3.2
EN 1993-1-8 §6.2.6.2 and §6.3.2
EN 1993-1-8 §6.2.6.3 and §6.3.2
EN 1993-1-8 §6.2.6.4 and §6.3.2
EN 1993-1-8 §6.2.6.5 and §6.3.2
EN 1993-1-8 §6.2.6.7 and §6.3.2
EN 1993-1-8 §6.2.6.8 and §6.3.2

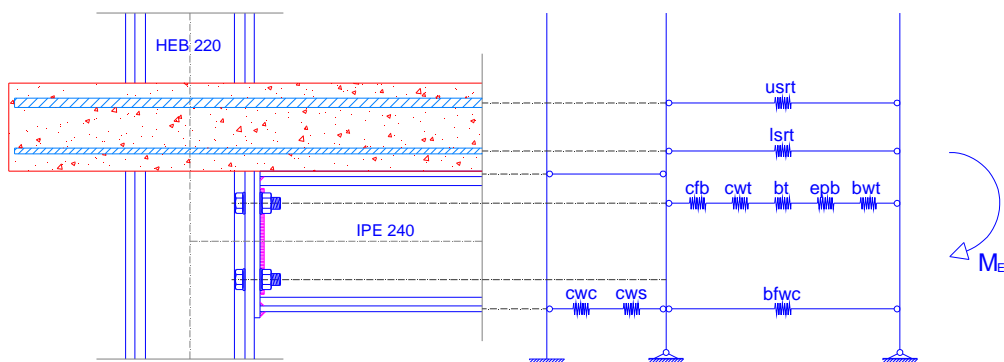


Figure 2-60. Single Side Beam-to-Column Joint connected on column flange (Type 1 and 2)

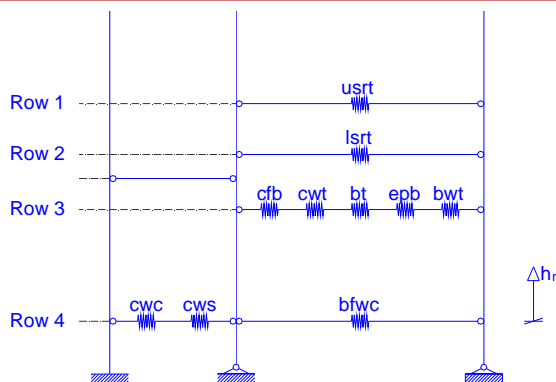


Figure 2-61. Arrangement of the components (Type 1 and 2)

Row 1 ($h_1 = 351.1 \text{ mm}$)

- usrt - Upper slab reinforcement in tension $F_{t,As1,Rd} = 499.10 \text{ kN}$ $k_{13,1,t} = 1.080 \text{ mm}$

Row 2 ($h_2 = 269.1 \text{ mm}$)

- lsrt - Lower slab reinforcement in tension $F_{t,As2,Rd} = 184.40 \text{ kN}$ $k_{13,2,t} = 0.435 \text{ mm}$

Row 3 ($h_3 = 180.1 \text{ mm}$)

- cwt - Column web in transverse tension $F_{t,wc,Rd} = 463.43 \text{ kN}$ $k_3 = 7.11 \text{ mm}$
- cfb - Column flange in bending $F_{t,cfb,Rd} = 339.74 \text{ kN}$ $k_4 = 34.66 \text{ mm}$
- epb - End-plate in bending $F_{t,epb,Rd} = 186.38 \text{ kN}$ $k_5 = 3.59 \text{ mm}$
- bwt - Beam web in tension $F_{t,wb,Rd} = 419.46 \text{ kN}$ $k_8 = \infty$
- bt - Bolt in tension $2 \cdot F_{t,Rd} = 352.80 \text{ kN}$ $k_{10} = 8.46 \text{ mm}$

Row 4 ($h_4 = 0 \text{ mm}$)

- cws - Column web panel in shear $V_{wp,Rd} = 515.02 \text{ kN}$ $k_1 = 3.77 \text{ mm}$
- cwc - Column web in transverse compression $F_{c,wc,Rd} = 544.80 \text{ kN}$ $k_2 = 2.59 \text{ mm}$
- bffc - Beam flange and web in compression $F_{c,fb,Rd} = 565.35 \text{ kN}$ $k_7 = \infty$

The design resistance moment of the composite joint with full shear connection is determined by analogy to provisions for steel joints given in EN 1993-1-8 §6.2.7 [2] taking account of the contribution of reinforcement as specified in EN 1994-1-1 §8.3.2(2) [8]. The moment plastic resistance of the joint is reached as consequence of the failure of the column web in shear.

$$M_{Rd} = F_{t,As1,Rd} \cdot h_1 + (V_{wp,Rd} - F_{t,As1,Rd}) h_2 = 179.52 \text{ kNm}$$

The rotational stiffness of the composite joint with full shear connection is determined by analogy to provisions for steel joints given in EN 1993-1-8 §6.2.7 [2] taking account of the contribution of reinforcement as specified in EN 1994-1-1 §8.3.2(2) [8].

The general method described in EN 1993-1-8 §6.3.3.1 [2] is applied in order to account for the 3 row in tension. In the considered case the effective stiffness coefficients are calculated based on EN 1993-1-8 §6.3.3.1(2) (6.30) [2].

The rotational stiffness of the joint is calculated as specified in EN 1993-1-8 §6.3.1(4) (6.27) [2].

$$S_{j,ini} = \frac{E_s \cdot z_{eq}^2}{\mu \left(\frac{1}{k_{eff,4}} + \frac{1}{k_{eq}} \right)} = 15814.5 \frac{kNm}{rad}$$

2.11.2 Joint type 2, X direction (single sided joint, $\beta=1$)

The components involved in the calculation of the resistance and stiffness of the joint are the same of the Joint type 1 and are illustrated in

Figure 2-60. Joints 1 and 2 are single side joints with the beam that is connected on the flange of the column, which differs for the amount of rebars within the effective width. The components which differ from Joint 1 are the upper slab reinforcement in tension (*usrt*) and the lower slab reinforcement in tension (*lsrt*). Arrangement of the components is reported in Figure 2-61.

Row 1 ($h_1 = 351.1 \text{ mm}$)

- usrt - Upper slab reinforcement in tension $F_{t,As1,Rd} = 406.90 \text{ kN}$ $k_{13,1,t} = 0.910 \text{ mm}$

Row 2 ($h_2 = 269.1 \text{ mm}$)

- lsrt - Lower slab reinforcement in tension $F_{t,As2,Rd} = 92.20 \text{ kN}$ $k_{13,2,t} = 0.230 \text{ mm}$

Row 3 ($h_3 = 180.1 \text{ mm}$)

- cwt - Column web in transverse tension $F_{t,wc,Rd} = 463.43 \text{ kN}$ $k_3 = 7.11 \text{ mm}$
- cfb - Column flange in bending $F_{t,cfb,Rd} = 339.74 \text{ kN}$ $k_4 = 34.66 \text{ mm}$
- epb - End-plate in bending $F_{t,epb,Rd} = 186.38 \text{ kN}$ $k_5 = 3.59 \text{ mm}$
- bwt - Beam web in tension $F_{t,wb,Rd} = 419.46 \text{ kN}$ $k_8 = \infty$
- bt - Bolt in tension $2 \cdot F_{t,Rd} = 352.80 \text{ kN}$ $k_{10} = 8.46 \text{ mm}$

Row 4 ($h_4 = 0 \text{ mm}$)

- cws - Column web panel in shear $V_{wp,Rd} = 515.02 \text{ kN}$ $k_1 = 3.77 \text{ mm}$
- cwc - Column web in transverse compression $F_{c,wc,Rd} = 544.80 \text{ kN}$ $k_2 = 2.59 \text{ mm}$
- bfwc - Beam flange and web in compression $F_{c,fb,Rd} = 565.35 \text{ kN}$ $k_7 = \infty$

The design resistance moment of the composite joint with full shear connection is determined by analogy to provisions for steel joints given in EN 1993-1-8 §6.2.7 [2] taking account of the contribution of reinforcement as specified in EN 1994-1-1 §8.3.2(2) [8]. The moment plastic resistance of the joint is reached as consequence of the failure of the column web in shear.

$$M_{Rd} = F_{t,As1,Rd} \cdot h_1 + F_{t,As2,Rd} \cdot h_2 + (V_{wp,Rd} - F_{t,As1,Rd} - F_{t,As2,Rd}) h_3 = 170.54 \text{ kNm}$$

The rotational stiffness of the composite joint with full shear connection is determined by analogy to provisions for steel joints given in EN 1993-1-8 §6.2.7 [2] taking account of the contribution of reinforcement as specified in EN 1994-1-1 §8.3.2(2) [8].

The general method described in EN 1993-1-8 §6.3.3.1 [2] is applied in order to account for the 3 row in tension. In the considered case the effective stiffness coefficients are calculated based on EN 1993-1-8 §6.3.3.1 (2) (6.30) [2].

The rotational stiffness of the joint is calculated as specified in EN 1993-1-8 §6.3.1(4) (6.27) [2].

$$S_{j,ini} = \frac{E_s \cdot z_{eq}^2}{\mu \left(\frac{1}{k_{eff,4}} + \frac{1}{k_{eq}} \right)} = 14392.1 \frac{kNm}{rad}$$

2.11.3 Joint type 3, X direction (double sided joint, $\beta=0$)

The components involved in the calculation of the resistance and stiffness of the joint are the same of the Joint type 1 and are illustrated in Figure 2-62. Joints 3 and 4 are double side joints with the beam that is connected on the flange of the column. These joints differ from the Joints 1 and 2 for the absence of the component column web panel in shear (cws). The components which differ from Joint 1 are the upper slab reinforcement in tension (usr), the lower slab reinforcement in tension (lsrt), the column web in transverse compression (cwc) and the column web in transverse tension (cwt). Only the calculation of these components is reported in the following.

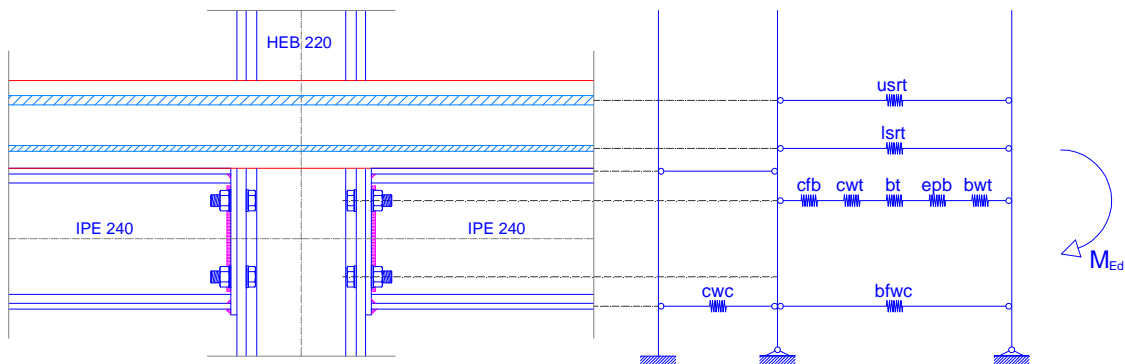


Figure 2-62. Double Side Beam-to-Column Joint connected on column flange (Type 3 and 4)

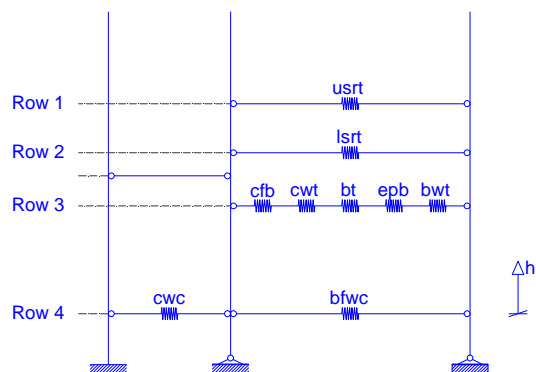


Figure 2-63. Arrangement of the components (Type 3 and 4)

Row 1 ($h_1 = 351.1 mm$)

• usrt	- Upper slab reinforcement in tension	$F_{t,As1,Rd} = 533.52 \text{ kN}$	$k_{13,1,t} = 2.660 \text{ mm}$
Row 2 ($h_2 = 269.1 \text{ mm}$)			
• lsrt	- Lower slab reinforcement in tension	$F_{t,As2,Rd} = 184.40 \text{ kN}$	$k_{13,2,t} = 1.170 \text{ mm}$
Row 3 ($h_3 = 180.1 \text{ mm}$)			
• cwt	- Column web in transverse tension	$F_{t,wc,Rd} = 547.76 \text{ kN}$	$k_3 = 7.11 \text{ mm}$
• cfb	- Column flange in bending	$F_{t,fb,Rd} = 339.74 \text{ kN}$	$k_4 = 34.66 \text{ mm}$
• epb	- End-plate in bending	$F_{t,epb,Rd} = 186.38 \text{ kN}$	$k_5 = 3.59 \text{ mm}$
• bwt	- Beam web in tension	$F_{t,wb,Rd} = 419.46 \text{ kN}$	$k_8 = \infty$
• bt	- Bolt in tension	$2 \cdot F_{t,Rd} = 352.80 \text{ kN}$	$k_{10} = 8.46 \text{ mm}$
Row 4 ($h_4 = 0 \text{ mm}$)			
• cwc	- Column web in transverse compression	$F_{c,wc,Rd} = 699.12 \text{ kN}$	$k_2 = 2.59 \text{ mm}$
• bfwc	- Beam flange and web in compression	$F_{c,fb,Rd} = 565.35 \text{ kN}$	$k_7 = \infty$

The design resistance moment of the composite joint with full shear connection is determined by analogy to provisions for steel joints given in EN 1993-1-8 §6.2.7 [2] taking account of the contribution of reinforcement as specified in EN 1994-1-1 §8.3.2(2) [8]. The moment plastic resistance of the joint is reached as consequence of the failure of the beam flange and web in compression.

$$M_{Rd} = F_{t,As1,Rd} \cdot h_1 + (F_{c,fb,Rd} - F_{t,As1,Rd}) h_2 = 195.88 \text{ kNm}$$

The rotational stiffness of the composite joint with full shear connection is determined by analogy to provisions for steel joints given in EN 1993-1-8 §6.2.7 [2] taking account of the contribution of reinforcement as specified in EN 1994-1-1 §8.3.2(2) [8].

The general method described in EN 1993-1-8 §6.3.3.1 [2] is applied in order to account for the 3 row in tension. In the considered case the effective stiffness coefficients are calculated based on EN 1993-1-8 §6.3.3.1(2) (6.30) [2].

The rotational stiffness of the joint is calculated as specified in EN 1993-1-8 §6.3.1(4) (6.27) [2].

$$S_{j,ini} = \frac{E_s \cdot z_{eq}^2}{\mu \left(\frac{1}{k_{eff,4}} + \frac{1}{k_{eq}} \right)} = 32741.4 \frac{\text{kNm}}{\text{rad}}$$

2.11.4 Joint type 4, X direction (double sided joint, $\beta=0$)

The components involved in the calculation of the resistance and stiffness of the joint are the same of the Joint type 1 and are illustrated in Figure 2-62. Joints 3 and 4 are double side joints with the beam that is connected on the flange of the column, which differs for the amount of rebars within the effective width. The components which differ from Joint 3 are the upper slab reinforcement in tension (*usrt*) and the lower slab reinforcement in tension (*lsrt*). Only the calculation of these two components is reported in the following. Arrangement of the components is reported in Figure 2-63.

Row 1 ($h_1 = 351.1 \text{ mm}$)

- usrt - Upper slab reinforcement in tension $F_{t,As1,Rd} = 454.85 \text{ kN}$ $k_{13,1,t} = 2.410 \text{ mm}$

Row 2 ($h_2 = 269.1 \text{ mm}$)

- lsrt - Lower slab reinforcement in tension $F_{t,As2,Rd} = 61.47 \text{ kN}$ $k_{13,2,t} = 0.530 \text{ mm}$

Row 3 ($h_3 = 180.1 \text{ mm}$)

- cwt - Column web in transverse tension $F_{t,wc,Rd} = 547.76 \text{ kN}$ $k_3 = 7.11 \text{ mm}$
- cfb - Column flange in bending $F_{t,cfb,Rd} = 339.74 \text{ kN}$ $k_4 = 34.66 \text{ mm}$
- epb - End-plate in bending $F_{t,epb,Rd} = 186.38 \text{ kN}$ $k_5 = 3.59 \text{ mm}$
- bwt - Beam web in tension $F_{t,wb,Rd} = 419.46 \text{ kN}$ $k_8 = \infty$
- bt - Bolt in tension $2 \cdot F_{t,Rd} = 352.80 \text{ kN}$ $k_{10} = 8.46 \text{ mm}$

Row 4 ($h_4 = 0 \text{ mm}$)

- cwc - Column web in transverse compression $F_{c,wc,Rd} = 699.12 \text{ kN}$ $k_2 = 2.59 \text{ mm}$
- bfwc - Beam flange and web in compression $F_{c,fb,Rd} = 565.35 \text{ kN}$ $k_7 = \infty$

The design resistance moment of the composite joint with full shear connection is determined by analogy to provisions for steel joints given in EN 1993-1-8 §6.2.7 [2] taking account of the contribution of reinforcement as specified in EN 1994-1-1 §8.3.2(2) [8]. The moment plastic resistance of the joint is reached as consequence of the failure of the beam flange and web in compression.

$$M_{Rd} = F_{t,As1,Rd} \cdot h_1 + F_{t,As2,Rd} \cdot h_2 + (F_{c,fb,Rd} - F_{t,As1,Rd} - F_{t,As2,Rd}) h_3 = 185.07 \text{ kNm}$$

The rotational stiffness of the composite joint with full shear connection is determined by analogy to provisions for steel joints given in EN 1993-1-8 §6.2.7 [2] taking account of the contribution of reinforcement as specified in EN 1994-1-1 §8.3.2(2) [8].

The general method described in EN 1993-1-8 §6.3.3.1 [2] is applied in order to account for the 3 row in tension. In the considered case the effective stiffness coefficients are calculated based on EN 1993-1-8 §6.3.3.1(2) (6.30) [2].

The rotational stiffness of the joint is calculated as specified in EN 1993-1-8 §6.3.1(4) (6.27) [2].

$$S_{j,ini} = \frac{E_s \cdot z_{eq}^2}{\mu \left(\frac{1}{k_{eff,4}} + \frac{1}{k_{eq}} \right)} = 30778.7 \frac{\text{kNm}}{\text{rad}}$$

2.11.5 Joint type 5, Y direction (double sided joint, $\beta=0$)

The components involved in the calculation of the resistance and stiffness of the joint illustrated in Figure 2-64 are reported in the follow:

- usrt - Upper slab reinforcement in tension
- lsrt - Lower slab reinforcement in tension
- epb - End-plate in bending EN 1993-1-8 §6.2.6.5 and §6.3.2

- bfwc - Beam flange and web in compression EN 1993-1-8 §6.2.6.7 and §6.3.2
- bwt - Beam web in tension EN 1993-1-8 §6.2.6.8 and §6.3.2
- bt - Bolt in tension

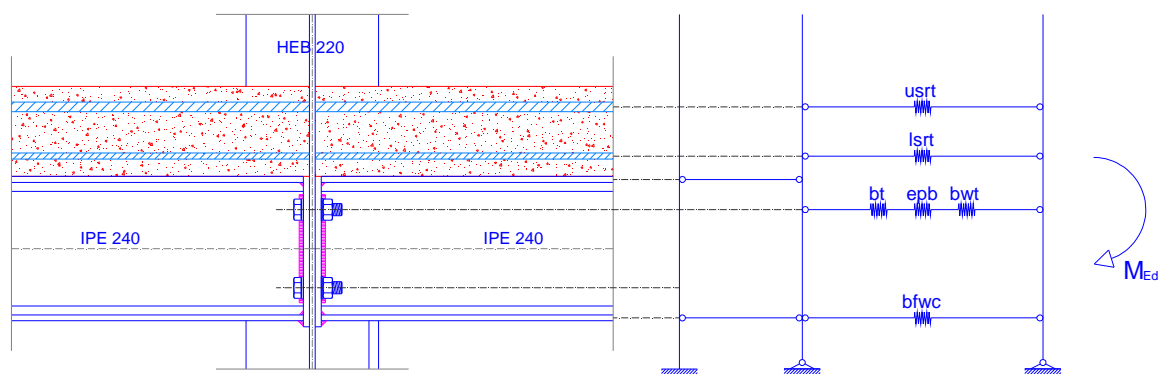


Figure 2-64. Double Side Beam-to-Column Joint connected on column web (Type 5 and 6)

Joints 5 and 6 are double side joints with the beam that is connected on the web of the column. These joints differ from the joints from 1 up to 4 for the absence of the following components:

- cws - Column web panel in shear
- cwc - Column web in transverse compression
- cwt - Column web in transverse tension
- cfb - Column flange in bending

The components which differ from those of Joint 1 are the upper slab reinforcement in tension (*usrt*), the lower slab reinforcement in tension (*lsrt*) and the bolt in tension (*bt*).

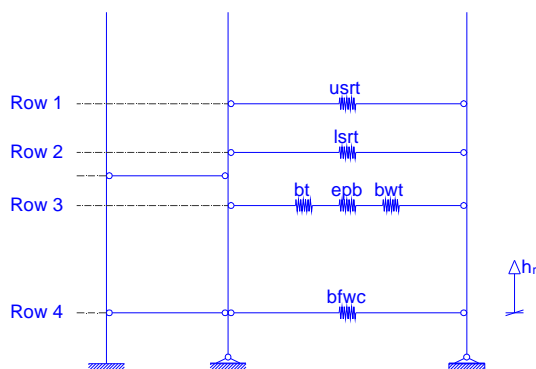


Figure 2-65. Arrangement of the components (Type 5 and 6)

Row 1 ($h_1 = 351.1 \text{ mm}$)

- usrt - Upper slab reinforcement in tension $F_{t,As1,Rd} = 454.85 \text{ kN}$ $k_{13,1,t} = 2.130 \text{ mm}$

Row 2 ($h_2 = 269.1 \text{ mm}$)

- lsrt - Lower slab reinforcement in tension $F_{t,As2,Rd} = 61.47 \text{ kN}$ $k_{13,2,t} = 0.500 \text{ mm}$

Row 3 ($h_3 = 180.1 \text{ mm}$)

- | | | |
|------------------------------|--|-----------------------------|
| • epb - End-plate in bending | $F_{t,epb,Rd} = 186.38 \text{ kN}$ | $k_5 = 3.59 \text{ mm}$ |
| • bwt - Beam web in tension | $F_{t,wb,Rd} = 419.46 \text{ kN}$ | $k_8 = \infty$ |
| • bt - Bolt in tension | $2 \cdot F_{t,Rd} = 352.80 \text{ kN}$ | $k_{10} = 15.73 \text{ mm}$ |

Row 4 ($h_4 = 0 \text{ mm}$)

- | | | |
|---|-----------------------------------|----------------|
| • bfwc - Beam flange and web in compression | $F_{c,fb,Rd} = 565.35 \text{ kN}$ | $k_7 = \infty$ |
|---|-----------------------------------|----------------|

The design resistance moment of the composite joint with full shear connection is determined by analogy to provisions for steel joints given in EN 1993-1-8 §6.2.7 [2] taking account of the contribution of reinforcement as specified in EN 1994-1-1 §8.3.2(2) [8]. The moment plastic resistance of the joint is reached as consequence of the failure of the beam flange and web in compression.

$$M_{Rd} = F_{t,As1,Rd} \cdot h_1 + F_{t,As2,Rd} \cdot h_2 + (F_{c,fb,Rd} - F_{t,As1,Rd} - F_{t,As2,Rd}) h_3 = 185.07 \text{ kNm}$$

The rotational stiffness of the composite joint with full shear connection is determined by analogy to provisions for steel joints given in EN 1993-1-8 §6.2.7 [2] taking account of the contribution of reinforcement as specified in EN 1994-1-1 §8.3.2(2) [8].

The general method described in EN 1993-1-8 §6.3.3.1 [2] is applied in order to account for the 3 row in tension. In the considered case the effective stiffness coefficients are calculated based on EN 1993-1-8 §6.3.3.1(2) (6.30) [2].

The rotational stiffness of the joint is calculated as specified in EN 1993-1-8 §6.3.1(4) (6.27) [2].

$$S_{j,ini} = \frac{E_s \cdot z_{eq}^2}{\mu \left(\frac{1}{k_{eff,4}} + \frac{1}{k_{eq}} \right)} = 82601.1 \frac{\text{kNm}}{\text{rad}} \quad \text{Moment resistance of the joint}$$

2.11.6 Joint type 6, Y direction (double sided joint, $\beta=0$)

The components involved in the calculation of the resistance and stiffness of the joint are the same of the Joint type 5 and are illustrated in Figure 2-64. The components which differ from Joint 5 are the upper slab reinforcement in tension (*usrt*) and the lower slab reinforcement in tension (*lsrt*). Arrangement of the components is reported in Figure 2-65.

Row 1 ($h_1 = 351.1 \text{ mm}$)

- | | | |
|--|------------------------------------|---------------------------------|
| • usrt - Upper slab reinforcement in tension | $F_{t,As1,Rd} = 533.52 \text{ kN}$ | $k_{13,1,t} = 2.330 \text{ mm}$ |
|--|------------------------------------|---------------------------------|

Row 2 ($h_2 = 269.1 \text{ mm}$)

- | | | |
|--|------------------------------------|---------------------------------|
| • lsrt - Lower slab reinforcement in tension | $F_{t,As2,Rd} = 184.40 \text{ kN}$ | $k_{13,2,t} = 1.090 \text{ mm}$ |
|--|------------------------------------|---------------------------------|

Row 3 ($h_3 = 180.1 \text{ mm}$)

- | | | |
|------------------------------|--|-----------------------------|
| • epb - End-plate in bending | $F_{t,epb,Rd} = 186.38 \text{ kN}$ | $k_5 = 3.59 \text{ mm}$ |
| • bwt - Beam web in tension | $F_{t,wb,Rd} = 419.46 \text{ kN}$ | $k_8 = \infty$ |
| • bt - Bolt in tension | $2 \cdot F_{t,Rd} = 352.80 \text{ kN}$ | $k_{10} = 15.73 \text{ mm}$ |

Row 4 ($h_4 = 0 \text{ mm}$)

- bfwc - Beam flange and web in compression $F_{c,fb,Rd} = 565.35 \text{ kN}$ $k_7 = \infty$

The design resistance moment of the composite joint with full shear connection is determined by analogy to provisions for steel joints given in EN 1993-1-8 §6.2.7 [2] taking account of the contribution of reinforcement as specified in EN 1994-1-1 §8.3.2(2) [8]. The moment plastic resistance of the joint is reached as consequence of the failure of the beam flange and web in compression.

$$M_{Rd} = F_{t,Asl,Rd} \cdot h_1 + (F_{c,fb,Rd} - F_{t,Asl,Rd}) h_2 = 195.88 \text{ kNm} \quad \text{Moment resistance} \quad \text{EN 1993-1-8 §6.2.7.2 [2].}$$

The rotational stiffness of the composite joint with full shear connection is determined by analogy to provisions for steel joints given in EN 1993-1-8 §6.2.7 [2] taking account of the contribution of reinforcement as specified in EN 1994-1-1 §8.3.2(2) [8].

The general method described in EN 1993-1-8 §6.3.3.1 [2] is applied in order to account for the 3 row in tension. In the considered case the effective stiffness coefficients are calculated based on EN 1993-1-8 §6.3.3.1(2) (6.30) [2].

The rotational stiffness of the joint is calculated as specified in EN 1993-1-8 §6.3.1(4) (6.27) [2].

$$S_{j,ini} = \frac{E_s \cdot z_{eq}^2}{\mu \left(\frac{1}{k_{eff,4}} + \frac{1}{k_{eq}} \right)} = 96749.0 \frac{\text{kNm}}{\text{rad}} \quad \text{Moment resistance of the joint}$$

2.11.7 Shear components for Joints

- Bolt in shear

The joints employ 4 bolts where 2 are in traction and 2 works in shear. The shear resistance of the single bolt is calculated as reported in EN 1993-1-8 §3.6.1 Table 3.4 [2]. The shear resistance has been reduced by factor 0,4/1,4 due to tension in bolts.

$$F_{v,Rd} = \frac{\alpha_v f_{ub} A}{\gamma_{M2}} = 98.00 \text{ kN} \quad \text{Resistance of the single bolt}$$

$$V_{Rd,1} = 252.1 \text{ kN}$$

- End plate in bearing

The bearing resistance of the end plate is calculated as reported in EN 1993-1-8 §3.6.1 Table 3.4 [2].

$$k_1 = \min\left(2.8 \frac{e_2}{d_0} / 1.7; 2.5\right) = 2.118 \quad \alpha_b = \min\left(\frac{f_{ub}}{f_u}; 1\right) = 1$$

$$F_{b,Rd} = \frac{k_1 \alpha_b f_u d t}{\gamma_{M2}} = 172.83 \text{ kN}$$

$$V_{Rd,2} = 691.3 \text{ kN}$$

- Column flange in bearing

The bearing resistance of the column flange is calculated as reported in EN 1993-1-8 §3.6.1 Table 3.4 [2].

$$k_1 = \min\left(2.8 \frac{e_2}{d_0} / 1.7; 2.5\right) = 2.5 \quad \alpha_b = \min\left(\frac{f_{ub}}{f_u}; 1\right) = 1$$

$$F_{b,Rd} = \frac{k_1 \alpha_b f_u d t}{\gamma_{M2}} = 326.40 \text{ kN}$$

$$V_{Rd,3} = 1305.60 \text{ kN}$$

- Shear resistance of joints

The shear resistance of the joint is equal to the shear resistance of the weakest component.

$$V_{Rd} = 252.1 \text{ kN}$$

2.11.8 Joint design for the Symmetric Configuration - ULS

- Joint type 1 - X direction (single side joint, $\beta=1$)

The maximum bending moment and the maximum shear force on the joint type 1 of the *Symmetric* structure are respectively $M_{Ed} = 4.68 \text{ kNm}$ and $V_{Ed} = 124.46 \text{ kN}$.

$$M_{Rd} = 179.52 \text{ kNm} > M_{Ed}$$

$$V_{Rd} = 252.1 \text{ kN} > V_{Ed}$$

- Joint type 2 - X direction (single side joint, $\beta=1$)

The maximum bending moment and the maximum shear force on the joint type 2 of the *Symmetric* structure are respectively $M_{Ed} = 5.87 \text{ kNm}$ and $V_{Ed} = 56.23 \text{ kN}$.

$$M_{Rd} = 170.54 \text{ kNm} > M_{Ed}$$

$$V_{Rd} = 252.1 \text{ kN} > V_{Ed}$$

- *Joint type 3 - X direction (double side joint, $\beta=0$)*

The maximum bending moment and the maximum shear force on the joint type 3 of the *Symmetric* structure are respectively $M_{Ed} = 98.05 \text{ kNm}$ and $V_{Ed} = 145.68 \text{ kN}$.

$$M_{Rd} = 195.88 \text{ kNm} > M_{Ed}$$

$$V_{Rd} = 252.1 \text{ kN} > V_{Ed}$$

- *Joint type 4 - X direction (double side joint, $\beta=0$)*

The maximum bending moment and the maximum shear force on the joint type 4 of the *Symmetric* structure are respectively $M_{Ed} = 33.89 \text{ kNm}$ and $V_{Ed} = 54.81 \text{ kN}$.

$$M_{Rd} = 185.07 \text{ kNm} > M_{Ed}$$

$$V_{Rd} = 252.1 \text{ kN} > V_{Ed}$$

- *Joint type 5 - Y direction (double side joint, $\beta=0$)*

The maximum bending moment and the maximum shear force on the joint type 5 of the *Symmetric* structure are respectively $M_{Ed} = 41.42 \text{ kNm}$ and $V_{Ed} = 56.11 \text{ kN}$.

$$M_{Rd} = 185.07 \text{ kNm} > M_{Ed}$$

$$V_{Rd} = 252.1 \text{ kN} > V_{Ed}$$

- *Joint type 6 - Y direction (double side joint, $\beta=0$)*

The maximum bending moment and the maximum shear force on the joint type 5 of the *Symmetric* structure are respectively $M_{Ed} = 109.18 \text{ kNm}$ and $V_{Ed} = 141.51 \text{ kN}$.

$$M_{Rd} = 195.88 \text{ kNm} > M_{Ed}$$

$$V_{Rd} = 252.1 \text{ kN} > V_{Ed}$$

2.11.9 Joint design for the Asymmetric Configuration - ULS

- *Joint type 1 - X direction (single side joint, $\beta=1$)*

The maximum bending moment and the maximum shear force on the joint type 1 of the *Asymmetric* structure are respectively $M_{Ed} = 16.63 \text{ kNm}$ and $V_{Ed} = 134.56 \text{ kN}$.

$$M_{Rd} = 179.52 \text{ kNm} > M_{Ed}$$

$$V_{Rd} = 252.1 \text{ kN} > V_{Ed}$$

- *Joint type 2 - X direction (single side joint, $\beta=1$)*

The maximum bending moment and the maximum shear force on the joint type 2 of the *Asymmetric* structure are respectively $M_{Ed} = 11.29 \text{ kNm}$ and $V_{Ed} = 62.10 \text{ kN}$.

$$M_{Rd} = 170.54 \text{ kNm} > M_{Ed}$$

$$V_{Rd} = 252.1 \text{ kN} > V_{Ed}$$

- *Joint type 3 - X direction (double side joint, $\beta=0$)*

The maximum bending moment and the maximum shear force on the joint type 3 of the *Asymmetric* structure are respectively $M_{Ed} = 104.31 \text{ kNm}$ and $V_{Ed} = 149.92 \text{ kN}$.

$$M_{Rd} = 195.88 \text{ kNm} > M_{Ed}$$

$$V_{Rd} = 252.1 \text{ kN} > V_{Ed}$$

- *Joint type 4 - X direction (double side joint, $\beta=0$)*

The maximum bending moment and the maximum shear force on the joint type 4 of the *Asymmetric* structure are respectively $M_{Ed} = 42.10 \text{ kNm}$ and $V_{Ed} = 63.86 \text{ kN}$.

$$M_{Rd} = 185.07 \text{ kNm} > M_{Ed}$$

$$V_{Rd} = 252.1 \text{ kN} > V_{Ed}$$

- *Joint type 5 - Y direction (double side joint, $\beta=0$)*

The maximum bending moment and the maximum shear force on the joint type 5 of the *Asymmetric* structure are respectively $M_{Ed} = 65.32 \text{ kNm}$ and $V_{Ed} = 74.25 \text{ kN}$.

$$M_{Rd} = 185.07 \text{ kNm} > M_{Ed}$$

$$V_{Rd} = 252.1 \text{ kN} > V_{Ed}$$

- *Joint type 6 - Y direction (double side joint, $\beta=0$)*

The maximum bending moment and the maximum shear force on the joint type 5 of the *Asymmetric* structure are respectively $M_{Ed} = 149.88 \text{ kNm}$ and $V_{Ed} = 173.56 \text{ kN}$.

$$M_{Rd} = 195.88 \text{ kNm} > M_{Ed}$$

$$V_{Rd} = 252.1 \text{ kN} > V_{Ed}$$

3 DESIGN OF THE EXPERIMENTAL TESTS

The 3-D full-scale tests were performed at the laboratory of Material and Testing of the University of Trento. The facilities of the laboratory were the starting point for planning the 3-D tests. The lab is equipped with a 42 m long strong floor and to the 9.5 m height reaction L shaped wall (Figure 3-1 and Figure 3-2). Holes in a regular pattern on both the floor and the reaction wall allowing an easy connection of specimens and actuators. Two bridge-cranes allow an easy handling of the specimens. A high pressure oil network characterized by 210 bar, 1500 l/min flow in the main line, 1200 l/min flow in the raising line and 600 kW oil pumps allows the effective connection of several actuators, also distributing them in far apart locations. A support for a queen post truss permanently located in the lab and an emergency escape at the end of the lab limited the available area for test to a square area with side of approximately 13.6 m (Figure 3-3).

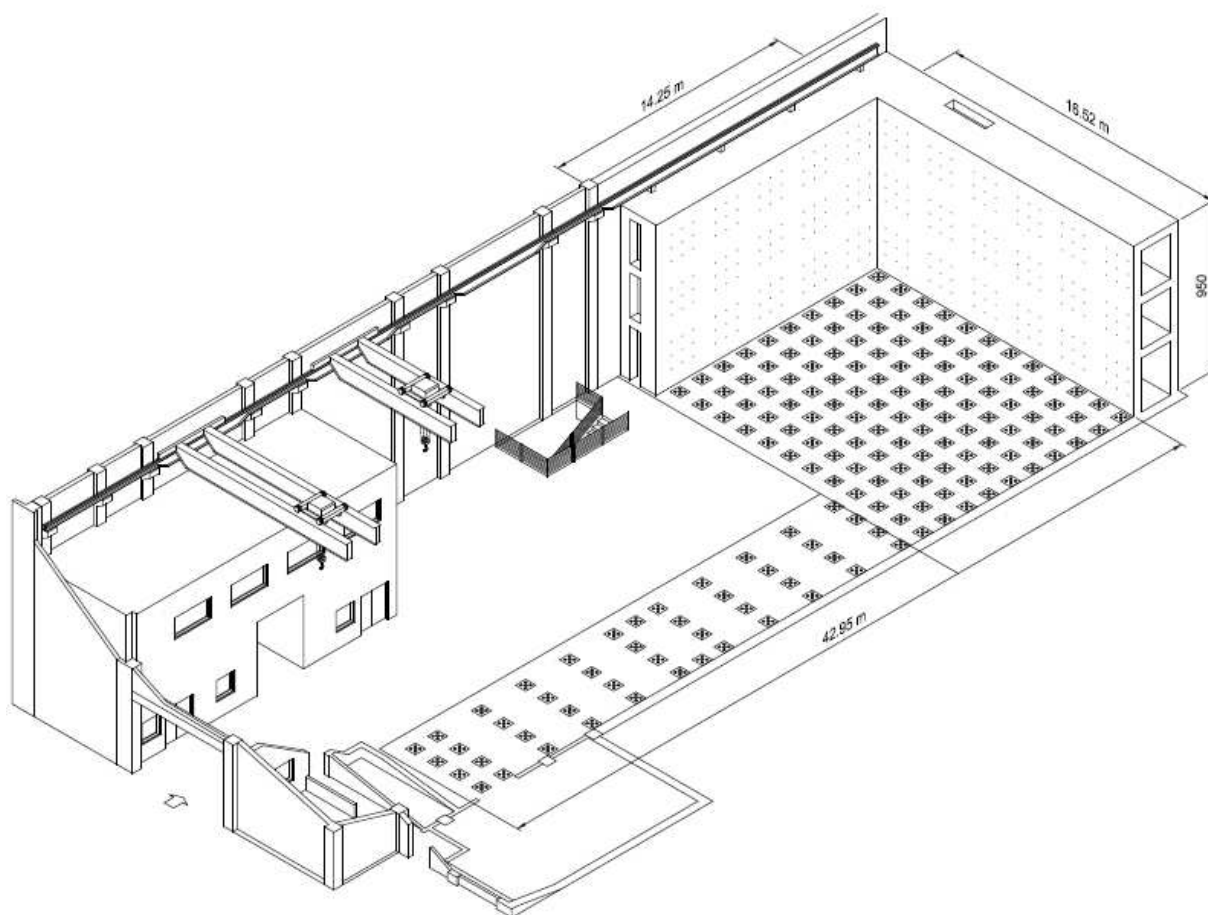


Figure 3-1: 3-D view of the laboratory of Material and Testing of the University of Trento

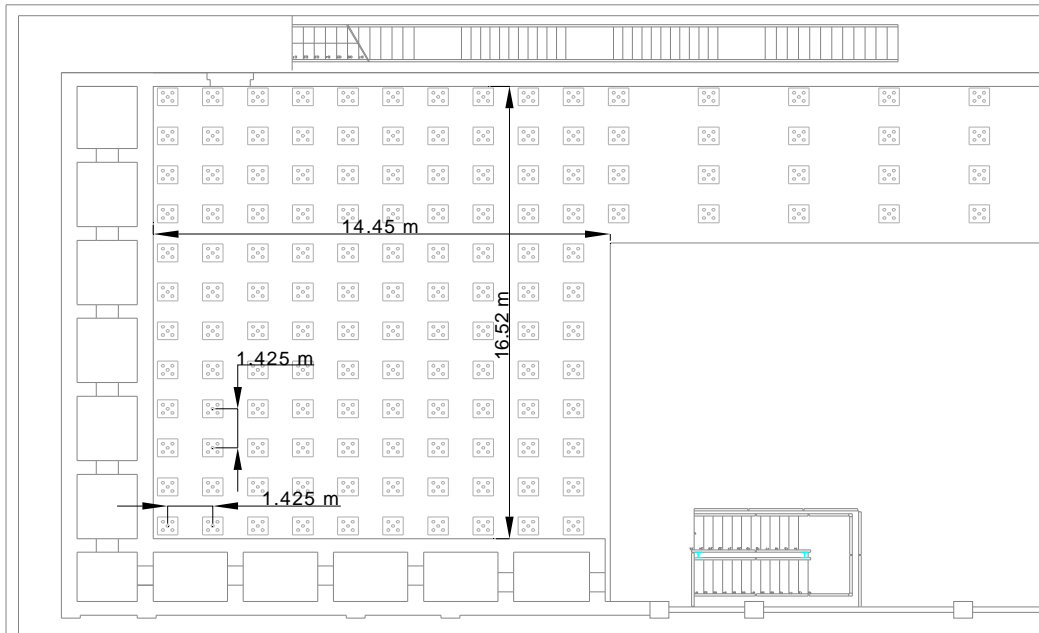


Figure 3-2: Plan view of the laboratory of Material and Testing of the University of Trento

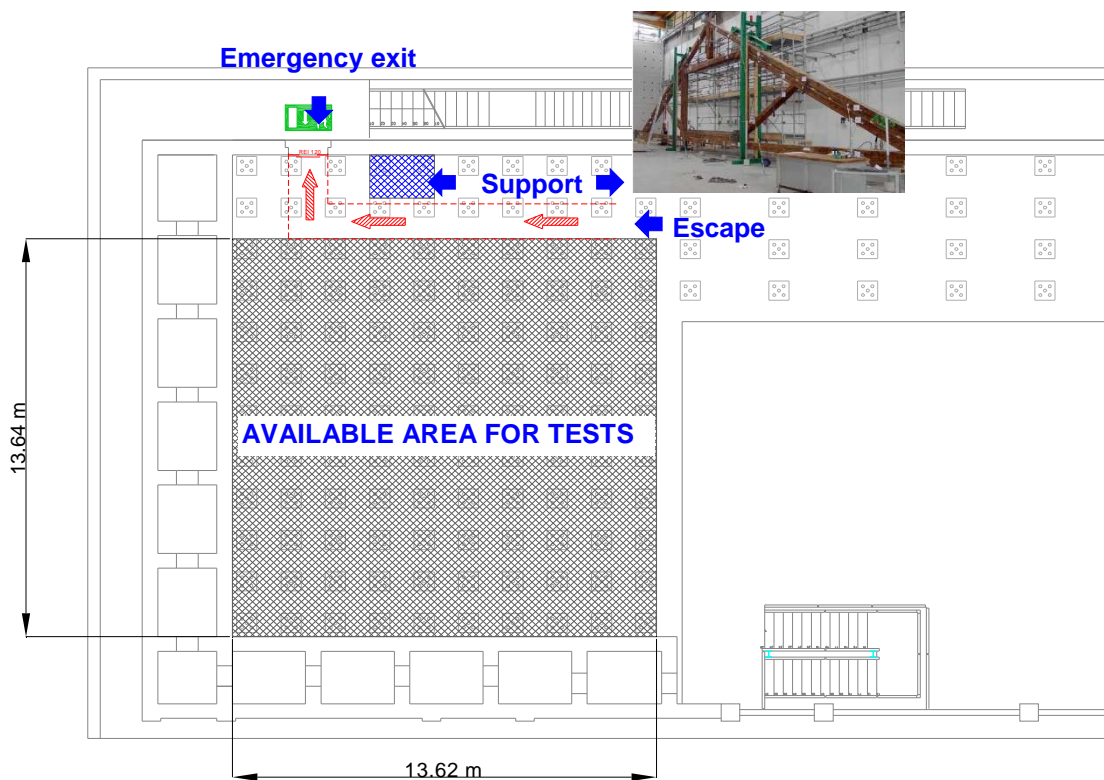


Figure 3-3: Available area for tests

The plan view of the lab shown in Figure 3-2 identify the pattern of the holes in the slab which allow the connection of specimens/counter frames to the slab. The position of these holes identifies possible positions of the columns of the 3-D specimens. The design of the reference

structure was hence carried out by considering the testing availability of all the partners involved in tests and in particular of UTRE.

The 3-D full scale experimental test were performed on a portion of the first floor of the corresponding full-frame, which will be referred to hereinafter as sub-frame. The floor framing plan of the sub-frames for the Symmetric and Asymmetric configurations are represented by the dotted area in Figure 3-4 and Figure 3-5 respectively which dimensions are in agreement with the lab testing facilities.

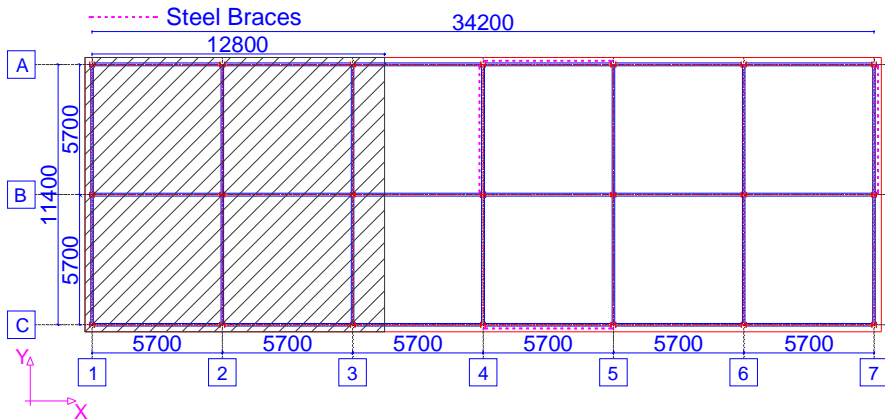


Figure 3-4: Floor Framing Plan - Symmetric Configuration (dimensions in mm)

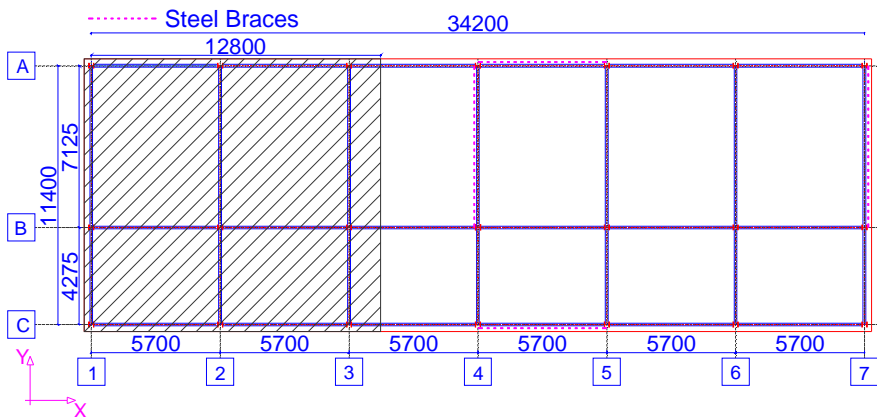


Figure 3-5: Floor Framing Plan - Asymmetric Configuration (dimensions in mm)

The final geometry of the two specimens and the layout of the slab rebars are presented in Figure 3-6. 'Symmetric' Structure. Slab reinforcements. (a) Lower layer; (b) upper layer (dimensions in m). The rebars layout showed in the figures are in agreement with ones calculated for the reference structures (Figure 2-38, Figure 2-39, Figure 2-50 and Figure 2-51).

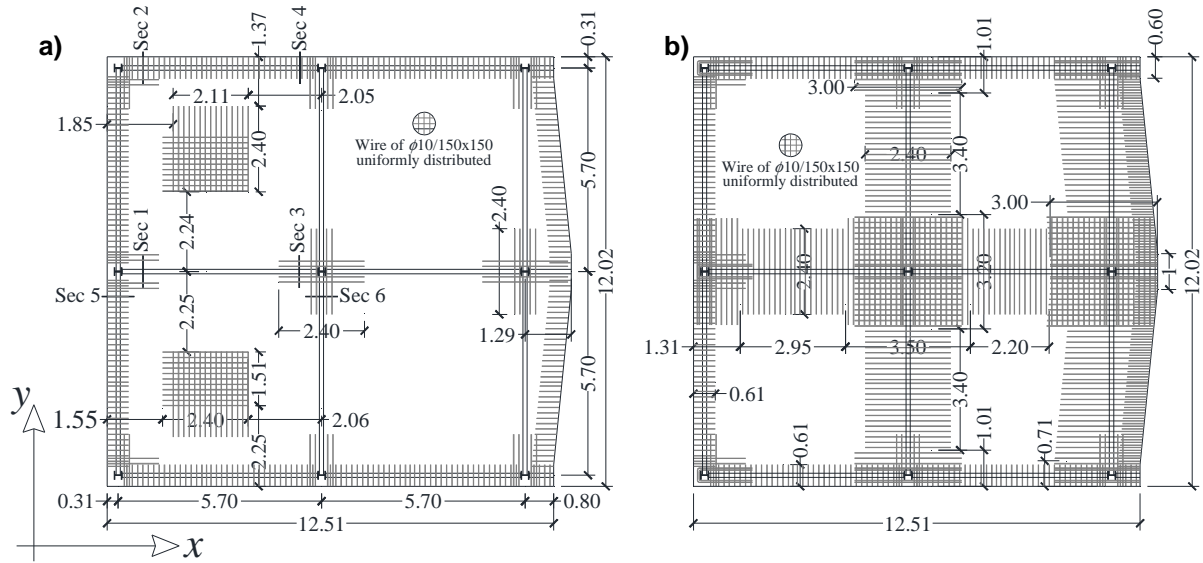


Figure 3-6. ‘Symmetric’ Structure. Slab reinforcements. (a) Lower layer; (b) upper layer (dimensions in m)

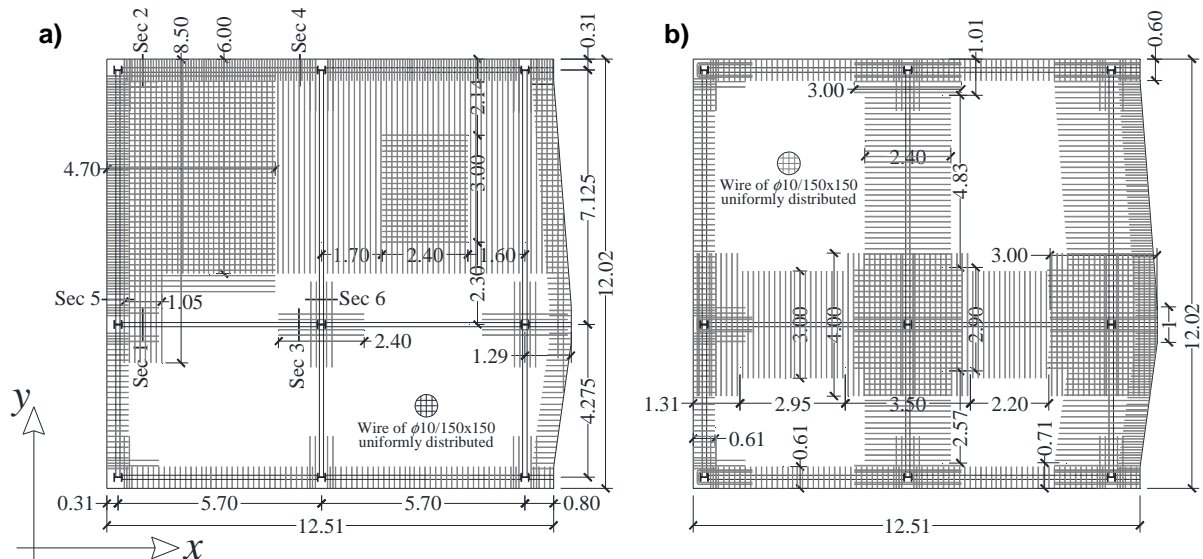


Figure 3-7. ‘Asymmetric’ structure. Slab reinforcements. (a) Lower layer; (b) upper layer (dimensions in m)

3.1 Numerical analysis of the experimental test

In order to design the experimental tests, refined Finite Element Models of the full-frames and sub-frames were developed by using the Abaqus program [9]; beams and columns are modeled as ‘Frame’ elements while the slabs are modeled as ‘Shell’ elements with quadrilateral elements with 4 nodes. The ‘Frame’ elements are modeled in the position corresponding their central axis, while the ‘Shell’ elements are modeled in the position corresponding the mid height of the concrete section. The ‘Shell’ elements are modeled with a constant thickness and, in order to reproduce the real distribution of the rebars in the slabs, accurate partitions and several sections accounting for different dimensions and spacing were adopted. Figure 3-8 show the partitions defined for the ‘Symmetric’ configuration, while Figure 3-9 refers to the ‘Asymmetric’ case [ref]. The representation considers the rebars excluding their anchorage length. The rebars

are embedded within the slab and the slab is rigidly connected to the beams through 'TIE' constraints [9]. In the preliminary study, a rigid beam-to-column connection is considered and the columns are fully fixed at the base. The loads are uniformly distributed on the slab and are gradually increased by using a smooth step. Different levels of meshing arrangements for the beams and the slabs have been considering in order to ensure an adequate structural response while minimizing the computational time of the simulations. Meshing of all the parts is carried out using the 'structured' technique. Mesh refinement with an average value of 200 mm has been used.

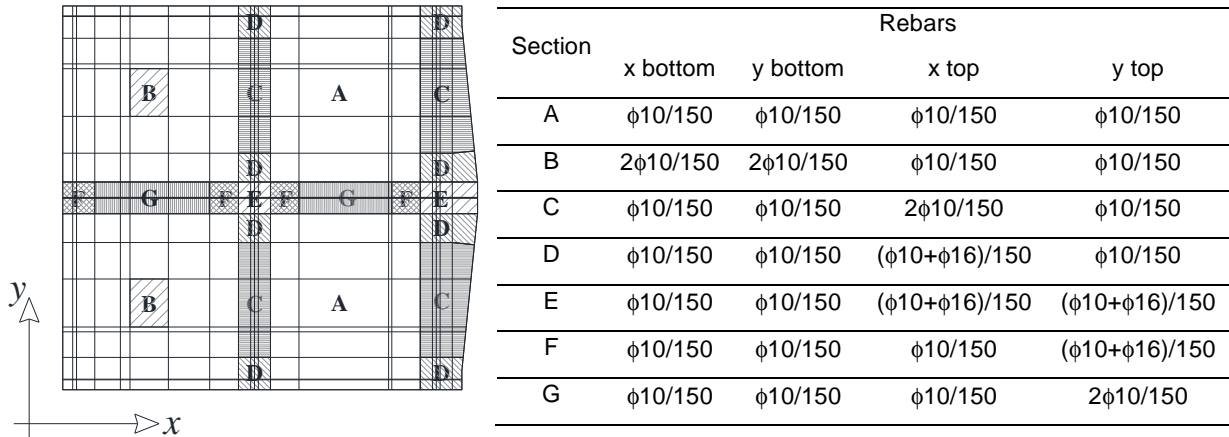


Figure 3-8. 'Symmetric' structure. (a) Concrete slab partitions; (b) slab section properties (measures in mm)

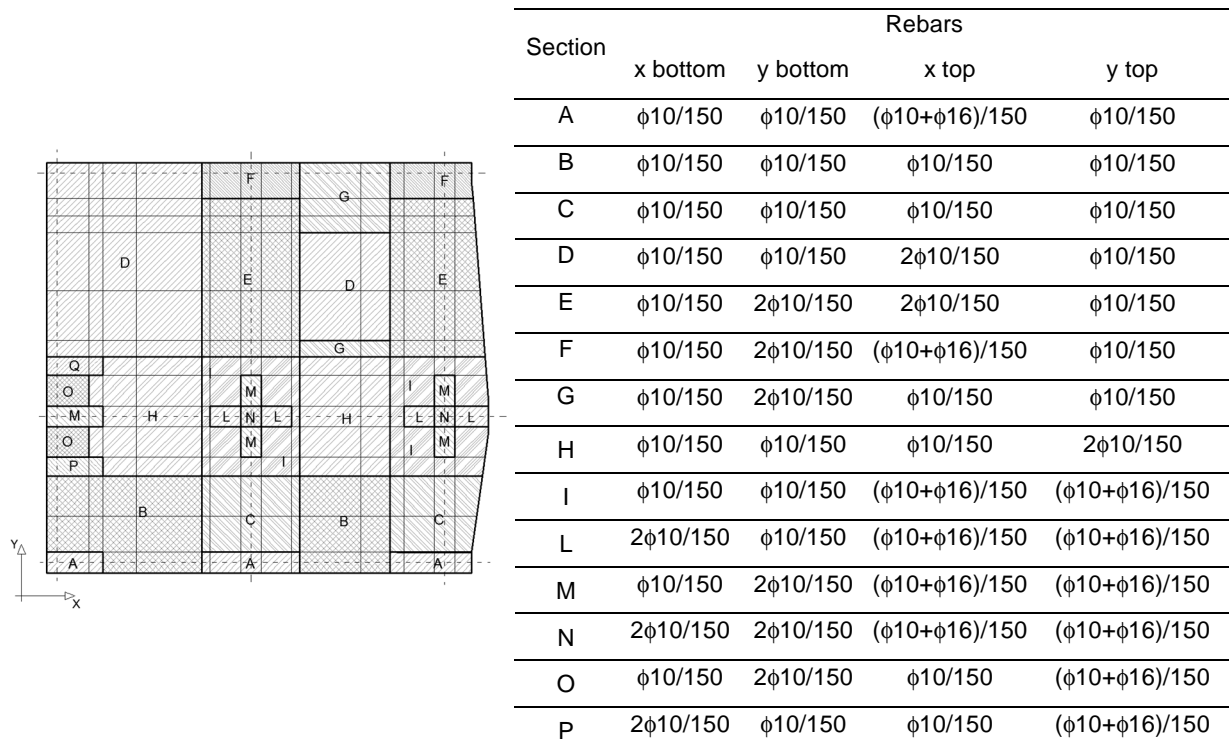


Figure 3-9. 'Asymmetric' structure. (a) Concrete slab partitions; (b) slab section properties (measures in mm)

The structural steel and the rebars are modeled by an elastic perfectly plastic material model based on the nominal values of the mechanical properties. The Young's modulus, E and the yield stress, f_y , are assumed equal to 200 GPa and 450 MPa and to 210 GPa and 355 MPa

for steel B450C and steel S355, respectively. The Poisson's coefficient is assumed equal to 0.3 for both the steel materials. Material non-linearity for the concrete is included in the FE model by the 'Concrete Damage Plasticity' option. The stress-strain relationships are defined in compression according to the Eurocode 2 [3] and in tension according to [10] including the effects of the tension stiffening. Stress-strain relationships for the concrete are reported in Figure 3-10. The von Mises yield criterion coupled with an isotropic hardening is assumed. All the material properties are defined accounting for the true values of stress, σ_t , and plastic strain, $\varepsilon_{t,pl}$ [11]. True stress-strain relationships and the plastic strain can be obtained based on the engineering values by the following equations:

$$\sigma_t = \sigma_{nom} (1 + \varepsilon_{nom}) \quad (1)$$

$$\varepsilon_t = \ln(1 + \varepsilon_{nom}) \quad (2)$$

$$\varepsilon_{t,pl} = \varepsilon_t - \varepsilon_{t,el} = \varepsilon_t - \frac{\sigma_t}{E} \quad (3)$$

where σ_{nom} is the engineering stress, ε_{nom} is the engineering strain, σ_t is the true stress, ε_t is the true strain, $\varepsilon_{t,pl}$ is the true plastic strain and $\varepsilon_{t,el}$ is the true elastic strain.

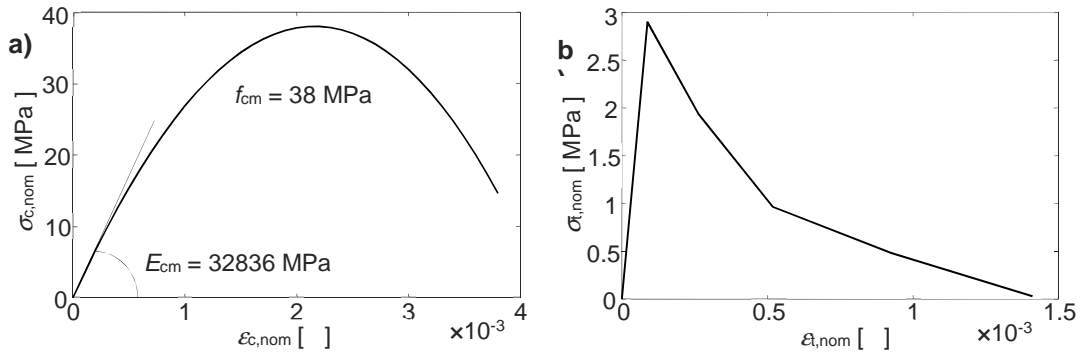


Figure 3-10. Concrete stress-strain relationships. (a) Compression and (b) tension behavior for concrete class C30/37 according to [3] and [10]

The numerical simulations of the tests, performed in ABAQUS [9], follow the three steps of the loading procedure. In the first step, the gravity load is applied on the slab defining the condition before the column's collapse; in the second step the central column is 'removed', while in the third step, additional load is applied onto the slab up to the collapse in order to get an appraisal of the available safety margin. The first step is performed by a static analysis while the second and third steps are performed by quasi-static analyses. The static analysis is performed with the ABAQUS/Standard solver; in this case the central column is fixed at the base and the analysis provides the vertical reaction force of the element. The equilibrium equations are solved using the static general analysis procedure. The standard 'Full Newton' solution technique is adopted together with an automatic incrementation scheme for the application of the loading. In the following steps, the quasi-static analyses are performed with the ABAQUS/Explicit solver which offer advantages while solving large non-linear problems. In the second step the central column is released and the reaction force from step 1 is applied at the base. A force in the opposite direction is increased in order to gradually reduce the force up to zero. In the third step the gravitational load on the slab is gradually increased. In these analyses, the dynamic equilibrium equations are solved using the central difference algorithm; the velocity of the column displacement is calibrated limiting the ratio between the kinetic energy and the internal energy (i.e. ≤ 0.01), ensuring that the dynamic effects are negligible. The response of the full-frame and sub-frame of the symmetric configuration in the three steps is reported in Figure 3-11.

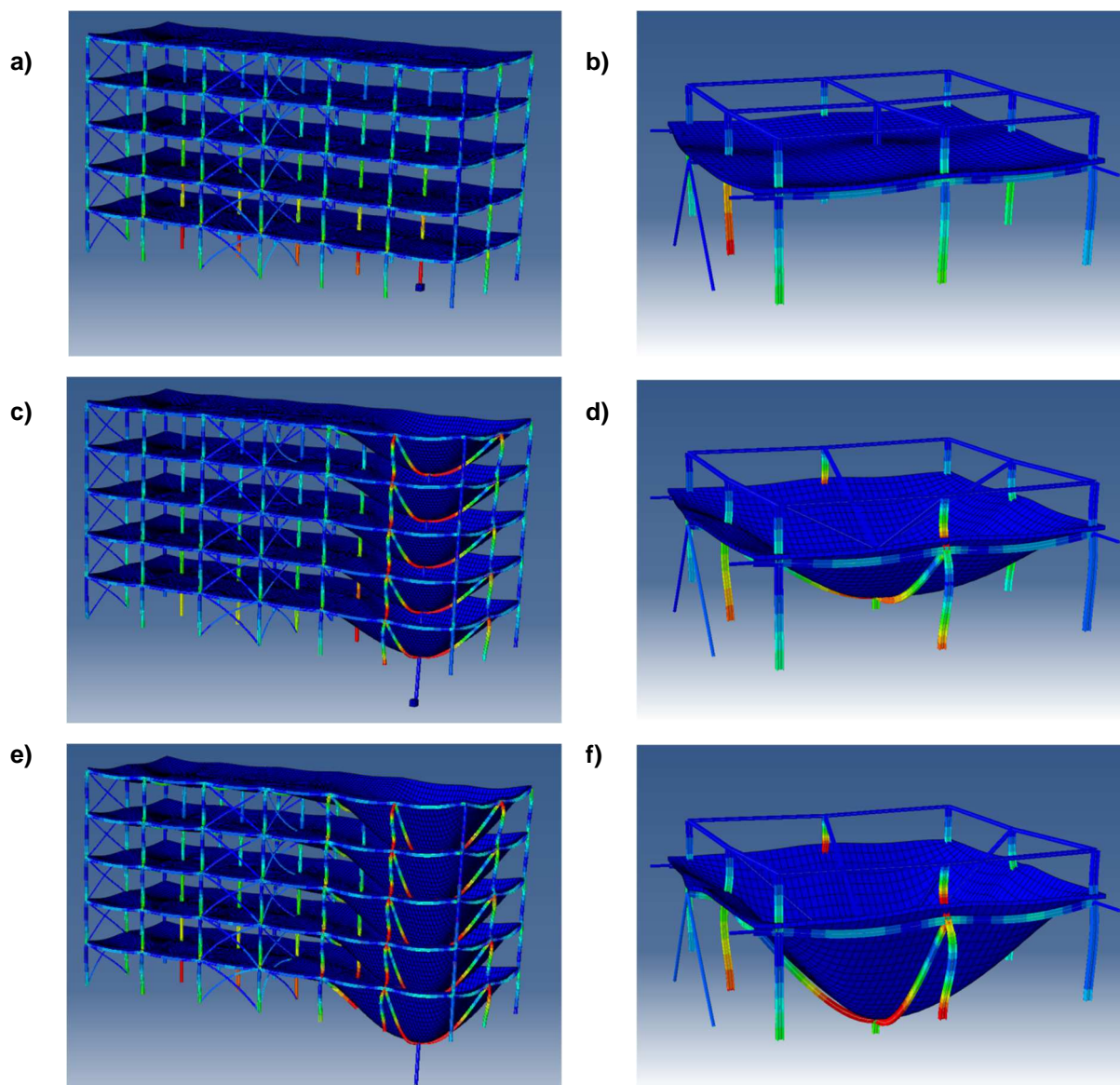


Figure 3-11. Sequence of collapse for the full-frame and sub-frame with the following loading steps: a) and b) Application of gravity load; c) and d) Removal of column; e) and f) Increase of load.

3.1.1 Sub-frame boundary conditions

The task of the experimentation is to investigate the behavior of the real structure subjected the collapse of a column. Hence, the sub-frame should be restrained in a way that permits simulation of the presence of the remaining part of the structure and this issue was of primary interest in the preliminary study for the test design.

The sub-frame is 'extracted' from the ground floor of the full-frame and hence the columns are fixed at the strong floor. The columns are longer than the story height, and continue up to the middle height of the second story, where they are connected among them by steel truss elements as represented in

Figure 3-12. This specimen's configuration allows for approximating well the distribution of the moments in the columns and the rotational stiffness of the beam-column joints.

While the definition of the columns' upper restraints was almost immediate, calibration of the connection between beams and slabs with the reaction system required greater attention. Three different restraining options, as illustrated in Figure 3-13, were considered in the analyses, and the main results in terms of deformations and internal forces were compared with the corresponding ones obtained by the analysis of the full-frame. In particular, the adequacy of the boundary restraints is checked by comparing the response at several significant sections of the structure reported in Figure 3-14. In order to limit the length of this report, only the results of the Symmetric configuration are reported and discussed in this section. Similar results have been obtained for the Asymmetric configuration.

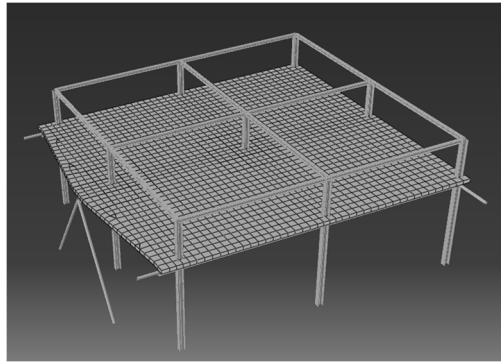


Figure 3-12. Sub-frame for the Symmetric configuration 3-D representation

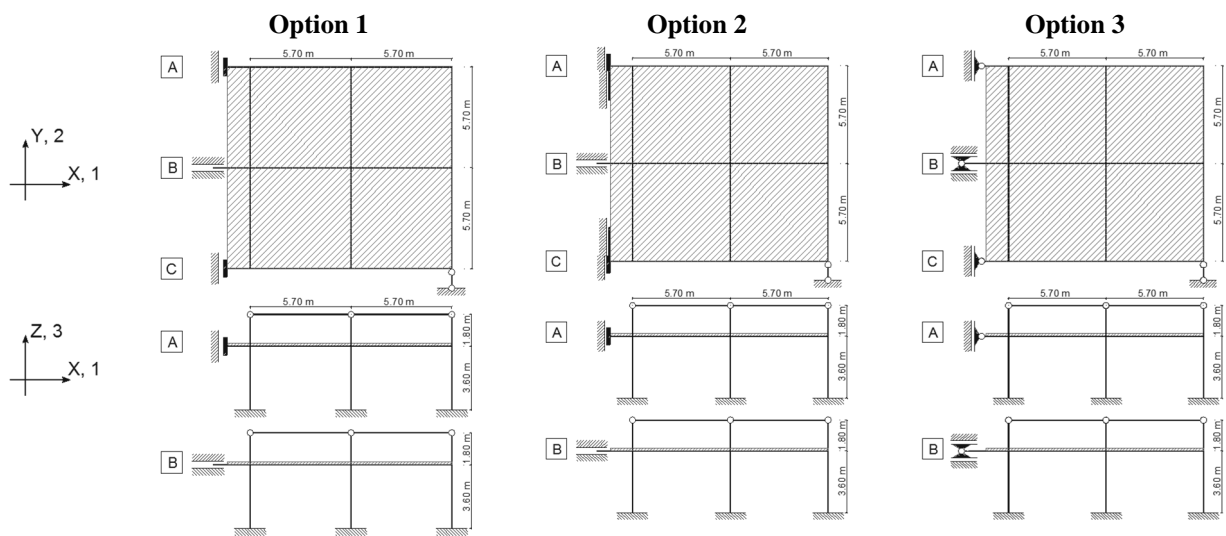


Figure 3-13. Restraining Options for the sub-Frame - Symmetric Configuration

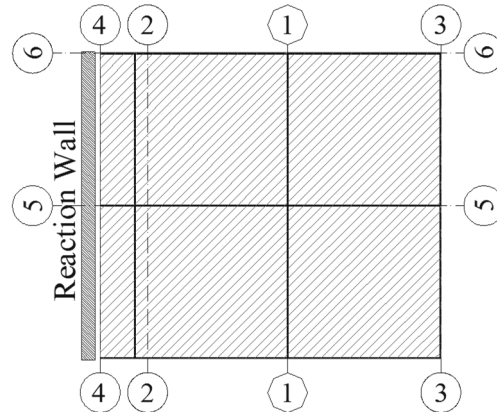


Figure 3-14. Significant Sections used for the comparison - Symmetric Configuration

In the Option 1 and 3, only the steel beams are restrained while the slab is not connected to the reaction wall. The presence of the bracings in full-frame prevents from any significant longitudinal displacement and hence, the relevant d.o.f. U1 is fully restrained in the sub-frame. This d.o.f. is left free at the central beam (B in Figure 3-13) where the vertical and lateral displacements (U2 and U3) are restrained. Besides, in the Option 1, the end rotations of beams A and C about both principal axes (R2 and R3) are restrained, and the central beam's end is restrained against rotations R2 and R3. In the Option 2, in addition to the restraints of the Option 1, also the parts of the slab adjacent to the lateral beams are connected, for a width of 0.5 m, to the reaction wall, restraining all the translational degrees of freedom. The Option 3 is similar to the Option 1 but all the rotations are released.

In order to permit the comparison between the results of the sub-frame and of the full-frame by neglecting the effects of the higher axial load on the columns of the full-frame, concentrated loads are applied on the columns of the sub-frame model and are varied during the analysis in order to simulate the axial force variation of the full-frame. The sequence of the concentrated loads applied on the columns is reported in Figure 3-15.

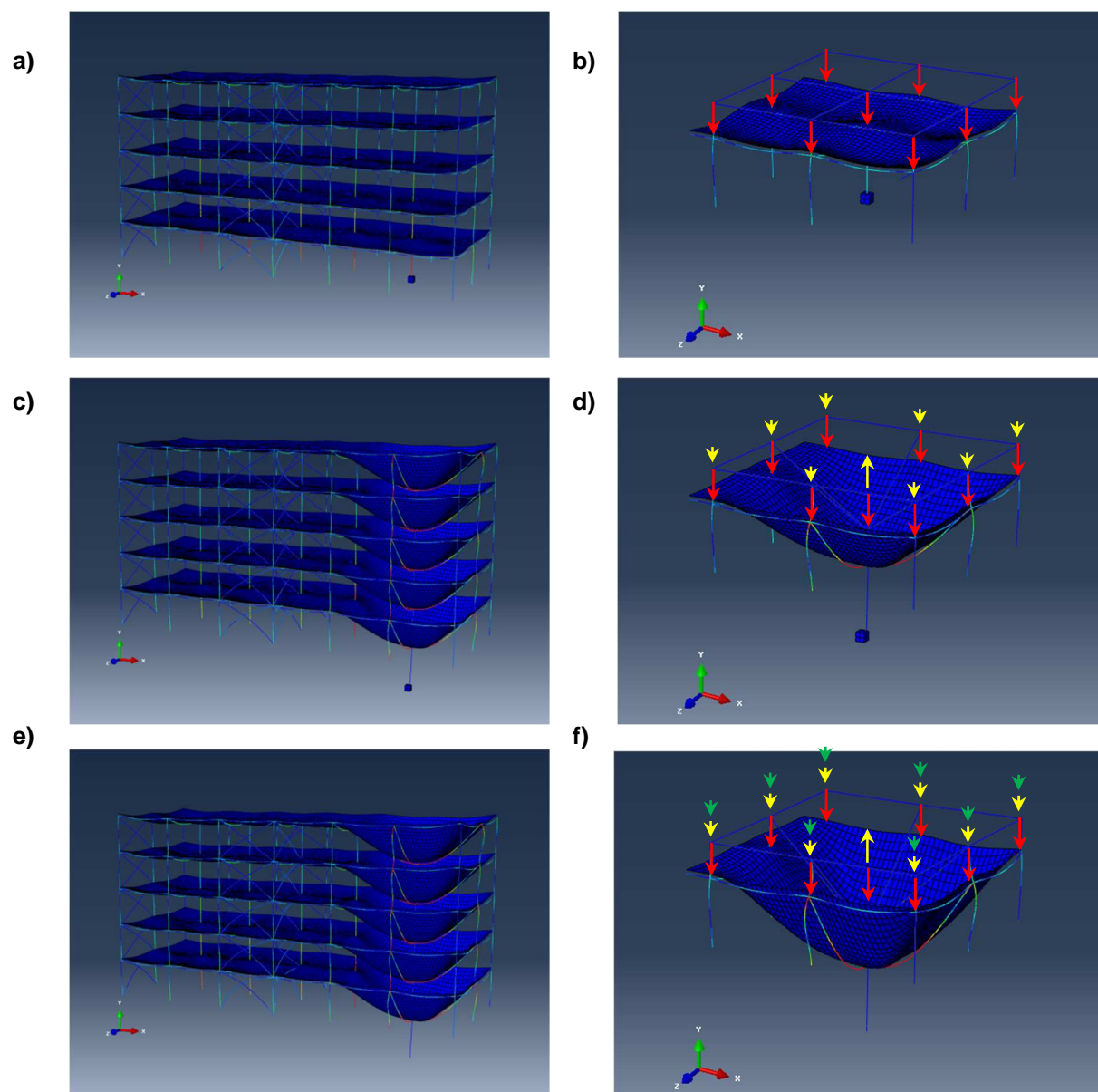


Figure 3-15. Sequence of collapse for the full-frame and sub-frame with the concentrated loads applied on the columns: a) and b) Application of gravity load; c) and d) Removal of column; e) and f) Increase of load

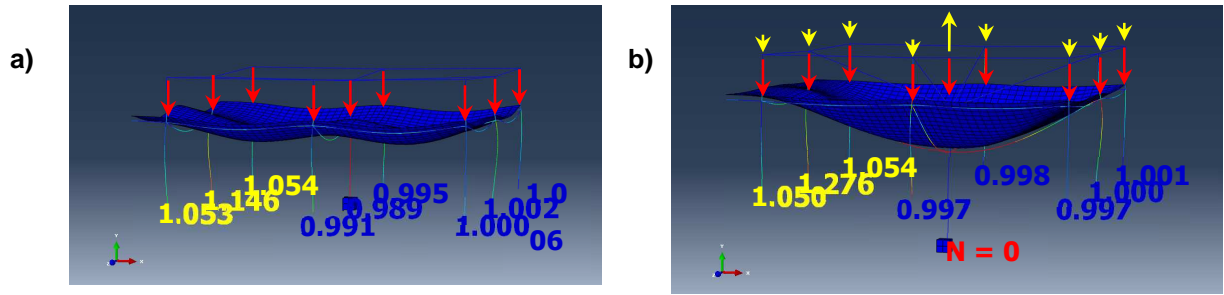


Figure 3-16. The ratios of the axial forces on the columns of full-frame and of sub-frame for: a) first step and b) second step

The ratios of the axial forces on the columns of full-frame and of sub-frame for the first and second steps of the loading sequence are reported in Figure 3-16. It is possible to observe that these values are very close to 1 in all the columns confirming that by this procedure is possible to well approximate the axial force of the full-frame. However, the shear forces in the beams are not simulated and hence the axial forces on the columns of the sub-frame close to the reaction wall are still lower with respect to those of the column of the full-frame.

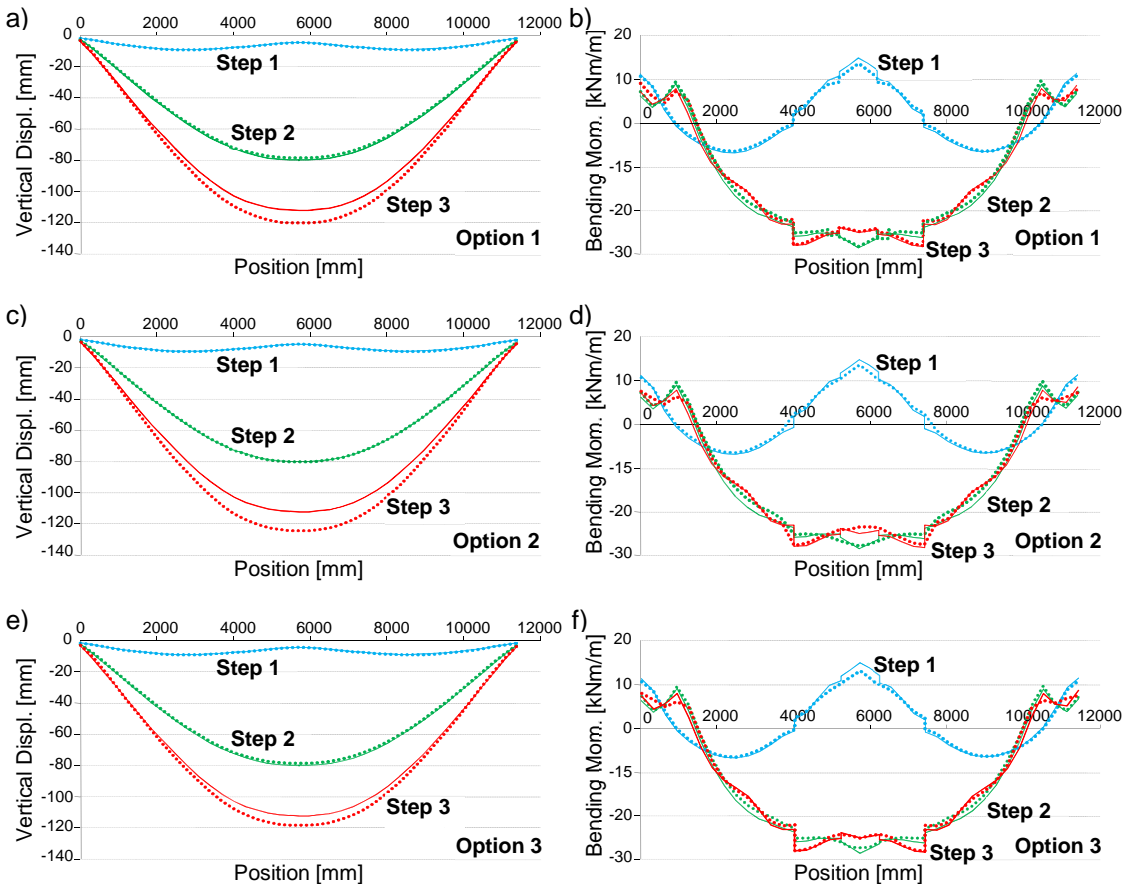


Figure 3-17. Comparison of the Vertical displacements and Bending moments on the Section 1 - Symmetric Configuration

Figure 3-17 shows the comparisons of the vertical displacements and bending moments on the slab positioned on the sections 1 of the sub-frame with one of the three restraining options and the full-frame. The dotted lines indicate the responses of the sub-frames while the continuous line is related to the full-frame. The responses are reported for three steps of the numerical

tests. In the step 1 the gravity load is applied on the slab, in step 2 the central column is completely removed, while in the step 3 the load on the slab is increased with a coefficient equal to 1.3. By looking at Figure 3-17 is possible to observe that there is no significant difference between the results obtained by the three restraining options. Moreover, is possible to observe that all of them are able to approximate more than satisfactorily the behavior of the full-frame in term of displacements and bending moments. Similar results are obtained also by comparing other quantities (i.e. shear, axial force, etc.).

Figure 3-18 shows the comparisons of the vertical displacements and bending moments on the slab positioned on the sections 2 of the sub-frame with one of the three restraining options and the full-frame. Similarly to section 1, also in this case for the first two steps of the analysis the response of the full-frame is well approximated by the sub-frame. Differently, the response of the third step of the analysis is not well captured. It is consequence of the buckling of the central column close to this significant section in the full-frame.

As showed in Figure 3-16 the columns close to this section are more compressed in the full-frame with respect to the sub-frame and the buckling of the central column as showed in Figure 3-19 is not reproduced in the model of the sub-frame. However, this phenomenon is not of interest in this study and there is no significant difference between the results obtained by the three restraining options.

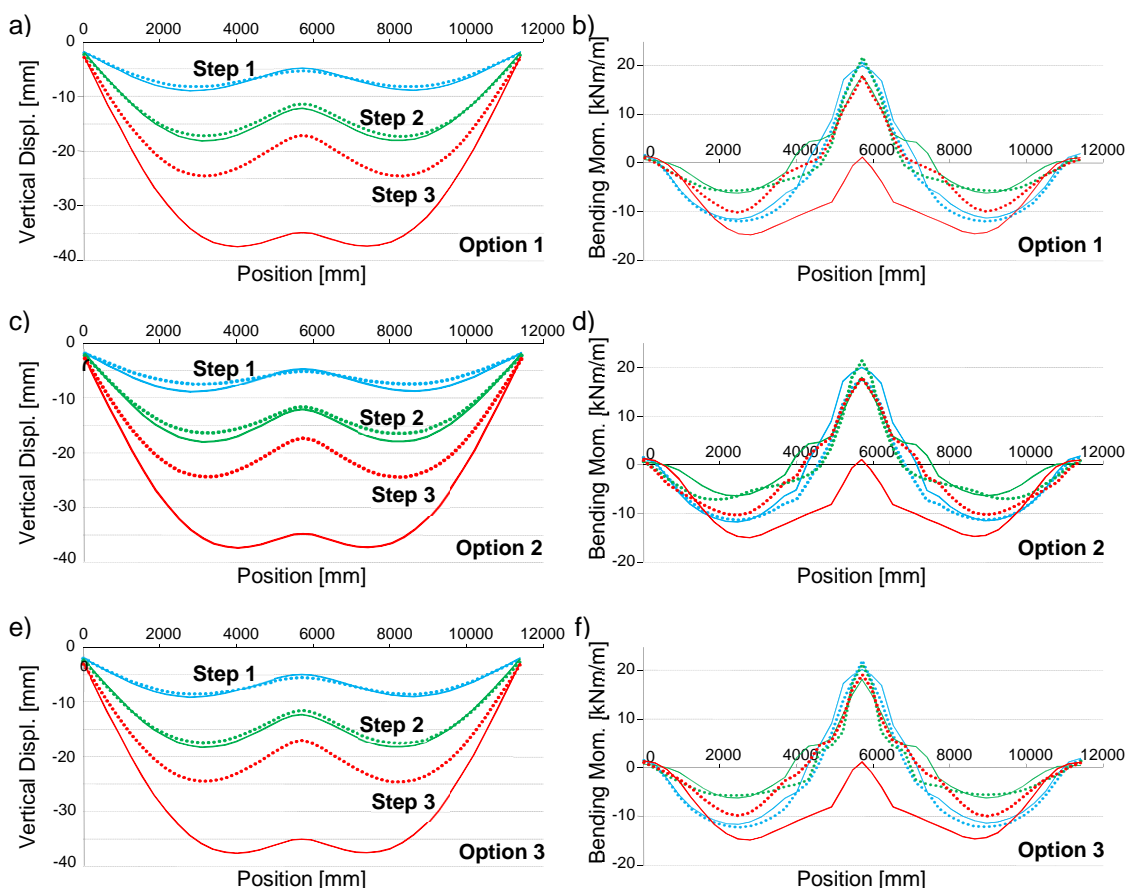


Figure 3-18. Comparison of the Vertical displacements and Bending moments on the Section 2 - Symmetric Configuration

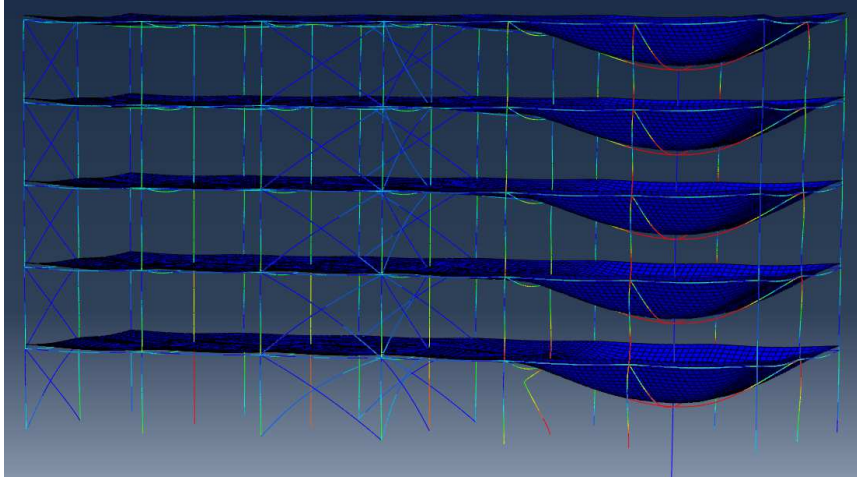


Figure 3-19. Third step of the analysis for the full-frame. Buckling of column.

Figure 3-20 shows the comparisons of the vertical displacements on the slab positioned on the section 4 of the sub-frame with one of the three restraining options and the full-frame. In this section, the response of the sub-frame is strictly related to the restraining option adopted. Figure 3-20 shows that no one of the considered options is able to reproduce well the behavior of the full-frame in this section.

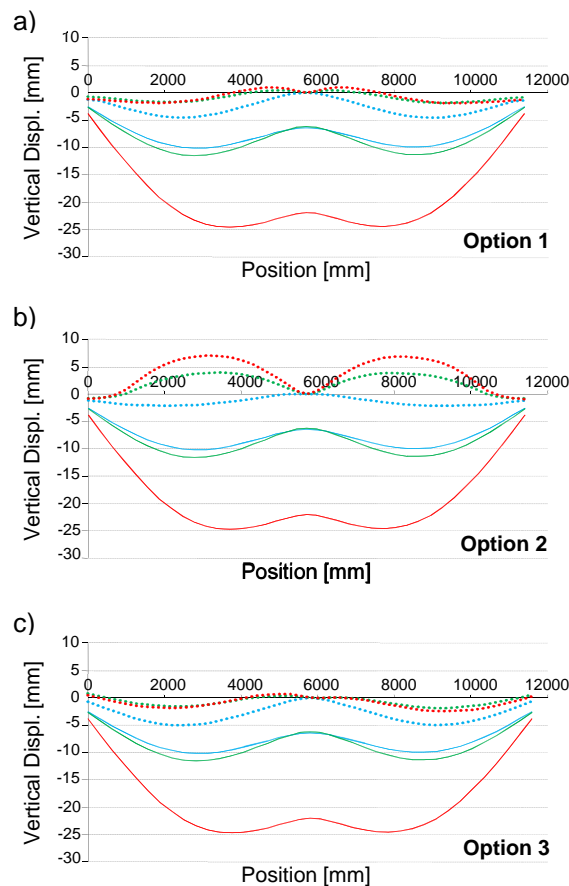


Figure 3-20. Comparison of the Vertical displacements on the Section 4 - Symmetric Configuration

These results indicate that the behavior of the floor subjected to the collapse of the central column is weakly sensitive to the boundary conditions used to reproduce the continuity of the full-frame and that the response on the sections of interest for the experimentation are well reproduced by the sub-frame independently from the response of the external sections. This outcome allows the use of the simplest restraining solution during the test.

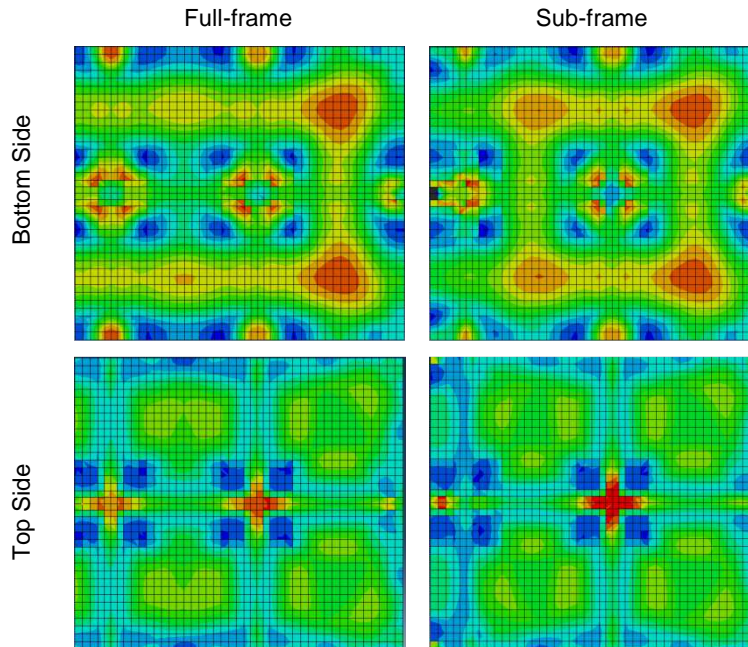


Figure 3-21. Comparison of the Von Mises Stresses on the slab - Step 1 - Symmetric Configuration

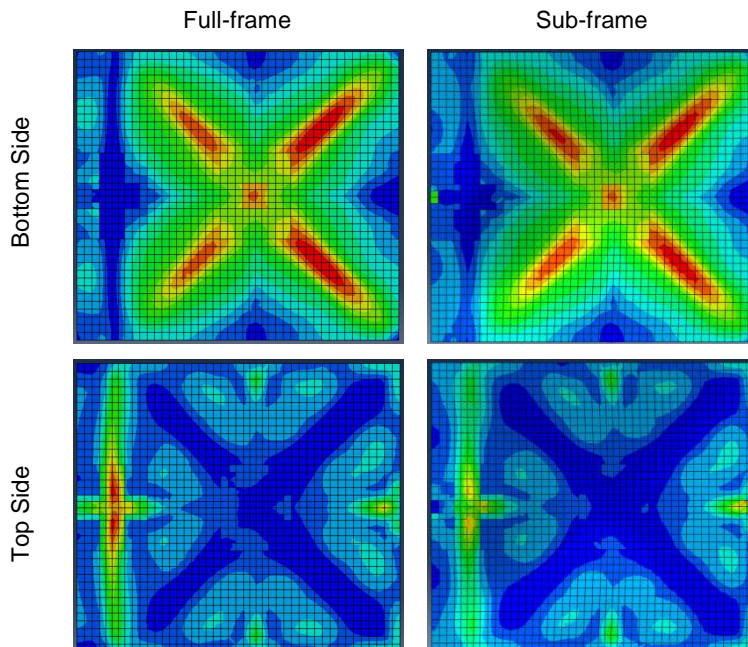


Figure 3-22. Comparison of the Von Mises Stresses on the slab - Step 2 - Symmetric Configuration

Figure 3-22 and Figure 3-22 compare the Von Mises stresses at the bottom and top side of the slab between the full-frame and the sub-frame modeled by using the restraints of Option 3 for

the first and second steps of the analysis. It is possible to observe that the distribution of the stresses obtained in the full-frame is well approximated by the sub-frame model. Analogous results have been obtained also by using the other restraint Options.

3.1.2 Increase of load after column removal

While performing the third step of the test's sequence, additional load should be applied onto the slab up to the collapse in order to get an appraisal of the available safety margin. However, application of a distributed load in the frame during the experimental test is not feasible and other solutions have been explored. During the first and second steps the presence of the column is simulated by using a hydraulic ram in which the compression force is gradually reduced down to zero. The hydraulic ram might then used to apply a tension force so simulating the increase of the vertical load in an 'easy' and feasible way. The influence on the frame response of this loading approach was explored by comparing the results of the numerical analysis of the full-frame and of the sub-frame by using the two different loading solutions. The responses are compared in terms of deformations and internal forces at several significant sections of the structure identified in Figure 3-14. However, in order to limit the length of this report, only the results related to section 1 of the Symmetric configuration are reported. Similar results have been obtained for the Asymmetric configuration.

Figure 3-23 shows the comparisons of the vertical displacements and bending moments on the slab positioned on the section 1 of the sub-frame restrained by option 3 with the concentrated load applied in the central column and the full-frame where the increase of load is made by increasing the distributed load on the slab. The dotted lines indicate the responses of the sub-frames while the continuous line is related to the full-frame. The responses are reported for three steps of the numerical tests and in the step 3 the load on the slab is increased with a load factor equal to 1.3. In this case the concentrated force is the equivalent force based on the influence area of the central column. The results for the step 3 indicates that the proposed solution is able to approximate more than satisfactorily the behavior of the full-frame in term of displacements (with an error of 1.5 %) and bending moments. Similar results were obtained also for the other 'significant' sections and by comparing other quantities (i.e. shear, axial force, etc.). The analyses demonstrate that is possible to apply a concentrated force in the central column to increase the vertical load during the test in order to investigate the available safety margin.

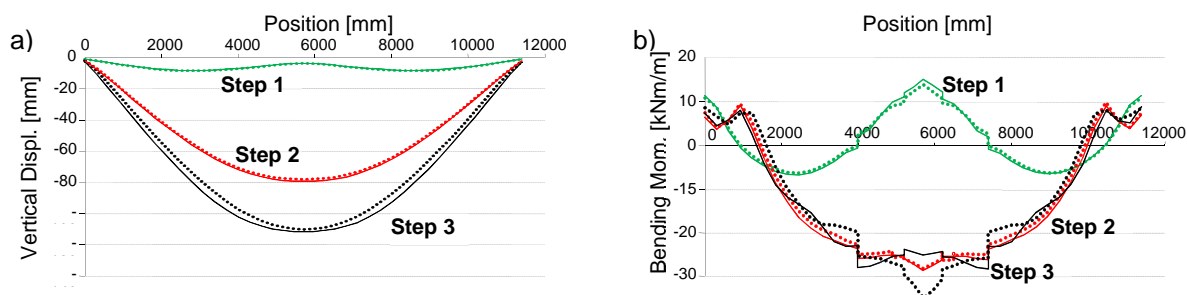


Figure 3-23. Comparison of the vertical displacements and bending moments of the Section 1 - Symmetric configuration

3.2 Design of the test setup

The numerical analysis showed that the behavior of the floor subjected to the collapse of the central column observed in the full-frame can be well simulated in the sub-frame by applying the boundary conditions reported in Figure 3-24. Only the steel beams are restrained while the slab is not connected to the reaction wall. The longitudinal displacement is fully restrained in the

lateral beams (joints A and C). This d.o.f. is left free at the central beam (B in Figure 3-24) while d.o.f. U2 and U3 are restrained. In all the connections, the rotations are released.

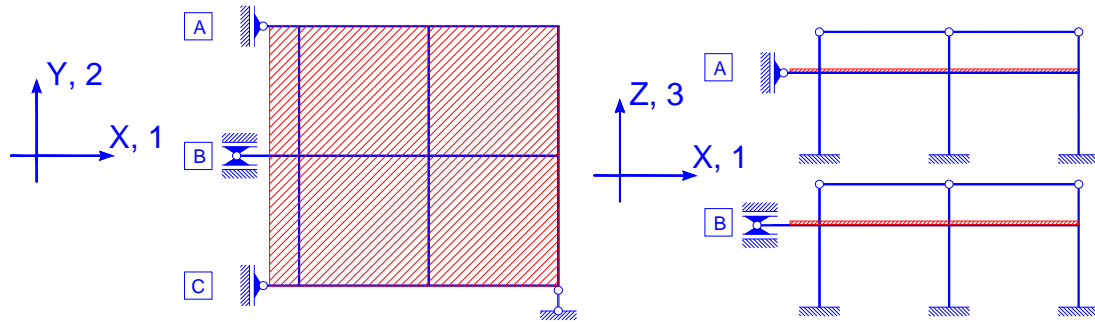


Figure 3-24. Boundary conditions for the sub-frame - Symmetric Configuration

Since the rotations are not restrained, the boundary conditions reported in Figure 3-24 have been obtained by using truss elements. The same elements of the test setup are going to be employed for both the Symmetric and Asymmetric configurations, hence, they have been designed by considering the worst condition among the two cases.

The specimens will be built inside the laboratory. Figure 3-25 and Figure 3-26 report the 3-D representation of the sub-frame and the relative position with respect to the reaction walls including the elements employed to reproduce appropriate boundary conditions.

Figure 3-27 shows the plan view of the experimental test for the Symmetric configuration while Figure 3-28 up to Figure 3-32 report the relative sections. These Figures include the indications of the lateral supports, of the central support, of the hydraulic ram and of the base supports.

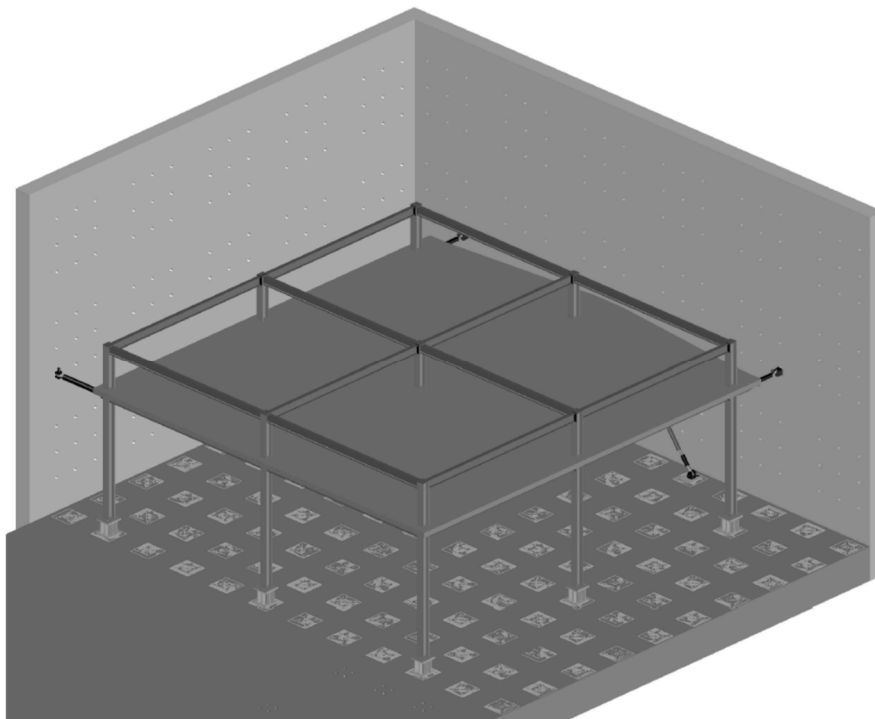


Figure 3-25. Symmetric 3-D specimen

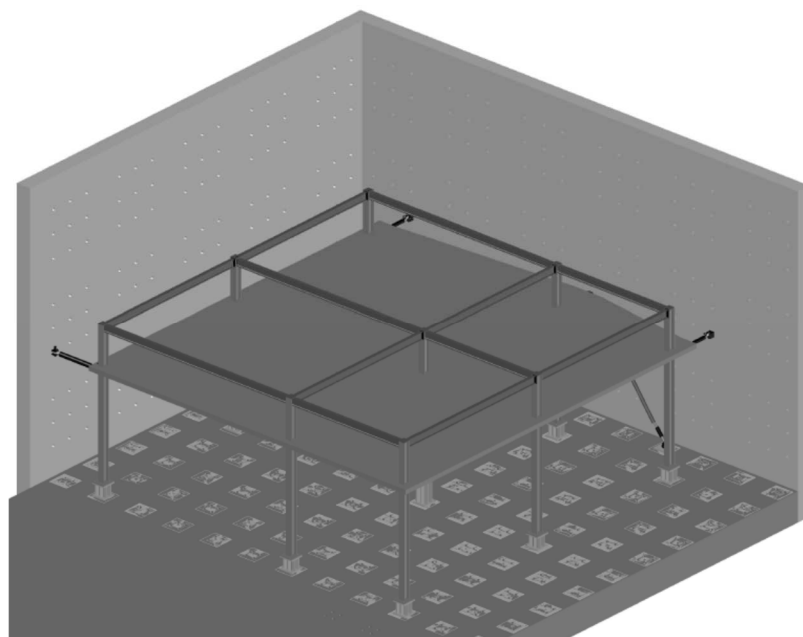


Figure 3-26. Asymmetric 3-D specimen

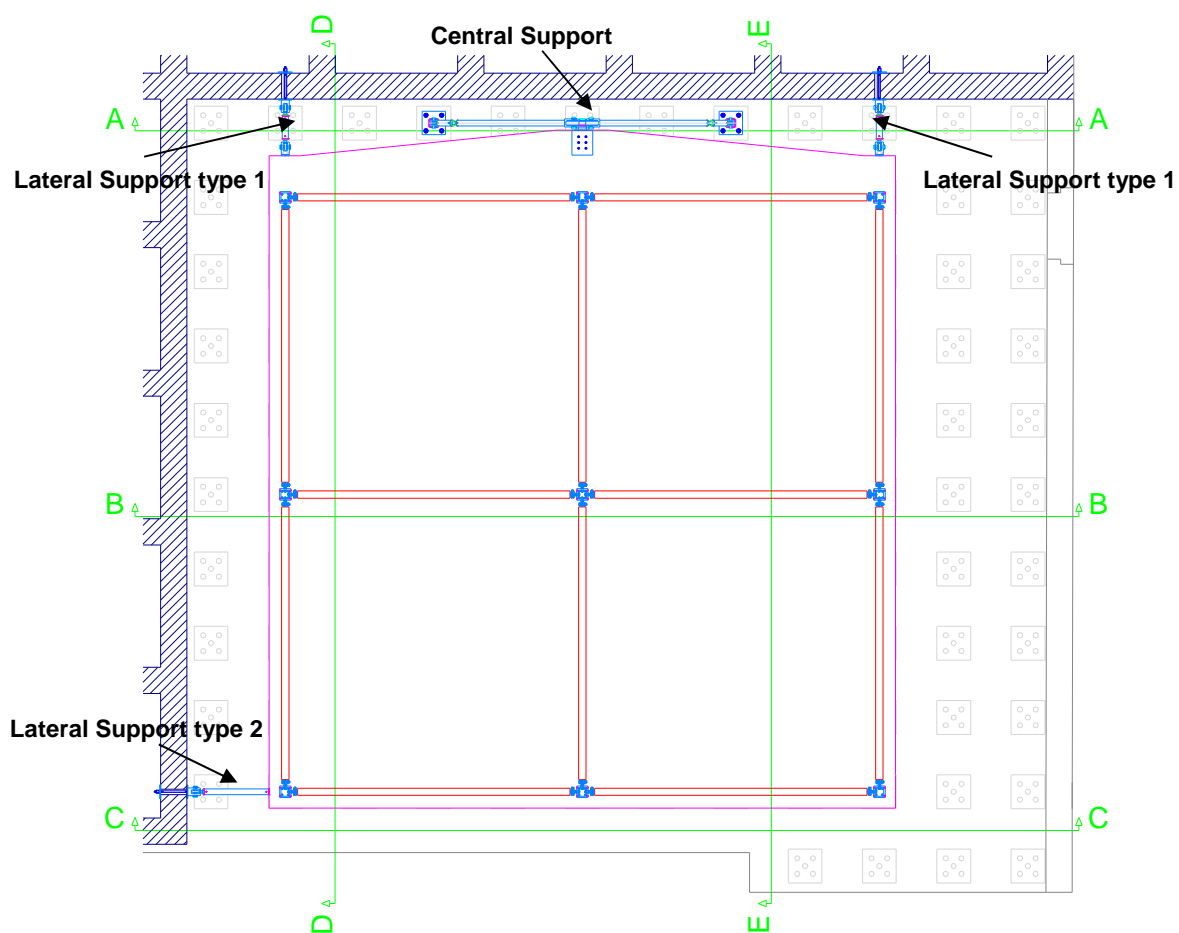


Figure 3-27. Plan View of the Experimental Tests for the Symmetric Configuration

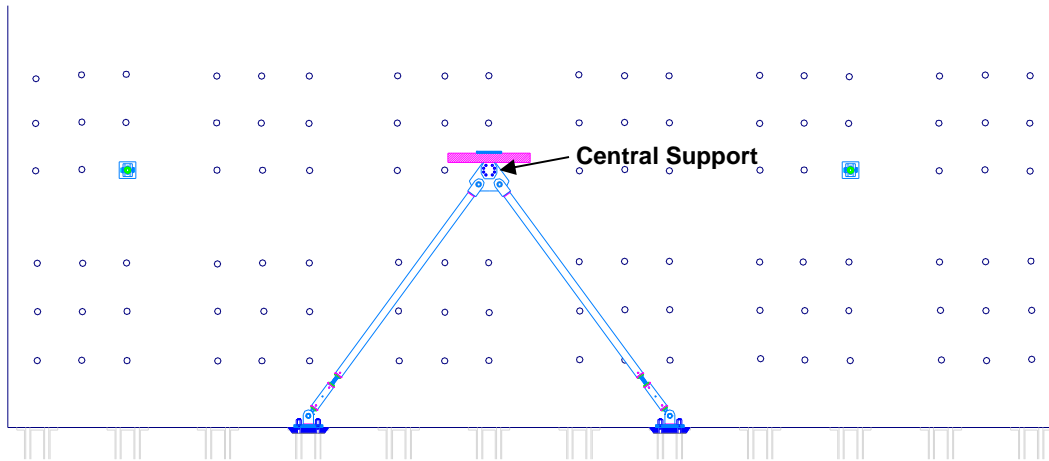


Figure 3-28. Section A-A of the experimental test setup for the Symmetric Configuration

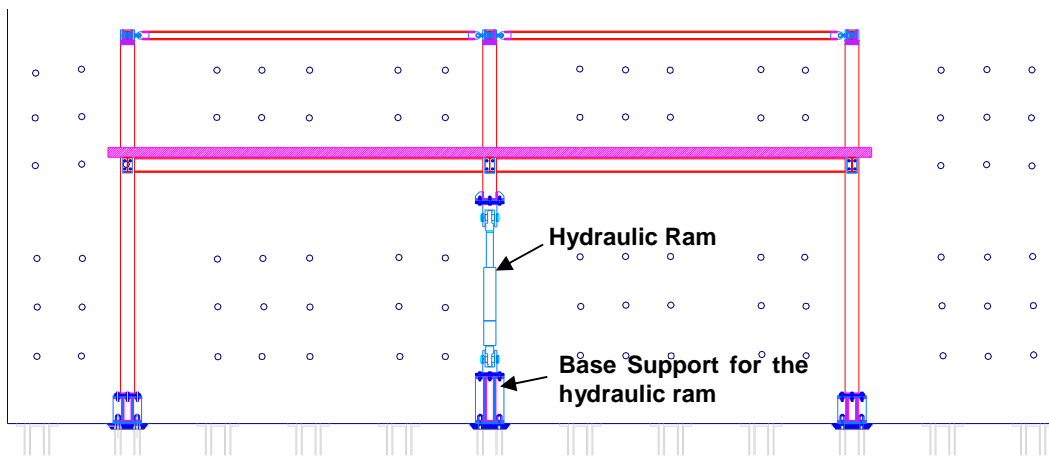


Figure 3-29. Section B-B of the experimental test setup for the Symmetric Configuration

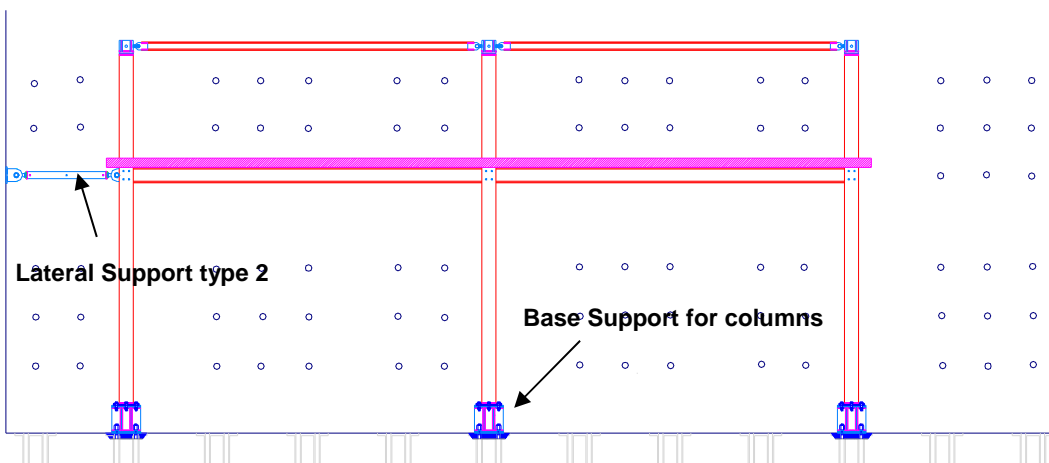


Figure 3-30. Section C-C of the experimental test setup for the Symmetric Configuration

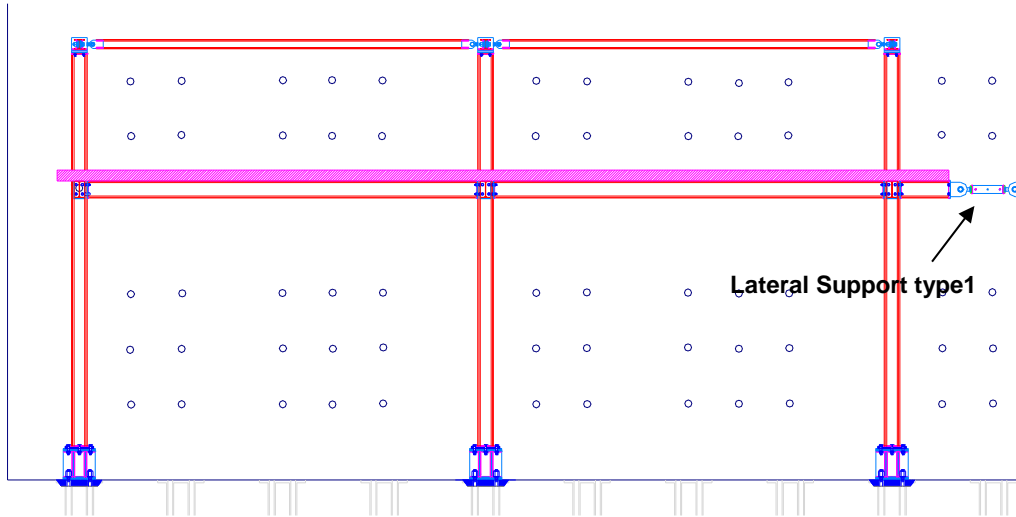


Figure 3-31. Section D-D of the experimental test setup for the Symmetric Configuration

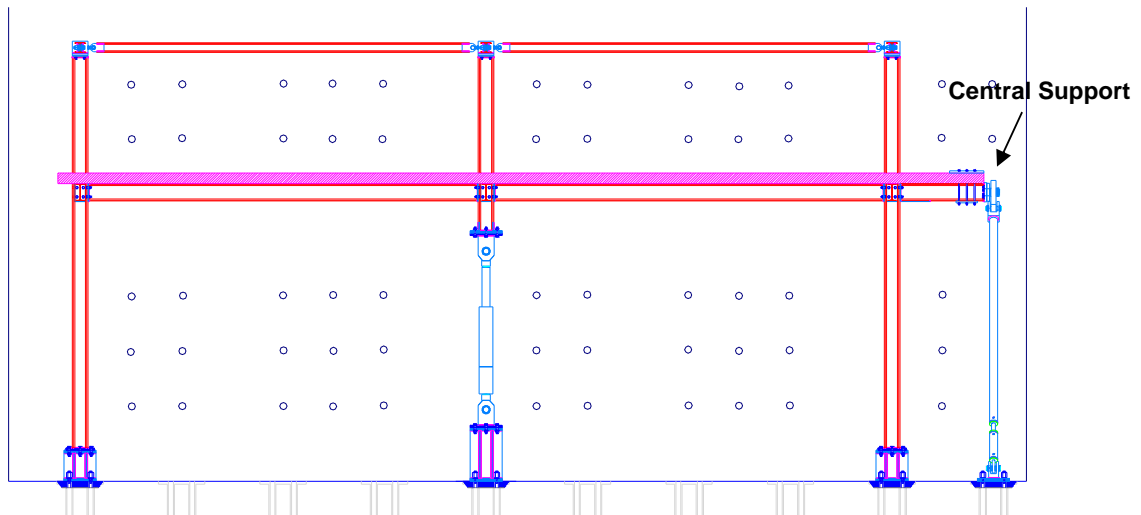


Figure 3-32. Section E-E of the experimental test setup for the Symmetric Configuration

3.2.1 Restraints of the lateral beams

The lateral supports are identical with the only difference that the lateral support type 2 is longer. Lateral support type 1 is reported in Figure 3-33. These connections are made by coupling two yokes and rod ends which are connected respectively to the counterwall from one side and to the steel beam from the other side. The rod ends are connected by a tubular steel element by a coupling system that permits the regulation of the length of the elements while assembling the test setup. The rod ends have the rotation that is fully released in the principal direction, while, in the other direction only a rotation of 6 degrees is permitted as reported in Figure 3-34. This solution have been adopted since the numerical analysis showed that in this direction the demand in terms of rotation is lower than 6 degrees.

Both the lateral supports have been designed to support a force in traction of 250 kN.

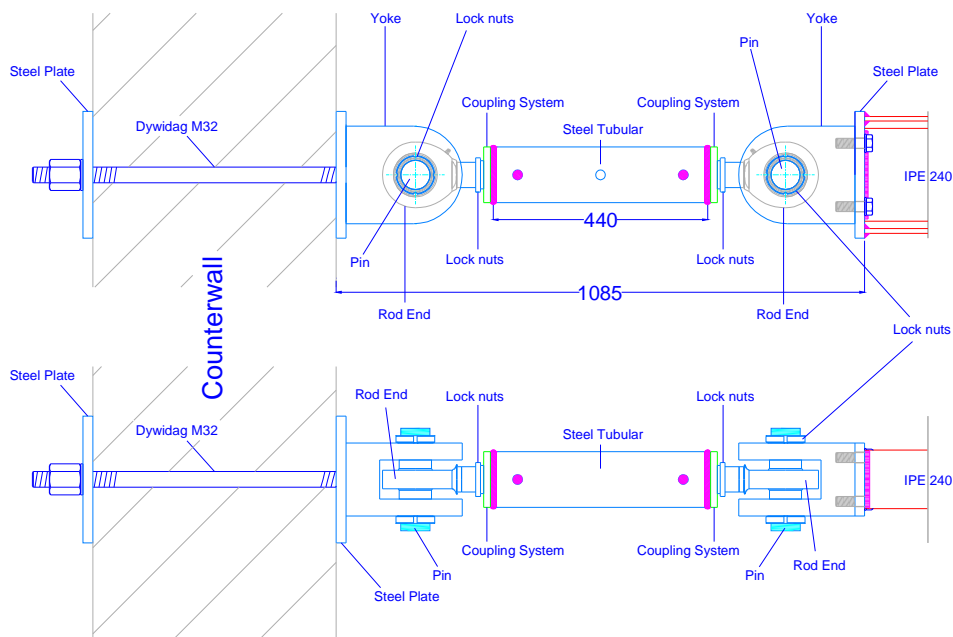


Figure 3-33. Lateral Support type 1

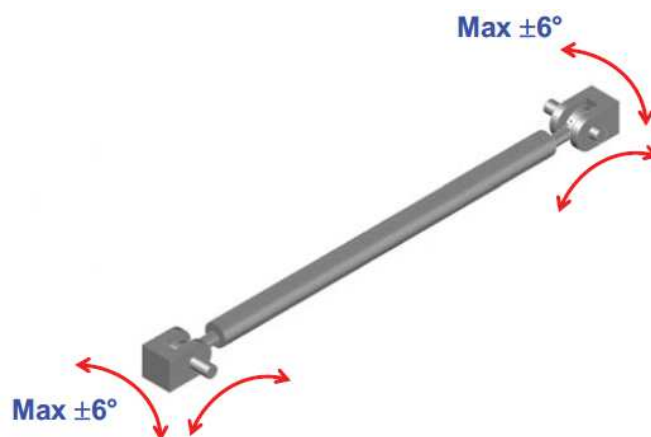


Figure 3-34. Behaviour of Lateral Supports

3.2.2 Restraints of the central beam

The central connection is made by two braces which restrain the vertical and the in plane lateral displacement of the central beam as shown in Figure 3-35. Differently, the out of plane lateral displacement is released. The braces are connected to the strong floor and to a steel plate in which is connected the central beam. Figure 3-36 reports a detailed representation of a single brace. The connection with the strong floor is made by yokes and rod ends while the steel plate in the top is equipped with spherical roller bearings in order to permit the connection with the yokes. In this case the braces are composed by two tubular steel elements as can be observed in Figure 3-36. The shorter element has been introduced in order to permit the length regulation of the brace. Also in this case the rod ends have the rotation that is fully released in the principal direction, while, in the other direction only a rotation of 6 degrees is permitted.

The actions on the steel braces have been obtained by the Abaqus model. Figure 3-37 and Figure 3-38 show the axial forces on the diagonal braces of the central joint restraint system

respectively for the Symmetric and Asymmetric frame. The braces of the central supports have been designed to support a force in traction of 250 kN. The shear force on the central beam transmitted by the central joint restraint system is reported in Figure 3-39.

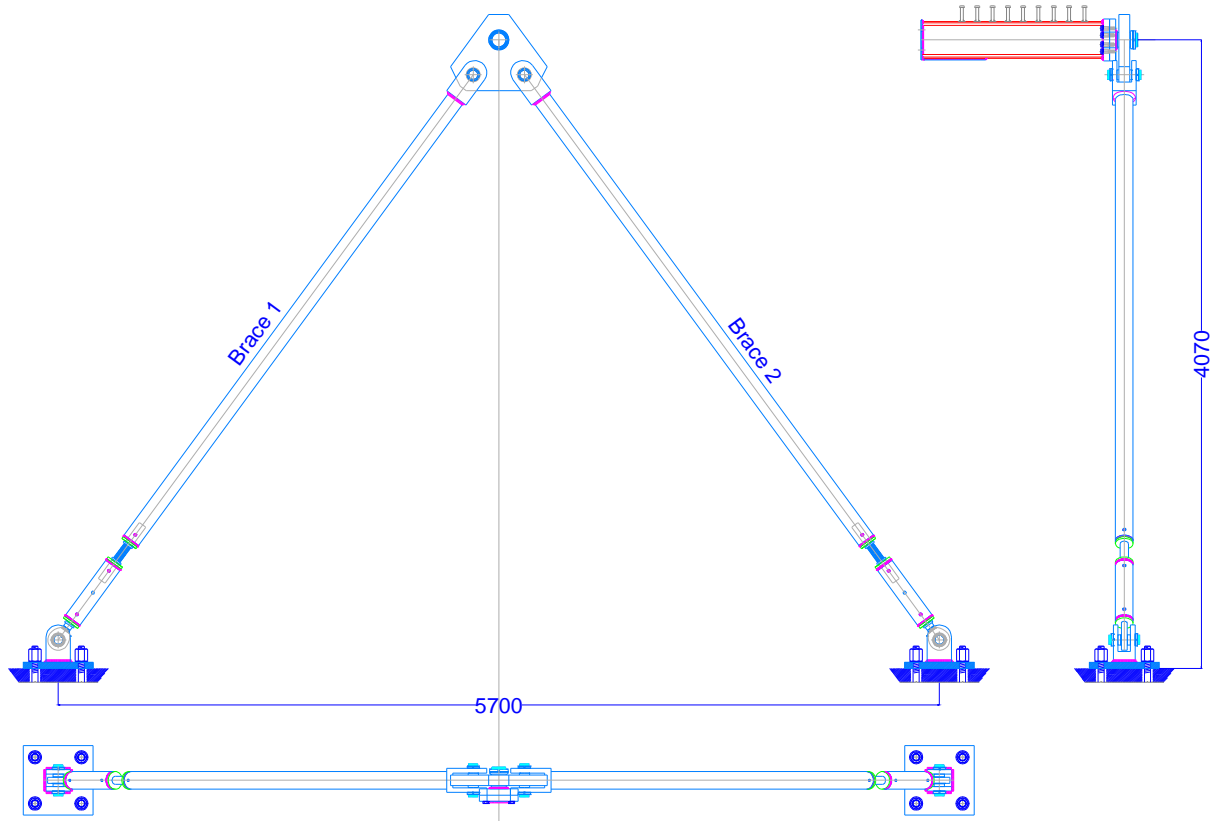


Figure 3-35. Central Support

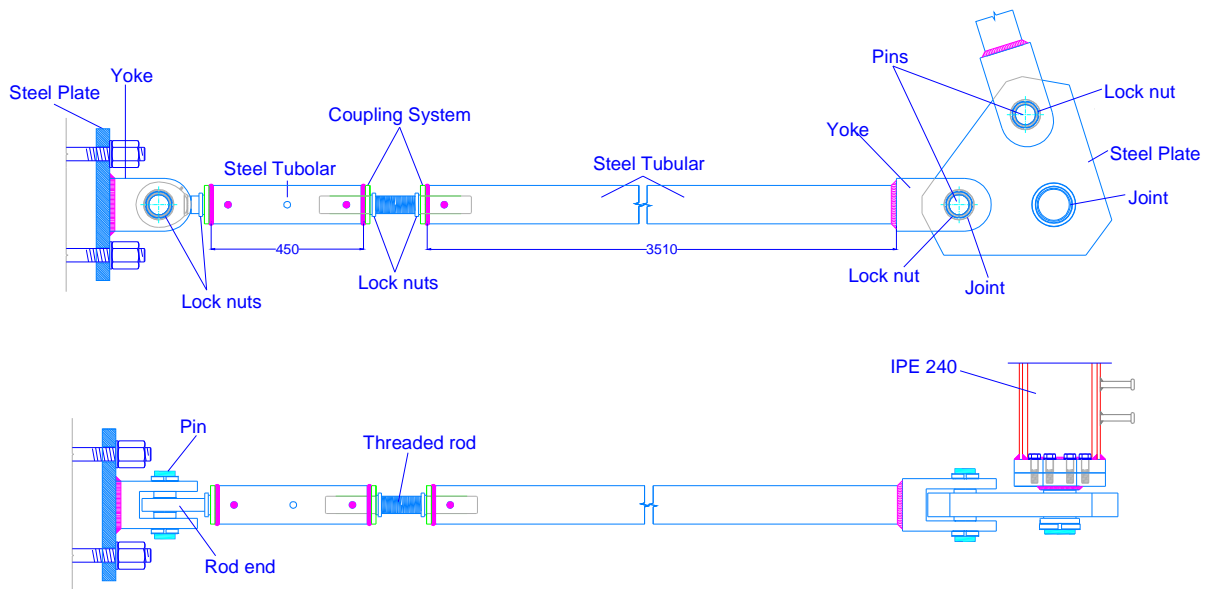


Figure 3-36. Central Support - One brace

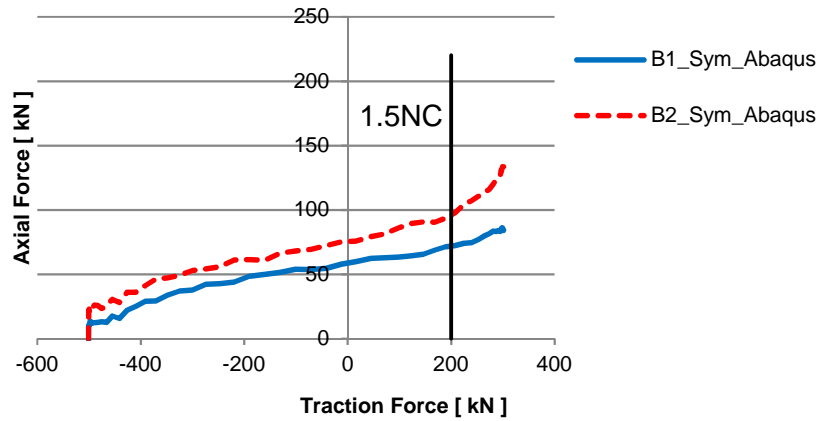


Figure 3-37. Axial Forces on the diagonal braces of the central joint restraint system of the Symmetric Frame

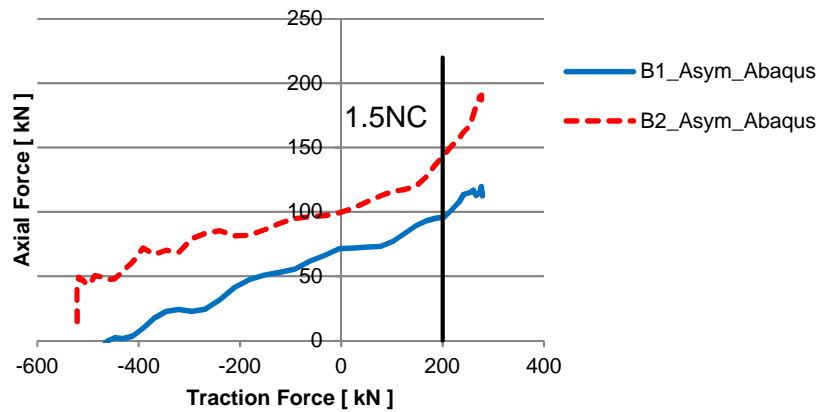


Figure 3-38. Axial Forces on the diagonal braces of the central joint restraint system of the Asymmetric Frame

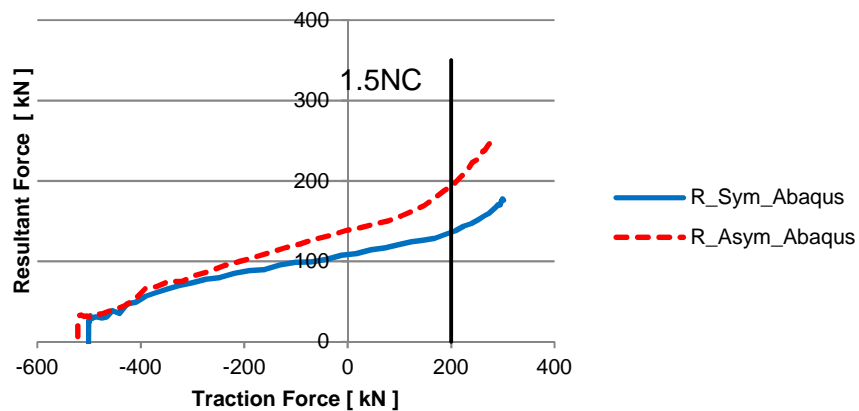


Figure 3-39. Resultant Vertical Force transmitted by the central joint restraint system

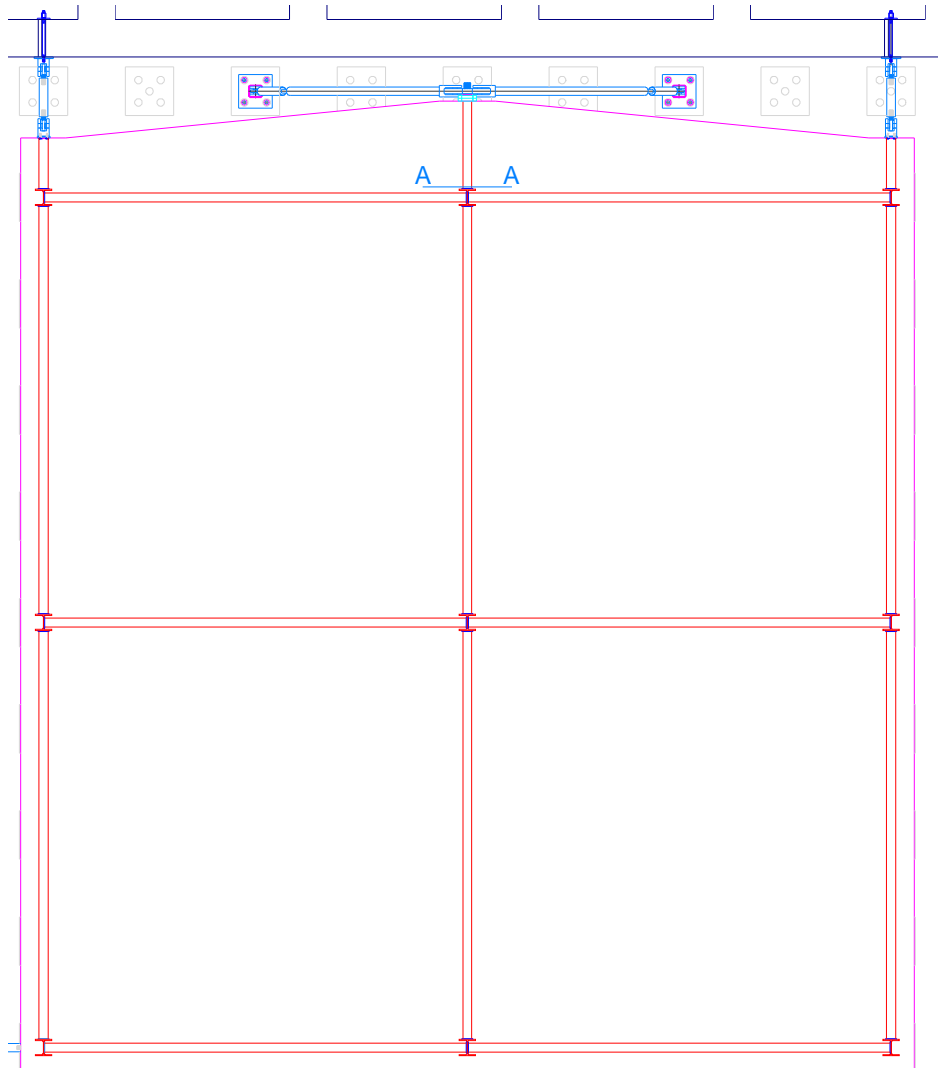


Figure 3-40. Symmetric Frame in the Laboratory. Section A-A

The forces on section A-A as illustrated in Figure 3-40 have been obtained as Free Body Cut in Abaqus. The evaluation of the bending moment on the composite section A-A is made by combining the actions of the beam and of the slab.

$$M_{Ed} = 186.909 \text{ kNm}$$

In order to achieve an adequate safety margin the lower flange of the beam is stiffened with a welded steel plate. The dimensions of the section of the steel plate are $10 \times 90 \text{ mm}^2$.

3.2.3 Column Supports

As can be observed from Figure 3-29, the central column is supported by a hydraulic ram. The hydraulic ram is introduced in order to permit simulation of the collapse of the central column, and it is arranged with a load cell to monitor the forces. The ends of hydraulic ram and load cell are pinned to the column from one side and to a base support from the other side. These connections, similarly to the other supports previously described are made by using yokes and rod ends.

Figure 3-41 reports the arrangement of the hydraulic ram. The hydraulic ram has a capacity in pulling of 600 kN and all the connecting parts have been designed to resist of this force.

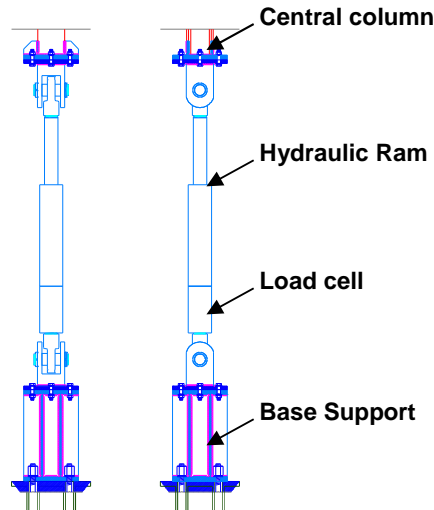


Figure 3-41. Arrangement of the Hydraulic Ram

Both, the hydraulic ram and all the columns are connected with base supports connected to the strong floor by Dywidag bars. Figure 3-42 give a 3-D representation of the base supports.

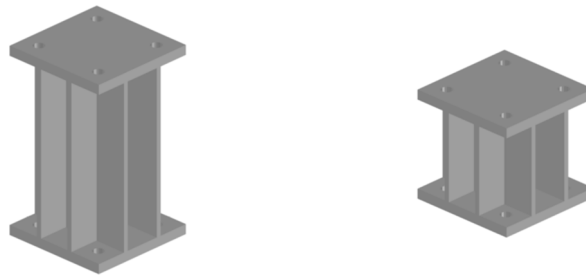


Figure 3-42. Base support a) for the hydraulic ram, b) for the columns

3.2.4 Column Supports

Moreover, as can be observed by the sections, the columns are longer than the story height, and continue up to the middle height of the second story, where they are connected among them by steel elements (HEB 140).

Figure 3-43 reports the central connection of the crowing beams.

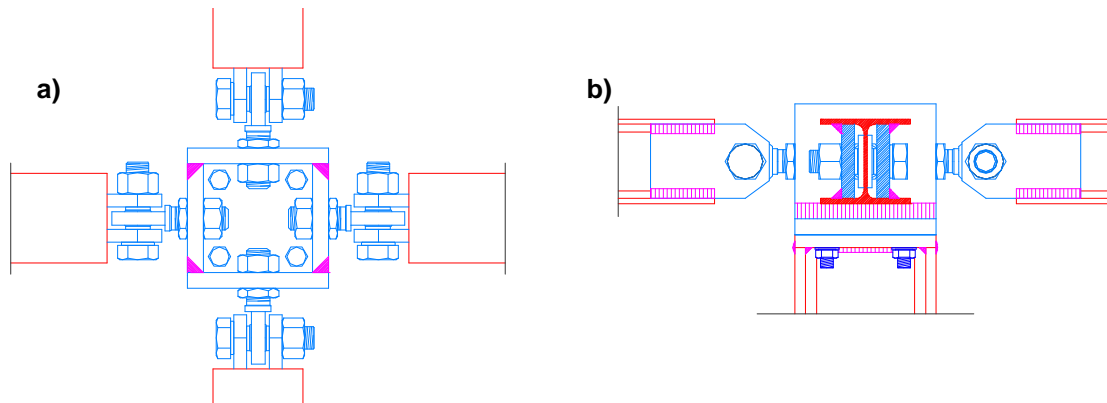


Figure 3-43. Central connection of the crowing beams. a) plan view, b) lateral view

Similar arrangement of the test is going to be employed also for the asymmetric configuration. Figure 3-44 reports the plan view of the experimental test for the symmetric and asymmetric structure.

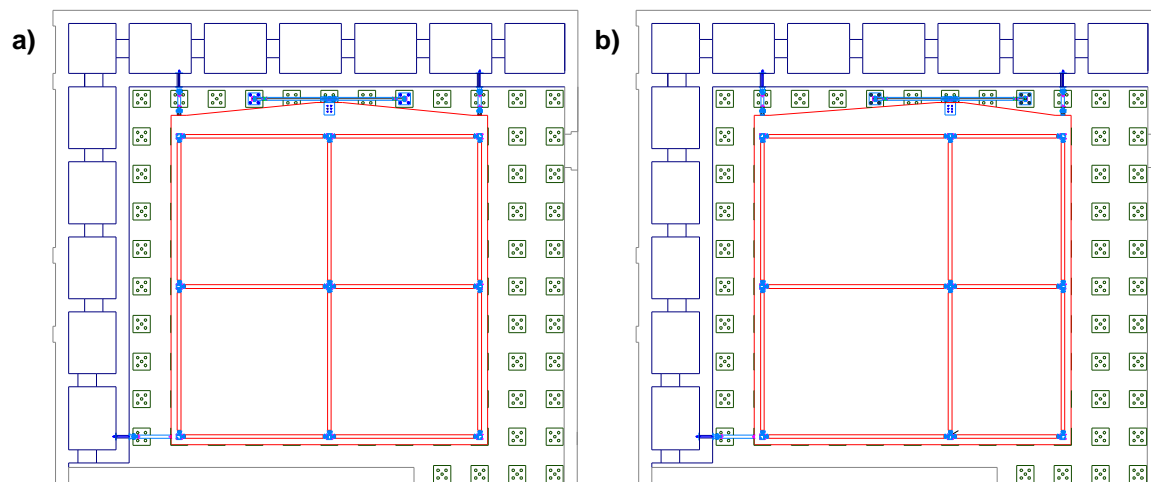


Figure 3-44. Plan View of the Experimental Tests for the a) Symmetric and b) Asymmetric Configuration

4 PRODUCTION OF THE SPECIMENS

In this section, a list of the pieces produced for the construction of the two specimens is given. All the drawings are reported in the annexes A-C.

Depending on the material to be provided, the material was provide by ArcelorMittal, local fabricators and local companies.

4.1 Steel components

Table 4-1 summarises the steel components needed for the construction of steel skeleton of the full-scale specimens.

Table 4-1. Summary of the steel components for the steel skeleton of the full-scale specimens

DESCRIPTION	DRAWING NAME	NUMBER OF PIECES	SPEC. CONFIGURATION	
			Symmetric	Asymmetric
Summary of the steel components	FST 01	-	X	X
COLUMNS TYPE 1				
Steel profile HEB220 length 5500mm	FST 02-09	18	X	X
Steel plate type B 400x400x30mm	FST 03-09	18	X	X
Steel plate type C 220x220x20mm	FST 03-09	18	X	X
Column assembly	FST 09	-	X	X
BEAMS				
Beam type 1 Steel profile IPE240 length 5460mm	FST 04	12	X	X
Beam type 2 Steel profile IPE240 length 5670mm	FST 05	6	X	
Beam type 3 Steel profile IPE240 length 7095mm	FST 06	3		X
Beam type 4 Steel profile IPE240 length 4246mm	FST 07	3		X
Beam type 5 Steel profile IPE240 length 1500mm	FST 08	6	X	X
Steel plate type A	FST 03-04-05-06-07-08	54	X	X

Figure 4-1and Figure 4-2 provide a plan view of the two full-scale specimens (steel skeleton) which allows identifying the position of the various steel components.

The profiles needed for the steel skeleton of both the specimens (Annex A) were produced by ArcelorMittal.

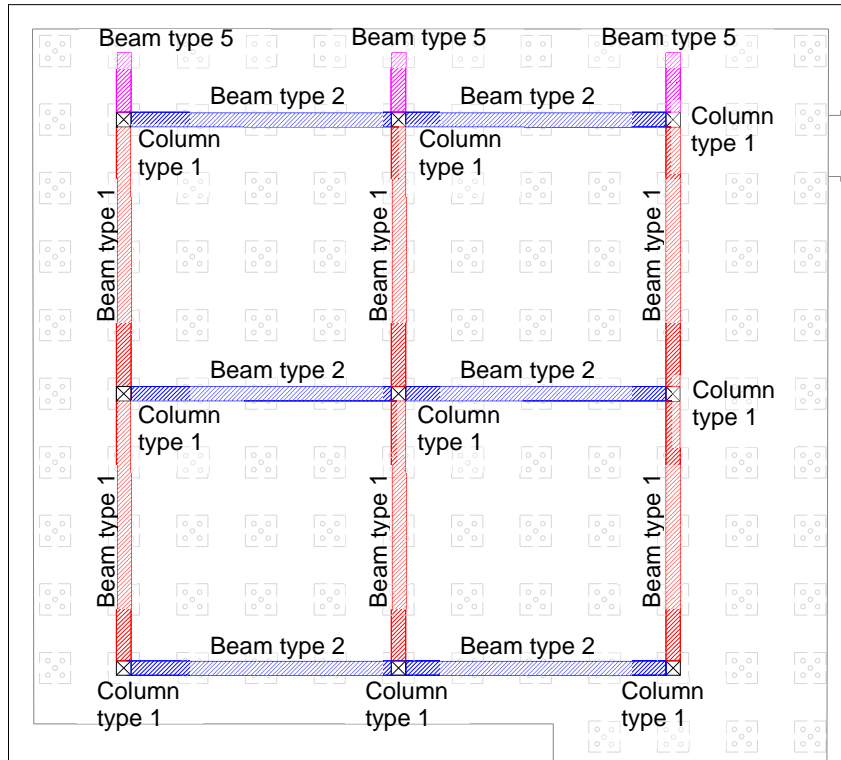


Figure 4-1. Steel profiles for the symmetric full-scale specimen

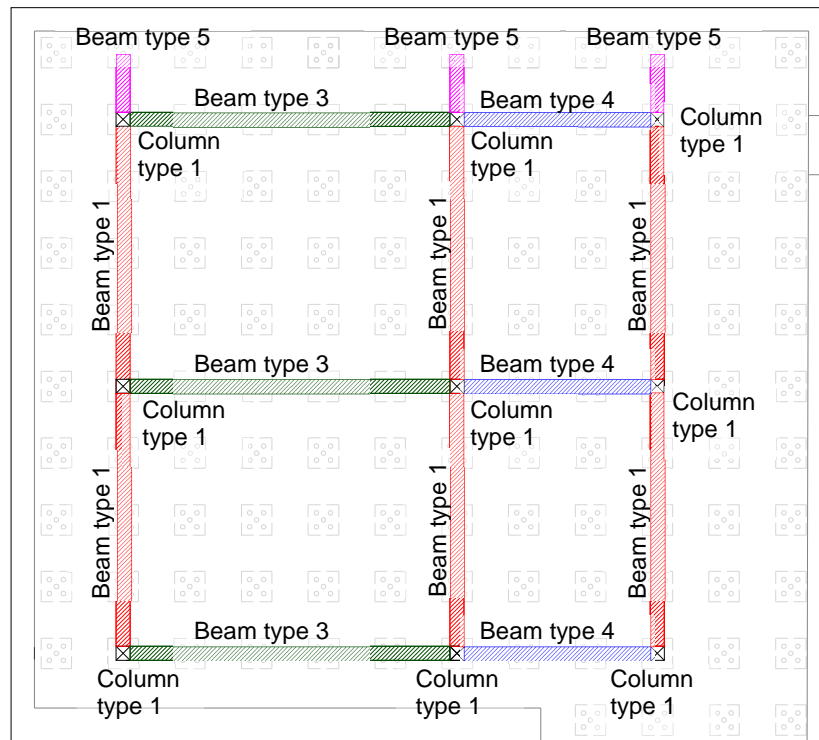


Figure 4-2. Steel profiles for the asymmetric full-scale specimen

4.2 Restraints

In order to reproduce the effect provided by the remaining part of the structure and the base connections, the specimens will be restrained to both the floor slab and the vertical walls of the laboratory. At this aim suitable restraints were identified through FE numerical investigations and accordingly designed. Furthermore, the columns of the specimens, at their upper ends, will be connected together in order to reproduce the effect provided by the levels of the structure above the one considered in the tests. Figure 4-3, Figure 4-4 and Figure 4-5 allow identifying the position of the restraints.

The main drawings related to the restraints are summarised in Table 4-2 and collected in Annex B. The restraints (Annex B) were produced by local fabricators.

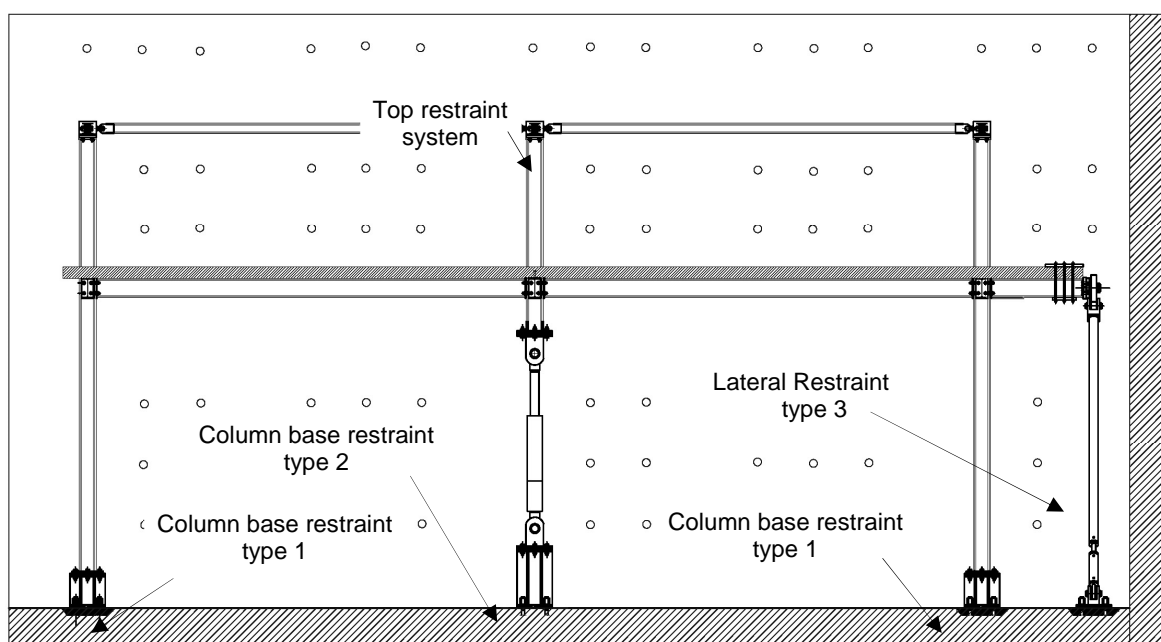


Figure 4-3. Restraints configuration for the full-scale specimens

Table 4-2. Summary of the restraints

DESCRIPTION	DRAWING NAME	NUMBER OF PIECES	SPECIMEN'S CONFIGURATION	
			Symmetric	Asymmetric
RESTRAINTS AT THE COLUMN'S BASE				
Column Base Restraint type 1	CBR1	8	X	X
Column Base Restraint type 2	CBR2	1	X	X
LATERAL RESTRAINTS				
Lateral Restraint type 1	LR1	1	X	X
Lateral Restraint type 2	LR2	2	X	X
Lateral Restraint type 3	LR3	1	X	X
TOP COLUMN RESTRAINTS				
Top connection type 1	TC1	1	X	X
Top connection type 2	TC2	4	X	X
Top connection type 3	TC3	4	X	X

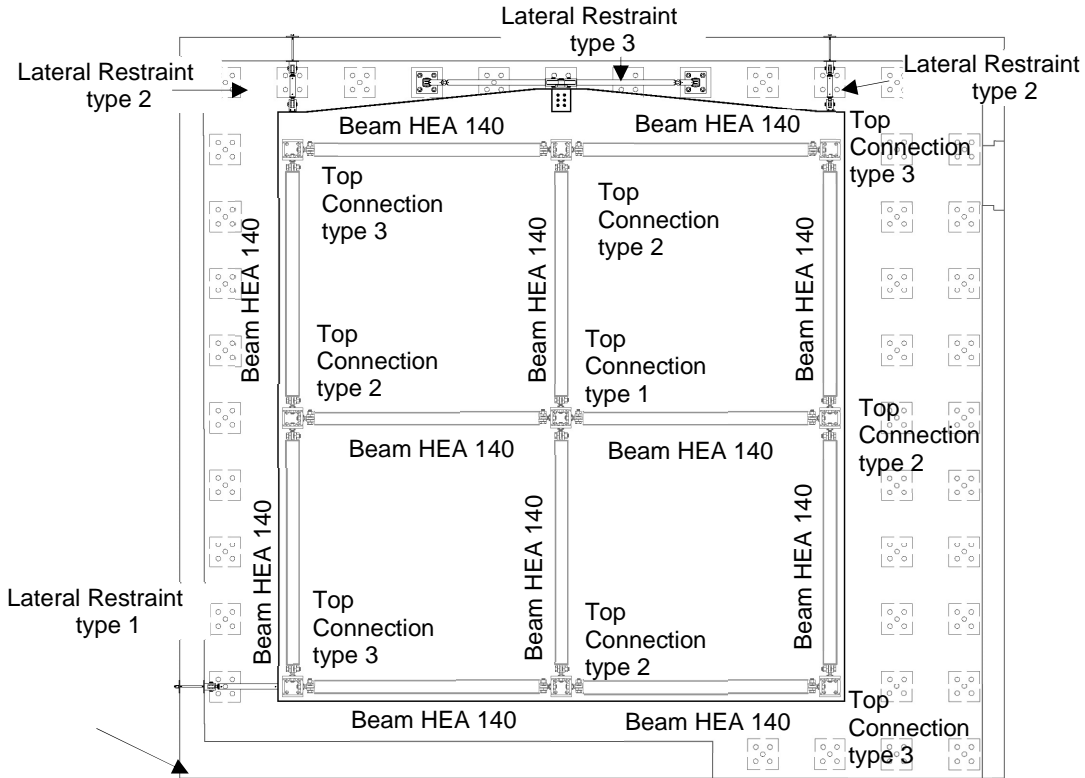


Figure 4-4. Restraints for the symmetric full-scale specimen

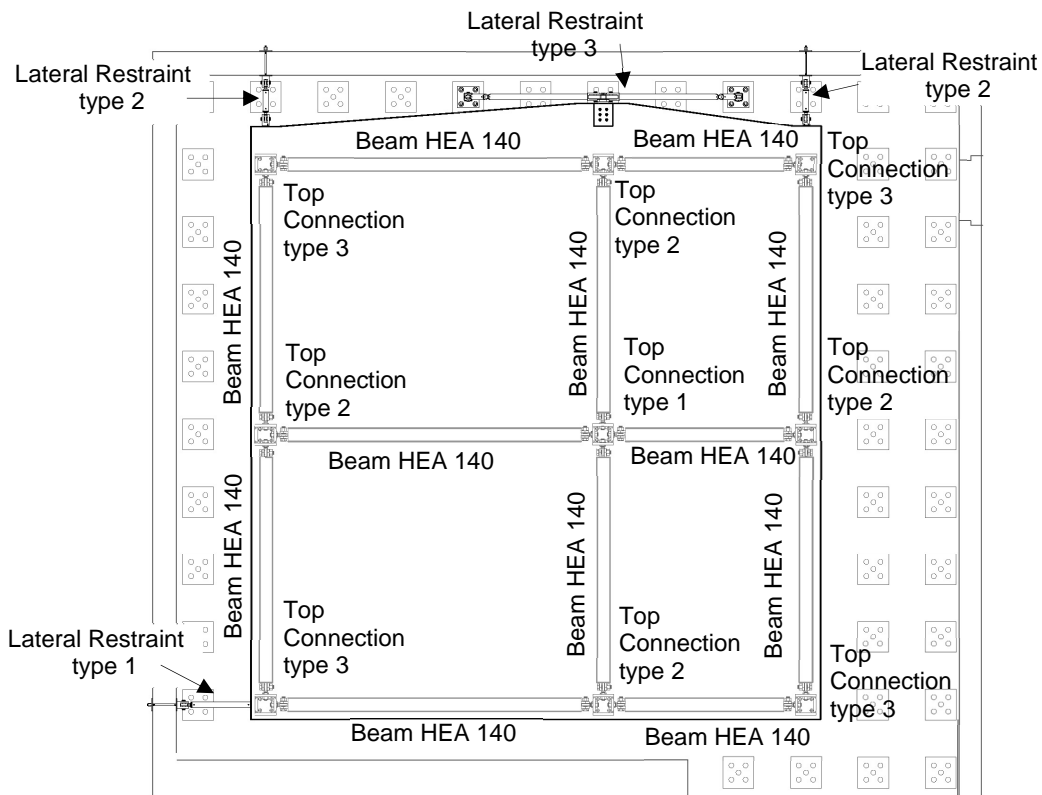


Figure 4-5. Restraints for the asymmetric full-scale specimen

4.3 Rebars

The reinforcement of the slabs of the two full-scale specimens is realized with an electrowelded wire mesh located on both the upper and the lower sides of the slab and additional rebars added where required by the design calculations.

A summary of the reinforcement needed for the slabs of the two full-scale specimens is reported in Table 4-3-Table 4-7. In detail:

- Table 4-3 summarises the electrowelded wire mesh required for both the specimens;
- Table 4-4 and Table 4-5 list the additional rebars for the symmetric specimen, for the lower and the upper side, respectively;
- Table 4-6 and Table 4-7 collect the additional rebars for the asymmetric specimen, related to the lower and the upper side, respectively.

A detailed description of the layout of the rebars for both the specimens is presented in Annex C.

Table 4-3-Table 4-7 and the drawings of Annex C have been sent to a local Company for their production.

Table 4-3. Summary of the electrowelded wires for the full-scale specimens (symmetric and asymmetric configuration)

ELECTROWELDED WIRES			
MESH TYPE 1			
N° panels	Dimensions mm	Nominal unitary weight kgf	Nominal total weight kgf
22	5500x2300	57,882	1273
MESH TYPE 2			
N° panels	Dimensions mm	Nominal unitary weight kgf	Nominal total weight kgf
62	7000x2300	74,493	4619
MESH TYPE 3			
N° panels	Dimensions mm	Nominal unitary weight kgf	Nominal total weight kgf
44	2150x1300	12,976	571

Table 4-4. Summary of the rebars for the symmetric configuration - Lower side

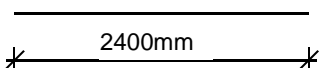
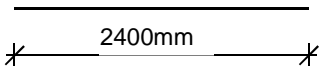
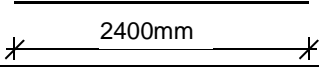
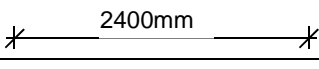
SLAB REBARS - LOWER SIDE - SYMMETRIC CONFIGURATION					
Position	Shape	Diameter mm	Length mm	Quantity n°	Nominal weight kgf
Pos. C		10	2400	22	33
Pos. D		10	2400	8	12
Pos. E		10	2400	30	44
Pos. F		10	2400	8	12
Total nominal weight (kgf)					153

Table 4-5. Summary of the rebars for the symmetric configuration - Upper side.

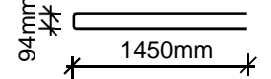
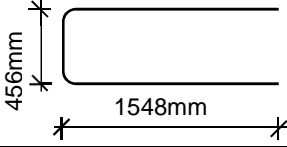
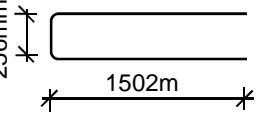
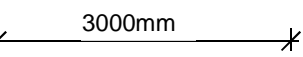
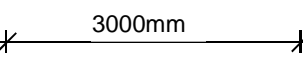
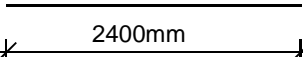

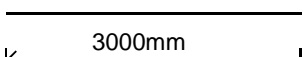
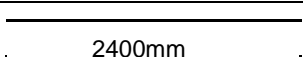
SLAB REBARS - UPPER SIDE - SYMMETRIC CONFIGURATION					
Position	Shape	Diameter mm	Length mm	Quantity n°	Nominal kgf
Pos. A		10	3000	28	52
Pos. G1		16	3500	3	17
Pos. G2		16	3200	3	15
Pos. H		16	3000	24	114
Pos. I		16	3000	48	227
Pos. L		10	2400	92	136
Pos. M		16	3000	12	57
Pos. N		16	3000	44	206
Pos. O		10	2400	35	52
Total nominal weight (kgf)					878

Table 4-6. Summary of the rebars for the asymmetric configuration - Lower side

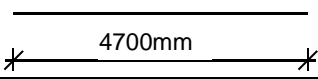
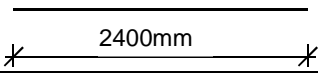
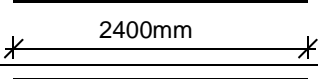
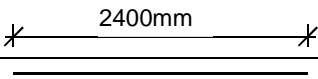
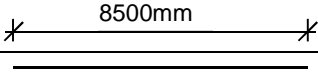
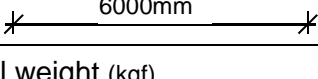
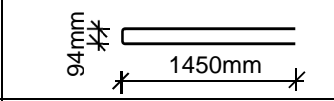
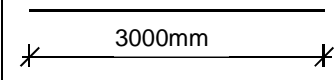
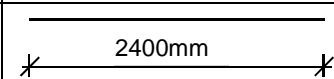
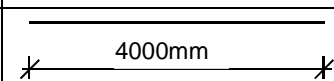
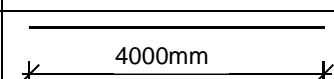
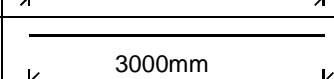
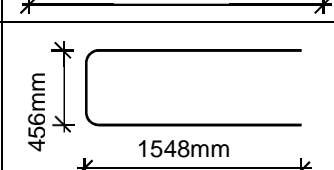
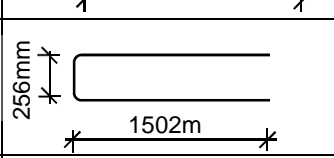
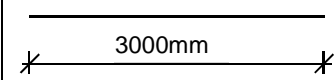
SLAB REBARS - LOWER SIDE - ASYMMETRIC CONFIGURATION					
Position	Shape	Diameter mm	Length mm	Quantity n°	Nominal weight kgf
Pos. C		10	4700	41	119
Pos. D		10	2400	8	12
Pos. E		10	2400	21	31
Pos. F		10	2400	8	12
Pos. G		10	8500	8	42
Pos. H		10	6000	76	281
Total nominal weight (kgf)					527

Table 4-7. Summary of the rebars for the asymmetric configuration - Upper side

SLAB REBARS - UPPER SIDE - ASYMMETRIC CONFIGURATION					
Position	Shape	Diameter mm	Length mm	Quantity n°	Nominal kgf
Pos. A		10	3000	28	52
Pos. I		16	3000	40	189
Pos. L		10	2400	98	145
Pos. M		16	4000	12	76
Pos. N		16	4000	45	284
Pos. O		10	3000	35	65
Pos. P1		16	3500	3	17
Pos. G2		16	3200	3	15
Pos. Q		16	3000	24	114
Total nominal weight (kgf)					957

5 CONCLUDING REMARKS

This document focuses on the design work related to two full scale tests carried out at the University of Trento in the framework of the European RFCS project 'Robust Impact design of steel and composite building structures' (acronym ROBUSTIMPACT) (Grant Agreement Number: RFSR-CT-2012-00029).

The study focuses on composite steel and concrete framed buildings and in particular on their response when subject to accidental actions. At this aim, two reference five-story buildings were designed according to the Eurocodes, and representative one story sub-frames 'extracted' from them. The sub-frames were built and tested at the Laboratory of Material and Structural Testing (LMST) of the University of Trento by simulating the loss of an internal column. In this document, the work performed to design the reference frames, to 'extract' representative sub-frames, and to design the test set-up is highlighted. In detail, the following subjects are analyzed:

- the selection and the definition of the reference buildings for the case studies;
- the design of the reference buildings according to the Eurocodes;
- the identification of the representative sub-structures (slab-beam system, columns and joints) from the reference structures to be experimentally investigated;
- the design of the test set-up.

6 ACKNOWLEDGEMENTS

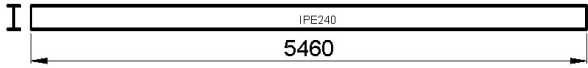
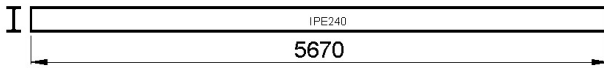
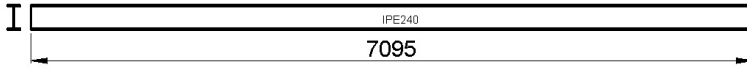
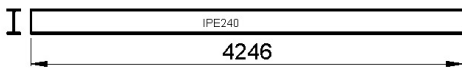
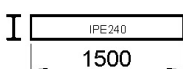
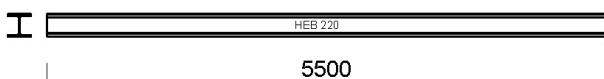
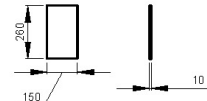
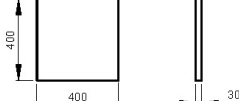
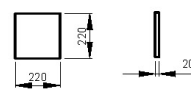
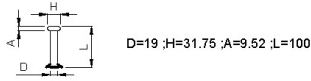

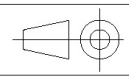
The experimental work presented in this document was supported by the European Commission under its Research Programme of the Research Fund for Coal and Steel (Project acronym Robust Impact, Grant Agreement Number: RFSR-CT-2012-00029) .

The Authors gratefully acknowledge prof. eng. Paolo Zanon, Mr. Stefano Girardi, Mr. Marco Graziadei and Mr. Alessandro Banterla for their valuable advices for the design of the experimental set-up.

7 LITERATURE

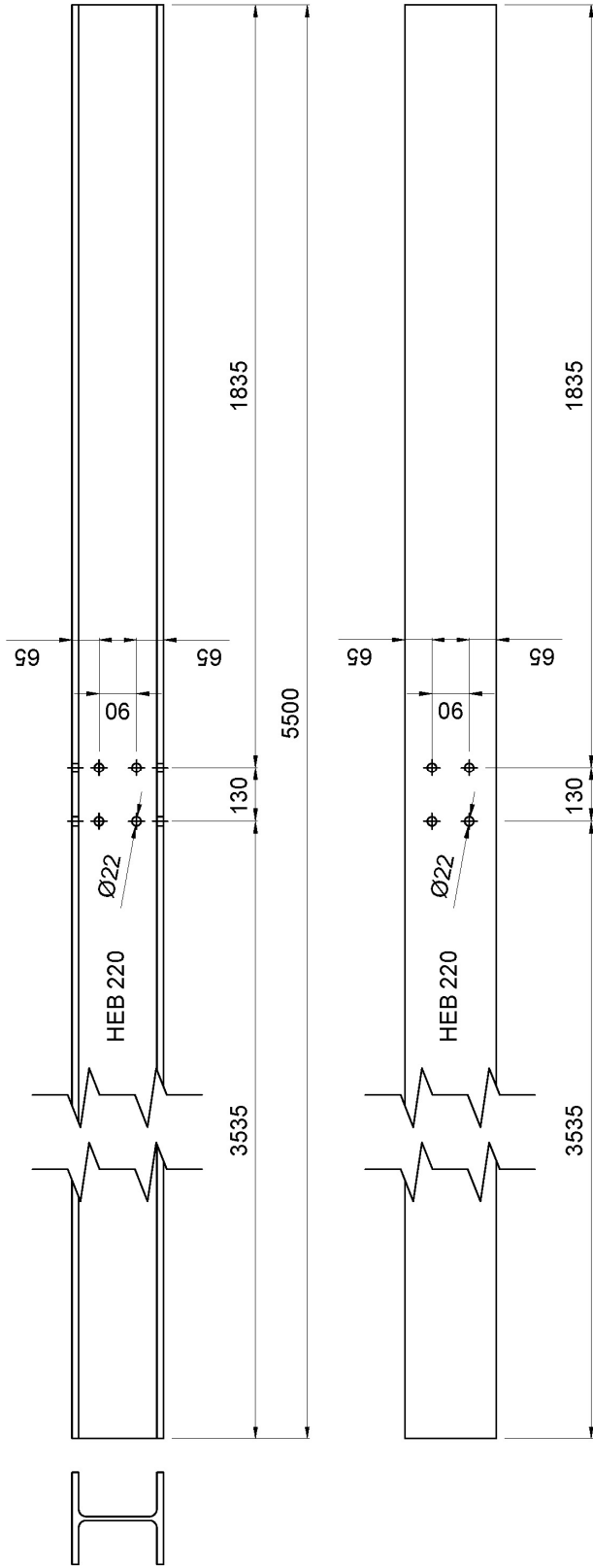
- [1] CSI SAP 2000 – Linear and nonlinear static and dynamic analysis and design of three-dimensional structures: Basic analysis reference manual, Computers and Structures, Inc. Berkeley, California, 2011.
- [2] EN 1993-1-8 – Eurocode 3: Design of steel structures - Part 1-8: Design of joints, EN 1993-1-8:2005, December 2010;
- [3] EN 1992-1-1 – Eurocode 2: Design of concrete structures - Part 1-1: General rules and rules for buildings, CEN 2004.
- [4] EN 1993-1-1 – Eurocode 3: Design of steel structures - Part 1-1: General rules and rules for buildings, CEN 2004.
- [5] EN 1991-1-4 – Eurocode 1: Actions on Structures - Part 1-4: General actions - Wind Actions, CEN 2004.
- [6] EN 1991-1-3 – Eurocode 1: Actions on Structures - Part 1-3: General actions - Snow Loads, CEN 2002.
- [7] EN 1990 – Eurocode 0: Basis of Structural Design, CEN 2002.
- [8] EN 1994-1-1 – Eurocode 4: Design of composite steel and concrete structures - Part 1-1: General rules and rules for buildings, CEN 2004.
- [9] ABAQUS – Analysis user's manual, version 6.10, Simulia Dassault Systems, 2010.
- [10] Allam SM, Shoukry MS, Rashad G, Hassan AS.. Evaluation of tension stiffening effect on the crack width calculation of flexural RC members. Alexandria Engineering Journal; 52: 163-173. 2013.
- [11] Fu F, Lam D, Ye J. Modeling semi-rigid composite joints with precast hollowcore slabs in hogging moment region. Journal of Constructional Steel Research; 64(12): 1408-1419. 2008.


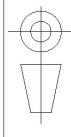
ANNEX A: FULL-SCALE TESTS - STEEL COMPONENTS

Beam Type 1 Number of pieces - 12 																																																																																											
Beam Type 2 Number of pieces - 6 																																																																																											
Beam Type 3 Number of pieces - 3 																																																																																											
Beam Type 4 Number of pieces - 3 																																																																																											
Beam Type 5 Number of pieces - 6 																																																																																											
Column type 1 Number of pieces - 18 																																																																																											
Plate type A Number of pieces - 54 	Plate type B Number of pieces - 18 	Plate type C Number of pieces - 18 																																																																																									
Shear Connector SD 3/4" x 4"; Mild Steel; 1182 Headed studs 																																																																																											
<table border="1" style="width: 100%; border-collapse: collapse; text-align: center;"> <thead> <tr> <th>Name</th> <th>Steel Grade</th> <th>Dimensions [mm]</th> <th>Weight [t]</th> <th>Number of pieces</th> <th>Total Weight [t]</th> <th>Drawing No.</th> </tr> </thead> <tbody> <tr> <td>Beam type 1</td> <td>S 355 JR</td> <td>240x120x5460</td> <td>0.168</td> <td>12</td> <td>2.011</td> <td>FST 04</td> </tr> <tr> <td>Beam type 2</td> <td>S 355 JR</td> <td>240x120x5670</td> <td>0.174</td> <td>6</td> <td>1.044</td> <td>FST 05</td> </tr> <tr> <td>Beam type 3</td> <td>S 355 JR</td> <td>240x120x7095</td> <td>0.218</td> <td>3</td> <td>0.653</td> <td>FST 06</td> </tr> <tr> <td>Beam type 4</td> <td>S 355 JR</td> <td>240x120x4246</td> <td>0.130</td> <td>3</td> <td>0.391</td> <td>FST 07</td> </tr> <tr> <td>Beam type 5</td> <td>S 355 JR</td> <td>240x120x1500</td> <td>0.046</td> <td>6</td> <td>0.276</td> <td>FST 08</td> </tr> <tr> <td>Column type 1</td> <td>S 355 JR</td> <td>220x220x5500</td> <td>0.393</td> <td>18</td> <td>7.079</td> <td>FST 02-09</td> </tr> <tr> <td>Plate type A</td> <td>S 355 JR</td> <td>260x150x10</td> <td>0.003</td> <td>54</td> <td>0.165</td> <td>FST 03-04-05-06-07-08</td> </tr> <tr> <td>Plate type B</td> <td>S 355 JR</td> <td>400x400x30</td> <td>0.038</td> <td>18</td> <td>0.678</td> <td>FST 03-09</td> </tr> <tr> <td>Plate type C</td> <td>S 355 JR</td> <td>220x220x20</td> <td>0.007</td> <td>18</td> <td>0.137</td> <td>FST 03-09</td> </tr> <tr> <td>Shear Coonectors</td> <td>SD 3/4"x 4"</td> <td>D=19; H=31.75; A=9.52; L=100</td> <td>---</td> <td>1182</td> <td>---</td> <td>FST 04-05-06-07-08</td> </tr> <tr> <td colspan="5">Total</td> <td>12.434</td> <td></td> </tr> </tbody> </table>								Name	Steel Grade	Dimensions [mm]	Weight [t]	Number of pieces	Total Weight [t]	Drawing No.	Beam type 1	S 355 JR	240x120x5460	0.168	12	2.011	FST 04	Beam type 2	S 355 JR	240x120x5670	0.174	6	1.044	FST 05	Beam type 3	S 355 JR	240x120x7095	0.218	3	0.653	FST 06	Beam type 4	S 355 JR	240x120x4246	0.130	3	0.391	FST 07	Beam type 5	S 355 JR	240x120x1500	0.046	6	0.276	FST 08	Column type 1	S 355 JR	220x220x5500	0.393	18	7.079	FST 02-09	Plate type A	S 355 JR	260x150x10	0.003	54	0.165	FST 03-04-05-06-07-08	Plate type B	S 355 JR	400x400x30	0.038	18	0.678	FST 03-09	Plate type C	S 355 JR	220x220x20	0.007	18	0.137	FST 03-09	Shear Coonectors	SD 3/4"x 4"	D=19; H=31.75; A=9.52; L=100	---	1182	---	FST 04-05-06-07-08	Total					12.434	
Name	Steel Grade	Dimensions [mm]	Weight [t]	Number of pieces	Total Weight [t]	Drawing No.																																																																																					
Beam type 1	S 355 JR	240x120x5460	0.168	12	2.011	FST 04																																																																																					
Beam type 2	S 355 JR	240x120x5670	0.174	6	1.044	FST 05																																																																																					
Beam type 3	S 355 JR	240x120x7095	0.218	3	0.653	FST 06																																																																																					
Beam type 4	S 355 JR	240x120x4246	0.130	3	0.391	FST 07																																																																																					
Beam type 5	S 355 JR	240x120x1500	0.046	6	0.276	FST 08																																																																																					
Column type 1	S 355 JR	220x220x5500	0.393	18	7.079	FST 02-09																																																																																					
Plate type A	S 355 JR	260x150x10	0.003	54	0.165	FST 03-04-05-06-07-08																																																																																					
Plate type B	S 355 JR	400x400x30	0.038	18	0.678	FST 03-09																																																																																					
Plate type C	S 355 JR	220x220x20	0.007	18	0.137	FST 03-09																																																																																					
Shear Coonectors	SD 3/4"x 4"	D=19; H=31.75; A=9.52; L=100	---	1182	---	FST 04-05-06-07-08																																																																																					
Total					12.434																																																																																						
 UNIVERSITÀ DEGLI STUDI DI TRENTO DIPARTIMENTO DI INGEGNERIA MECCANICA E STRUTTURALE Laboratorio Prove Materiali e Strutture				Part No. F_{ull} Scale S Test T		RFCS project N° RFSR-CT-2012-0029 Proposal acronym: ROBUSTIMPACT Organisation acronym: UNITRE Note: All dimensions are illustrated in the individual drawings																																																																																					
		Material: FST 01 Drawing No.: FST 01 Date: 13/09/2013 Review: Revised by: Designed by:		SCALE: Date: 13/09/2013 Reference file: Frame_Test_RobustImpact_UNITRE_FST_TST_000		The design is property of the University of Trento. Copy or reuse this document without permission is not allowed and will be punished in accordance with the law.																																																																																					

MOMENT RESISTING STEEL-CONCRETE COMPOSITE FRAMES UNDER THE COLUMN LOSS SCENARIO:
 DESIGN OF THE REFERENCE FRAMES AND OF THE FULL-SCALE SUB-FRAME SPECIMENS

Column type 1



	UNIVERSITÀ DEGLI STUDI DI TRENTO DIPARTIMENTO DI INGEGNERIA MECCANICA E STRUTTURALE Laboratorio Prove Materiali e Strutture	
	Part No.	
Full Scale Test	RFCS project N° RFSR-CT-2012-0029 Proposal acronym: ROBUSTIMPACT Organisation acronym: UNITRE	SCALE Drawing No. S 355 JR Date 15/06/2013 Revision
Note: All dimensions are illustrated in the individual drawings	FST 02	Reference file Frame_1_Full_ScaleImpact_COLUMN_FST_000
This drawing is property of the University of Trento. Copy or use this document without permission is not allowed and will be punished in accordance with the law.		

**MOMENT RESISTING STEEL-CONCRETE COMPOSITE FRAMES UNDER THE COLUMN LOSS SCENARIO:
DESIGN OF THE REFERENCE FRAMES AND OF THE FULL-SCALE SUB-FRAME SPECIMENS**

Plate type A

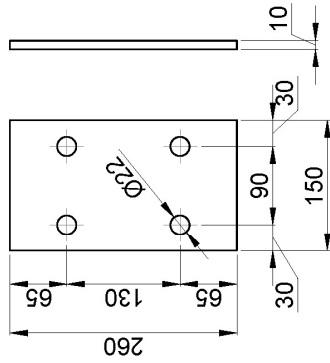


Plate type C

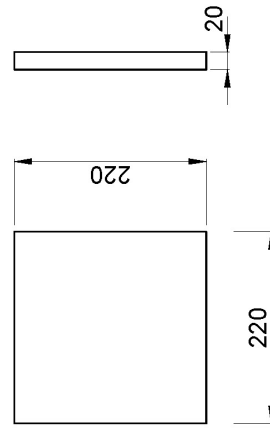
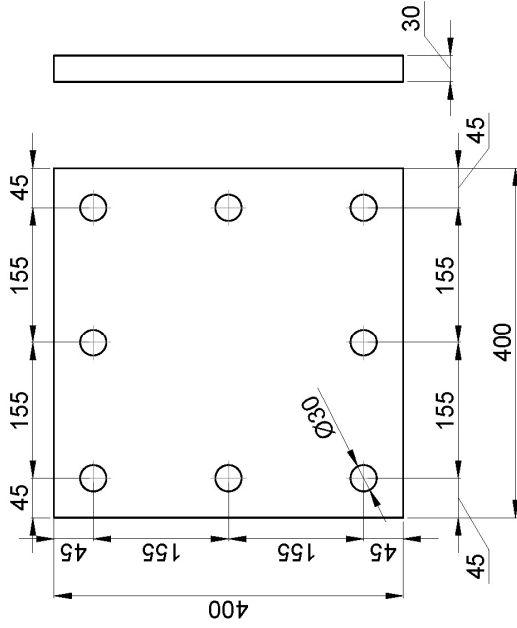

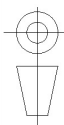
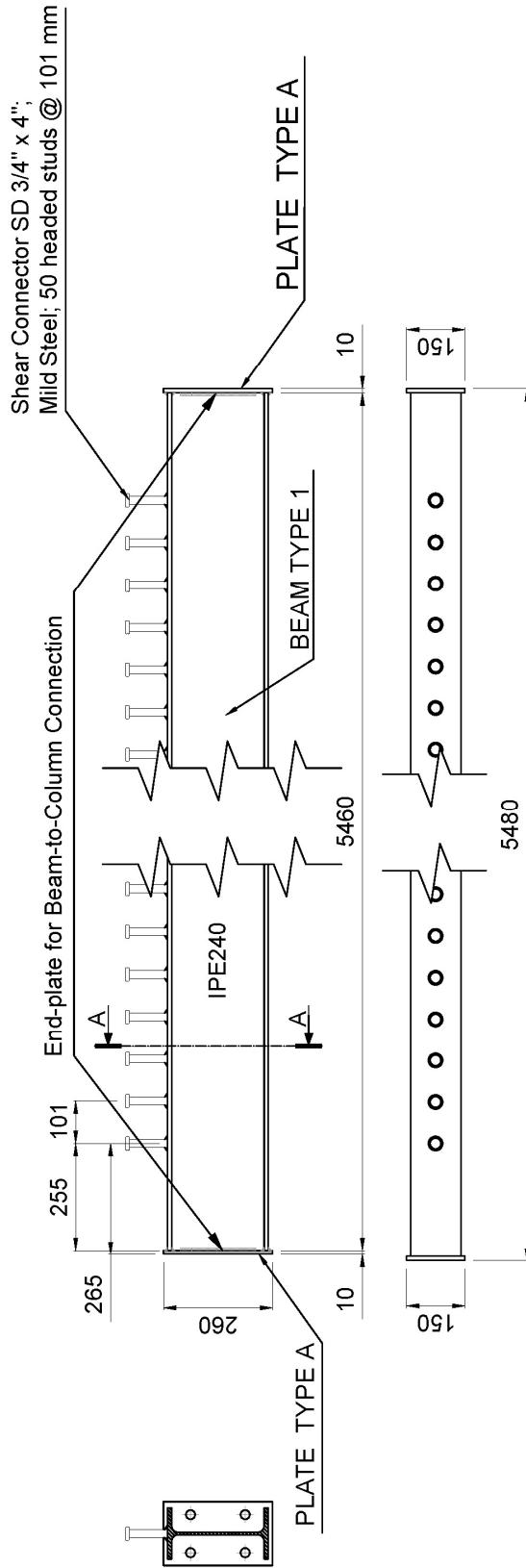


Plate type B

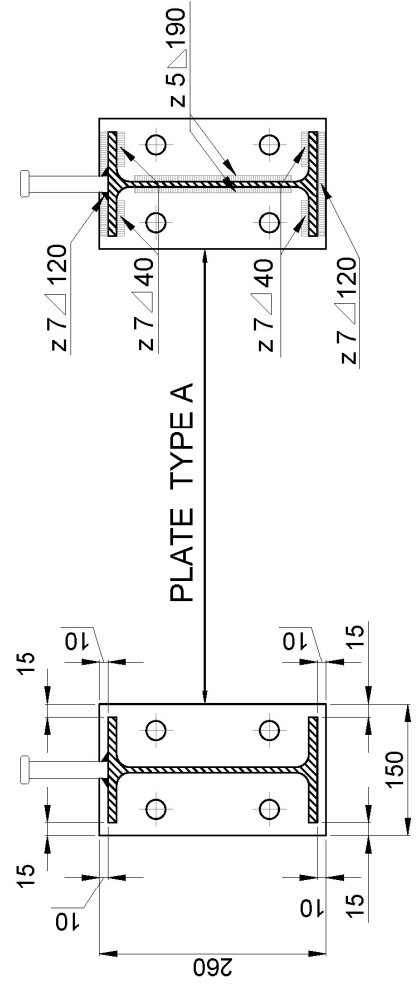



	UNIVERSITÀ DEGLI STUDI DI TRENTO <small>DIPARTIMENTO DI INGEGNERIA, MECCANICA E STRUTTURALE</small> Laboratorio Prove Materiali e Strutture	
Part No. F ull S cale T est		RFCS project N° RFSR-CT-2012-0029 Proposal acronym: ROBUSTIMPACT Organisation acronym: UNTIRE
Note: All dimensions are illustrated in the individual drawings		Material: S 355 JR Drawing No.: 13/06/2013 Date: 13/06/2013 Review:
Revises by:		Reference file:
Designed by:		File name: "RobustImpact_UNTIRE_fig_1_000"
This design is property of the University of Trento. Copy or use without permission is not allowed and will be punished in accordance with the law.		

Number of pieces - 12

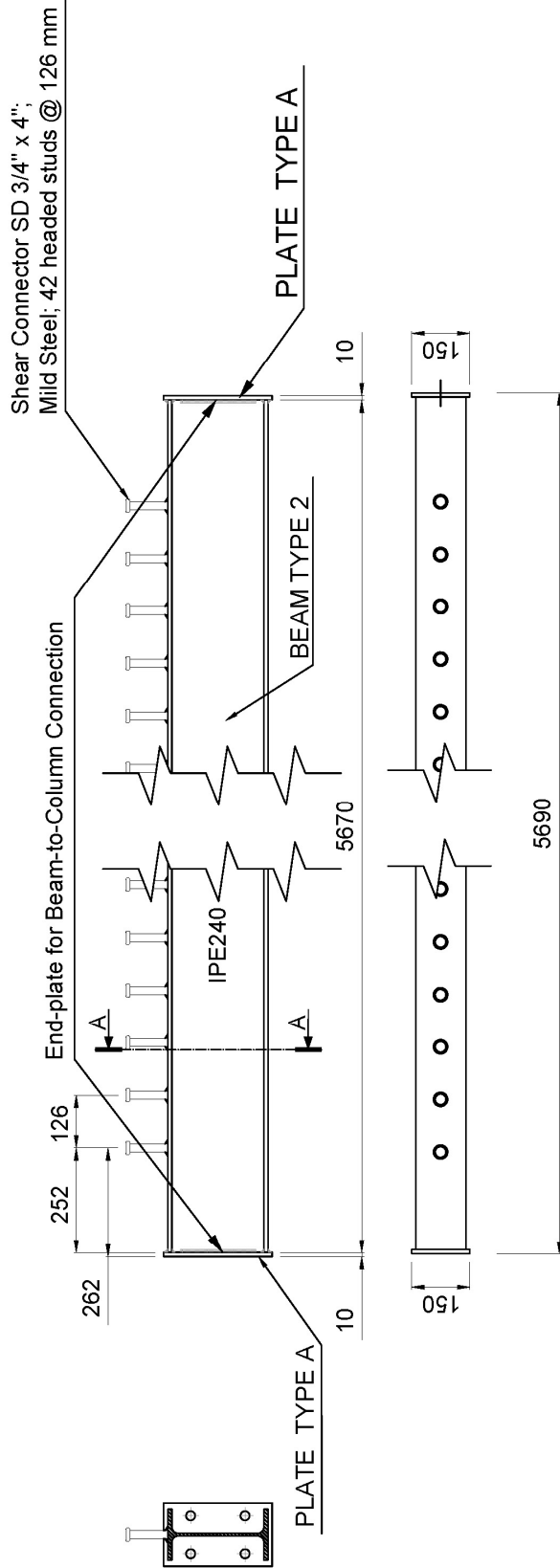


SEC. A-A SCALE 1:5

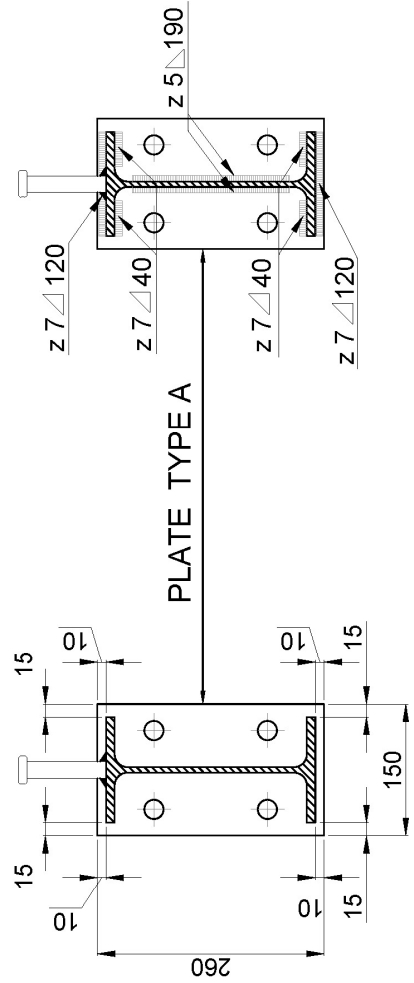



 UNIVERSITÀ DEGLI STUDI DI TRENTO DIPARTIMENTO DI INGEGNERIA, ARCHITETTURA E STRUTTURE Laboratorio Prove Materiali e Strutture	Part No.	Full Scale Test	Note: All dimensions are illustrated in the individual drawings	Material: S 355 JR	SCALE: 13/06/2013
				Drawing No.	Reviewer
RFCS project N° RFSR-CT-2012-0029 Proposal acronym: ROBUSTIMPACT Organisation acronym: UNITRE		Referred by:			
This design is property of the University of Trento. Copy or use without permission is not allowed and will be punished in accordance with the law.		Reference file:			

Number of pieces - 6



SEC. A-A SCALE 1:5

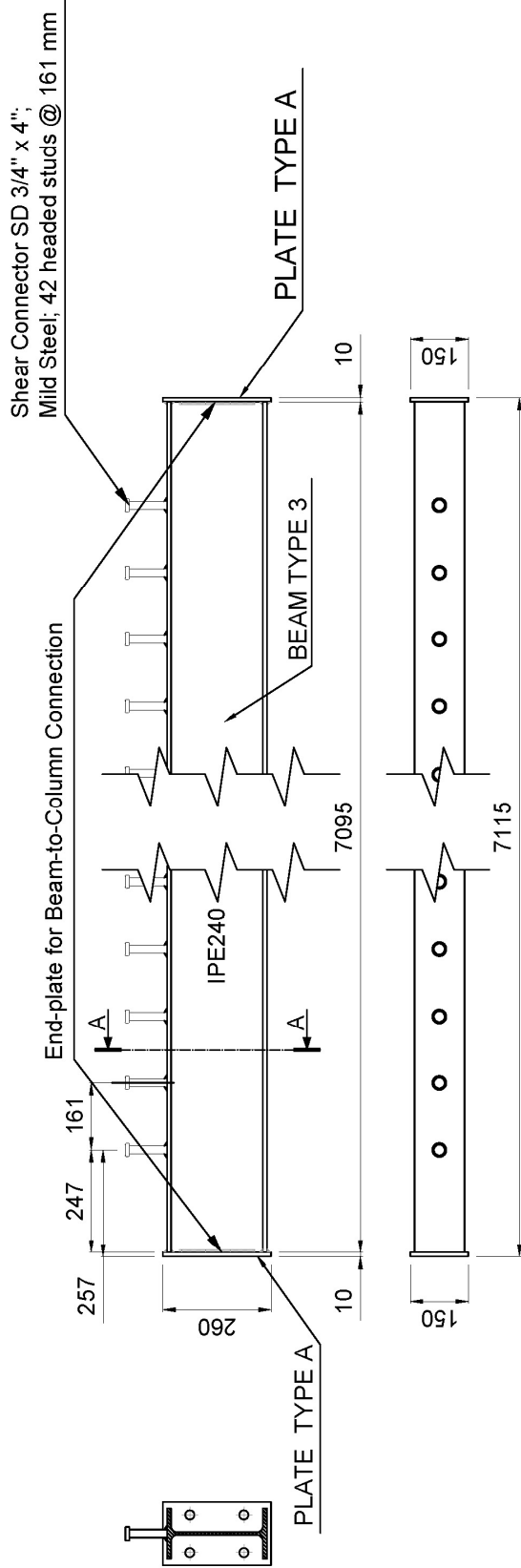


 UNIVERSITÀ DEGLI STUDI DI TRENTO DIPARTIMENTO DI INGEGNERIA, ARCHITETTURA E STRUTTURE Laboratorio Prove Materiali e Strutture	Part No.	F S T	Full Scale Test	Note: All dimensions are illustrated in the individual drawings	Material: S 355 JR
					Drawing No.: 13/06/2013
RFCS project N° RFSR-CT-2012-0029 Proposal acronym: ROBUSTIMPACT Organisation acronym: UNITRE		SCALE Date: 13/06/2013 Reviewer:			
Revisited by: Drawn by:		Reference file: Form: "Full_Jobname_impact_UNITRE_fig_300"			

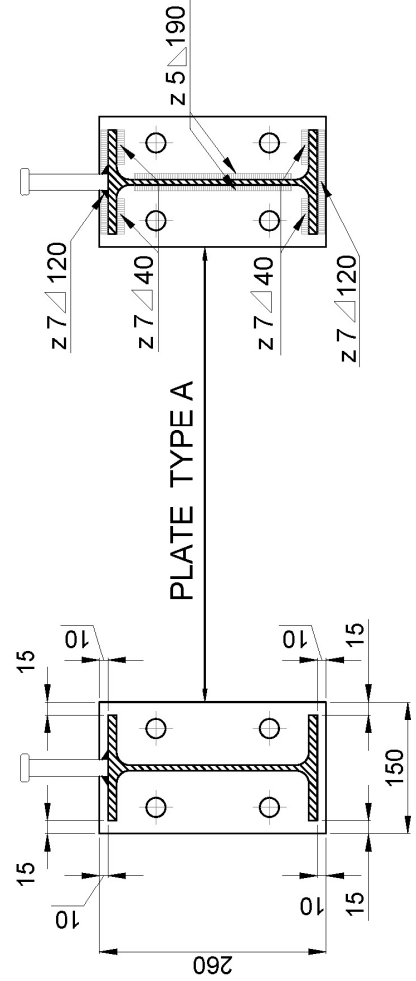
This design is property of the University of Trento. Copy or use this document without permission is not allowed and will be punished in accordance with the law.


MOMENT RESISTING STEEL-CONCRETE COMPOSITE FRAMES UNDER THE COLUMN LOSS SCENARIO:
 DESIGN OF THE REFERENCE FRAMES AND OF THE FULL-SCALE SUB-FRAME SPECIMENS

Number of pieces - 3



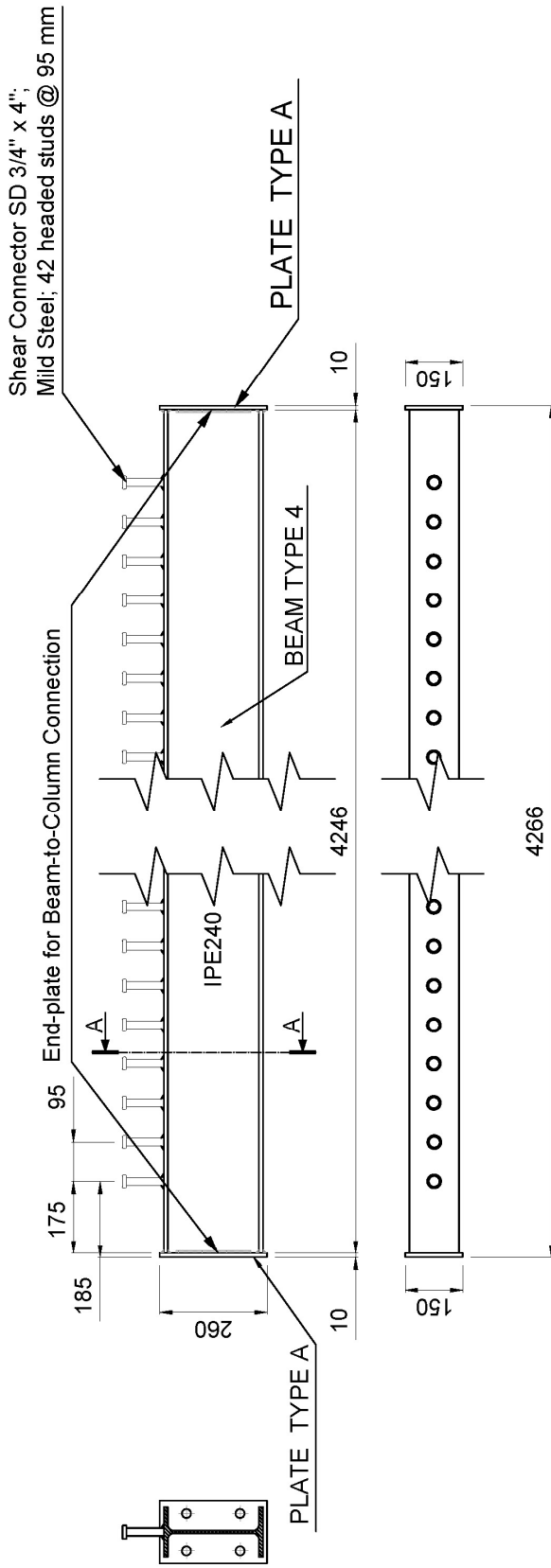
SEC. A-A SCALE 1:5



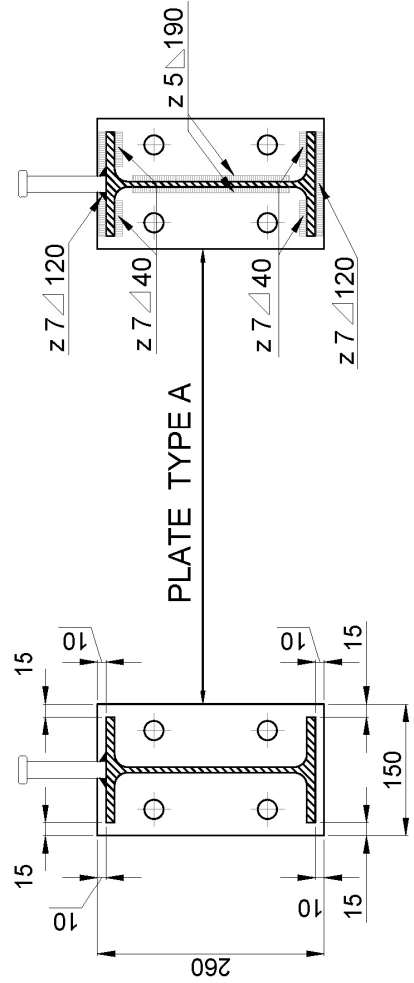
 UNIVERSITÀ DEGLI STUDI DI TRENTO DIPARTIMENTO DI INGEGNERIA AEROSPAZIALE E STRUTTURALE Laboratorio Prove Materiali e Strutture	Part No.	RFS project N° RFSR-CT-2012-0029 Proposal acronym: ROBUSTIMPACT Organisation acronym: UNITRE	
		Material: S 355 JR	SCALE: 13/06/2013 Drawing No.
F S T Test	Note: All dimensions are illustrated in the individual drawings	Drawing No. FST 06 Revision	Reference file: Forme_Inf_LaboratorioIMPACT_UNITRE_Inf_500


This design is property of the University of Trento. Copy or use this document without permission is not allowed and will be punished in accordance with the law.

Number of pieces - 3

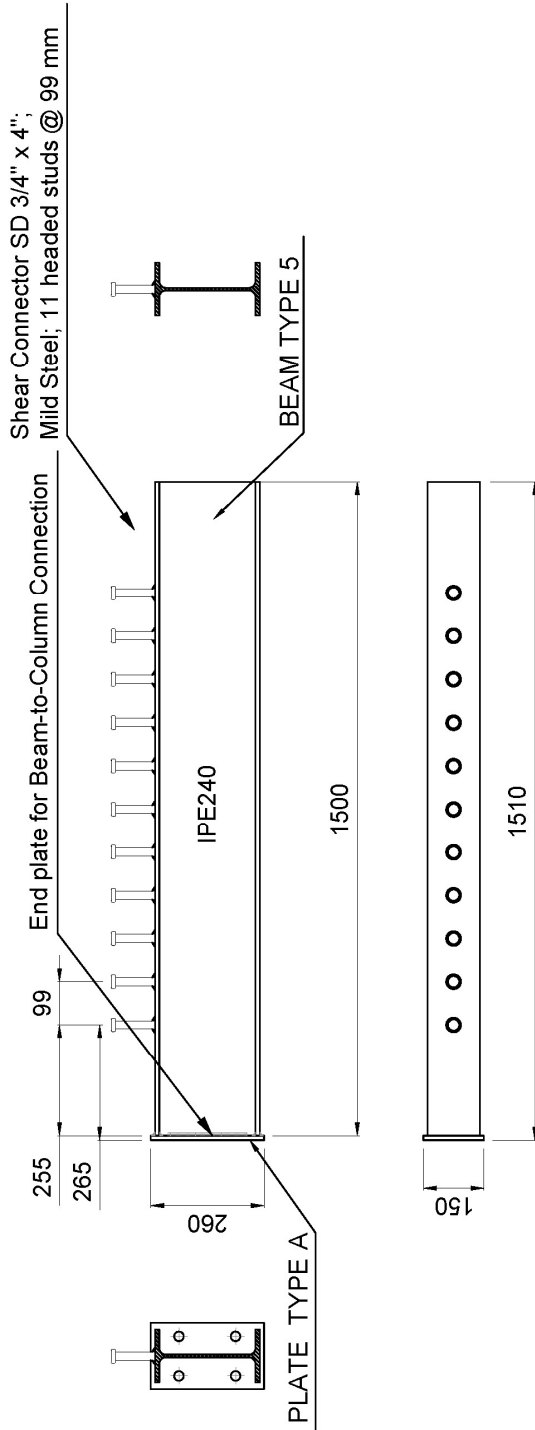


SEC. A-A SCALE 1:5

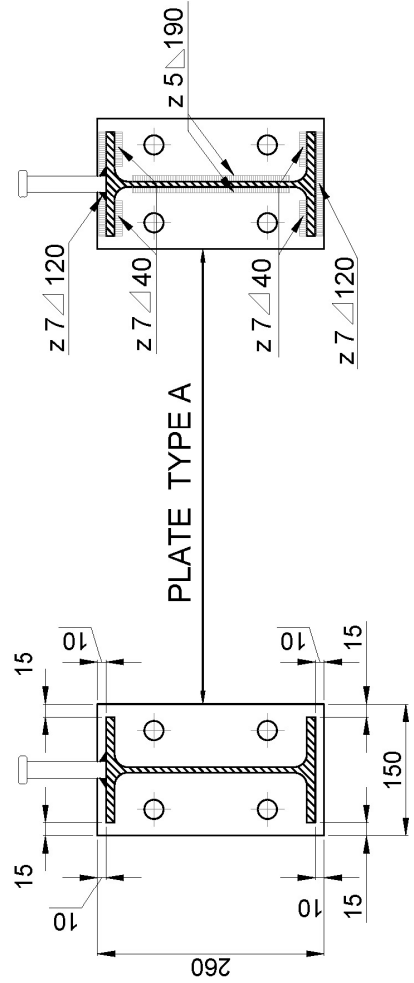



 UNIVERSITÀ DEGLI STUDI DI TRENTO DIPARTIMENTO DI INGENGERIA AEROSPAZIALE E STRUTTURALE Laboratorio Prove Materiali e Strutture	Part No. F ull S cale T est	Project No. RFSR-CT-2012-0029 Proposal acronym: ROBUSTIMPACT Organisation acronym: UNITRE	
		Note: All dimensions are illustrated in the individual drawings	Material: S 355 JR Drawing No.: 13/06/2013 Date: 13/06/2013 Reviewer: Reference file: Form: "Prod_LaboratorioImpact_UNITRE_07_000"

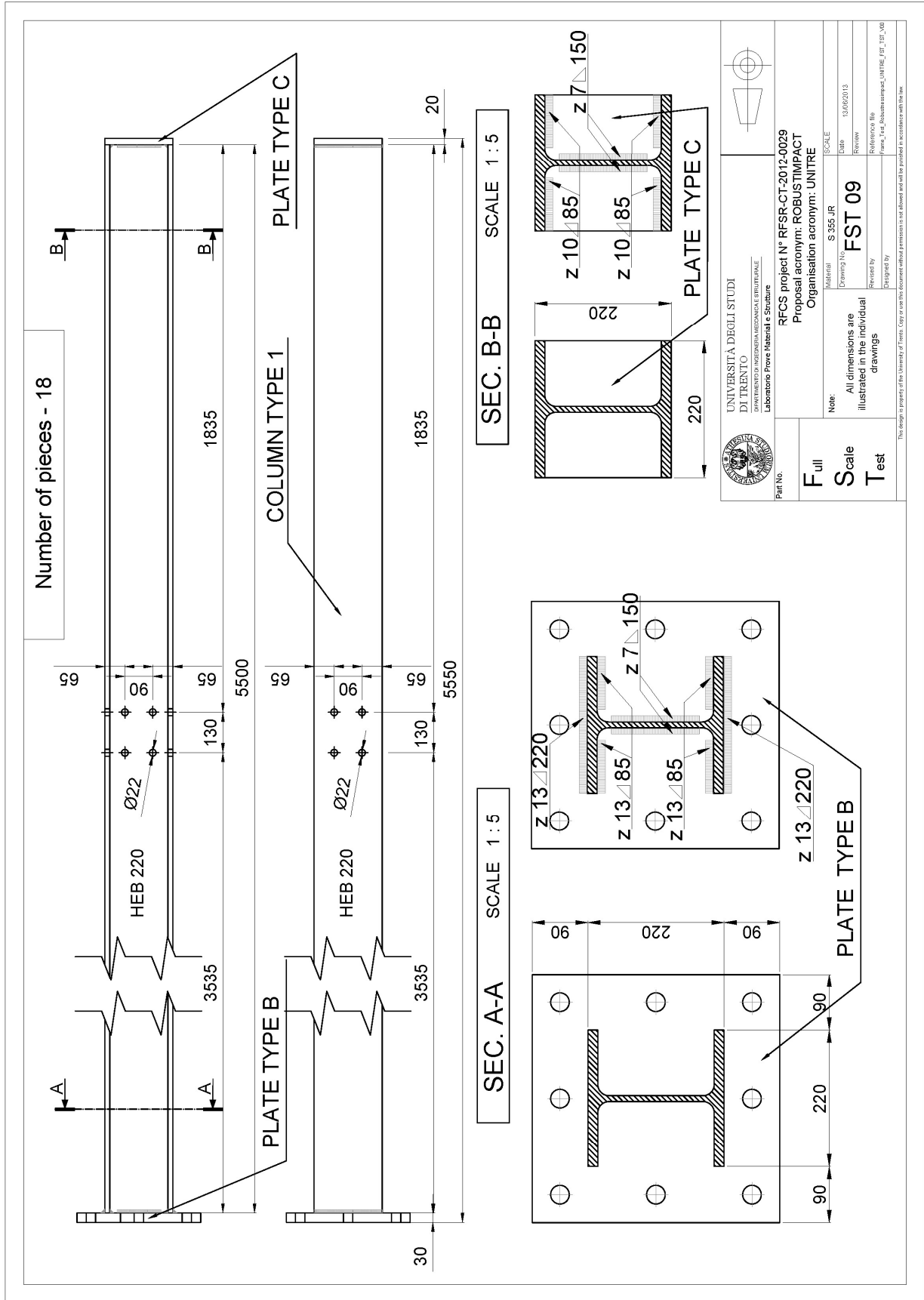
Number of pieces - 6



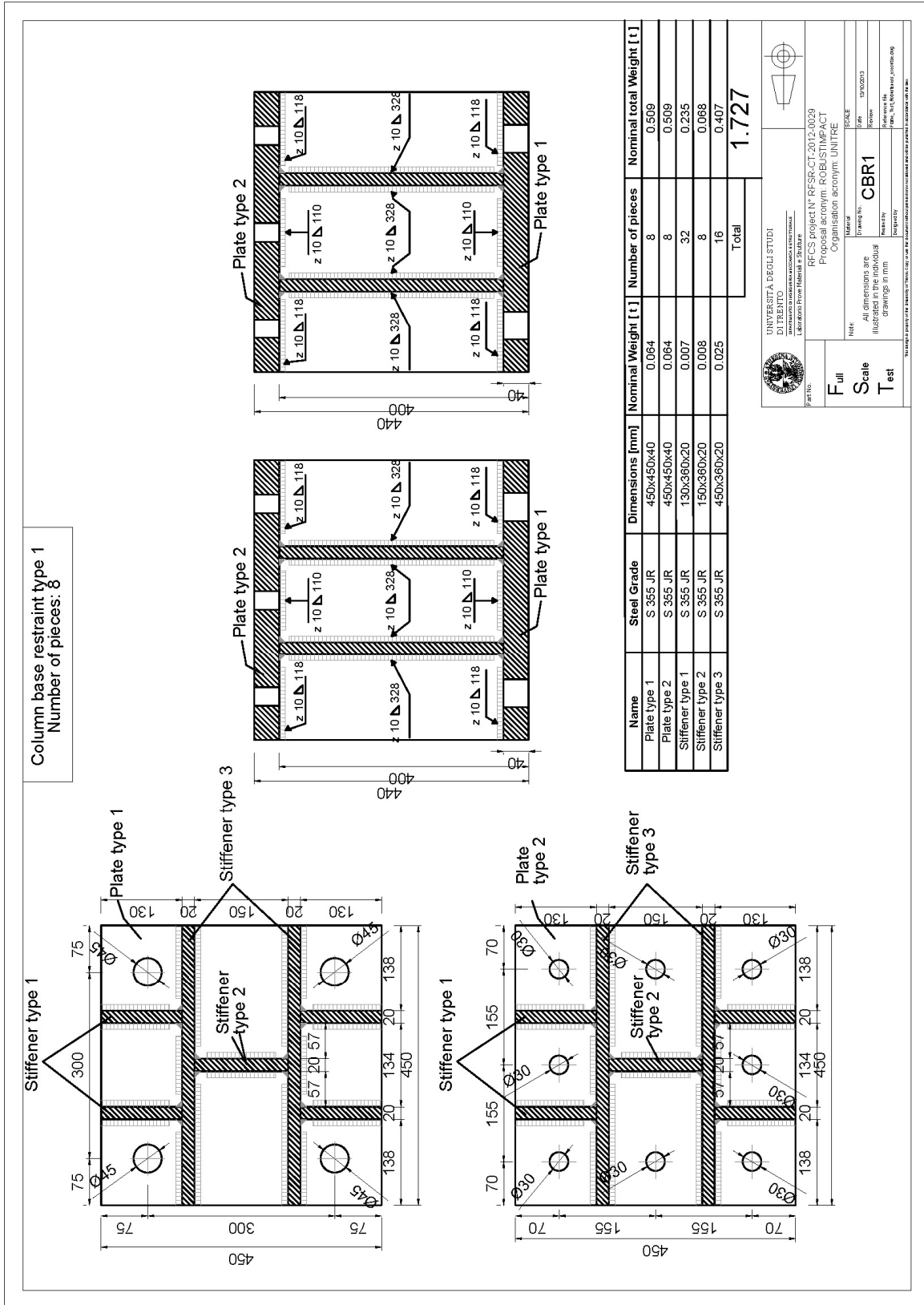
SEC. A-A SCALE 1 : 5



 UNIVERSITÀ DEGLI STUDI DI TRENTO DIPARTIMENTO DI INGEGNERIA AEROSPAZIALE E STRUTTURALE Laboratorio Prove Materiali e Strutture	RFCS project N° RFSR-CT-2012-0029 Proposal acronym: ROBUSTIMPACT Organisation acronym: UNITRE	Material: S 355 JR	SCALE: 13/06/2013
		Drawing No: FST 08	Review:
Part No.	Note: All dimensions are illustrated in the individual drawings	Designed by:	Reference file: Form_1741_Jobnameimpact_UNITRE_fig_000
Full Scale Test			
This design is property of the University of Trento. Copy or use this document without permission is not allowed and will be punished in accordance with the law.			

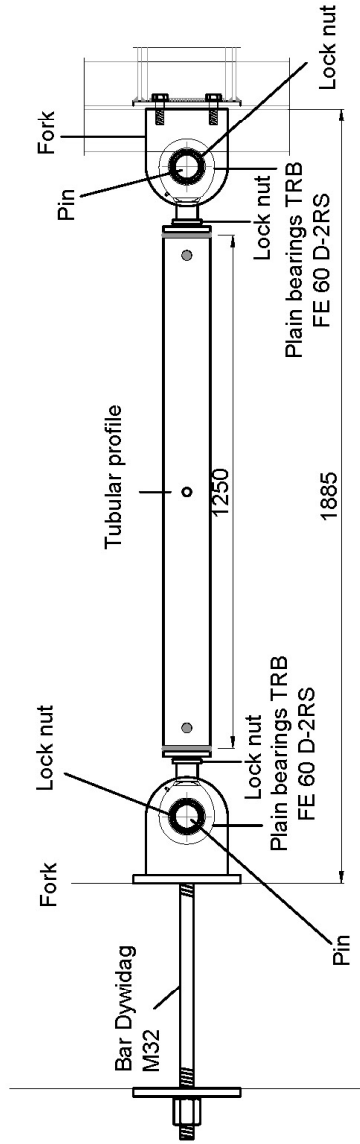



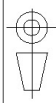
ANNEX B: RESTRAINTS



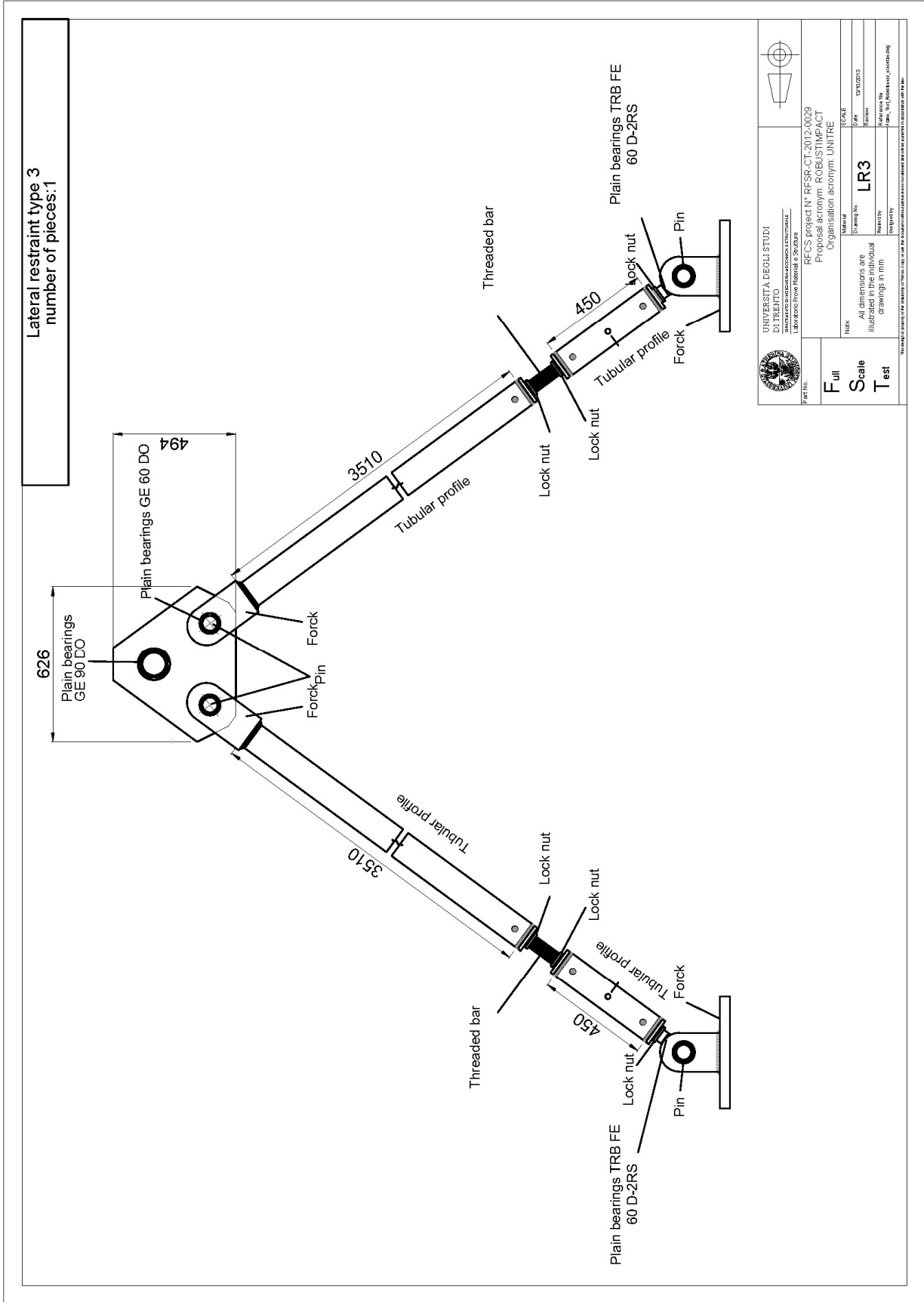
**MOMENT RESISTING STEEL-CONCRETE COMPOSITE FRAMES UNDER THE COLUMN LOSS SCENARIO:
DESIGN OF THE REFERENCE FRAMES AND OF THE FULL-SCALE SUB-FRAME SPECIMENS**

Lateral restraint type 1
number of pieces: 1



 UNIVERSITÀ DEGLI STUDI DI TRENTO <small>UNIVERSITY OF TRENTO</small> LABORATORIO PROVA MATERIALI E STRUTTURE	
Part No. F ull S cale T est	
Note: All dimensions are illustrated in the individual drawings in mm.	
Project No. LR1	Date: 19/02/20
Organisation acronym: UNITRE	Revision:
Reference file:	Project file:
Tutti i diritti sono riservati. È vietata espressamente la ristampa o l'uso non autorizzato senza permesso scritto dalla Università degli Studi di Trento.	

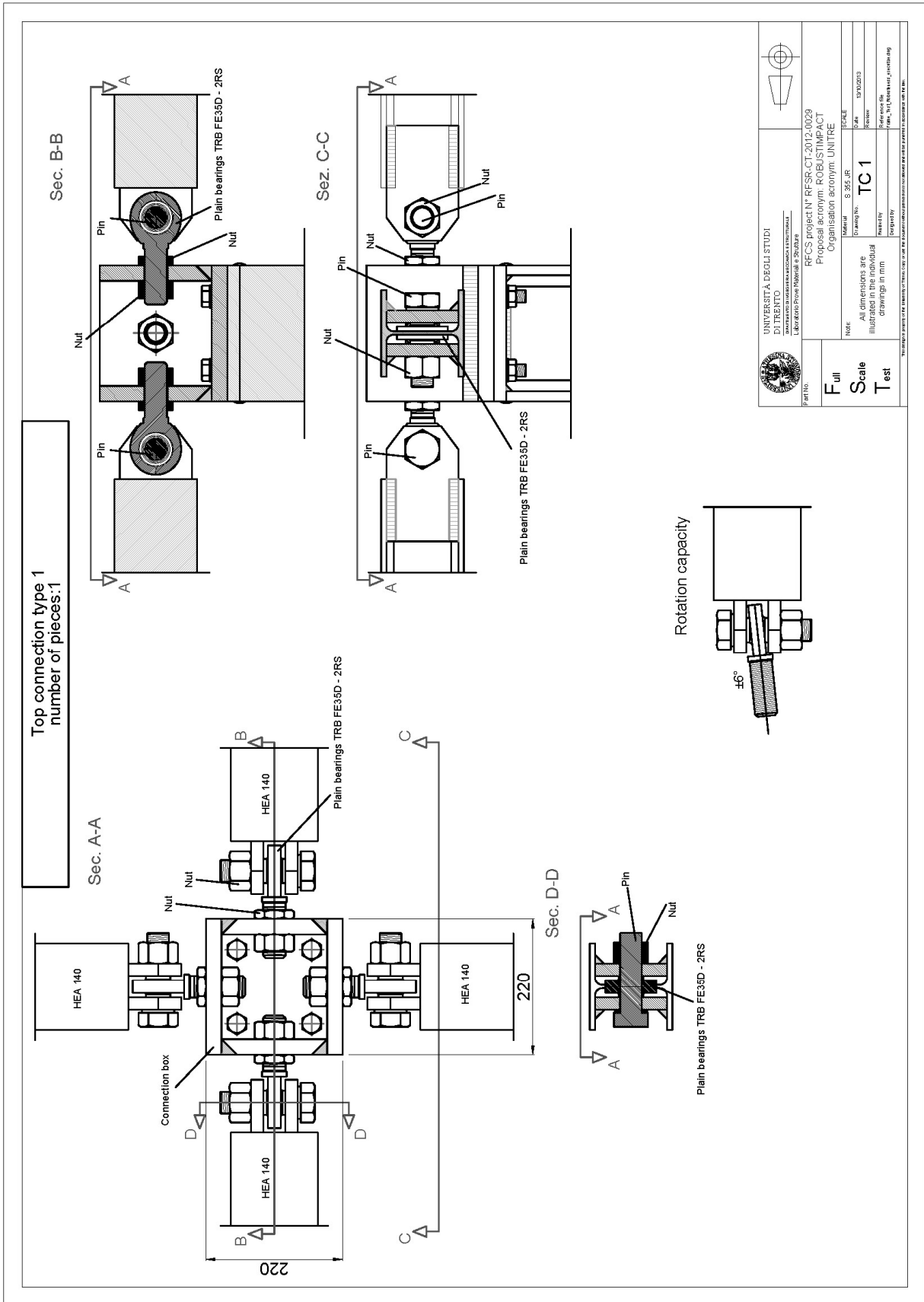
**MOMENT RESISTING STEEL-CONCRETE COMPOSITE FRAMES UNDER THE COLUMN LOSS SCENARIO:
DESIGN OF THE REFERENCE FRAMES AND OF THE FULL-SCALE SUB-FRAME SPECIMENS**



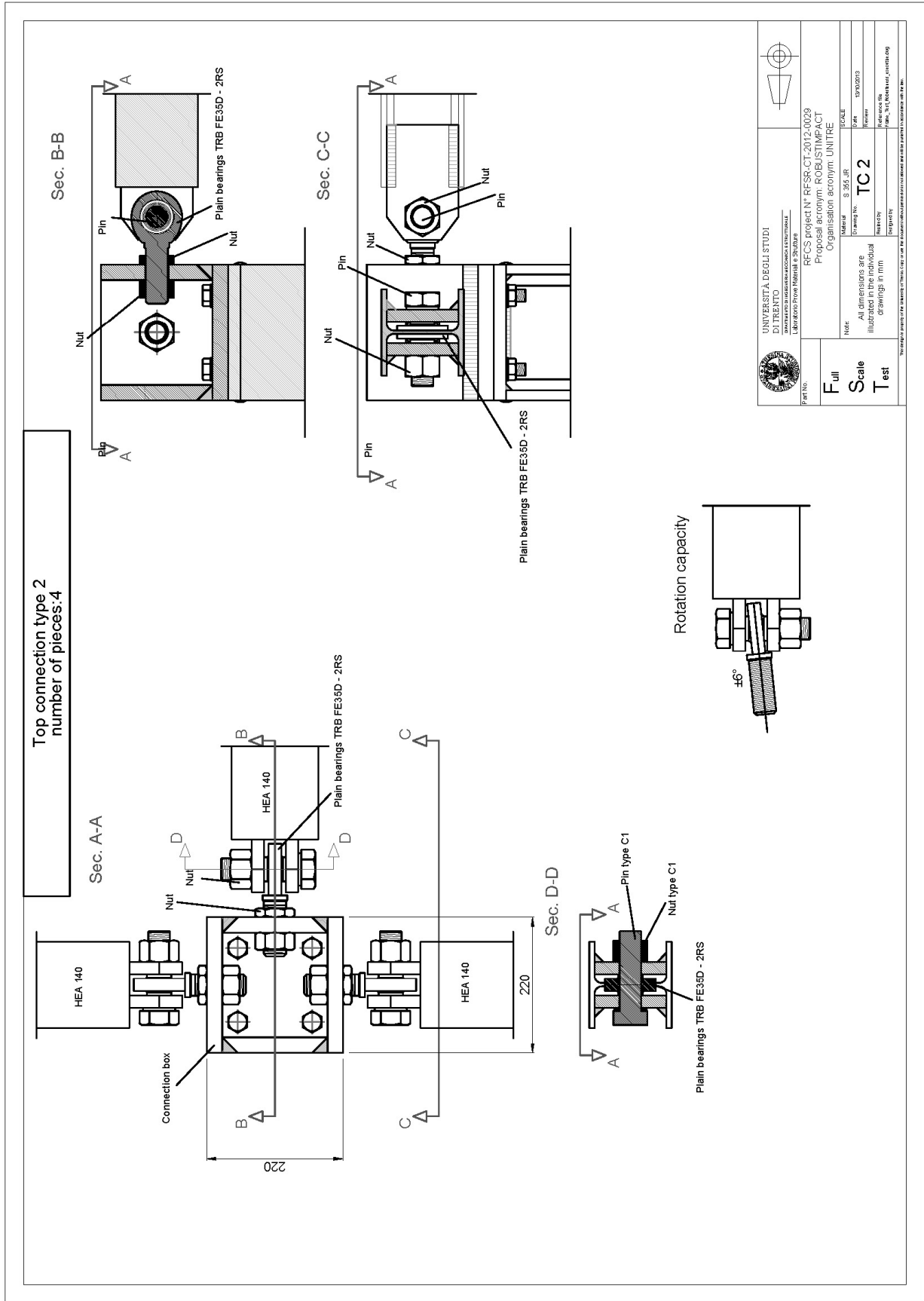
	UNIVERSITÀ DEGLI STUDI DI TRENTO LABORATORIO DI STRUTTURE IN ACCIAIO E LEGHE ALUMINICHE LABORATORIO PER I MATERIALI E I SISTEMI
PART No.	RECS project N° REFSR-CT-2012-0029 Proposal acronym: ROBUSTIMPACT Organisation acronym: UNITRE
F ull	Material
S cale	Drawing No. LR3
T est	Date: 19/02/2013
	Revision
	Reference No.
	Drawing in mm
	Company
	Scale: 1:1 (Not for printing)

*The drawing is subject to the approval of Trento City Council for the approval of the project and the approval of the project.

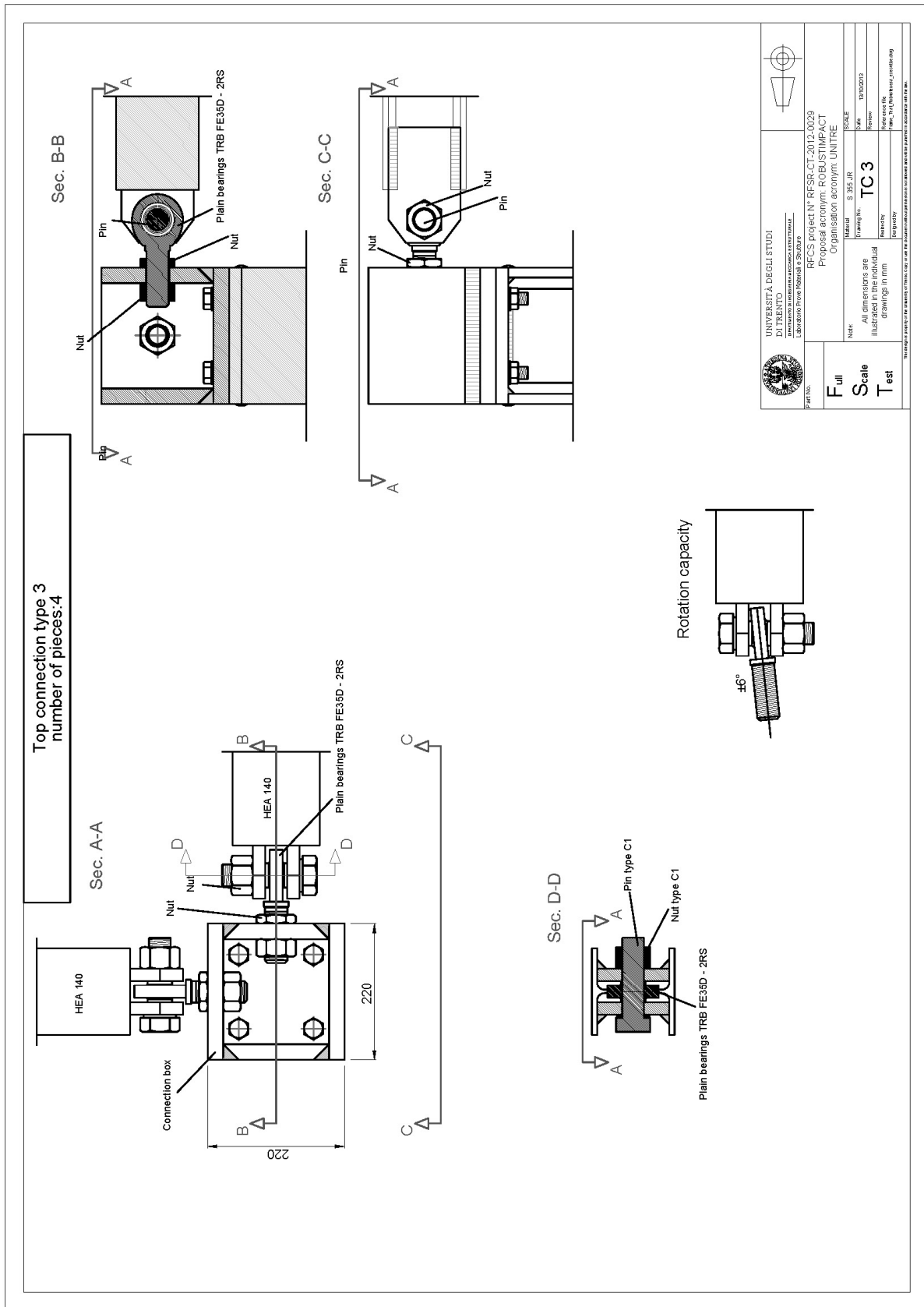
MOMENT RESISTING STEEL-CONCRETE COMPOSITE FRAMES UNDER THE COLUMN LOSS SCENARIO:
 DESIGN OF THE REFERENCE FRAMES AND OF THE FULL-SCALE SUB-FRAME SPECIMENS



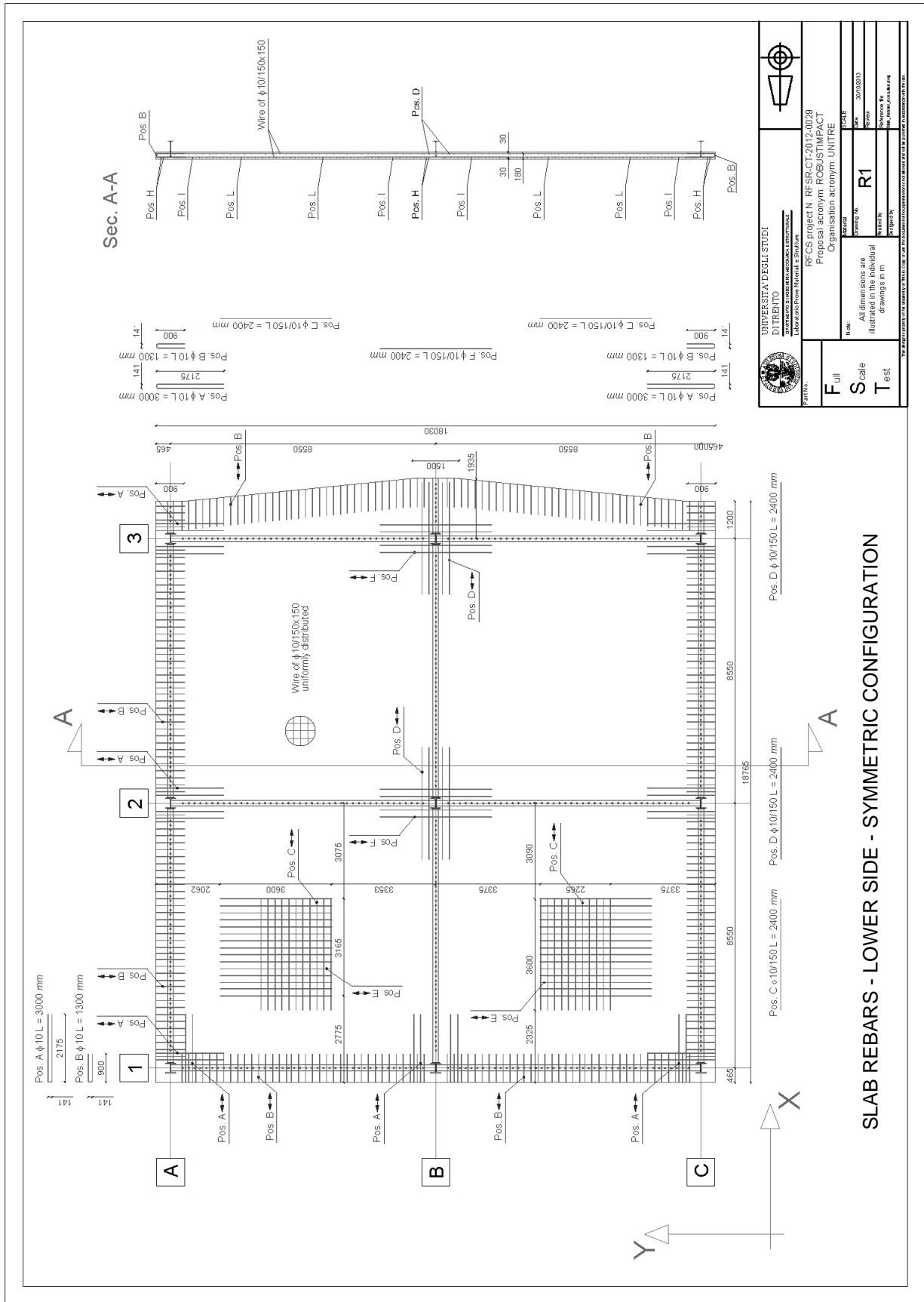
MOMENT RESISTING STEEL-CONCRETE COMPOSITE FRAMES UNDER THE COLUMN LOSS SCENARIO:
 DESIGN OF THE REFERENCE FRAMES AND OF THE FULL-SCALE SUB-FRAME SPECIMENS

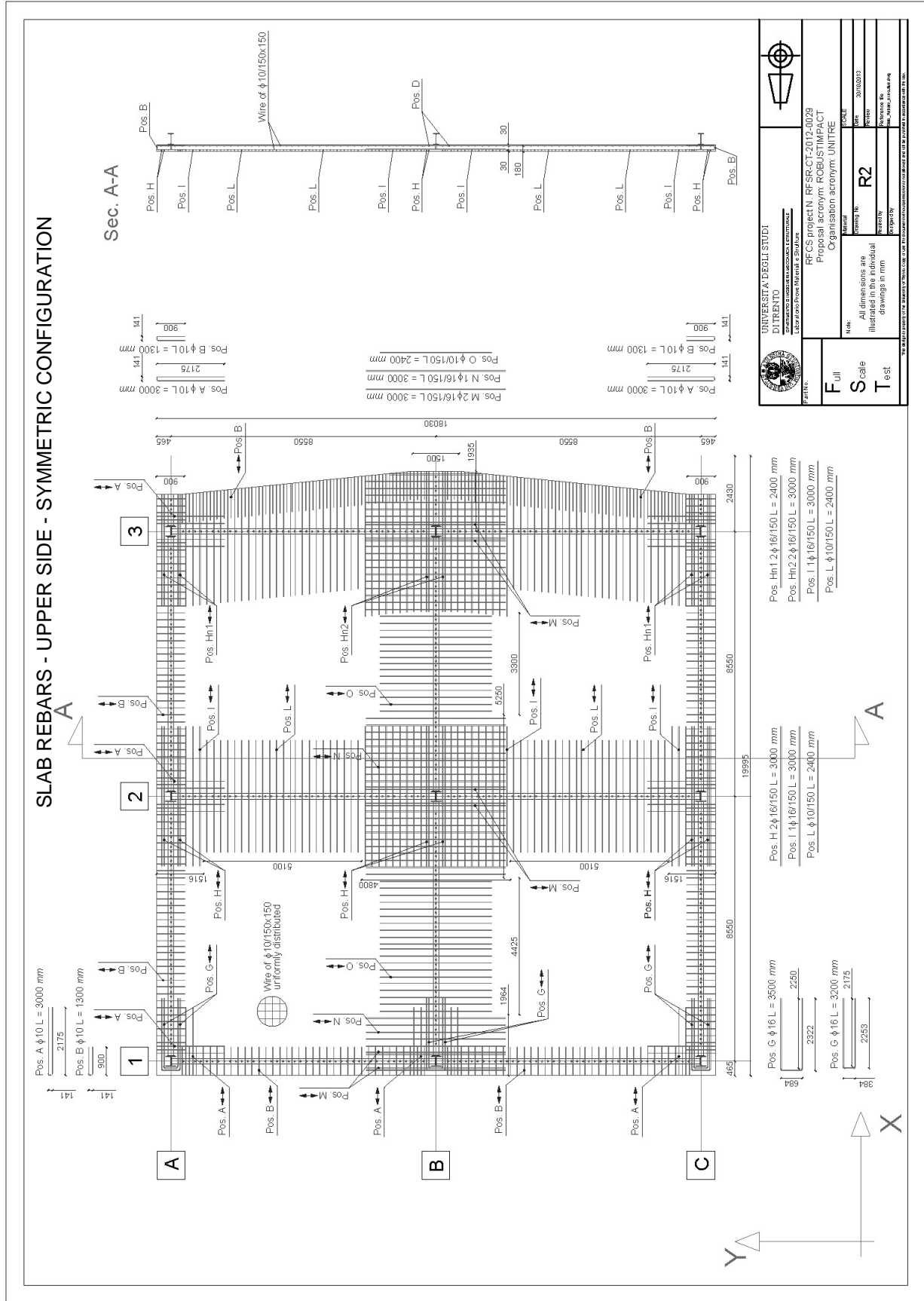


**MOMENT RESISTING STEEL-CONCRETE COMPOSITE FRAMES UNDER THE COLUMN LOSS SCENARIO:
DESIGN OF THE REFERENCE FRAMES AND OF THE FULL-SCALE SUB-FRAME SPECIMENS**

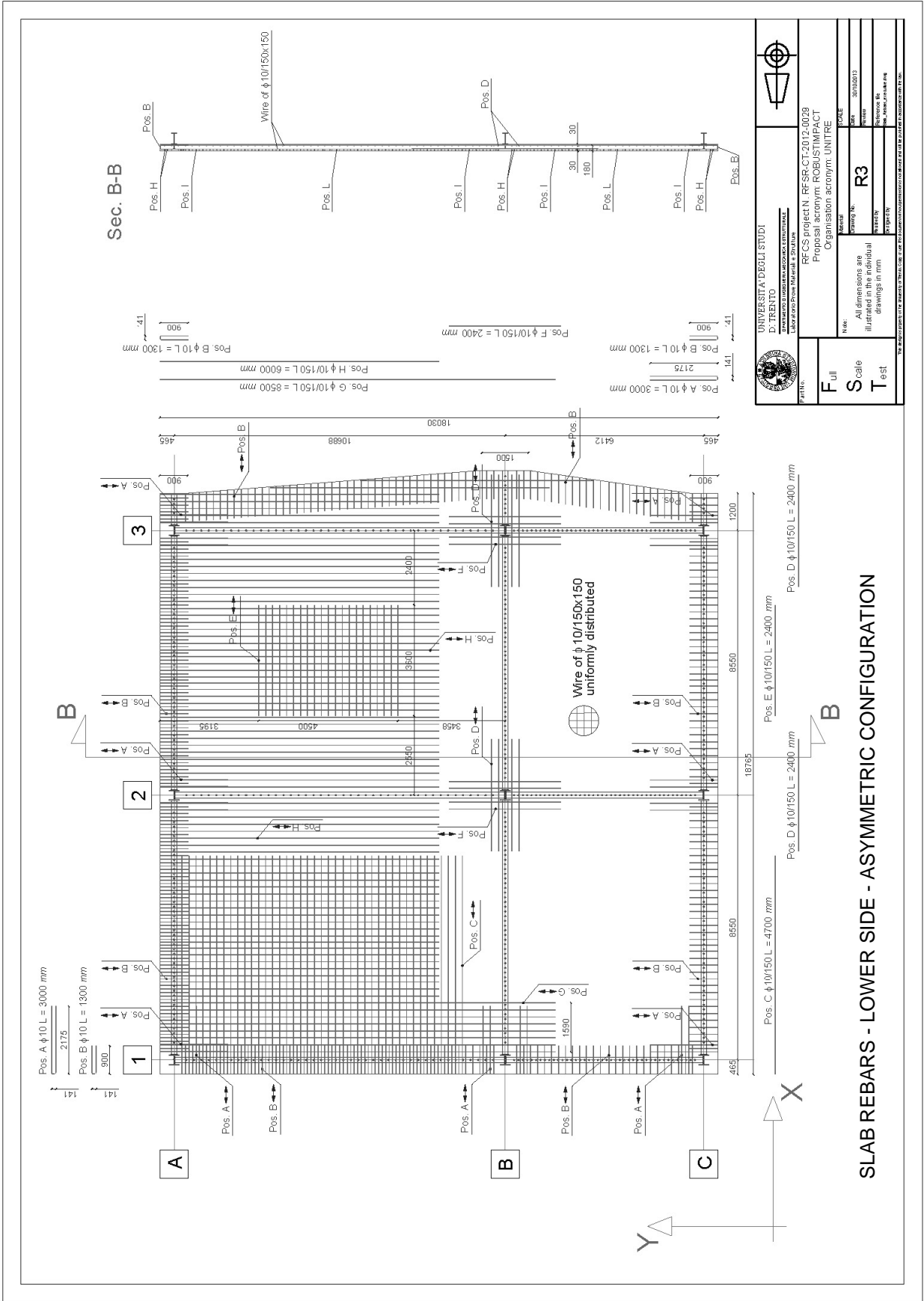


ANNEX C: SLAB'S REINFORCEMENT





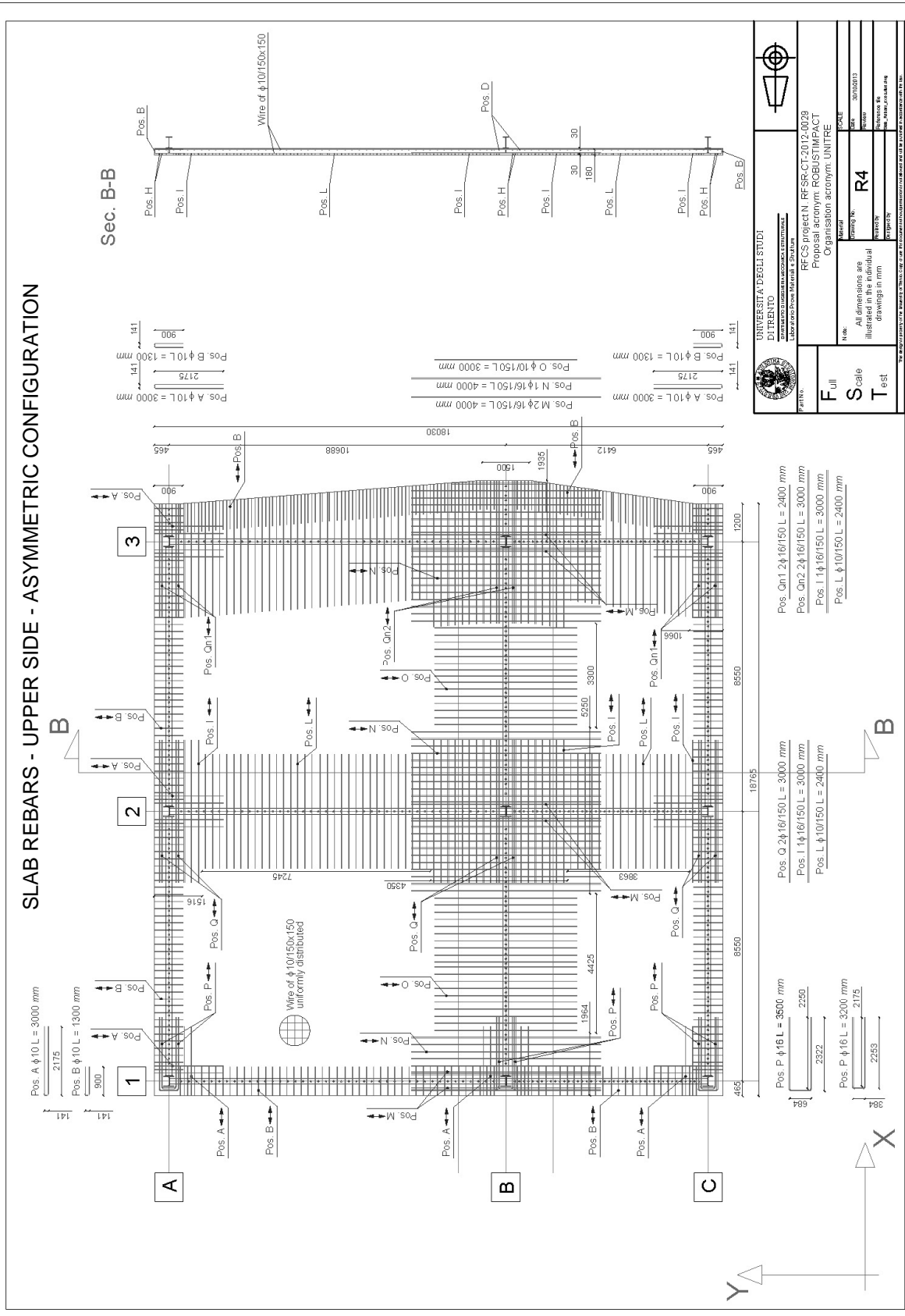
**MOMENT RESISTING STEEL-CONCRETE COMPOSITE FRAMES UNDER THE COLUMN LOSS SCENARIO:
DESIGN OF THE REFERENCE FRAMES AND OF THE FULL-SCALE SUB-FRAME SPECIMENS**



 UNIVERSITA' DEGLI STUDI D. TRENTO DIPARTIMENTO DI INGEGNERIA E SCIENZE MECCANICHE E STRUTTURE	 RFCS Project N. RF3P-CT-2012-0038 Proprietary acronym: ROBUSTIMPACT Organisation acronym: UNITIFE	Project NO.: R3 Version: 30/06/2013 Author: [Name] Check: [Name]
		Note: All dimensions are illustrated in the individual drawings in mm.
Scale: Full Scale Test		Project No.: R3 Version: 30/06/2013 Author: [Name] Check: [Name]

SLAB REBARS - LOWER SIDE - ASYMMETRIC CONFIGURATION

SLAB REBARS - UPPER SIDE - ASYMMETRIC CONFIGURATION



UNIVERSITA' DEGLI STUDI DI TRENTO FACOLTA' DI INGEGNERIA CORSO VITTORIO VENETO 1, 38100 TRENTO, ITALY	Project No. _____ Date: 03/10/2023 Scale: R4 Drawing No. _____ Revision No. _____ Author: _____ Checked: _____
Project Name: R4 Proposal acronym: ROBUSTIMPACT Organisation acronym: UNITRE	Scale: R4 Drawing No. _____ Revision No. _____ Author: _____ Checked: _____

